GRADIENTS AND NON-ADIABATIC DERIVATIVE COUPLING TERMS FOR SPIN-ORBIT WAVEFUNCTIONS

DISSERTATION

Lachlan T. Belcher, Captain, USAF
AFIT/DS/ENP/11-J01

DEPARTMENT OF THE AIR FORCE
AIR UNIVERSITY

AIR FORCE INSTITUTE OF TECHNOLOGY

Wright-Patterson Air Force Base, Ohio

AFIT/DS/ENP/11-J01

GRADIENTS AND NON-ADIABATIC DERIVATIVE COUPLING TERMS FOR SPIN-ORBIT WAVEFUNCTIONS

DISSERTATION

Presented to the Faculty

Department of Engineering Physics

Graduate School of Engineering and Management

Air Force Institute of Technology

Air University

Air Education and Training Command

In Partial Fulfillment of the Requirements for the

Degree of Doctor of Philosophy

Lachlan T. Belcher, BS, MS

Captain, USAF

June 2011

AFIT/DS/ENP/11-J01

GRADIENTS AND NON-ADIABATIC DERIVATIVE COUPLING TERMS FOR SPIN-ORBIT WAVEFUNCTIONS

Lachlan T. Belcher, BS, MS

Captain, USAF

Approved:

_____//SIGNED//_____	_____
David E. Weeks, PhD (Chairman)	Date
_____//SIGNED//_____	_____
Glenn P. Perram, PhD (Member)	Date
_____//SIGNED//_____	_____
William P. Baker, PhD (Member)	Date
_____//SIGNED//_____	_____
Gary S. Kedziora, PhD (Member)	Date

Accepted

_____//SIGNED//_____	_____
M.U. Thomas	Date
Dean, Graduate School of	
Engineering and Management	

AFIT/DS/ENP/11-J01

Abstract

Analytic gradients of electronic eigenvalues require one calculation per nuclear geometry, compared to 3n calculations for finite difference methods, where n is the number of nuclei. Analytic non-adiabatic derivative coupling terms, which are calculated in a similar fashion, are used to remove non-diagonal contributions to the kinetic energy operator, leading to more accurate nuclear dynamics calculations than those that employ the Born-Oppenheimer approximation, i.e., that assume off-diagonal contributions are zero. The current methods and underpinnings for calculating both of these quantities for MRCI-SD wavefunctions in COLUMBUS are reviewed. Before this work, these methods were not available for wavefunctions of a relativistic MRCI-SD Hamiltonian. A formalism for calculating the density matrices, analytic gradients, and analytic derivative coupling terms for those wavefunctions is presented. The results of a sample calculation using a Stuttgart basis for K He are presented. Density matrices predict the MRCI eigenvalues to approximately 10^{-10} hartree. Analytic gradients match finite central-difference gradients to within one percent. The non-adiabatic coupling angle calculated by integrating the radial analytic derivative coupling terms matches the same angle approximated by the Werner method to within 0.02 radians. Non-adiabatic energy surfaces for K He are presented.

For Pooki

Acknowledgments

I would like to thank the members of my committee for their time and dedication to this project. I would like to thank Dr. Kedziora for the countless hours he has put into guiding me through FORTRAN and COLUMBUS. Finally, I would like to thank Dr. Weeks for carefully and thoughtfully selecting a rich and challenging research topic which leveraged the entirety of my faculties.

Lachlan T. Belcher

Table of Contents

Page

List of Figures

Figure Page

Figure Page

List of Tables

Table Page

GRADIENTS AND NON-ADIABATIC DERIVATIVE COUPLING TERMS FOR SPIN-ORBIT WAVEFUNCTIONS

I. Introduction

Computational chemistry is a useful theoretical companion of spectroscopy and other experimental approaches to understand the complex interaction between atoms and molecules. It seeks to explain the chemical phenomena observed by experimental science and further to predict the nature of future experimental results. Over the past several decades, computers have grown in size and speed, and the methods of computational chemistry have matured. As needs are identified, the field of computational chemistry has grown to meet those needs. For example, the coupling between electronic states and nuclear degrees of freedom, quantified by *Derivative Coupling Terms* (DCT) was largely ignored until recently. Now that field, known as *non-adiabatic chemistry*, is growing, and continues to explain a number of phenomena.

Suppose we have a system of interest which involves a transition from one energy state to another. The Diode-Pumped Alkali Laser (DPAL) is one such system in which non-adiabatic dynamics plays an important role. In a DPAL, the alkali atoms are

pumped to the excited $2P_{3/2}$ state from which they transition to the $2P_{1/2}$ state via collision with a gas, creating a population inversion in the $2P_{1/2}$ state; finally they lase to the ground state (see schematic in Figure 1). To model the transition of the system, the nuclear wavefunction can be represented as a two-component vector,

$$\begin{pmatrix} \Xi_{P_{3/2}} \\ \Xi_{P_{1/2}} \end{pmatrix} \tag{1}$$

and the Hamiltonian which will propagate it can be represented as

$$\mathbf{H} = \mathbf{K} + \mathbf{V} = -\sum_{\alpha} \frac{1}{m_\alpha} \begin{pmatrix} \nabla_\alpha & 0 \\ 0 & \nabla_\alpha \end{pmatrix}^2 + \begin{pmatrix} \varepsilon_{P_{3/2}} & 0 \\ 0 & \varepsilon_{P_{1/2}} \end{pmatrix} \tag{2}$$

where α indexes the nuclei and the $\varepsilon's$ are the potential energy values (determined by the electronic Schrodinger equation). We restrict the discussion that follows to a diatomic system consisting of an alkali atom and a noble gas atom. Because this Hamiltonian is completely diagonal, a wavefunction that is prepared in the $2P_{3/2}$ state

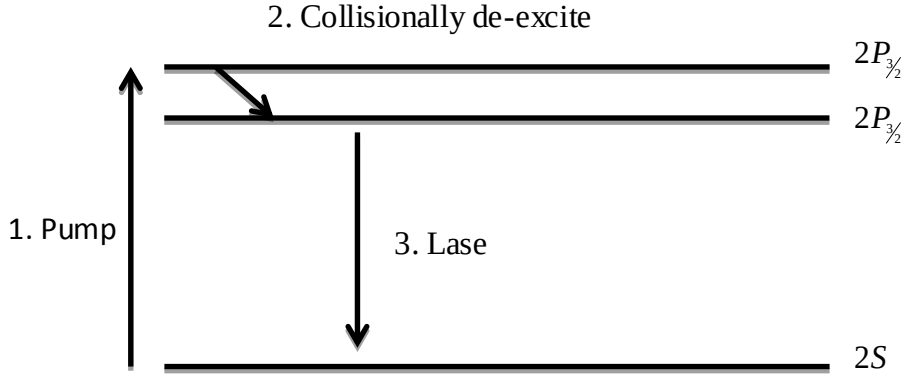

Figure 1. Schematic of DPALS

will never couple to the $2P_{1/2}$ state (note that this Hamiltonian does not account for interaction with an electromagnetic field or vacuum fluctuations). This Hamiltonian is *adiabatic* in that it does not allow a wavefunction to transition between potential energy surfaces, and is a result of the *Born-Oppenheimer Approximation* which completely decouples the electronic and nuclear dynamics.

Such systems cannot be studied under the Born-Oppenheimer Approximation, and a more realistic albeit complicated Hamiltonian must be employed:

$$\mathbf{H} = -\sum_{\alpha} \frac{1}{2m_{\alpha}} \begin{pmatrix} \nabla_{\alpha} & P_{\alpha} \\ -P_{\alpha} & \nabla_{\alpha} \end{pmatrix}^2 + \begin{pmatrix} \varepsilon_{P_{3/2}} & 0 \\ 0 & \varepsilon_{P_{1/2}} \end{pmatrix} \tag{3}$$

The off-diagonal values in the kinetic energy operator are the DCTs which are a result of the coupling of electronic and nuclear dynamics. They are not, in general, negligible, but they do allow a nuclear wavefunction to transition between the two levels.

Unfortunately, these terms also introduce off-diagonal derivative operators into the kinetic energy operator, making the propagation equations difficult to solve. To remedy this shortcoming, we may introduce a unitary transformation, which is calculated from the DCTs, to the Hamiltonian to diagonalize the kinetic energy operator:

$$\begin{aligned} \mathbf{U}^{\dagger}\mathbf{H}\mathbf{U} &= -\sum_{\alpha} \frac{1}{2m_{\alpha}} \mathbf{U}^{\dagger} \begin{pmatrix} \nabla_{\alpha} & P_{\alpha} \\ -P_{\alpha} & \nabla_{\alpha} \end{pmatrix}^2 \mathbf{U} + \mathbf{U}^{\dagger} \begin{pmatrix} \varepsilon_{P_{3/2}} & 0 \\ 0 & \varepsilon_{P_{1/2}} \end{pmatrix} \mathbf{U} \\ &= -\sum_{\alpha} \frac{1}{2m_{\alpha}} \begin{pmatrix} \nabla_{\alpha} & 0 \\ 0 & \nabla_{\alpha} \end{pmatrix}^2 + \begin{pmatrix} \varepsilon_1 & \varepsilon_{12} \\ \varepsilon_{12} & \varepsilon_2 \end{pmatrix} \end{aligned} \tag{4}$$

This transformation results in two new *diabatic* potential energy curves, ε_1 and ε_2, as well as a *coupling curve*, ε_{12}. This diabatic form of the Hamiltonian still allows transitions between the two states, but now results in tractable nuclear dynamics equations.

In order to construct this form of the Hamiltonian, we must be able to calculate the DCTs, P_α, and from them the transformation matrix $\mathbf{U}$. Shepard's method of analytic gradients [**1**] [**2**] [**3**] [**4**] and Lischka's adaptation of it to DCTs [**5**] [**6**] has made their calculation possible in COLUMBUS [**7**] [**8**] [**9**] [**10**], a popular quantum chemistry code package. While Yabushita has implemented the ability to calculate the wavefunctions and energies of open-shell systems, including spin-orbit systems, in COLUMBUS [**11**], the analytic calculation of the DCTs (and energy gradients) for such systems has not been available for *Configuration Interaction* (CI) calculations.

Previously, a number of methods were available to approximate inclusion of spin-orbit coupling into DCTs. For example, code is available to calculate spin-orbit DCTs for a *Mulit-Configuration Self-Consistent Field* (MCSCF) [**12**]; however, MCSCF calculations are generally smaller than CI calculations, and thus produce less-accurate wavefunctions. Spin-orbit coupling can also be added perturbatively to the non-relativistic Hamiltonian (see, e.g., [**13**] [**14**] [**15**]); however, perturbative approaches are generally not applicable to larger atoms. It is also possible to perform a spin-orbit calculation to create the CI wavefunctions, but then use a non-relativistic approach to calculate the DCTs and resultant transformation which are applied to the entire

wavefunction [**16**] [**17**] [**18**]; however, this method is not as rigorous as including the spin-orbit effects in the DCTs.

Werner introduced a rudimentary yet extremely fast way to calculate the non-adiabatic coupling angle by examining the CI coefficients of the wavefunction, the derivative of which is the DCT [**12**]. Because of the speed and ease of calculation, we will use this last method as a quick validation of the method presented herein.

The recent experimental work at the Air Force Institute of Technology on DPALs has given impetus to the theoretical effort in the system's nuclear dynamics, and hence a need for accurate, open-shell spin-orbit DCTs. This dissertation reviews the established methods available in COLUMBUS and then presents the formalism whereby they can be augmented to produce analytic gradients and DCTs for open-shell spin-orbit wavefunctions. This formalism has been implemented in an experimental version of COLUMBUS at the Department of Defense Super-computing Resource Center (DSRC) at Wright-Patterson Air Force Base, OH [**19**]. The alkali-noble gas system of K He has been chosen to validate the code due to its simplicity, the availability of a spin-orbit potential, and its potential application to DPALs. The resultant gradients, DCTs, and adiabatic potential energy surfaces of K He, the last of which may be used for the nuclear dynamics calculation, are presented herein.

II. Background

Second-Quantization of the Fine-Structure Hamiltonian

The energy operator, or *Hamiltonian*, will be the principal quantum-mechanical tool used in this paper to derive the quantities of interest to us, *viz*, energy eigenvalues, energy gradients, and derivative coupling terms. The Hamiltonian obeys the eigenvalue equation

$$\hat{H}\left|\Psi_I\right\rangle = E^I\left|\Psi_I\right\rangle \tag{5}$$

in which Ψ_I are the solution wavefunctions, and the E^I are the corresponding energy eigenvalues. A brief introduction to the Hamiltonian, and the Schrödinger equation, is discussed in Appendix A.

The Electronic Hamiltonian

For the atomic and molecular systems which we will explore in this paper, we can formulate a Hamiltonian in which the kinetic energy of each particle and each pair-wise Coulombic potential energy are represented, all of which are linearly superimposed [**20**]:

$$H = -\sum_{\alpha}\frac{\nabla_{\alpha}^2}{2m_{\alpha}} - \sum_{i}\frac{\nabla_{i}^2}{2} + \tfrac{1}{2}\sum_{\alpha,\beta}\frac{Z_{\alpha}Z_{\beta}}{\left|\vec{r}_{\alpha}-\vec{r}_{\beta}\right|} + \tfrac{1}{2}\sum_{i,j}\frac{1}{\left|\vec{r}_{i}-\vec{r}_{j}\right|} - \sum_{\alpha,i}\frac{Z_{\alpha}}{\left|\vec{r}_{\alpha}-\vec{r}_{i}\right|} \tag{6}$$

where Z_{α} and m_{α} are the charge and mass, respectively, of the α^{th} nucleus; $\vec{r}_i$ and $\vec{r}_{\alpha}$ are the position of the i^{th} electron and α^{th} nucleus, respectively; and ∇_{α}^2 and ∇_i^2 are the Laplacian operators of the α^{th} nucleus and the i^{th} electron, respectively. In this

equation and for the remainder of the paper we will use atomic units for which the mass of the electron, the charge of the electron, and $\hbar$ are all equal in magnitude to unity. The terms in equation (6) are, from left to right:

1. The nuclear kinetic energy summed over the nuclei
2. The electronic kinetic energy summed over electrons
3. The nuclear potential energy summed over nuclear pairs
4. The electronic potential energy summed over electron pairs
5. The nuclear-electronic potential energy summed over nucleus-electron pairs

This Hamiltonian is often split into a nuclear Hamiltonian

$$H_n = -\sum_{\alpha} \frac{\nabla_{\alpha}^2}{2m_{\alpha}} \tag{7}$$

and an electronic Hamiltonian

$$H_e = -\sum_{i} \frac{\nabla_i^2}{2} + \tfrac{1}{2}\sum_{i,j} \frac{1}{\left|\vec{r}_i - \vec{r}_j\right|} - \sum_{\alpha,i} \frac{Z_{\alpha}}{\left|\vec{r}_{\alpha} - \vec{r}_i\right|} \tag{8}$$

Notably missing from either Hamiltonian is the nuclear potential term. This term will be the same for all electronic eigenvalues, so it will not affect the calculations to come; rather, it will be added to the final energy as an offset.

Effective Core Potentials

The above electronic Hamiltonian is known as an *all-electron* Hamiltonian, since it is assumed that i indexes all electrons belonging to the atoms in the system. For larger systems or small systems with larger atoms, the two-electron interaction term can become quite cumbersome to calculate. It is expedient, then, to replace some of

the core electrons that play a lesser role in the chemistry with an *Effective Core Potential* (ECP), while dealing with the more important valence electrons individually [**21**] [**22**]. The resultant electronic Hamiltonian is

$$H_e = -\sum_i \frac{\nabla_i^2}{2} + \tfrac{1}{2}\sum_{i,j} \frac{1}{\left|\vec{r}_i - \vec{r}_j\right|} - \sum_{\alpha,i} \frac{Z_\alpha}{\left|\vec{r}_\alpha - \vec{r}_i\right|} + \sum_i U^{ECP}\left(\vec{r}_i\right) \tag{9}$$

where i indexes the valence electrons and possibly some subset of the core electrons. The ECP captures the approximate effects of the core electrons on the valence set.

Relativistic Effects

The above electronic Hamiltonian, while powerful, does not take into account the effects of relativity on the energy eigenvalues. Appendix B addresses the Breit-Pauli Hamiltonian, a more accurate and relativistic energy operator. While we will not explicitly use the Breit-Pauli Hamiltonian in our calculations, we will be using one of the quantities derived from it. We include the largest relativistic contribution in the valence region, the spin-orbit contribution, by means of a *Relativistic ECP* (RECP),

$$H_e = -\sum_i \frac{\nabla_i^2}{2} + \tfrac{1}{2}\sum_{i,j} \frac{1}{\left|\vec{r}_i - \vec{r}_j\right|} - \sum_{\alpha,i} \frac{Z_\alpha}{\left|\vec{r}_\alpha - \vec{r}_i\right|} + \sum_i U^{RECP}\left(\vec{r}_i\right) \tag{10}$$

which is calculated by transforming the solutions to the Dirac-Hartree-Fock equations [**23**] [**24**]. The RECP is calculated in two pieces: an *Averaged Relativistic Electron Potential* (AREP), which approximates the average fine-structure contribution, and a *Spin-Orbit Potential* (SOP), which effects the actual splitting of the energy eigenfunctions. The spin-orbit potential may be defined as [**11**]

$$H_{so} \equiv \sum_{\alpha,i,l} \xi_l(i,\alpha)\vec{\sigma}_i \cdot \vec{l}_{i\alpha} \tag{11}$$

in which $\vec{\sigma}_i$ is the spin vector of the i^{th} electron, $\vec{l}_{i\alpha}$ is the orbital angular momentum vector of the i^{th} electron with respect to the α^{th} nucleus, and $\xi_l(i,\alpha)$ is a numerically-calculated radial potential term. (Compare this term to the term h_{so} in equation (306) of Appendix B). Making these corrections to the electronic Hamiltonian in equation (9) yields a spin-orbit electronic Hamiltonian:

$$H_e = -\sum_i \frac{\nabla_i^2}{2} + \tfrac{1}{2}\sum_{i,j} \frac{1}{\left|\vec{r}_i - \vec{r}_j\right|} - \sum_{\alpha,i} \frac{Z_\alpha}{\left|\vec{r}_\alpha - \vec{r}_i\right|} + \sum_i U^{AREP}(\vec{r}_i) + H_{so} \tag{12}$$

One- and Two-Electron Operators

The electronic Hamiltonian in equation (12) has two types of integrals with which we will be concerned: the one-electron operators (those that sum only over one electronic coordinate) and the two-electron operators (those that sum over two electronic coordinates). We define the operators

$$\begin{aligned} \hat{h}(i) &\rightarrow -\frac{\nabla_i^2}{2} - \sum_\alpha \left(\frac{Z_\alpha}{\left|\vec{r}_\alpha - \vec{r}_i\right|} \right) + U^{AREP}(\vec{r}_i) \\ \hat{h}^{so}(i) &\rightarrow \sum_{\alpha,l} \left(\xi_l(i,\alpha)\vec{\sigma}_i \cdot \vec{l}_{i\alpha} \right) \\ \hat{g}(i,j) &\rightarrow \frac{1}{\left|\vec{r}_i - \vec{r}_j\right|} \end{aligned} \tag{13}$$

so that the electronic Hamiltonian may be written in the more compact form

$$\hat{H} = \sum_i \hat{h}(i) + \sum_i \hat{h}^{so}(i) + \tfrac{1}{2}\sum_{i,j} \hat{g}(i,j) \tag{14}$$

Second Quantization

The Hamiltonian introduced in the previous section is the *first-quantized* Hamiltonian. Some of the distinguishing features of the first-quantization are [**3**]:

1. It is constructed from the fundamental characteristics of the particles (mass, charge, position).
2. It depends on the number of electrons, N, and thus it confines its eigenfunctions to have N electrons.
3. There is no requirement that the functions on which it operates be antisymmetric or even built from an orbital basis.
4. The choice of orbital basis has no effect on the form of the Hamiltonian.

In contrast, we wish to form a *second-quantized* Hamiltonian that is constructed from an orbital basis and is unconfined by electron number. Furthermore, this Hamiltonian will be represented in a space of antisymmetric many-electron functions, known as *Configuration State Functions* (CSFs).

Consider the spin-orbital projectors,

$$|r(i)\mu(\omega_i)\rangle\langle r(i)\mu(\omega_i)| \tag{15}$$

where $r(i)$ signifies the i^{th} electron in the r^{th} spatial orbital and $\mu(\omega_i)$ signifies the same electron in the μ^{th} spin state. Through completeness,

$$\sum_{r,\mu}|r(i)\mu(\omega_i)\rangle\langle r(i)\mu(\omega_i)| = \hat{1} \tag{16}$$

which we can now insert judiciously into the first-quantized Hamiltonian:

$$
\begin{aligned}
H = & \sum_{i} \sum_{r,\mu} |\, r(i)\mu(\omega_i)\rangle\langle r(i)\mu(\omega_i)\,| h(i) \sum_{s,\nu} |\, s(i)\nu(\omega_i)\rangle\langle s(i)\nu(\omega_i)\,| \\
& + \tfrac{1}{2} \sum_{i,j\neq i} \sum_{r,\mu} |\, r(i)\mu(\omega_i)\rangle\langle r(i)\mu(\omega_i)\,| g(i,j) \sum_{s,\nu} |\, s(i)\nu(\omega_i)\rangle\langle s(i)\nu(\omega_i)\,| \\
& + \sum_{i} \sum_{r,\mu} |\, r(i)\mu(\omega_i)\rangle\langle r(i)\mu(\omega_i)\,| h^{so}(i) \sum_{s,\nu} |\, s(i)\nu(\omega_i)\rangle\langle s(i)\nu(\omega_i)\,|
\end{aligned}
\tag{17}
$$

A word of caution: equation (16) is only true for a complete (i.e. infinite) set of orbitals. All computational chemistry calculations use a finite basis, and thus equation (16) is not necessarily true. The result of this approximation is that the second-quantized Hamiltonian at the end of this section is not exactly equal to the first-quantized Hamiltonian at the beginning. However, in order to use a first-quantized Hamiltonian in calculations, it too must at some point be projected into a working CSF basis; if this basis is the same as the one found in equation (16), then the first- and second-quantized Hamiltonians will have the same representation [**3**].

Since the sums over spin-orbitals are independent, they can be combined. Further, since $h(i)$ and $g(i,j)$ are not functions of spin, the spins are not involved in those integrals:

$$
\begin{aligned}
H = & \sum_{i} \sum_{r,\mu,s,\nu} |\, r(i)\mu(\omega_i)\rangle\langle r(i)\,| h(i) \,|\, s(i)\rangle\langle \mu(\omega_i)\,|\, \nu(\omega_i)\rangle\langle s(i)\nu(\omega_i)\,| \\
& + \tfrac{1}{2} \sum_{i,j\neq i} \sum_{r,\mu,s,\nu} |\, r(i)\mu(\omega_i)\rangle\langle r(i)\,| g(i,j) \,|\, s(i)\rangle\langle \mu(\omega_i)\,|\, \nu(\omega_i)\rangle\langle s(i)\nu(\omega_i)\,| \\
& + \sum_{i} \sum_{r,\mu,s,\nu} |\, r(i)\mu(\omega_i)\rangle\langle r(i)\mu(\omega_i)\,| h^{so}(i) \,|\, s(i)\nu(\omega_i)\rangle\langle s(i)\nu(\omega_i)\,|
\end{aligned}
\tag{18}
$$

For compactness, let us rename the integrals:

$$
\begin{aligned}
h_{rs} &\equiv \langle r(i)\,| h(i) \,|\, s(i)\rangle \\
g_{rs}(j) &\equiv \langle r(i)\,| g(i,j) \,|\, s(i)\rangle \\
h^{so}_{r\mu s\nu} &\equiv \langle r(i)\mu(\omega_i)\,| h^{so}(i) \,|\, s(i)\nu(\omega_i)\rangle
\end{aligned}
\tag{19}
$$

Note that since g started as a two-electron operator, it still has an electron dependence after a single integration. The orthonormality of the spin functions eliminates one of the spin sums in the non-spin terms:

$$\begin{aligned} H = & \sum_i \sum_{r,\mu,s} \left| r(i)\mu(\omega_i) \right\rangle \left\langle s(i)\mu(\omega_i) \right| h_{rs} \\ & + \tfrac{1}{2} \sum_{i,j\neq i} \sum_{r,\mu,s} \left| r(i)\mu(\omega_i) \right\rangle \left\langle s(i)\mu(\omega_i) \right| g_{rs}(j) \\ & + \sum_i \sum_{r,\mu,s,\nu} \left| r(i)\mu(\omega_i) \right\rangle \left\langle s(i)\nu(\omega_i) \right| h^{so}_{r\mu s\nu} \end{aligned} \tag{20}$$

In order to remove all electron dependence from g, we again apply completeness:

$$\begin{aligned} H = & \sum_i \sum_{r,\mu,s} |r(i)\mu(\omega_i)\rangle\langle s(i)\mu(\omega_i)| h_{rs} + \\ & \tfrac{1}{2} \sum_{i,j\neq i} \sum_{r,\mu,s} \sum_{t,\rho,u,\sigma} |r(i)\mu(\omega_i)\rangle\langle s(i)\mu(\omega_i)| t(j)\rho(\omega_j)\rangle\langle t(j)\rho(\omega_j)| g_{rs}(j) |u(j)\sigma(\omega_j)\rangle\langle u(j)\sigma(\omega_j)| \\ & + \sum_i \sum_{r,\mu,s,\nu} |r(i)\mu(\omega_i)\rangle\langle s(i)\nu(\omega_i)| h^{so}_{r\mu s\nu} \end{aligned} \tag{21}$$

Following the same prescription as equations (18) and (20), the spin functions ρ and σ are removed from the integral and one of the spin sums is eliminated. We now define the integral

$$g_{rstu} \equiv \langle t(j)| g_{rs}(j) |u(j)\rangle \tag{22}$$

and we have

$$\begin{aligned} H = & \sum_i \sum_{r,\mu,s} |r(i)\mu(\omega_i)\rangle\langle s(i)\mu(\omega_i)| h_{rs} \\ & + \tfrac{1}{2} \sum_{i,j\neq i} \sum_{r,\mu,s} \sum_{t,\rho,u} |r(i)\mu(\omega_i)\rangle\langle s(i)\mu(\omega_i)| t(j)\rho(\omega_j)\rangle\langle u(j)\rho(\omega_j)| g_{rstu} \\ & + \sum_i \sum_{r,\mu,s,\nu} |r(i)\mu(\omega_i)\rangle\langle s(i)\nu(\omega_i)| h^{so}_{r\mu s\nu} \end{aligned} \tag{23}$$

Let us define the creation and annihilation operators

$$\hat{a}^{\dagger}_{r\mu} \equiv \frac{1}{\sqrt{N+1}} \sum_i |\, r(i)\,\mu(\omega_i)\rangle$$
$$\hat{a}_{r\mu} \equiv \sqrt{N} \sum_{i'} \langle r(i')\,\mu(\omega_{i'})\,| \tag{24}$$

(see Appendix C). The product of a raising and a lowering operator with identical indices will only have non-zero results on the diagonal of an operator matrix.

$$\begin{aligned} \hat{a}^{\dagger}_{r\mu}\hat{a}_{r\mu} &= \left(\frac{1}{\sqrt{N+1}} \sum_i |\, r(i)\,\mu(\omega_i)\rangle \right) \left(\sqrt{N+1} \sum_{i'} \langle r(i')\,\mu(\omega_{i'})\,| \right) \\ &= \sum_i |\, r(i)\,\mu(\omega_i)\rangle\langle r(i)\,\mu(\omega_i)\,| \end{aligned} \tag{25}$$

We can now place these operators into the Hamiltonian:

$$\begin{aligned} H = & \sum_{r,\mu,s} \hat{a}^{\dagger}_{r\mu}\hat{a}_{s\mu} h_{rs} \\ & + \tfrac{1}{2} \sum_{i,j\neq i} \sum_{r,\mu,s} \sum_{t,\rho,u} |\, r(i)\,\mu(\omega_i)\rangle\langle s(i)\,\mu(\omega_i)\,|\, t(j)\,\rho(\omega_j)\rangle\langle u(j)\,\rho(\omega_j)\,|\, g_{rstu} \\ & + \sum_{r,\mu,s,\nu} \hat{a}^{\dagger}_{r\mu}\hat{a}_{s\nu} h^{so}_{r\mu s\nu} \end{aligned} \tag{26}$$

Note that the pair of operators for the non-relativistic one-electron integral is spin preserving, but the pair for the spin-orbit integral is not. Note also that the g term appears to have four creation/annihilation operators; however, since $j = i$ is not allowed, one pair of these operators is short of a complete sum. We can correct this omission by adding and subtracting the $j = i$ term:

$$\begin{aligned} H = & \sum_{r,\mu,s} \hat{a}^{\dagger}_{r\mu}\hat{a}_{s\mu} h_{rs} \\ & + \tfrac{1}{2} \sum_{r,\mu,s} \sum_{t,\rho,u} \sum_{i,j} [\left| r(i)\,\mu(\omega_i) \right\rangle \left\langle s(i)\,\mu(\omega_i) \right| \left| t(j)\,\rho(\omega_j) \right\rangle \left\langle u(j)\,\rho(\omega_j) \right| \\ & - \left| r(i)\,\mu(\omega_i) \right\rangle \left\langle s(i)\,\mu(\omega_i) \right| \left| t(i)\,\rho(\omega_i) \right\rangle \left\langle u(i)\,\rho(\omega_i) \right|] g_{rstu} \\ & + \sum_{r,\mu,s,\nu} \hat{a}^{\dagger}_{r\mu}\hat{a}_{s\nu} h^{so}_{r\mu s\nu} \end{aligned} \tag{27}$$

Now the second term includes a complete integral over the electronic variable i :

$$\langle s(i)\,\mu(\omega_i)\,|\,t(i)\,\rho(\omega_i)\rangle = \delta_{st}\delta_{\mu\rho} \tag{28}$$

and the Hamiltonian is simplified as

$$\begin{aligned} H = & \sum_{r,\mu,s} \hat{a}^{\dagger}_{r\mu}\hat{a}_{s\mu}h_{rs} \\ & + \tfrac{1}{2}\sum_{r,\mu,s}\sum_{t,\rho,u}\left(\hat{a}^{\dagger}_{r\mu}\hat{a}_{s\mu}\hat{a}^{\dagger}_{t\rho}\hat{a}_{u\rho} - \hat{a}^{\dagger}_{r\mu}\hat{a}_{u\rho}\delta_{st}\delta_{\mu\rho}\right)g_{rstu} \\ & + \sum_{r,\mu,s,\nu}\hat{a}^{\dagger}_{r\mu}\hat{a}_{s\nu}h^{so}_{r\mu s\nu} \end{aligned} \tag{29}$$

Let us further define [**11**] [**3**]

$$\begin{aligned} \hat{E}_{rs} &\equiv \sum_{\mu}^{2}\hat{a}^{\dagger}_{r\mu}\hat{a}_{s\mu} \\ \hat{e}_{rstu} &\equiv \hat{E}_{rs}\hat{E}_{tu} - \hat{E}_{ru}\delta_{st} \\ \hat{E}_{r\mu s\nu} &\equiv \hat{a}^{\dagger}_{r\mu}\hat{a}_{s\nu} \end{aligned} \tag{30}$$

such that the final form of the second-quantized spin-orbit Hamiltonian takes the form

$$H = \sum_{r,s}\hat{E}_{rs}h_{rs} + \tfrac{1}{2}\sum_{r,s,t,u}\hat{e}_{rstu}g_{rstu} + \sum_{r,\mu,s,\nu}\hat{E}_{r\mu s\nu}h^{so}_{r\mu s\nu} \tag{31}$$

In a later section we will see that the $\hat{E}_{rs}$ are generators of the Unitary Group. For this reason, the second-quantized form of the Hamiltonian will be central to the computational chemistry techniques we discuss in later sections.

Density Matrices

One tool available from second quantization of the Hamiltonian will be vitally important to the construction of analytic gradients and DCTs is the d*ensity matrix*. Let $|\Psi_I\rangle$ be an eigenfunction of the Hamiltonian in equation (31). Then its energy eigenvalue is

$$
\begin{aligned}
E^I &= \langle \Psi_I | H | \Psi_I \rangle \\
&= \sum_{r,s} \langle \Psi_I | \hat{E}_{rs} h_{rs} | \Psi_I \rangle + \tfrac{1}{2} \sum_{r,s,t,u} \langle \Psi_I | \hat{e}_{rstu} g_{rstu} | \Psi_I \rangle + \sum_{r,\mu,s,\nu} \langle \Psi_I | \hat{E}_{r\mu s\nu} h^{so}_{r\mu s\nu} | \Psi_I \rangle
\end{aligned} \tag{32}
$$

Since the integral matrices are not functions of electronic coordinates, they commute with the eigenfunctions and we have

$$
E^I = \sum_{r,s} h_{rs} \langle \Psi_I | \hat{E}_{rs} | \Psi_I \rangle + \tfrac{1}{2} \sum_{r,s,t,u} g_{rstu} \langle \Psi_I | \hat{e}_{rstu} | \Psi_I \rangle + \sum_{r,\mu,s,\nu} h^{so}_{r\mu s\nu} \langle \Psi_I | \hat{E}_{r\mu s\nu} | \Psi_I \rangle \tag{33}
$$

We define the quantities

$$
\begin{aligned}
D_{rs} &\equiv \langle \Psi_I | \hat{E}_{rs} | \Psi_I \rangle \\
d_{rstu} &\equiv \langle \Psi_I | \hat{e}_{rstu} | \Psi_I \rangle
\end{aligned} \tag{34}
$$

to be elements of the one-electron and two-electron density matrices, respectively. The spin-orbit density matrix, which would appear in the last term of equation (33), will be addressed in Chapter III. For many transition properties between wavefunctions, including DCTs, it is necessary to use *transition* density matrices which we similarly define as

$$
\begin{aligned}
D^{JI}_{rs} &\equiv \langle \Psi_J | \hat{E}_{rs} | \Psi_I \rangle \\
d^{JI}_{rstu} &\equiv \langle \Psi_J | \hat{e}_{rstu} | \Psi_I \rangle
\end{aligned} \tag{35}
$$

These matrices will appear often in the derivations in Chaper III as well as the appendices.

Gauge Theory

The many-body problem

Systems of more than two bodies are, in general, not analytically tractable [**25**]. The sole example of a two–body problem is the hydrogen atom (or exotic variants thereof) consisting of one proton and one electron; even the basic hydrogen molecule has no analytic solution. The energies and eigenfunctions of the hydrogen atom were solved analytically long ago; indeed, this was one of the primary reasons for the introduction of quantum mechanics [**26**]. The desire to understand molecules from diatoms to proteins and beyond requires various types of approximations. This is the *many-body problem* that is fundamental to this field, which forces us to look for computational solutions to molecular problems.

Another problem that faces computational chemistry is the disparate nature of the particles involved. Electrons are light and fast compared to the massive, lumbering nuclei (which, for most calculations, are modeled as a single particle). The vastly different sizes of these two particles leads to two separate timescales and separates the problem of molecular dynamics into an electronic and a nuclear piece (see the separation of the Hamiltonian, equations (7) and (8)).

The Born-Oppenheimer Approximation

The *Born-Oppenheimer* approximation attempts to effect this separation. In this section, let r represent the collection of electronic coordinates, and let R represent the collection of nuclear coordinates. Assume we have a complete set of orthonormal electronic wavefunctions such that

$$\langle \psi_i \,|\, \psi_j \rangle = \delta_{ij} \tag{36}$$

The solution to the Schrödinger equation (equation (5)) can be expanded in this basis:

$$|\, \Psi_I \rangle = \sum_i \Xi_{Ii} \,|\, \psi_i \rangle \tag{37}$$

which is called the *Born-Oppenheimer expansion* [**27**]. As we will see shortly, these coefficients are actually the nuclear wavefunctions. Alternatively, we can write

$$|\, \Psi_I \rangle \rightarrow \begin{pmatrix} \Xi_{I1} \\ \Xi_{I2} \\ \Xi_{I3} \\ \vdots \end{pmatrix} \equiv \vec{\Xi}_I \tag{38}$$

in the matrix representation. The Born-Oppenheimer approximation takes advantage of the different timescales discussed in the last section by assuming the Hamiltonian can be partitioned into fast and slow, or electronic and nuclear, operators. The Schrödinger equation can be cast as

$$\sum_i \left(\hat{H}_e + \hat{H}_n - E^I \right) \Xi_{Ii} \,|\, \psi_i \rangle = 0 \tag{39}$$

where $\hat{H}_n$ is the part of the full Hamiltonian that depends on nuclear operators and $\hat{H}_e$ depends on electronic operators, as defined in equations (7) and (8), respectively. Consider the integral equation

$$\langle \psi_j \,|\, \sum_i \left(\hat{H}_e + \hat{H}_n - E^I \right) \Xi_{Ii} \,|\, \psi_i \rangle = 0 \tag{40}$$

which is expanded as

$$\sum_i \left(\langle \psi_j \,|\, \hat{H}_e \Xi_{Ii} \,|\, \psi_i \rangle + \langle \psi_j \,|\, \hat{H}_n \Xi_{Ii} \,|\, \psi_i \rangle - \langle \psi_j \,|\, E^I \Xi_{Ii} \,|\, \psi_i \rangle \right) = 0 \tag{41}$$

In the first term, the Hamiltonian acts on the bra and pulls out an eigenvalue, while the Ξ_{Ii} does not participate in the integration, leaving a delta function. In the third term, neither E^I nor Ξ_{Ii} participates in the integration, leaving another delta function:

$$\varepsilon_j \Xi_{Ij} + \sum_i \langle \psi_j \,|\, \hat{H}_n \Xi_{Ii} \,|\, \psi_i \rangle - E^I \Xi_{Ij} = 0 \tag{42}$$

To interpret the second term, it is best to project it into coordinate space by employing the identity

$$\sum_{r,R} |\, r, R \rangle \langle r, R \,| = \hat{1} \tag{43}$$

where

$$\begin{aligned} \psi_i \left(r; R \right) &\rightarrow \langle r, R \,|\, \psi_i \rangle \\ \Xi_{Ii} \left(R \right) &\rightarrow \langle r, R \,|\, \Xi_{Ii} \rangle \\ -\sum_\alpha \frac{\nabla_\alpha^2}{2m_\alpha} &\rightarrow \langle r, R \,|\, \hat{H}_n \,|\, r, R \rangle \\ \varepsilon_j \left(R \right) &\rightarrow \langle r, R \,|\, \varepsilon_j \,|\, r, R \rangle \\ E^I \left(R \right) &\rightarrow \langle r, R \,|\, E^I \,|\, r, R \rangle \end{aligned} \tag{44}$$

Note that while the ψ_i are strictly functions of electronic coordinates, they are parameterized by the nuclear coordinates [**27**]. Since the total wavefunction must be a function of both nuclear and electronic coordinates, this leaves the nuclear dependence in the Ξ_{Ii} term. The form of the nuclear Hamiltonian in coordinate space comes from equation (7). (Note that by including the kinetic energy operator but not the potential energy operator, we have inherently prepared for the coordinate representation since it is the momentum operator that will be represented by a derivative operator. Were we

to prepare for the momentum representation, we might choose to keep the potential energy operator and not the kinetic.) In the coordinate representation, equation (42) is

$$\varepsilon_j(R)\Xi_{Ij}(R)-\sum_{i,\alpha}\frac{1}{2m_\alpha}\int dr\,\psi_j^*(r;R)\nabla_\alpha^2\left[\Xi_{Ii}(R)\psi_i(r;R)\right]-E^I(R)\Xi_{Ij}(R)=0 \qquad (45)$$

The derivative operator must be distributed across the product in brackets in the usual fashion:

$$\begin{aligned}\nabla_\alpha^2\left[\psi_i(r;R)\Xi_{Ii}(R)\right]&=\nabla_\alpha\cdot\left[\psi_i(r;R)\nabla_\alpha\Xi_{Ii}(R)+\Xi_{Ii}(R)\nabla_\alpha\psi_i(r;R)\right]\\&=2\nabla_\alpha\psi_i(r;R)\cdot\nabla_\alpha\Xi_{Ii}(R)+\psi_i(r;R)\nabla_\alpha^2\Xi_{Ii}(R)+\Xi_{Ii}(R)\nabla_\alpha^2\psi_i(r;R)\end{aligned} \qquad (46)$$

which leads to the equation

$$\begin{aligned}&\varepsilon_j(R)\Xi_{Ij}(R)-\sum_{i,\alpha}\frac{1}{2m_\alpha}\int dr\left\{2\psi_j^*(r;R)\nabla_\alpha\psi_i(r;R)\cdot\nabla_\alpha\Xi_{Ii}(R)\right.\\&\left.+\psi_j^*(r;R)\psi_i(r;R)\nabla_\alpha^2\Xi_{Ii}(R)+\psi_j^*(r;R)\nabla_\alpha^2\left[\psi_i(r;R)\right]\cdot\Xi_{Ii}(R)\right\}-E^I(R)\Xi_{Ij}(R)=0\end{aligned} \qquad (47)$$

Each term in this Schrödinger equation operates on $\Xi_{Ii}(R)$ or $\Xi_{Ij}(R)$. Therefore, the terms can be collected as follows:

$$\begin{aligned}&\left[-\sum_\alpha\frac{1}{2m_\alpha}\nabla_\alpha^2+\varepsilon_j(R)-E^I(R)\right]\Xi_{Ij}(R)=\\&\qquad\sum_{i,\alpha}\frac{1}{2m_\alpha}\int dr\left[2\psi_j^*(r;R)\nabla_\alpha\psi_i(r;R)\cdot\nabla_\alpha+\psi_j^*(r;R)\nabla_\alpha^2\psi_i(r;R)\right]\Xi_{Ii}(R)\end{aligned} \qquad (48)$$

The left-hand side of this equation is devoid of electronic dependence, while the right-hand side involves operators which take derivatives of electronic functions with respect to nuclear coordinates. We can compactly rewrite the right-hand side as

$$\sum_i\Lambda_{ji}(r;R)\Xi_{Ii}(R) \qquad (49)$$

where

$$\Lambda_{ji}(R) \equiv \sum_{\alpha} \frac{1}{2m_{\alpha}} 2P_{ji}(R) \cdot \nabla_{\alpha} + Q_{ji}(R)$$
$$P_{ji}^{\alpha}(R) \equiv \int dr\, \psi_j^*(r;R) \nabla_{\alpha} \psi_i(r;R) \leftrightarrow \left\langle \psi_j \middle| \nabla_{\alpha} \psi_i \right\rangle \tag{50}$$
$$Q_{ji}^{\alpha}(R) \equiv \int dr\, \psi_j^*(r;R) \nabla_{\alpha}^2 \psi_i(r;R) \leftrightarrow \left\langle \psi_j \middle| \nabla_{\alpha}^2 \psi_i \right\rangle$$

leading to the more compact Schrödinger equation

$$\left[-\sum_{\alpha} \frac{1}{2m_{\alpha}} \nabla_{\alpha}^2 + \varepsilon_j(R) - E^I(R) \right] \Xi_{Ij}(R) = \sum_i \Lambda_{ji}(R) \Xi_{Ii}(R) \tag{51}$$

or, in matrix representation,

$$\left[-\sum_{\alpha} \frac{1}{2m_{\alpha}} \mathbf{I} \nabla_{\alpha}^2 + \boldsymbol{\varepsilon}(R) - \mathbf{I} E^I(R) \right] \vec{\Xi}_I(R) = \boldsymbol{\Lambda}(R) \vec{\Xi}_I(R) \tag{52}$$

Note that all matrices on the left are diagonal matrices, while the matrix on the right side is unrestricted. If we assume that derivatives of electronic functions with respect to nuclear coordinates, or DCTs, are negligible compared to the rest of the equation, the right side of equation (51) or (52) is summarily zero, and we have the *adiabatic nuclear wave equation* [**28**]:

$$\left[-\sum_{\alpha} \frac{1}{2m_{\alpha}} \mathbf{I} \nabla_{\alpha}^2 + \boldsymbol{\varepsilon}(R) - \mathbf{I} E^I(R) \right] \vec{\Xi}_I(R) = \vec{0} \tag{53}$$

which is the extent of the Born-Oppenheimer approximation; nuclear and electronic dynamics have been completely separated.

Adiabatic chemistry, the subject of most computational chemistry, relies on the Born-Oppenheimer approximation and the resultant adiabatic equation above. The lumbering nuclei are frozen in space and the electronic Schrödinger equation is solved around them. The eigenvalues of that equation, $\boldsymbol{\varepsilon}$, parameterized by the nuclear

coordinates, serve as the adiabatic potential energy surface in equation (53). (The term *surface* is used loosely, since it will have as many dimensions as there are internal nuclear coordinates.) This approximation is feasible because the timescale of the electrons is so short that the nuclei are shepherded by the electronic wavefunction (rather than by information about the precise location of individual particles), which adjusts, for practical calculations, instantaneously to the nuclear motion. Since all operators in the nuclear equation are diagonal, these equations are simply solved, and the nuclear dynamics can be studied with relative ease.

Non-adiabatic Chemistry

Though adiabatic chemistry provides a straightforward way to tackle nuclear dynamics, the Born-Oppenheimer approximation is a compromise. The term *adiabatic* in this sense refers to the fact that the complete separation of fast and slow variables does not allow the nuclear wavefunction to pass from one potential energy surface (or set of electronic eigenvalues) to another quantum mechanically, a *diabatic* process, by transferring electronic potential energy to nuclear kinetic energy. This means that a molecule has no way, apart from electromagnetic interaction, of changing its electronic state. We know this premise to be false, as chemistry is wrought with examples of molecules which, after briefly contacting another, rebound with a higher (or lower) energy level. For problems in which these transitions are critical, the field of non-adiabatic chemistry is more appropriate.

Non-adiabatic chemistry still relies, at least partially, on the Born-Oppenheimer approximation. It still requires that the Hamiltonian be separated into nuclear and

electronic operators, and that the wavefunction be a product of nuclear and electronic wavefunctions (this latter requirement being fundamental to gauge theory, as explained shortly); however, it relaxes the assumption that the elements of the DCT matrix in equation (52) are negligible. To understand where these terms are not negligible, consider the following derivation, beginning with the electronic Schrödinger equation [**29**]:

$$\hat{H}_e \,|\, \psi_i \rangle = \varepsilon_i \,|\, \psi_i \rangle \,. \tag{54}$$

Taking the nuclear derivative of this equation and integrating against ψ_j where $j \neq i$ yields

$$\langle \psi_j \,|\, \nabla \hat{H}_e \,|\, \psi_i \rangle + \langle \psi_j \,|\, \hat{H}_e \,|\, \nabla \psi_i \rangle = \langle \psi_j \,|\, \nabla \varepsilon_i \,|\, \psi_i \rangle + \langle \psi_j \,|\, \varepsilon_i \,|\, \nabla \psi_i \rangle \tag{55}$$

where

$$\nabla \equiv \sum_{\alpha} \nabla_{\alpha} \tag{56}$$

In the second term, the electronic Hamiltonian acts on the bra pulling out an eigenvalue; in the third term the derivative of the eigenvalue is not involved in the integration, and the integral evaluates to zero by orthogonality; in the fourth term the eigenvalue is not involved in the integral, but it does not evaluate to zero:

$$\langle \psi_j \,|\, \nabla \hat{H}_e \,|\, \psi_i \rangle + \varepsilon_j \langle \psi_j \,|\, \nabla \psi_i \rangle = \varepsilon_i \langle \psi_j \,|\, \nabla \psi_i \rangle \tag{57}$$

The result gives an alternate definition to the elements of the $\mathbf{P}$ matrix part of the DCT, which were defined in equation (50):

$$\vec{P}_{ji} = \langle \psi_j \,|\, \nabla \psi_i \rangle = \frac{\langle \psi_j \,|\, \nabla \hat{H}_e \,|\, \psi_i \rangle}{\varepsilon_i - \varepsilon_j} \tag{58}$$

where

$$\vec{\mathbf{P}} = \sum_\alpha \vec{\mathbf{P}}^\alpha \tag{59}$$

(Note that $\vec{\mathbf{P}}$ is a vector; with this understanding, we will drop the arrow notation). Thus we see that elements of $\mathbf{P}$ and hence $\mathbf{\Lambda}$ become significant when the energy eigenvalues of two distinct wavefunctions become very close. Note that when $\varepsilon_i = \varepsilon_j$, P_{ji} is undefined; such points are called conical intersections [**30**]. For the diatomic systems that will be the focus of this paper, such crossings occur only between wavefunctions of dissimilar spatial symmetries, which will not be subject to derivative coupling) [**31**].

Derivative Coupling Terms

Given that there are certain points in the nuclear manifold where the DCTs become significant, they deserve closer scrutiny. Consider again the matrix equation (52), now including the definitions (50):

$$\left[-\sum_\alpha \frac{1}{2m_\alpha} \mathbf{I} \nabla_\alpha^2 + \boldsymbol{\varepsilon} - \mathbf{I} E^I \right] \vec{\Xi}_I = \sum_\alpha \frac{1}{2m_\alpha} \left[2\left(\mathbf{P}^\alpha \cdot \mathbf{I} \nabla_\alpha \right) + \mathbf{Q}^\alpha \right] \vec{\Xi}_I \tag{60}$$

where the nuclear coordinate dependence of operators and functions is understood and has been dropped from the notation for simplicity. Since the DCT has second nuclear derivatives in it, it is part of the kinetic energy term rather than the potential:

$$\left[-\sum_{\alpha}\frac{1}{2m_{\alpha}}\left[\mathbf{I}\nabla_{\alpha}^{2}+2\left(\mathbf{P}^{\alpha}\cdot\mathbf{I}\nabla_{\alpha}\right)+\mathbf{Q}^{\alpha}\right]+\boldsymbol{\varepsilon}-\mathbf{I}E^{I}\right]\vec{\Xi}_{I}=0 \tag{61}$$

In this form of the equation both $\mathbf{P}^{\alpha}$ and $\mathbf{Q}^{\alpha}$ have non-zero off-diagonal derivative components which make this set of equations very difficult to solve in its current form. We require a similarity transformation which will diagonalize the kinetic energy term but may undiagonalize the potential energy term $(\boldsymbol{\varepsilon})$, a compromise which yields an equation with no off-diagonal derivative operators. This transformation takes the equation from the adiabatic basis to a diabatic basis. Diagonal elements of $\boldsymbol{\varepsilon}$ in this diabatic basis are the diabatic potential energy surfaces and are coupled by the off diagonal elements of $\boldsymbol{\varepsilon}$. This transformation from the adiabatic to the diabatic basis is called the *non-adiabatic transformation.*

In order to find that transformation, it is first necessary to manipulate the form of the DCTs [**27**]. Let us first derive an alternate form of $\mathbf{Q}^{\alpha}$. In order to accomplish this, we first calculate the divergence of $\mathbf{P}^{\alpha}$:

$$\begin{aligned}\left(\mathbf{I}\nabla_{\alpha}\cdot\mathbf{P}^{\alpha}\right)_{ij}&=\nabla_{\alpha}\cdot\int dr\,\psi_{j}^{*}(r)\nabla_{\alpha}\psi_{i}(r)\\&=\int dr\,\nabla_{\alpha}\left(\psi_{j}^{*}(r)\right)\cdot\nabla_{\alpha}\psi_{i}(r)+\int dr\,\psi_{j}^{*}(r)\nabla_{\alpha}^{2}\psi_{i}(r)\\&=\int dr\,\nabla_{\alpha}\left(\psi_{j}^{*}(r)\right)\cdot\nabla_{\alpha}\psi_{i}(r)+\mathbf{Q}_{ij}^{\alpha}\end{aligned} \tag{62}$$

Now consider $\mathbf{P}^{\alpha 2}$:

$$\left(\mathbf{P}^{\alpha}\cdot\mathbf{P}^{\alpha}\right)_{ij}=\sum_{k}\int dr'\psi_{i}^{*}(r')\nabla_{\alpha}\psi_{k}(r')\cdot\int dr\,\psi_{k}^{*}(r)\nabla_{\alpha}\psi_{j}(r) \tag{63}$$

Since $\mathbf{P}^{\alpha}$ is antisymmetric,

$$P_{ik}^{\alpha}=-P_{ki}^{\alpha}\rightarrow\int dr\,\psi_{i}^{*}\nabla_{\alpha}\psi_{k}=-\int dr\,\psi_{k}^{*}\nabla_{\alpha}\psi_{i} \tag{64}$$

and so it follows that

$$\left(\mathbf{P}^{\alpha}\cdot\mathbf{P}^{\alpha}\right)_{ij}=-\sum_{k}\int dr'\nabla_{\alpha}\left[\psi_{i}(r')\right]\psi_{k}^{*}(r')\cdot\int dr\,\psi_{k}^{*}(r)\nabla_{\alpha}\psi_{j}(r) \tag{65}$$

Furthermore, if the electronic eigenfunctions are real,

$$\left(\mathbf{P}^{\alpha}\cdot\mathbf{P}^{\alpha}\right)_{ij}=-\sum_{k}\int dr'\nabla_{\alpha}\left[\psi_{i}^{*}(r')\right]\psi_{k}(r')\int dr\,\psi_{k}^{*}(r)\nabla_{\alpha}\psi_{j}(r) \tag{66}$$

which can be rewritten as

$$\left(\mathbf{P}^{\alpha}\cdot\mathbf{P}^{\alpha}\right)_{ij}=-\int dr\int dr'\sum_{k}\left[\psi_{k}(r')\psi_{k}^{*}(r)\right]\nabla_{\alpha}\left[\psi_{i}^{*}(r')\right]\nabla_{\alpha}\psi_{j}(r) \tag{67}$$

The double integral over the sum of k-indexed functions is a completeness identity (analogous to $\sum_{k}|\psi_{k}\rangle\langle\psi_{k}|$), and produces a dirac delta function:

$$-\int dr\int dr'\sum_{k}\left[\psi_{k}(r')\psi_{k}^{*}(r)\right]\nabla_{\alpha}\left[\psi_{i}^{*}(r')\right]\nabla_{\alpha}\psi_{j}(r)=-\int dr\int dr'\,\delta(r-r')\nabla_{\alpha}\left[\psi_{i}^{*}(r')\right]\nabla_{\alpha}\psi_{j}(r) \tag{68}$$

and thus we conclude that

$$\left(\mathbf{P}^{\alpha}\cdot\mathbf{P}^{\alpha}\right)_{ij}=-\int dr\,\nabla_{\alpha}\psi_{i}^{*}(r)\cdot\nabla_{\alpha}\psi_{j}(r) \tag{69}$$

Thus $-\left(\mathbf{P}^{\alpha}\cdot\mathbf{P}^{\alpha}\right)_{ij}$ is the term added to $\mathbf{Q}_{ij}^{\alpha}$ in equation (62). This means that $\mathbf{Q}^{\alpha}$ and $\mathbf{P}^{\alpha}$ are related by

$$\mathbf{Q}^{\alpha}=\left(\mathbf{I}\nabla_{\alpha}\cdot\mathbf{P}^{\alpha}\right)+\mathbf{P}^{\alpha 2} \tag{70}$$

We can use this relationship to eliminate $\mathbf{Q}^{\alpha}$ in equation (61):

$$\left[-\sum_{\alpha}\frac{1}{2m_{\alpha}}\left[\mathbf{I}\nabla_{\alpha}^{2}+2\left(\mathbf{P}^{\alpha}\cdot\mathbf{I}\nabla_{\alpha}\right)+\left(\mathbf{I}\nabla_{\alpha}\cdot\mathbf{P}^{\alpha}\right)+\mathbf{P}^{\alpha 2}\right]+\boldsymbol{\varepsilon}-\mathbf{I}E^{I}\right]\vec{\Xi}_{I}=0 \tag{71}$$

Since $\mathbf{P}^{\alpha}$ and ∇_{α} are non-commuting operators, $\left(\mathbf{P}^{\alpha}\cdot\mathbf{I}\nabla_{\alpha}\right)\neq\left(\mathbf{I}\nabla_{\alpha}\cdot\mathbf{P}^{\alpha}\right)$. Furthermore, note that

$$\mathbf{I}\nabla_{\alpha}\cdot\left(\mathbf{P}^{\alpha}\vec{\Xi}_{I}\right)=\left(\mathbf{I}\nabla_{\alpha}\cdot\mathbf{P}^{\alpha}\right)\vec{\Xi}_{I}+\mathbf{P}^{\alpha}\cdot\mathbf{I}\nabla_{\alpha}\vec{\Xi}_{I} \tag{72}$$

so that the operator relationship

$$\left(\mathbf{I}\nabla_{\alpha}\cdot\mathbf{P}^{\alpha}\right)=\mathbf{I}\nabla_{\alpha}\cdot\mathbf{P}^{\alpha}-\mathbf{P}^{\alpha}\cdot\mathbf{I}\nabla_{\alpha} \tag{73}$$

can be substituted into equation (71), yielding

$$\left[-\sum_{\alpha}\frac{1}{2m_{\alpha}}\left(\mathbf{I}\nabla_{\alpha}+\mathbf{P}^{\alpha}\right)^{2}+\boldsymbol{\varepsilon}-\mathbf{I}E^{I}\right]\vec{\Xi}_{I}=0 \tag{74}$$

Note that this equation looks like the adiabatic nuclear Schrödinger equation (equation(53)), with the exception that $-i\sum_{\alpha}\mathbf{I}\nabla_{\alpha}+\mathbf{P}^{\alpha}$ has replaced $-i\sum_{\alpha}\mathbf{I}\nabla_{\alpha}$ as the momentum operator. This form is called the *gauge-covariant momentum* [**32**] for reasons that will be made clear in the next section (*cf.* the momentum operator in the Dirac equation, equation (289) in Appendix B).

This simplification has not changed the difficult nature of the equations as $\mathbf{P}^{\alpha}$ still has off-diagonal derivative operators. A transformation is still necessary; however, with the $\mathbf{P}^{\alpha}$ identified in this form as the *gauge potential* [**32**](in electrodynamics the vector potential plays the same role), we can use the constructs of gauge theory to find that transformation.

Derivative Coupling Terms in Gauge Theory

By separating the wavefunction and Hamiltonian into nuclear and electronic parts, the Born-Oppenheimer approximation has set the stage for casting non-adiabatic chemistry in the language of gauge theory. The nuclear coordinates serve as an *external manifold*, which is a Hilbert space. At each point on the manifold there is an *internal space*, which is the space spanned by the electronic wavefunctions. Hence the point on the nuclear manifold parameterizes the electronic wavefunctions. Together, these spaces form a *fiber bundle*, for which the derivative coupling matrix serves as the gauge potential. If the internal-space basis did not change as a function of nuclear coordinates, the gauge potential would be everywhere zero, and the fiber bundle would be considered *trivial*. This is the algebraic equivalent of the complete Born-Oppenheimer approximation which considers those changes negligible. But, as the electronic wavefunctions do change with nuclear position, the fiber bundle is non-trivial, and the gauge potential serves as a *connection* that dictates how the internal space slowly rotates as a function of external coordinates. According to fiber bundle theory, the bundle at each point on the manifold is equivalent to any other, and they can be transformed one into the other by a *gauge transformation.* That is, although the electronic basis functions at different nuclear positions are not the same, they differ only by a unitary transformation, which will be the non-adiabatic transformation mentioned previously. By understanding the underlying theory of gauge potentials, we can see the utility of the derivative coupling terms in effecting that transformation.

Gauge-covariant derivative

In this section we introduce an alternative perspective on the gauge covariant derivative in equation (74). The total differential of the vector in equation (38),

$$d\vec{\Xi}_I = \begin{pmatrix} d\Xi_{I1} \\ d\Xi_{I2} \\ d\Xi_{I3} \\ \vdots \end{pmatrix} \tag{75}$$

produces a vector representing the change in the components of $\vec{\Xi}_I$; however, this is not the total *change* of $|\Psi_I\rangle$, as it does not account for a change in the basis [**32**]. The total change, represented by the total differential of the wavefunction, using equation(37), is

$$d|\Psi_I\rangle = \sum_i \left(d\Xi_{Ii} |\psi_i\rangle + \Xi_{Ii} |d\psi_i\rangle \right) \tag{76}$$

where the Ξ_I are the nuclear wave functions and the $|\psi_i\rangle$ are the electronic wavefunctions, and the total differentials are defined as

$$\begin{aligned} d|\Psi_I\rangle &\equiv \sum_{\alpha,k} \frac{\partial}{\partial R_{\alpha k}} |\Psi_I\rangle dR_{\alpha k} \\ d\Xi_{Ii} &\equiv \sum_{\alpha,k} \frac{\partial}{\partial R_{\alpha k}} \Xi_{Ii} dR_{\alpha k} \end{aligned} \tag{77}$$

The first term under the summation in equation (76) looks like a standard differential, i.e., it takes the differential of each component of the eigenvector as in equation (75). The second term, however, takes into account the change in the internal (electronic)

space due to a change in external (nuclear) space. To develop the meaning of $|d\psi_i\rangle$, consider that we effect a change in $|\psi_i\rangle$ via a unitary transformation:

$$\hat{U}|\psi_i\rangle = \sum_j c_j |\psi_j\rangle \tag{78}$$

Since the group of unitary transformations of degree n, $U(n)$, (which can be represented as the set of all $n \times n$ unitary matrices) is a compact Lie group, it can be expressed as the exponentiation of the underlying Lie algebra $u(n)$ [**33**]:

$$\hat{\mathbf{U}}\left(\theta_1(R), \theta_2(R), \ldots\right) = \prod_a \exp\left(\theta_a(R)\hat{\mathbf{X}}_a\right) \tag{79}$$

where the θ_γ are the parameters and the $\hat{\mathbf{X}}_a$ are the generators. An infinitesimal rotation of the wavefunction is effected by [**32**]

$$\hat{\mathbf{U}}\left(d\theta_1(R), d\theta_2(R), \ldots\right)|\psi_i\rangle = \prod_a \exp\left(d\theta_a(R)\hat{\mathbf{X}}_a\right)\ldots|\psi_i\rangle = |\psi_i\rangle + |d\psi_i\rangle \tag{80}$$

This can be shown by using the Taylor series expansion of exp and keeping only linear terms:

$$\hat{\mathbf{U}}\left(d\theta_1(R), d\theta_2(R), \ldots\right)|\psi_i\rangle = \left(\hat{\mathbf{I}} + \sum_a d\theta_a(R)\hat{\mathbf{X}}_a\right)|\psi_i\rangle = |\psi_i\rangle + |d\psi_i\rangle \tag{81}$$

This implies that

$$\left(\sum_a d\theta_a(R)\hat{\mathbf{X}}_a\right)|\psi_i\rangle = |d\psi_i\rangle \tag{82}$$

We can now substitute the left-hand side of this equation into equation (76):

$$
\begin{aligned}
d\,|\Psi_I\rangle &= \sum_i d\Xi_{Ii}\,|\psi_i\rangle + \sum_a d\theta_a(R)\hat{\mathbf{X}}_a \sum_i \Xi_{Ii}\,|\psi_i\rangle \\
&\rightarrow d\vec{\Xi}_I + \sum_a d\theta_a(R)\mathbf{X}_a\vec{\Xi}_I
\end{aligned}
\tag{83}
$$

where, in the second line, we have collected the coefficients into vectors and consider the matrix form of the generators. The second term has now become an operator simply multiplied by the original wavefunction. We recognize that the total differential of the eigenfunction $|\Psi_I\rangle$ is more than just the total differential of the vector components, and give it the symbol d':

$$
\begin{aligned}
d\,|\Psi_I\rangle &= \sum_i d\Xi_{Ii}\,|\psi_i\rangle + \sum_a d\theta_a(R)\hat{\mathbf{X}}_a \sum_i \Xi_{Ii}\,|\psi_i\rangle \rightarrow \\
d'\vec{\Xi}_I &= d\vec{\Xi}_I + \sum_a d\theta_a(R)\mathbf{X}_a\vec{\Xi}_I
\end{aligned}
\tag{84}
$$

where again in the second line we have moved from the abstract operator-ket form of the equation to the matrix-vector form. Since we can choose the nuclear coordinates to be independent of each other, the total derivatives are equal to their partial derivatives:

$$
\frac{\partial'}{\partial R_{\alpha k}}\vec{\Xi}_I = \frac{\partial}{\partial R_{\alpha k}}\vec{\Xi}_I + \sum_a \frac{\partial}{\partial R_{\alpha k}}\theta_a(R)\mathbf{X}_a\vec{\Xi}_I \tag{85}
$$

which we can collect into vector form:

$$
\mathbf{I}\nabla'_\alpha\vec{\Xi}_I = \mathbf{I}\nabla_\alpha\vec{\Xi}_I + \sum_a \nabla_\alpha\theta_a(R)\mathbf{X}_a\vec{\Xi}_I \tag{86}
$$

and rename

$$
\mathbf{P}^\alpha = \sum_a \nabla_\alpha\theta_a(R)\mathbf{X}_a \tag{87}
$$

to find the relationship

$$
\sum_\alpha \mathbf{I}\nabla'_\alpha\vec{\Xi}_I = \left(\sum_\alpha \mathbf{I}\nabla_\alpha + \mathbf{P}^\alpha\right)\vec{\Xi}_I\,; \tag{88}
$$

This is the *gauge-covariant gradient* as found in equation (74).

This derivation in gauge theory reveals several characteristics of the derivative coupling terms. First of all, it recognizes $\mathbf{P}^{\alpha}$ as the gauge potential. Specifically from equation (87), we see that the matrix of derivative coupling terms is the sum of the gradients of the rotation parameters multiplied by their respective generators. Thus the DCTs are directly connected to the rotations between electronic eigenfunctions at different points in nuclear space. Since unitary generators are antihermitian, this relationship shows that $\mathbf{P}^{\alpha}$ is antihermitian (or antisymmetric in the case of real wavefunctions) as well. Its antisymmetry implies that the diagonal elements, i.e. $\langle \psi_i | \nabla_{\alpha} \psi_i \rangle$, are zero, which further implies the gradient of a real wavefunction has no projection onto the wavefunction itself.

The non-adiabatic transformation

The purpose of our introduction to gauge theory was to find the non-adiabatic transformation to make equation (74) more easily solvable, i.e., to transform it into an equation in which $\mathbf{P}^{\alpha}$ is diagonal (since $\mathbf{P}^{\alpha}$ is antisymmetric, its diagonal form will actually be the zero matrix). We can use the form of $\mathbf{P}^{\alpha}$ in terms of rotations (equation (87)) to find that transformation. The transformation is position dependent, and will vary based on nuclear coordinates. For that reason it is categorized as a *local gauge transformation* [**27**]. The effect of applying this transformation everywhere on the nuclear manifold will be to align all the internal spaces; that is, it will remove the nuclear coordinate parameterization from the electronic wavefunctions. There will still be an

arbitrary but constant rotation common to all the functions, similar to the choice of a potential energy offset. Since this part of the transformation is common to the entire manifold, it is a *global gauge transformation* [**27**] and can be set arbitrarily.

Consider a global gauge transformation $\mathbf{U}^\dagger$ on the vector $\mathbf{I}\nabla_\alpha \vec{\Xi}_I(R)$ [**27**]:

$$\mathbf{U}^\dagger \mathbf{I}\nabla_\alpha \vec{\Xi}_I(R) = \mathbf{U}^\dagger \mathbf{I}\nabla_\alpha \left(\mathbf{U}\mathbf{U}^\dagger \vec{\Xi}_I(R)\right) = \mathbf{I}\nabla_\alpha \left(\tilde{\Xi}_I(R)\right) \tag{89}$$

where $\mathbf{U}^\dagger \vec{\Xi}_I(R) \equiv \tilde{\Xi}_I(R)$. The nature of the del operator has not changed, and so it is globally gauge invariant. Now consider a local gauge transformation, $\mathbf{U}^\dagger(R)$:

$$\begin{gathered}\mathbf{U}^\dagger(R)\mathbf{I}\nabla_\alpha \vec{\Xi}_I(R) = \mathbf{U}^\dagger(R)\mathbf{I}\nabla_\alpha \left(\mathbf{U}(R)\mathbf{U}^\dagger(R)\vec{\Xi}_I(R)\right) = \\ \mathbf{U}^\dagger(R)\mathbf{I}\nabla_\alpha \left(\mathbf{U}(R)\right)\tilde{\Xi}_I(R) + \mathbf{I}\nabla_\alpha \left(\tilde{\Xi}_I(R)\right)\end{gathered} \tag{90}$$

Note that $\mathbf{U}^\dagger(R)\left(\mathbf{I}\nabla_\alpha \vec{\Xi}_I(R)\right) \neq \mathbf{I}\nabla_\alpha \left(\tilde{\Xi}_I(R)\right)$, and so a gauge transformation changes the nature of the del operator, and hence the nature of the Schrödinger equation. Thus the bare del operator is not gauge-covariant. Now consider instead the transformation of the vector $\left(\mathbf{I}\nabla_\alpha + \mathbf{P}^\alpha(R)\right)\vec{\Xi}_I(R)$:

$$\begin{gathered}\mathbf{U}^\dagger(R)\left(\mathbf{I}\nabla_\alpha + \mathbf{P}^\alpha(R)\right)\vec{\Xi}_I(R) = \\ \mathbf{U}^\dagger(R)\mathbf{I}\nabla_\alpha \left(\mathbf{U}(R)\right)\tilde{\Xi}_I(R) + \mathbf{I}\nabla_\alpha \left(\tilde{\Xi}_I(R)\right) + \mathbf{U}^\dagger(R)\mathbf{P}^\alpha(R)\mathbf{U}(R)\left(\tilde{\Xi}_I(R)\right)\end{gathered} \tag{91}$$

If we define

$$\tilde{\mathbf{P}}^\alpha(R) \equiv \mathbf{U}^\dagger(R)\mathbf{P}^\alpha(R)\mathbf{U}(R) + \mathbf{U}^\dagger(R)\mathbf{I}\nabla_\alpha \left(\mathbf{U}(R)\right) \tag{92}$$

then we see that

$$\mathbf{U}^\dagger(R)\left(\mathbf{I}\nabla_\alpha + \mathbf{P}^\alpha(R)\right)\vec{\Xi}_I(R) = \left(\mathbf{I}\nabla_\alpha + \tilde{\mathbf{P}}^\alpha(R)\right)\tilde{\Xi}_I(R) \tag{93}$$

and the form of the gauge-covariant gradient operator is unchanged by the transformation. If we apply the above local gauge transformation to equation (74) we find

$$\left[-\sum_{\alpha}\frac{1}{2m_{\alpha}}\left(\mathbf{I}\nabla_{\alpha}+\tilde{\mathbf{P}}^{\alpha}\right)^{2}+\tilde{\boldsymbol{\varepsilon}}-\mathbf{I}E^{I}\right]\tilde{\Xi}_{I}=0 \tag{94}$$

and indeed, the nature of the equation has not changed. For these equations to be put into a form in which they are most easily solved, we require that $\tilde{\mathbf{P}}=\mathbf{0}$. From equation (92), this condition implies that

$$\mathbf{P}^{\alpha}\left(R\right)\mathbf{U}\left(R\right)=-\mathbf{I}\nabla_{\alpha}\left(\mathbf{U}\left(R\right)\right) \tag{95}$$

Combining this equation with the form of $\mathbf{P}$ from (87) leads to the equation

$$\sum_{\alpha,m'}\nabla_{\alpha}\theta'_{m'}\left(R\right)\mathbf{X}'_{m'}\mathbf{U}\left(R\right)=-\sum_{\alpha,m}\mathbf{I}\nabla_{\alpha}\left(\mathbf{U}\left(R\right)\right) \tag{96}$$

Since $\mathbf{U}\left(R\right)$ is unitary it can be expressed as a sum of exponentiated parameter-generator products [**34**],

$$\mathbf{U}\left(R\right)=\sum_{m}\exp\left[\theta_{m}\left(R\right)\mathbf{X}_{m}\right] \tag{97}$$

and equation (96) can be rewritten as

$$\sum_{\alpha,m'}\nabla_{\alpha}\theta'_{m'}\left(R\right)\mathbf{X}'_{m'}\sum_{m}\exp\left[\theta_{m}\left(R\right)\mathbf{X}_{m}\right]=-\sum_{\alpha,m}\mathbf{I}\nabla_{\alpha}\exp\left[\theta_{m}\left(R\right)\mathbf{X}_{m}\right] \tag{98}$$

If $\mathbf{P}^{\alpha}$ is calculated, the $\theta'_{m'}\left(R\right)$ are known parameters used to solve for the $\theta_{m}\left(R\right)$. The del operator on the right-hand side of the equation pulls out the derivatives of the arguments of the exponential function yielding

$$\sum_{\alpha,m'} \nabla_\alpha \theta'_{m'}(R)\mathbf{X}'_{m'} \sum_m \exp\left[\theta_m(R)\mathbf{X}_m\right] = -\sum_{\alpha,m} \nabla_\alpha \left[\theta_m(R)\right]\mathbf{X}_m \exp\left[\theta_m(R)\mathbf{X}_m\right]$$
$$\sum_{\alpha,m'} \nabla_\alpha \theta'_{m'}(R)\mathbf{X}'_{m'}\mathbf{U}(R) = -\sum_{\alpha,m} \nabla_\alpha \left[\theta_m(R)\right]\mathbf{X}_m\mathbf{U}(R) \tag{99}$$

While it is true that the set $\mathbf{X}'_{m'}$ and the set $\mathbf{X}''_m$ span the same space, they are not necessarily the same set, and hence we cannot conclude that the parameters θ'_m and θ''_m are the same for all m. In this case, there is no clear path to discover the parameters which will transform $\tilde{\mathbf{P}}^\alpha$ to $\mathbf{0}$, and an approximate method must be used [**27**]. The exception to this case is when only two surfaces are coupled, and hence only one generator and parameter are present,and we can indeed conclude that

$$\theta'' = -\theta' \tag{100}$$

is the condition for which the unitary gauge transformation will yield $\tilde{\mathbf{P}}^\alpha = \mathbf{0}$ for all α.

Consider the simple example of coupling a two-level system with only one nuclear coordinate. The DCT matrix is

$$\mathbf{P}(R) = \begin{pmatrix} 0 & \left\langle \psi_1 \middle| \frac{\partial}{\partial R} \psi_2 \right\rangle \\ -\left\langle \psi_1 \middle| \frac{\partial}{\partial R} \psi_2 \right\rangle & 0 \end{pmatrix} = -\left\langle \psi_1 \middle| \frac{\partial}{\partial R} \psi_2 \right\rangle \begin{pmatrix} 0 & -1 \\ 1 & 0 \end{pmatrix} \tag{101}$$

while the unitary transformation is

$$\mathbf{U}(R) = \mathbf{exp}\left[\theta(R)\begin{pmatrix} 0 & -1 \\ 1 & 0 \end{pmatrix}\right] \tag{102}$$

By equation (87), we know that $-\left\langle \psi_1 \middle| \frac{\partial}{\partial R} \psi_2 \right\rangle = \frac{\partial}{\partial R}\theta'$, and hence the correct parameter for the local gauge transformation satisfies the equation [**29**]

$$\theta(R_0) + \int_{R_0}^{R} dR \left\langle \psi_1 \middle| \frac{\partial}{\partial R} \psi_2 \right\rangle = \theta(R) \tag{103}$$

(R_0 is chosen arbitrarily, and determines the global gauge.) In this manner, the local gauge transformations can be determined on the nuclear manifold, leading to solvable equations of the form

$$\left[-\sum_{\alpha} \frac{1}{2m_\alpha} \mathbf{I}\nabla_\alpha^2 + \tilde{\boldsymbol{\varepsilon}} - \mathbf{I}E^I \right] \tilde{\Xi}_I = 0 \tag{104}$$

where $\mathbf{I}\nabla_\alpha^2$ and $\mathbf{I}E^I$ are diagonal, but $\tilde{\boldsymbol{\varepsilon}}$ is not. It is to this end that finding the derivative coupling terms, i.e. $\langle \psi_i | \nabla \psi_j \rangle$, is important.

Wavefunctions and the Graphical Unitary Group Approach

In order to perform a calculation of molecular energy properties, we must find a suitable representation of the Hamiltonian. Let us assume that a suitable set of one-electron molecular orbital basis functions (MOs) has been furnished by an established *Multi-Configuration Self Consistent Field* (MCSCF) procedure [**20**] [**35**]. From these MOs, we produce a basis of CSFs, which are antisymmetric many-electron functions, in which the electronic Hamiltonian and its wavefunctions will be represented. Our basis of choice, which is the one used in the COLUMBUS programs, is the *Gel'fand-Tsetlin basis* [**7**] [**8**] [**9**] [**10**] [**36**]. The procedure to build this basis is known as the *Unitary Group Approach* (UGA). This section will present the construction of the Gel'fand-Tsetlin basis via UGA, its value, and how it is implemented.

The Unitary Group

Irreducible Representation

Many of the characteristics of a group are discoverable in abstract or operator form; however, often it is necessary to use a matrix representation of the group to better understand its nature. For any given group there are several matrix representations. For example, the group SU(2) has a *defining representation* on 2×2 matrices, but has a *regular representation* in 3×3 matrices [**34**].

The most useful matrix representation we will encounter for our purposes will be the *irreducible representation*, or *irrep*. For a non-abelian group, not all elements commute and hence not all can be diagonal matrices in the same representation. The irreducible representation is the basis in which all group operators are block-diagonalized. While not as advantageous as a purely diagonal representation, the block-diagonal form does have the advantage of reducing the effort of $n\times n$ matrix diagonalizations to separate 1×1, 2×2, 3×3 etc. diagonalizations (*n.b.* these separate blocks are also called irreps [**37**]).

Building the CSF space

For a given molecular system, we assume a collection of N indistinguishable electrons and, for each, a vector space V of n orthonormal orbitals. The space in which such a system exists is the N^{th}-rank tensor product of V, $V^{\otimes N}$, which is n^N dimensional [**38**]. This is known as the *carrier space,* and is conceptualized in Figure 2. Given these two groups of objects, i.e. electrons and orbitals, there are two distinct

ways to enumerate our basis. In the first place, we could leave the orbitals fixed and permute the electrons among them. In the second place, we could leave the electrons fixed and rotate the orbitals around them. The latter method is the Unitary Group Approach, while the former is the *Symmetric Group Approach* (SGA) [**39**]. A discussion of the SGA, not as relevant to the path of this discussion, can be found in Appendix J.

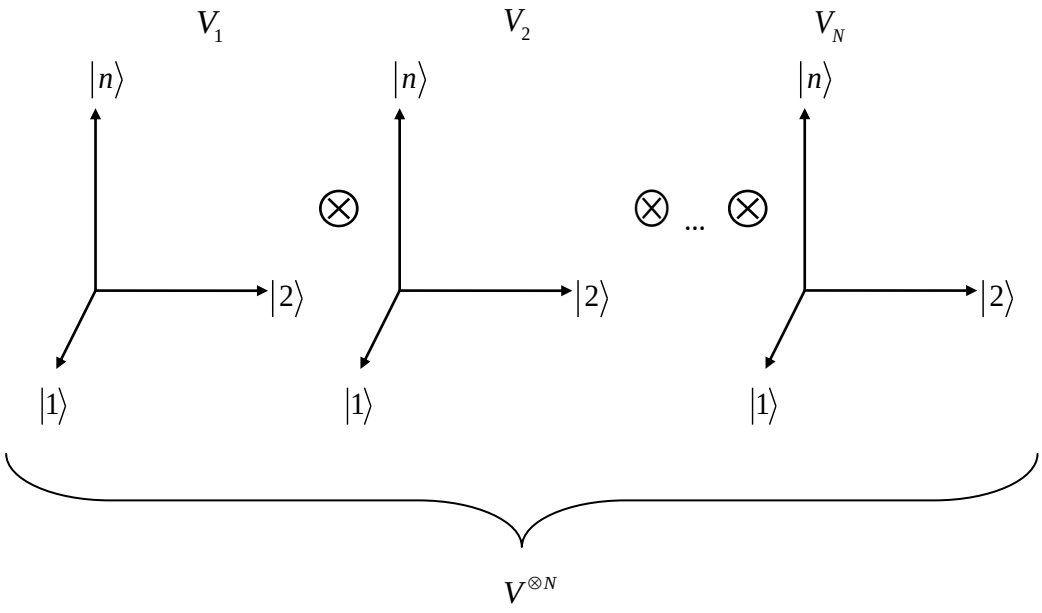

Figure 2. Visualization of carrier space of *N* electrons and *n* orbitals

Generators of the Unitary Group

The Unitary group is of particular importance to the field of Quantum Chemistry because of the manner in which the second-quantized Hamiltonian is constructed. The anticommutation relation [**40**] of the raising and lowering operators from definition (24)

$$\left\{\hat{a}^{\dagger}_{r\mu}, \hat{a}_{r\mu}\right\} \equiv \hat{a}^{\dagger}_{r\mu}\hat{a}_{r\mu} + \hat{a}_{r\mu}\hat{a}^{\dagger}_{r\mu} = \hat{1} \tag{105}$$

(see Appendix C) lead to the following commutation relation between the operators introduced in equation (30) [**34**]:

$$\begin{aligned}
\left[E_{rs}, E_{tu}\right] &= \left[\sum_{\mu'} a^{\dagger}_{r\mu'}a_{s\mu'}, \sum_{\mu} a^{\dagger}_{t\mu}a_{u\mu}\right] \\
&= \sum_{\mu'\mu}\left[a^{\dagger}_{r\mu'}a_{s\mu'}, a^{\dagger}_{t\mu}a_{u\mu}\right] = \sum_{\mu'\mu}\left(a^{\dagger}_{r\mu'}a_{s\mu'}a^{\dagger}_{t\mu}a_{u\mu} - a^{\dagger}_{t\mu}a_{u\mu}a^{\dagger}_{r\mu'}a_{s\mu'}\right) \\
&= \sum_{\mu'\mu}\left\{a^{\dagger}_{r\mu'}\left(\delta_{st}\delta_{\mu'\mu} - a^{\dagger}_{t\mu}a_{s\mu'}\right)a_{u\mu} - a^{\dagger}_{t\mu}\left(\delta_{ur}\delta_{\mu'\mu} - a^{\dagger}_{r\mu'}a_{u\mu}\right)a_{s\mu'}\right\} \\
&= \sum_{\mu'\mu}\left(a^{\dagger}_{r\mu'}a_{u\mu}\delta_{st}\delta_{\mu'\mu} - a^{\dagger}_{r\mu'}a^{\dagger}_{t\mu}a_{s\mu'}a_{u\mu} - a^{\dagger}_{t\mu}a_{s\mu'}\delta_{ur}\delta_{\mu'\mu} + a^{\dagger}_{t\mu}a^{\dagger}_{r\mu'}a_{u\mu}a_{s\mu'}\right) \\
&= E_{ru}\delta_{st} - E_{ts}\delta_{ur} + \sum_{\mu'\mu}\left(-a^{\dagger}_{r\mu'}a^{\dagger}_{t\mu}a_{s\mu'}a_{u\mu} + a^{\dagger}_{t\mu}a^{\dagger}_{r\mu'}a_{u\mu}a_{s\mu'}\right)
\end{aligned} \tag{106}$$

Since raising operators commute with each other, and lowering operators do as well, the terms left under the summation sum to zero, leaving

$$\left[E_{rs}, E_{tu}\right] = E_{ru}\delta_{st} - E_{ts}\delta_{ur} \tag{107}$$

We will show that these operators represent generators of the Unitary group.

Let $\mathbf{U}$ be an element of the group $\mathbf{U}(n)$ (the set of all $n \times n$ unitary matrices). Unitary matrices obey the bilinear condition

$$\mathbf{U}^{\dagger}\mathbf{U} = \mathbf{1} \tag{108}$$

If we let

$$\mathbf{U} = \exp(\mathbf{K}) \tag{109}$$

Then we have the condition from equation (108)

$$\exp(\mathbf{K})^{\dagger}\exp(\mathbf{K}) = \exp\left(\mathbf{K}^{\dagger}\right)\exp(\mathbf{K}) = \mathbf{1} \tag{110}$$

Since $\mathbf{U}$ and $\mathbf{U}^\dagger$ commute, so do $\mathbf{K}$ and $\mathbf{K}^\dagger$, and

$$\exp\left(\mathbf{K}^\dagger\right)\exp\left(\mathbf{K}\right)=\exp\left(\mathbf{K}+\mathbf{K}^\dagger\right) \tag{111}$$

which leads to the condition

$$\mathbf{U}^\dagger\mathbf{U}=\mathbf{1}\rightarrow\mathbf{K}+\mathbf{K}^\dagger=0 \tag{112}$$

Element-wise, this condition indicates that

$$\mathbf{K}_{ij}+\left(\mathbf{K}_{ji}\right)^*=0 \tag{113}$$

or that $\mathbf{K}$ is antihermitian. In the most general case $\mathbf{K}$ will be complex, and can be split into an antisymmetric real part and a symmetric imaginary part:

$$\mathbf{K}=\mathbf{A}+i\mathbf{S} \tag{114}$$

Without further restriction, this indicates $\frac{n^2-n}{2}$ parameters for $\mathbf{A}$ and $\frac{n^2+n}{2}$ parameters for $\mathbf{S}$, or a total of n^2 parameters for $\mathbf{K}$. This is the same number of parameters as $GL(n,R)$, the group of all $n\times n$ non-singular real matrices [**34**]. Consequently, the generators of $U\left(n\right)$ are linear combinations of the generators of $GL(n,R)$, and we can use either set of generators to construct $\mathbf{U}$. In the most general formulation, a unitary operator can be constructed from generators as

$$\mathbf{U}=\mathbf{exp}\left(\sum_{rs}\theta_{rs}\mathbf{E}_{rs}\right) \tag{115}$$

(*Cf*. equation (79); these formulations are *not* equivalent; that is, the same parameters used in either case will lead to different results. However, they are both equally valid.)

Since the argument of the exponent must be antihermitian, one of the following restrictions must apply:

1. The $\mathbf{E}_{rs}$ are antihermitian (i.e., generators of $U(n)$), while the θ_{rs} are unrestricted real
2. The $\mathbf{E}_{rs}$ are split into a set of symmetric and a set of antisymmetric matrices; the former take imaginary parameters and the latter take real parameters
3. The $\mathbf{E}_{rs}$ are unrestricted (i.e. generators of $GL(n,R)$) while $\theta_{rs} = -\theta_{sr}^{*}$

We shall choose to use the $GL(n,R)$ generators which are unrestricted; thus we will confine ourselves to condition 3. The generators E_{ij} of $GL(n,R)$ are sparse matrices with only one non-zero entry; specifically,

$$\left(E_{ij}\right)_{kl} = \delta_{ik}\delta_{jl} \tag{116}$$

(Consequently, the generators associated with $\mathbf{A}$ would have the form $E_{ij} - E_{ji}$ and those associated with $\mathbf{S}$ would have the form $E_{ij} + E_{ji}$.) For example, in matrix form, the generator $E_{2,3}$ would be

$$E_{2,3} = \begin{pmatrix} 0 & 0 & 0 & \cdots \\ 0 & 0 & 1 & \cdots \\ 0 & 0 & 0 & \cdots \\ \vdots & \vdots & \vdots & \ddots \end{pmatrix} \tag{117}$$

It is clear through matrix multiplication in this representation that

$$E_{ij}E_{kl} = E_{il}\delta_{ik} \tag{118}$$

and hence the generators obey the commutation relation

$$\left[E_{ij}, E_{kl}\right] = E_{il}\delta_{jk} - E_{jk}\delta_{il} \tag{119}$$

This is the exact commutation relation we saw in equation (106), and thus we see that the second-quantized Hamiltonian applied to a system with n orbitals is constructed from the generators of $U(n)$. This connection is why the unitary group will be so important in outlining a basis in which to express the Hamiltonian; that process is the UGA [**38**]. Note that the generators in equation (30) were summed over spin, and so the unitary generators do not distinguish spin-up from spin-down. We can also create the operators [**38**]

$$E_{\mu\nu} = \sum_{r}^{n} a_{r\mu}^{\dagger} a_{r\nu} \tag{120}$$

for functions of spin rather than for functions of electronic coordinate. They obey the same commutation relation; however, since μ and ν can be selected from two spin states, these operators correspond to the generators of $U(2)$. The complete space in which we represent the Hamiltonian for n orbitals is the direct product space of the spatial functions and the spin functions, $U(n) \otimes U(2)$, which is a subgroup of $U(2n)$.

Note that the spin index necessarily remains in the generators from which the spin-orbit Hamiltonian is constructed (see equations (29), (30)). The spin-orbit Hamiltonian is constructed out of generators from $U(2n)$, and the CSFs span an irrep of a subgroup of this space.

Young frames

Before discussing the representation of the unitary group, it is necessary to make a short aside to the subject of *Young frames*, which will provide a useful labeling

scheme. Every integer N can be partitioned a number of ways. For example, 3 can be partitioned into 3, 2+1, or 1+1+1. Table 1 enumerates the partitions of the first five integers. We can also use boxes to indicate the partitions, as shown in Figure 3. These box figures are called Young Frames [**39**]. To prevent redundancy when creating these frames, it is necessary to impose the rule that a row be equal to or shorter than the row above it, and each row be left-justified. Figure 4 is an example of a Young frame which is not allowed.

These frames were first used to label irreps of the symmetric group; however, because of their close connection, they can also be used to label the irreps of the unitary group, as the succeeding discussion will reveal.

Table 1. Partitions of Integers 1 through 5

1	2	3	4	5
1	2	3	4	5
	1+1	2+1	3+1	4+1
		1+1+1	2+2	3+2
			2+1+1	3+1+1
			1+1+1+1	2+2+1
				1+1+1+1+1

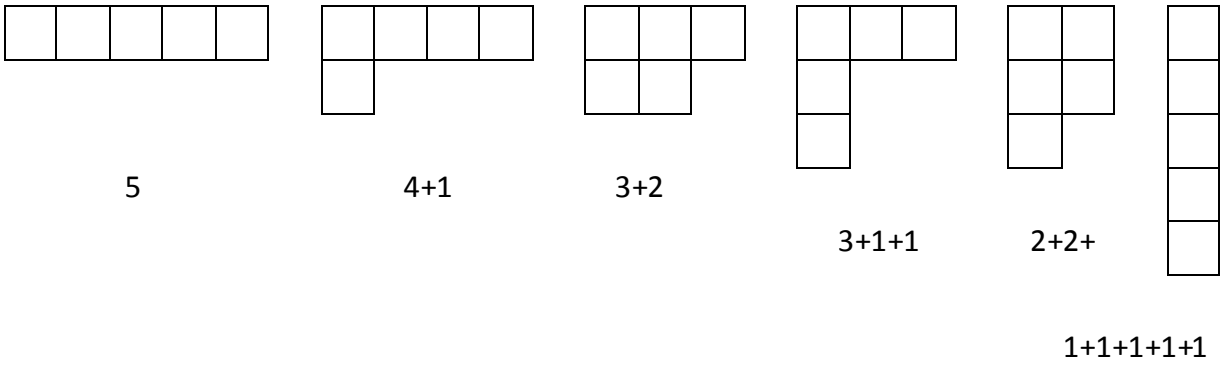

Figure 3. Young frames for partitions of 5

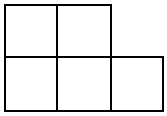

Figure 4. Illegal Young frame

Irreps of the unitary group

The group $U(n-1)$ is contained in $U(n)$, as each group contains the generators of the smaller groups. As an example, the generators of $U(2)$

$$\begin{pmatrix}1 & 0\\ 0 & 0\end{pmatrix},\begin{pmatrix}0 & 1\\ 0 & 0\end{pmatrix},\begin{pmatrix}0 & 0\\ 1 & 0\end{pmatrix},\begin{pmatrix}0 & 0\\ 0 & 1\end{pmatrix} \tag{121}$$

can be expressed in $U(3)$ as

$$\begin{pmatrix}1 & 0 & 0\\ 0 & 0 & 0\\ 0 & 0 & 1\end{pmatrix},\begin{pmatrix}0 & 1 & 0\\ 0 & 0 & 0\\ 0 & 0 & 1\end{pmatrix},\begin{pmatrix}0 & 0 & 0\\ 1 & 0 & 0\\ 0 & 0 & 1\end{pmatrix},\begin{pmatrix}0 & 0 & 0\\ 0 & 1 & 0\\ 0 & 0 & 1\end{pmatrix} \tag{122}$$

Thus we have the group subduction chain

$$U(1) \subset U(2) \subset U(3) \subset \ldots \subset U(n-1) \subset U(n) \tag{123}$$

It should be clear that *the unitary group* $U(\infty)$ contains all these, $\bigcup_n U(n)$.

Each unitary group $U(n)$ is a continuous group and will have uncountably infinite elements. Even though the *defining representation* [**34**] of the group $U(n)$ are the $n \times n$ matrices, it can be represented by infinitely large matrices with an infinite number of finite irreps, as it is a continuous but compact group [**38**]. The irreps of $U(n)$ can be labeled with Young frames of at most n rows [**38**]. Figure 5 shows the first few irreps of the unitary group and the subgroups.

The Gel'fand Tsetlin basis

Weyl tableaux

In the UGA we will use Weyl tableaux to label eigenfunctions [**38**], which are Young frames whose boxes are populated with tokens, (usually numbers, but it must be a set that has definite ordering), according to the following rules:

1. The number must be equal to or greater than the number to the left
2. The number must be strictly greater than the number above

In the UGA, the boxes will represent electrons and the numbers will represent orbitals (or spin states), thus mimicking the indistinguishability of the electrons. Since the numbers represent orbitals, it would seem this system allows an orbital to be assigned to more than two electrons, violating the exclusion principle; however, it will be revealed shortly that the principle of antisymmetry prohibits such Weyl tableaux.

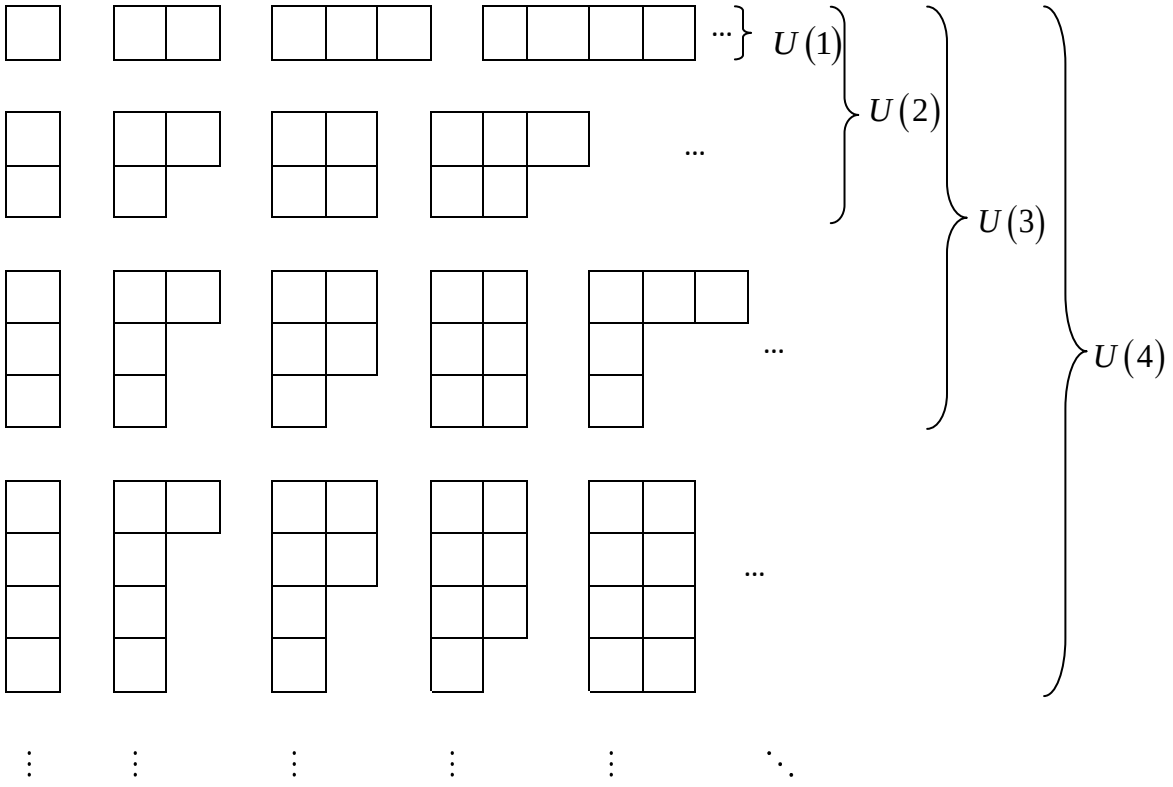

Figure 5. Young frame representation of the irreps of the Unitary Group

Spin States

As noted previously, the spin generators are those of $U(2)$; from Figure 5 it is clear that the spin irreps will only be represented by one- or two- row frames. Since there are only two spin states, spin-up and -down, there will also be only two tokens, 1 and 2, or α and β, to distribute among the boxes. Figure 6 shows as an example the possible spin states for a four- electron system. Note that each box in the top row represents adding spin 1/2 to the total, while each box in the bottom row subtracts spin 1/2. Thus the first column of Figure 6, the totally symmetric irrep, represents the $4\times\frac{1}{2}=2$ spin state or quintet; the second column represents the triplet, and the third

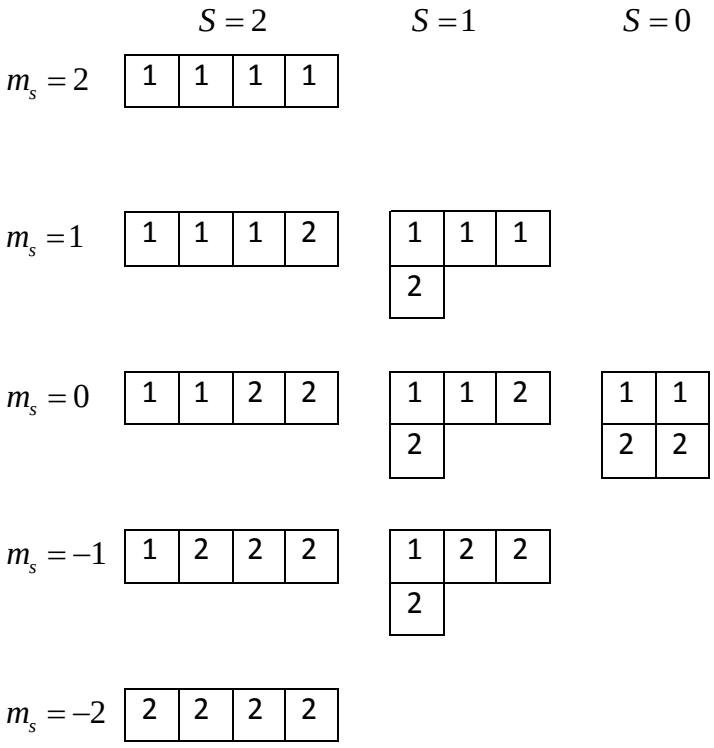

Figure 6. Four-electron spin states

represents the singlet. Within the framework of the total spin, the system can have a projection onto the z-axis from $+S$ to $-S$ in integer increments. The z spin component of a state can be calculated by adding 1/2 for each 1 and subtracting 1/2 for each 2, and so in Figure 6 we see the spin-structure we expect out of a four-electron system. Note that, since in a given Weyl tableau for $U(2)$ there are two rows and two numbers, any column with two rows must have a 1 in the top box and a 2 in the bottom. Thus the only variability in the m_s projection is within the single-box columns. For this reason, each multiplet does not have a unique frame; that is, any number of two-boxed columns could be added to the Young frame and the same multiplet would result. See Figure 7 for an example of various doublets. If we were only interested in spin states, we could

restrict ourselves to single-row irreps, which happen also to be the irreps of $SU(2)$ [**38**]; nevertheless, we will find the complete $U(2)$ irreps invaluable in choosing the correct irreps for the spatial state, as we will see shortly. Furthermore, we can use these irreps to label the nodes on the genealogical construction graph, Figure 8 (see also Appendix I). The genealogical construction graph shows the ways, given an N - electron spin function, to construct $N+1$-electron spin functions. A number of paths (always stepping to the right) can be taken from the origin to each node; each path represents a different way to couple angular momenta to get to the final state. While the Young frames label the nodes, they give no indication of the path taken to that node. Appendix J gives the relationship between paths and spin functions.

Figure 7. Different Young frames all representing doublets

Spatial States

Recall that the wavefunction should transform as a member of an irrep of a subgroup of $U(2n)$ since there are $2n$ total spin-orbitals. Further, if we restrict the total electronic wavefunction to be made up of antisymmetric tensor products of occupied spin-orbitals, it must reside completely in the totally antisymmetric irrep of $U(2n)$, which is represented by a single column of N boxes. We have, however,

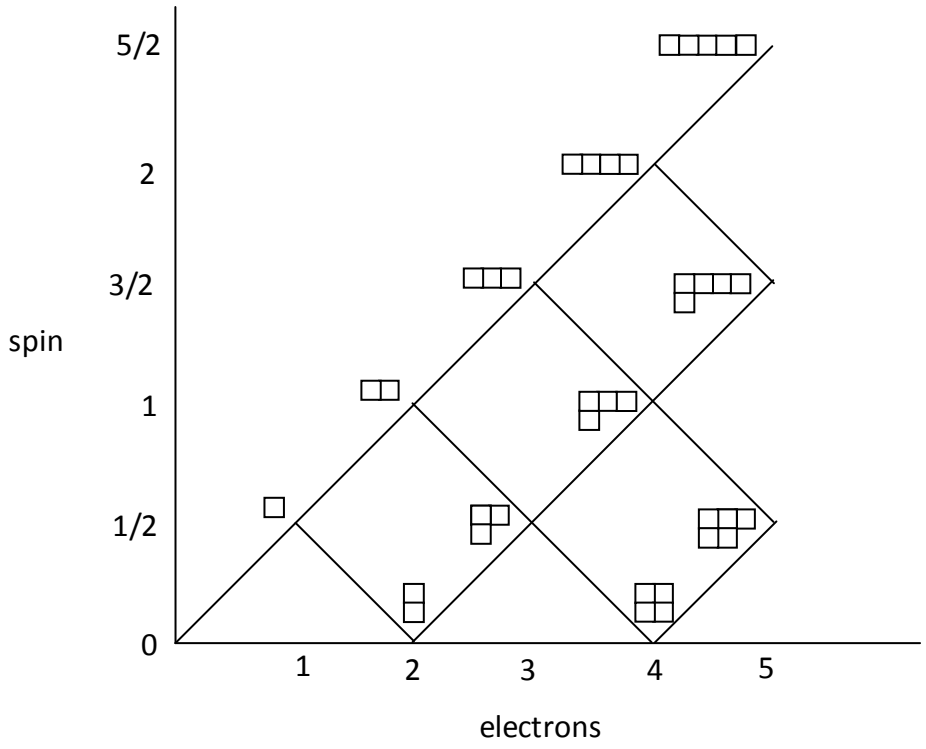

Figure 8. Tableaux-labeled genealogical spin construction graph [41**]**

restricted our calculations to the $U(n)\otimes U(2)$ subgroup (by restricting spin coupling), and so the irreps must be in the subduction chain from the antisymmetric irrep of $U(2n)$ to that group. This results in a spin-dependent Gel'fand-Tsetlin basis. This will only be the case when the spatial irrep and the spin irrep are *mutually conjugate* Young frames; that is, the frames interchange numbers of rows and columns [**38**]. Figure 9 shows an example of mutually conjugate Young frames that would result in a legitimate antisymmetric wavefunction. Since the spin irreps can have no more than two rows, this antisymmetry condition requires that the spatial irreps can have no more than two columns. This also means a number will appear no more than twice in the Weyl tableau

spatial irrep; that is, an orbital will be assigned to no more than two electrons. Since the spatial and spin Young frames must be mutually conjugate, the spatial Young frame gives the spin Young frame, and so it will be unnecessary to display both; the spatial frame will be sufficient. We will, however, lose the z-projection fo the spin, which will be important for constructing spin-orbit wavefunctions and calculating their properties. Fortunately, an alternative simple accounting system for m_s will be considered later.

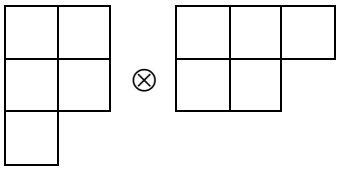

Figure 9. Mutually conjugate Young frames

An example: two electrons and two orbitals

To help solidify the meaning of the Weyl tableaux, a simple example is in order. Consider the case of two electrons in two orbitals. We will work in the subgroup $U(2)\otimes U(2)\subset U(4)$. The possible spin states are a singlet and a triplet:

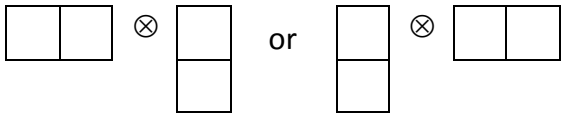

where we have retained the spin frames for illustration. For the singlet, the only Weyl tableau allowed is

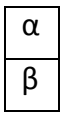

This tableau represents a totally antisymmetric spin state in which both electrons have been given different spins. This is the familiar function

$$\tfrac{1}{\sqrt{2}}\left[\alpha\beta-\beta\alpha\right] \tag{124}$$

where position indicates electron dependence (i.e., the first function in a product is of electron 1, the second is of electron 2, etc). For the triplet, there are three Weyl tableaux:

| α | α |

| α | β |

| β | β |

These tableaux represent totally symmetric spin states. The first, two spin-ups; the second, a mix; and the third, two spin-downs. These correspond to the spin functions

$$\begin{matrix}\alpha\alpha\\ \tfrac{1}{\sqrt{2}}\left[\alpha\beta+\beta\alpha\right]\\ \beta\beta\end{matrix} \tag{125}$$

Since there are only two orbitals, the spatial tableaux are the same as the spin tableaux, and represent analogous functions, but with orbitals rather than spin states. When paired, they result in the following states:

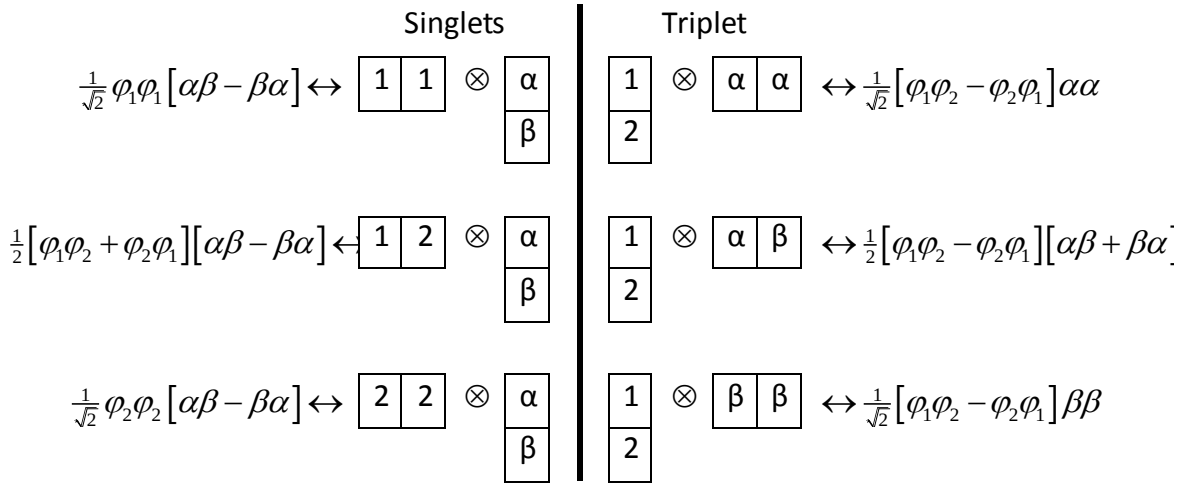

These are precisely the antisymmetric wavefunctions we expect to find for the 2-electron, 2-orbital system; thus these tableaux label a spin-adapted basis for the system.

In this example the antisymmetry was carried completely by either the spatial or the spin piece, with the other being symmetric. The general case is not this clean, as pairs of tableaux which contain neither single rows nor single columns are, on their own, neither symmetric nor antisymmetric, yet their product must be completely antisymmetric. As an example, a 3-electron, 2-orbital system has two doublets (i.e., two paths from the origin in Figure 8),

$$\begin{cases} \frac{1}{\sqrt{6}}\left[2\alpha\alpha\beta-\left(\alpha\beta\alpha+\beta\alpha\alpha\right)\right] \\ \frac{1}{\sqrt{6}}\left[\left(\alpha\beta\beta+\beta\alpha\beta\right)-2\beta\beta\alpha\right] \\ \frac{1}{\sqrt{2}}\left[\alpha\beta\alpha-\beta\alpha\alpha\right] \\ \frac{1}{\sqrt{2}}\left[\alpha\beta\beta-\beta\alpha\beta\right] \end{cases} \tag{126}$$

corresponding to the Weyl tableaux

α	α
β	

and

α	β
β	

none of which have definite parity. A product of such tableaux is not as simple as a product of a spatial and a spin determinant, but rather is a linear combination of determinants which is antisymmetric. Shavitt has developed a correspondence between the more complicated Weyl tableaux and Slater determinants; [**42**] may be consulted to see how to express CSFs in terms of Slater determinants.

The Subduction Chain

As stated previously in equation (123), each unitary group contains all unitary subgroups in the subgroup chain. Each Weyl tableau represents a unique subduction of an element of $U(n)$ to $U(1)$. The subduction of a tableau in $U(n)$ to $U(n-1)$ requires removing from the tableau any boxes assigned to the n^{th} orbital. Subsequent subduction to $U(n-2)$ would then remove any boxes assigned to the $(n-1)^{th}$ orbital, and so forth [**38**].

Consider the following Weyl tableau in a seven-electron, seven-orbital system,

2	3
3	4
5	5
6	

which is a doublet. The tableau resides in $U(7)$, which has tableaux of no more than seven rows. To subduce to $U(6)$, we must remove any boxes assigned to the seventh orbital. Since there are none, this tableau remains unchanged in $U(6)$. Following the prescription above, this tableau labels the subduction chain in Figure 10.

Paldus Tableaux

Each frame in the chain can be described by

1. the number of two-element rows (= a)
2. the number of one-element rows (= b)
3. the number of zero-element rows (= c)

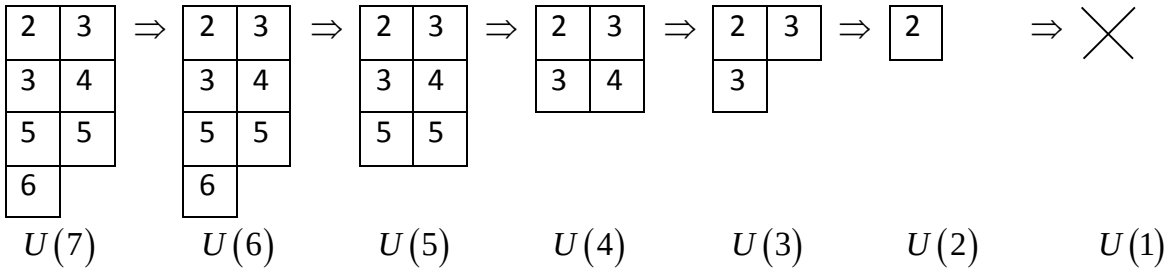

Figure 10. Subduction chain for an example doublet Weyl tableau where *N*=7, *n*=7

This last number is calculated to be the number of possible allowed rows in the subgroup (i.e., n rows for $U(n)$) minus the number or rows in the Young frame. Thus we can label the above subduction chain with the numbers a, b, and c in order of decreasing orbital number (see Table 2). The orbital number column can be discarded since it is the sum of a, b, and c, and we create the more simplified table, a *Paldus Tableau,* as shown in Figure 11 [**42**]. The Paldus Tableau is equivalent to the subduction chain of Figure 10, and is hence equivalent to the original Weyl Tableau.

Table 2. Subduction chain from Figure 10 in table form

Orbital	a	b	c
7	3	1	3
6	3	1	2
5	3	0	2
4	2	0	2
3	1	1	1
2	0	1	1
1	0	0	1
0	0	0	0

$$\begin{bmatrix} 3 & 1 & 3 \\ 3 & 1 & 2 \\ 3 & 0 & 2 \\ 2 & 0 & 2 \\ 1 & 1 & 1 \\ 0 & 1 & 1 \\ 0 & 0 & 1 \\ 0 & 0 & 0 \end{bmatrix}$$

Figure 11. Paldus Tableau corresponding to the subduction chain in Figure 10

Gel'fand Tableaux

Finally, we can alternatively label each frame in the subduction chain as a row of numbers whose length is equal to n. Starting from the left, we insert a 2 for every two-element row, followed by a 1 for every one-element row, ending with zeros. This is very closely related to the Paldus Tableau; for example, the top row of the Paldus Tableau in Figure 11, indicating three 2s, one 1, and three 0s, would have the form 2 2 2 1 0 0 0.

When each row is thus labled, the result is a *Gel'fand tableau*. The Gel'fand tableau in Figure 12 is equivalent to the Paldus tableau in Figure 11. Thus each Weyl, Paldus, or Gel'fand tableau represents a specific CSF. A Young frame, a Paldus tableau top row, or a Gel'fand tableau top row represents a family (or irrep) of CSFs for a system of n orbitals, N electrons, and a specific multiplet.

Ordering tableaux

All of the tableaux in this irrep can be ordered. Each tableau set has its specific ordering rules, but those for the Gel'fand tableau are most intuitive. The top row will be

$$\begin{bmatrix} 2 & 2 & 2 & 1 & 0 & 0 & 0 \\ & 2 & 2 & 2 & 1 & 0 & 0 \\ & & 2 & 2 & 2 & 0 & 0 \\ & & & 2 & 2 & 0 & 0 \\ & & & & 2 & 1 & 0 \\ & & & & & 1 & 0 \\ & & & & & & 0 \end{bmatrix}$$

Figure 12. Gel'fand tableau corresponding to the subduction chain in Figure 10

the same for the entire irrep. The elements of each subsequent row must follow the betweenness condition; that is, each must fall inclusively between the two elements situated in the row directly above it. The Gel'fand tableaux can be ordered according to the following rule: If tableau A and tableau B have the first k rows in coincidence, then the one with the greater number of 2s in the $(k+1)^{th}$ row is greater; if the number of 2s in the $(k+1)^{th}$ row is in coincidence, the one with the greater number of 1s in that row is the greater tableau. Figure 13 shows the order of the Gel'fand tableaux for the system of three orbitals and four electrons in a singlet, followed by the Paldus tableaux and Weyl Tableaux, including the subduction chain. They are labeled above lexically. The basis, thus ordered and spin adapted, is the *Gel'fand Tsetlin basis* [**38**]. This is the basis COLUMBUS uses to calculate the CI wavefunctions and the density matrices upon which analytic gradients and DCTs will be built, and shall be the basis we discuss in the remainder of this paper. In the next section, we will discuss how this basis is used in the graphical approach specifically used in COLUMBUS.

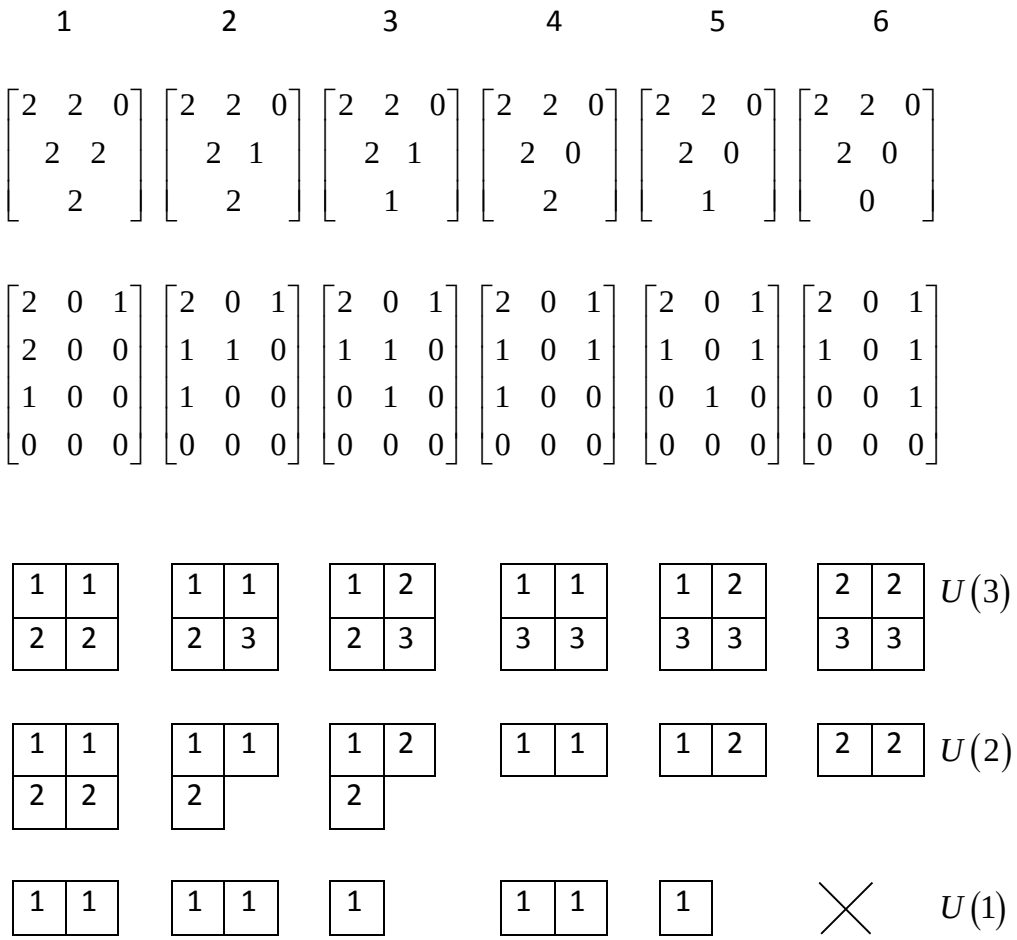

Figure 13. Gel'fand Tsetlin Basis for *N*=4, *n*=3, singlet

Distinct Row Tables

Each line in the Paldus tableau format, or each shape in the Weyl tableau format, in Figure 13 occurs often in an entire N-electron basis where $n >> N$. By taking advantage of these redundancies, we can greatly reduce the size of the displayed basis information [**43**]. The *Distinct Row Table* (DRT) contains only as many rows as there are *distinct* rows in the set of Paldus tableaux, with a fixed number of columns. For Figure 13, there are eight distinct rows; while there is not much savings in notation (and thus

disk space) at this level, the DRTs of larger bases of realistic problems are much smaller than their Paldus or Weyl tableaux counterparts. For example, a 30-orbital, 10-electron singlet system has over four million CSFs, but the DRT has only 511 rows [**43**]. Table 3 shows the DRT for the basis in Figure 13. The first column label, j, gives the index of the one-electron basis function, which is also the unitary subgroup to which the row belongs. The second column label, k, gives a unique index to each row. The next three column labels, a_k, b_k, and c_k, label the row itself using the Paldus step numbers (see Table 2).

The rest of the DRT essentially shows two sets of data: how each row is connected to the next, and how each row is lexically ordered with respect to others. To understand the first point, one must see that, in addition to removing an orbital, there

Table 3. DRT for three-orbital, four electron singlet basis

j	k	a_k	b_k	c_k	k_{0k}	k_{1k}	k_{2k}	k_{3k}	y_{1k}	y_{2k}	y_{3k}	x_k
3	1	2	0	1	2		3	4		1	3	6
2	2	2	0	0				5			0	1
	3	1	1	0		5		6	0	0	1	2
	4	1	0	1	5		6	7		1	2	3
1	5	1	0	0				8			0	1
	6	0	1	0		8			0	1	1	1
	7	0	0	1	8				1	1	1	1
0	8	0	0	0								1

are four possible electron-related actions, indexed by the step number d, to subduce one row to another:

1. Remove no electrons, spin remains the same ($d = 0$)
2. Remove an unpaired electron, spin goes down ($d = 1$)
3. Remove a paired electron, spin goes up ($d = 2$)
4. Remove a pair of electrons, spin remains the same ($d = 3$)

(Because only four such actions are available, a CSF can, in addition to the tableaux in Figure 13, be identified by the total spin and the order of these steps taken in the subduction chain. This will be useful in calculating elements of spin-orbit generators later on.) The next four columns of the DRT show to which row the given row subduces via one of the four subduction steps listed above. These indices are called the *downward-chaining indices* [**43**]. For example, row $k = 1$ subduces to row 2 via a $d = 0$ step; to row 3 via a $d = 2$ step; and to row 4 via a $d = 3$ step. A $d = 1$ step is not allowed from row 1, because it has no unpaired electrons. The final five columns are labeled by *counting indices.* The final column of the DRT gives the weight, labeled by x_k, and counts the number of distinct subtableaux that have that row at the top. The y indices, labeled by the step vector d, count the number of subductions that occur lexically before the given subduction. There is no column for y_{0k} since the $d = 0$ step always has the greatest weight. For example, row 1 subduces to row 2 via a $d = 0$ step in one tableau. Row 1 subduces to row 3 via a $d = 2$ step in two distinct Paldus subtableaux; they are still weighted lower than only one tableau, so y_{2k} also counts 1. Finally row 1

subduces to row 4 via a $d = 3$ step in three distinct tableaux, which are weighted lower than the previous three tableaux, and so receives a count of 3. This can be seen by comparing the DCT in Table 3 with the lexically ordered tableaux in Figure 13. Note that in this form of counting, a row which occurs in multiple Paldus tableaux but whose subduction chain is identical is only counted once. For example, the subduction $[1 \quad 0 \quad 0] \rightarrow [0 \quad 0 \quad 0]$ occurs in three different Paldus tableaux in Figure 13, but is only counted once in the DRT.

The Shavitt Graph

While the highly-ordered nature of the DRT is useful for programming, it is difficult to comprehend. The *Shavitt graph* is a compact, graphical representation of the DRT which is more useful for human-readability [**43**]. Figure 14 shows the Shavitt graph corresponding to Table 3. Each row is represented by its number in a circle. The rows

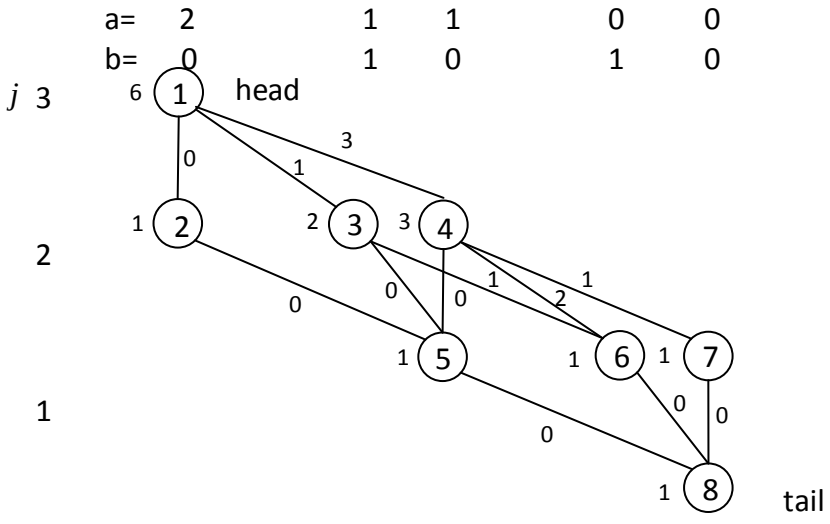

Figure 14. Shavitt graph *N*=4, *n*=3 singlet

k are distributed in a grid according to the values of j, a, and b. To the left of each circle is the x counting index. Each line or *arc* represents a valid subduction, labeled by its arc weight, which is the appropriate y index. The d index is represented by the slope of the arc. Each walk from tail (bottom) to head (top) represents one of the CSFs. Figure 15 highlights the six walks that represent the CSFs for the example basis. Each walk is assigned a weight by the sum of the arc weights it traverses; thus between a pair of walks, the higher weight (lower number) is assigned to the walk that begins with the left-most arc [**43**].

Representing the Non-Relativistic Hamiltonian Elements

Elements of the non-relativistic second-quantized Hamiltonian are calculated as

$$\langle \varphi_m | H | \varphi_n \rangle = \sum_{r,s} \langle \varphi_m | \hat{E}_{rs} | \varphi_n \rangle h_{rs} + \tfrac{1}{2} \sum_{r,s,t,u} \langle \varphi_m | \hat{e}_{rstu} | \varphi_n \rangle g_{rstu} \qquad (127)$$

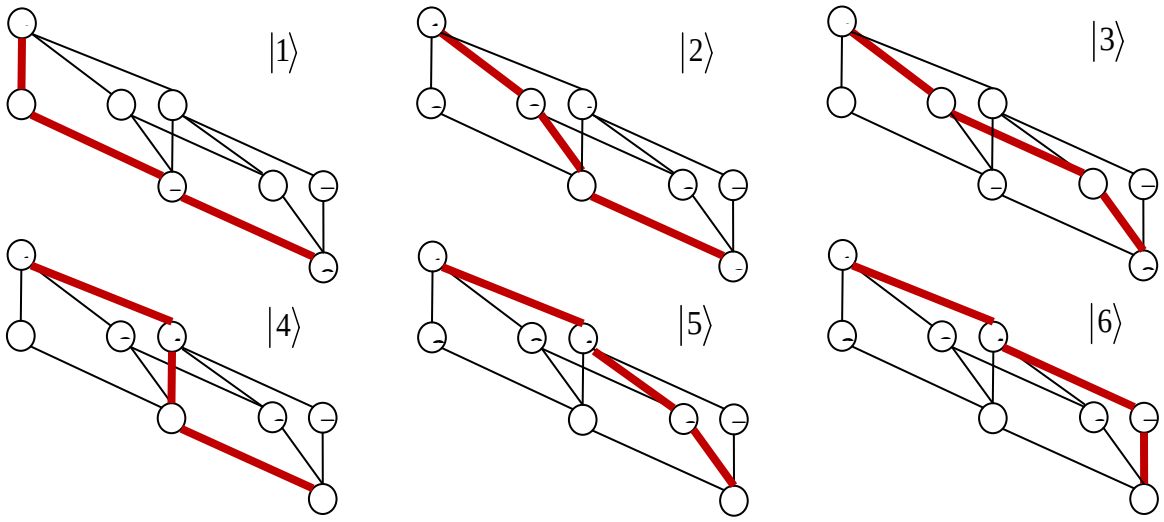

Figure 15. CSFs of *N*=4, *n*=3 singlet basis represented by walks

where the bra and ket are CSFs from the Gel'fand-Tsetlin basis. This formulation shows that the one-and two- electron integrals act as coefficients, and it is fundamentally the representation of the unitary group generators in the Gel'fand-Tsetlin basis we are calculating. The $\hat{E}_{ij}$ can be divided into three types of operators:

1. Diagonal or weight operators where $i = j$
2. Upper triangular or raising operators where $i > j$
3. Lower triangular or lowering operators where $i < j$

The CSFs are eigenvectors of the weight operators, with the relationship

$$\langle \varphi_m | \hat{E}_{ii} | \varphi_n \rangle = \delta_{mn} n_i \tag{128}$$

where n_i is the occupancy of the i^{th} orbital. The raising and lowering operators are adjoints of one another, so we will only consider raising operators here. There are several conditions which must be fulfilled so that the product $\langle \varphi_m | \hat{E}_{ij} | \varphi_n \rangle$ be non-zero; the equivalent of these on the Shavitt graph is that the two walks $|\varphi_m\rangle$ and $|\varphi_n\rangle$ must be joined from tail to the $i-1$ level and from the j^{th} level to the head [**43**]. Between these two levels, the walks form a loop, for which $|\varphi_n\rangle$ must always be to the right. Figure 16 shows an example of a non-zero loop value for the raising operator $\hat{E}_{21}$ in the example basis. The walks $|2\rangle$ (solid) and $|3\rangle$ (hashed) are joined at levels 0 and 2 with $|2\rangle$ on the left of the loop. Their common walk is represented by the dotted line.

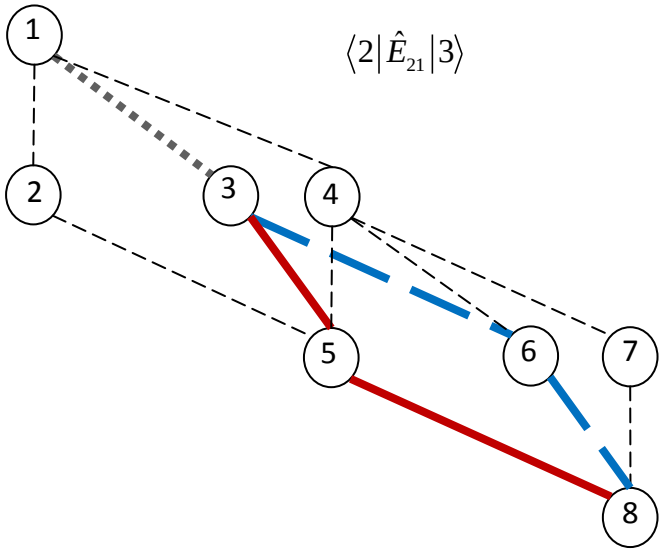

Figure 16. Example non-zero unitary generator element

To calculate the loop value, the loop is divided into segments. Each segment is a portion of the loop sitting between two j-indices, e.g., $[j-1, j]$, $[j, j+1]$,...$[i-1, i]$. A segment is given an index k which is equal to the top index on the Shavitt graph or the latter in the pair $[j,k]$. In the example in Figure 16, there are two sections, $[0,1]$ and $[1,2]$, shown explicitly in Figure 17. Figure 18 shows the seven different segment types, Q_k. Just like the generators, the segments can be classified as weight (W), raising (R), or lowering (L), and further identified as being unjoined (no overbar), joined at the top (overbar), or joined at the bottom (underbar). Again in these Figures, the bra is solid and the ket is hashed. Additionally, each segment can be identified by the step number of the bra and ket, $d_k^{'}$ and d_k, respectively, (where the primed quantity indicates the

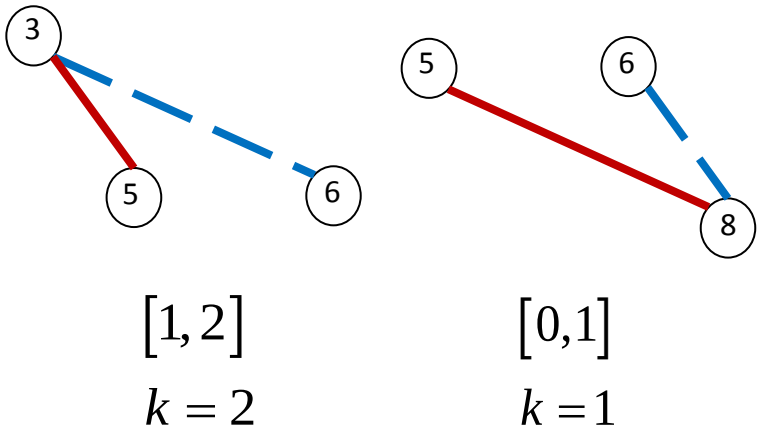

Figure 17. Segments of the loop in Figure 16

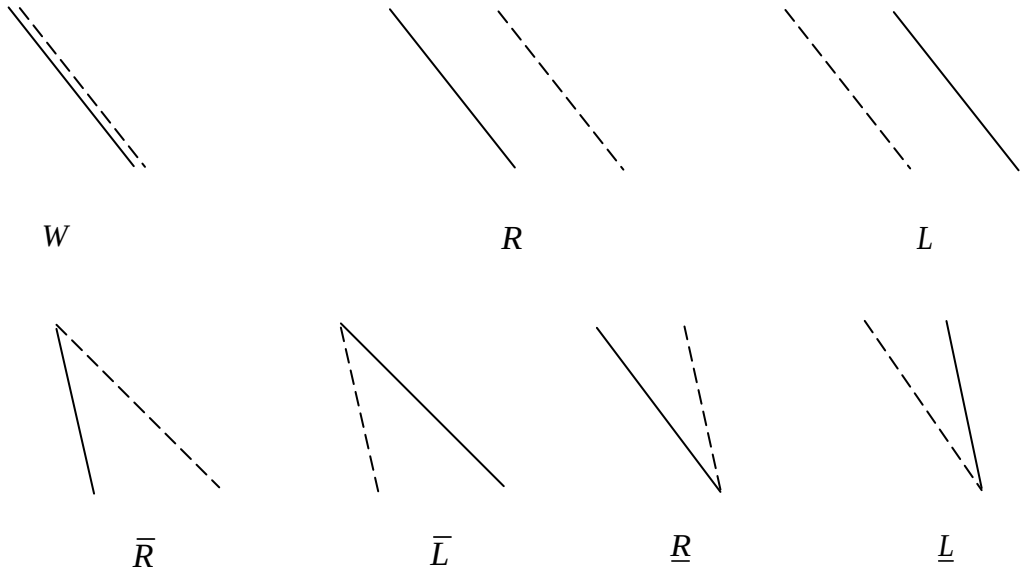

Figure 18. The different segment types, weight (W), raising (R), and lowering (L)

bra), and the values of b at the top of each segment, b_k' and b_k. As an alternative to this last requirement, we may specify the difference in the b_k values in addition to only

one of the b_k values; Shavitt chooses to specify b_k and define $\Delta b_k \equiv b_k - b'_k$ [**42**]. Segments with the same Q_k, d'_k, d_k, and Δb_k have congruent shapes; these parameters are collected into a single symbol

$$T_k \equiv \{Q_k; d'_k\, d_k; \Delta b_k\} \tag{129}$$

called the *segment shape symbol*. For example, the shape symbols for the segments in Figure 17 are

$$\begin{aligned} T_1 &= \{\underline{R}; 3, 1; 1\} \\ T_2 &= \{\overline{R}; 1, 3; 0\} \end{aligned} \tag{130}$$

The value of a segment, $W(T_k, b_k)$ is completely determined by its shape symbol and b_k. The matrix element of the unitary generator between the two CSFs is the product of these segment values:

$$\langle m' | \hat{E}_{ij} | m \rangle = \prod_{k=j}^{i} W(T_k, b_k) \tag{131}$$

The values of $W(T_k, b_k)$ are given in Table III of [**42**].

Matrix elements of generator products (e_{ijkl}) are calculated in a similar although more complicated manner [**42**].

The spin-orbit Hamiltonian elements

Adding the spin-orbit operator to the Hamiltonian does not perfectly fit into the above calculations for two reasons; first, the generators in that operator are not spin-free; and second, the Shavitt graphs require more than one total spin irrep. We shall present Yabushita's solution to the latter problem first [**11**].

Multi-spin Shavitt graph

When introducing spin-orbit coupling, our example system is incomplete; although it contains singlet CSFs, these could now couple with triplet or even higher CSFs, which must be included in the Shavitt graph. Figure 19 shows this graph, with exclusively triplet arcs and nodes marked with hashes (see Figure 14). Unlike the single-spin Shavitt graph, this graph now has two heads, one for each possible total spin. This means that Hamiltonian elements between CSFs of different spins will not create closed loops. In order to calculate coupling coefficients between CSFs of different spins, Yabushita devised a scheme [**11**] where an additional index is added to the top of the graph and the closed-loop formalism is used. This can be thought of as adding an additional artificial electron and orbital to the Shavitt Graph (see Figure 20), creating an irrep of $U(n+1)$ that will subduce to both the singlet and the triplet. In this example, the left and right hashed arcs in Figure 20 represent the subductions

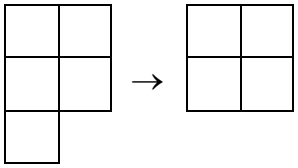

and

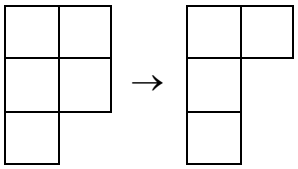

respectively.

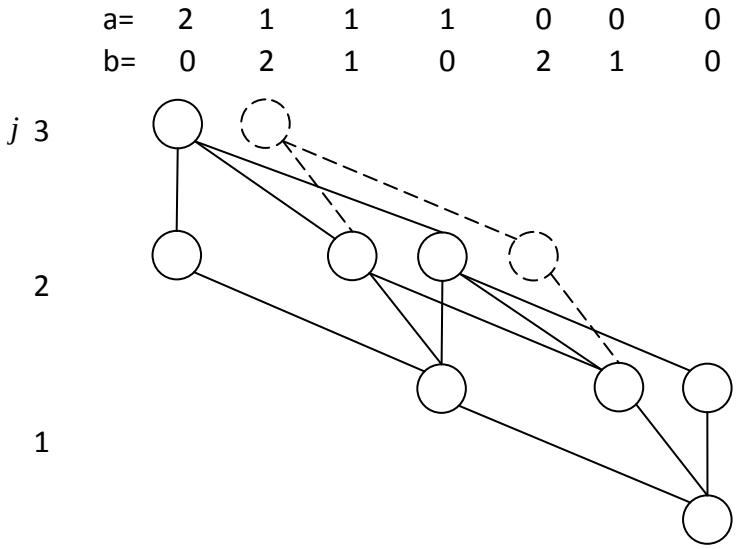

Figure 19. Mixed-Spin Shavitt graph for the *N*=4, *n*=3 singlet and triplet basis

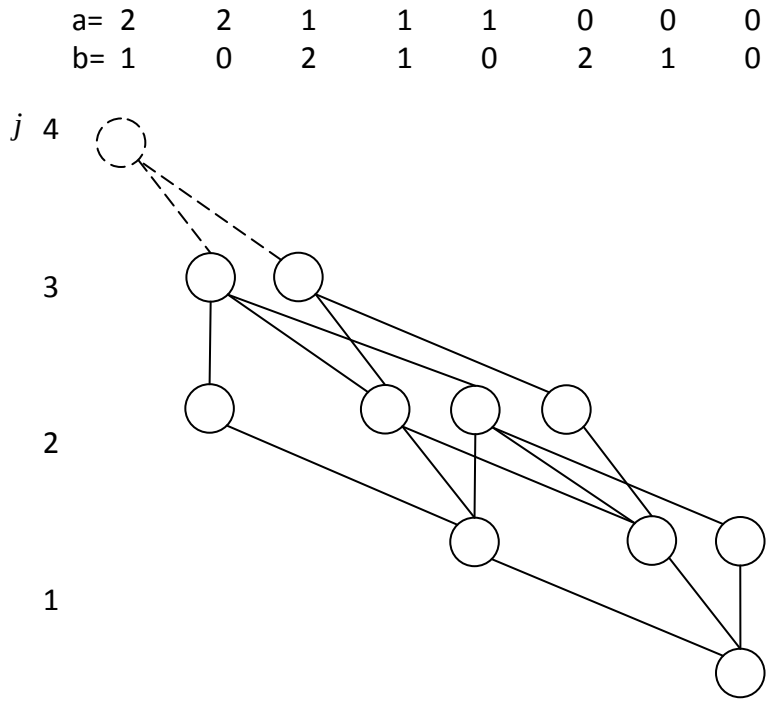

Figure 20. Mixed-spin Shavitt graph for the *N*=4, *n*=3 singlet and triplet basis with artificial U(n+1) head

Spin-orbit generators

Now that loops between CSFs of different spins are built, we can calculate the matrix elements of the generators. The spin-orbit generators defined in (30) are different from the spin-free generators used in the previous subsection; nevertheless, the spin-orbit generators can be expressed in terms of the spin-free generators [**44**]. To understand this process, we first note that each CSF is properly identified by its subduction steps ($\vec{d}$), total spin (s), and z-projection of spin (m_s). As mentioned previously, the subduction chain can be identified by the order of steps, d, taken. Thus we can identify a CSF by the ket

$$\left|\vec{d}\, S\, M\right\rangle \tag{132}$$

For example, the CSF $\left|1\right\rangle$ in Figure 13 may be represented by

$$\left|1\right\rangle \leftrightarrow \left|\vec{d} = \begin{pmatrix} 0 \\ 3 \\ 3 \end{pmatrix} S = 0\, M = 0\right\rangle \tag{133}$$

(since the example system is a singlet, the z-projection is necessarily zero. For non-zero spins, the physical, two-column Weyl tableaux do not specify that projection without their accompanying two-row spin Weyl tableaux). Thus the matrix element of the spin-orbit Hamiltonian is evaluated as

$$\left\langle \vec{d}\,'S'M'\left|\hat{H}_{so}\right|\vec{d}\, S\, M\right\rangle = \sum_{r,\mu,s,\nu} \left\langle \vec{d}\,'S'M'\left|\hat{E}_{r\mu s\nu}\right|\vec{d}\, S\, M\right\rangle h^{so}_{r\mu s\nu} \tag{134}$$

(see equations (19) and (31)). Let us define

$$\vec{q}(i) \equiv -\frac{1}{2c^2}\sum_{\alpha}\frac{Z_\alpha}{r_{i\alpha}^3}\vec{L}_{i\alpha} \tag{135}$$

(where i is the coordinate of the i^{th} electron), so that

$$h^{so}(i) = \vec{\sigma}(\omega_i)\cdot\vec{q}(i) \tag{136}$$

(where ω_i is the spin coordinate of the i^{th} electron), even though in the actual implementation the matrix elements are replaced by spin-orbit potential matrix elements [**45**]. Since we know that $\vec{q}(i)$ is a three-component vector, we can also cast it as a rank-one spherical tensor by defining [**11**] [**46**]

$$\begin{aligned} q_1(i) &= -\sqrt{\tfrac{1}{2}}\left(q_x(i) + iq_y(i)\right) \\ q_0(i) &= q_z(i) \\ q_1(i) &= \sqrt{\tfrac{1}{2}}\left(q_x(i) - iq_y(i)\right) \end{aligned} \tag{137}$$

(we can treat $\vec{\sigma}_i$ equivalently), whereby the spin-orbit operator can be recast as

$$h^{so}(i) = \sum_{\gamma}(-1)^{\gamma} q_{-\gamma}(i)\sigma_{\gamma}(\omega_i) \tag{138}$$

Thus

$$\begin{aligned} h^{so}_{r\mu s\nu} &= \langle r(i)\mu(\omega_i)|h^{so}(i)|s(i)\nu(\omega_i)\rangle \\ &= \langle r(i)\mu(\omega_i)|\sum_{\gamma}(-1)^{\gamma} q_{-\gamma}(i)\sigma_{\gamma}(\omega_i)|s(i)\nu(\omega_i)\rangle \\ &= \sum_{\gamma}(-1)^{\gamma}\langle r|q_{-\gamma}|s\rangle\langle\mu|\sigma_{\gamma}|\nu\rangle \end{aligned} \tag{139}$$

and equation (134) becomes

$$\begin{aligned}\left\langle \vec{d}\,'S'M'\middle|\hat{H}_{so}\middle|\vec{d}\,SM\right\rangle &= \sum_{r,\mu,s,\nu}\left\langle \vec{d}\,'S'M'\middle|\hat{E}_{r\mu s\nu}\middle|\vec{d}\,SM\right\rangle \sum_{\gamma}(-1)^{\gamma}\langle r\,|\,q_{-\gamma}\,|\,s\rangle\langle\mu\,|\,\sigma_{\gamma}\,|\,\nu\rangle \\ &= \sum_{r,s,\gamma}(-1)^{\gamma}\langle r\,|\,q_{-\gamma}\,|\,s\rangle\left\langle \vec{d}\,'S'M'\middle|\sum_{\mu,\nu}\hat{E}_{r\mu s\nu}\langle\mu\,|\,\sigma_{\gamma}\,|\,\nu\rangle\middle|\vec{d}\,SM\right\rangle \\ &= \sum_{r,s,\gamma}(-1)^{\gamma}\langle r\,|\,q_{-\gamma}\,|\,s\rangle\left\langle \vec{d}\,'S'M'\middle|\hat{Z}_{\gamma}(r,s)\middle|\vec{d}\,SM\right\rangle\end{aligned} \tag{140}$$

where we have defined

$$\hat{Z}_{\gamma}(r,s)\equiv\sum_{\mu,\nu}\hat{E}_{r\mu s\nu}\langle\mu\,|\,\sigma_{\gamma}\,|\,\nu\rangle \tag{141}$$

which is itself a rank-one spherical tensor. By the Wigner-Eckart theorem (see Appendix I), the integration of that tensor can be cast as a product of separate geometric and dynamic pieces [**46**]:

$$\left\langle \vec{d}\,'S'M'\middle|\hat{Z}_{\gamma}(r,s)\middle|\vec{d}\,SM\right\rangle=(-1)^{S'-M'}\begin{pmatrix}S' & 1 & S\\ -M' & \gamma & M\end{pmatrix}\left\langle \vec{d}\,'S'\|\,Z(i,j)\,\|\,\vec{d}\,S\right\rangle \tag{142}$$

where

$$\begin{pmatrix}S' & 1 & S\\ -M' & \gamma & M\end{pmatrix} \tag{143}$$

is the Wigner 3-J symbol [**46**], another incarnation of the Clebsch-Gordan coefficients discussed in Appendix I, and $\left\langle \vec{d}\,'S'\|\,Z(i,j)\,\|\,\vec{d}\,S\right\rangle$ is known as the *reduced matrix element* [**46**]. The spin-orbit Hamiltonian can be expressed as

$$\left\langle \vec{d}\,'S'M'\middle|\hat{H}_{so}\middle|\vec{d}\,SM\right\rangle=\sum_{r,s,\gamma}(-1)^{S'-M'+\gamma}\langle r\,|\,q_{-\gamma}\,|\,s\rangle\begin{pmatrix}S' & 1 & S\\ -M' & \gamma & M\end{pmatrix}\left\langle \vec{d}\,'S'\|\,Z(i,j)\,\|\,\vec{d}\,S\right\rangle \tag{144}$$

For this element to be non-zero, $\vec{d}\,'$must be obtained from $\vec{d}$ by substituting orbital r for orbital s in $\vec{d}$; further, $\gamma=M'-M$ must be satisfied [**11**]; thus the summation is dropped:

$$\left\langle \vec{d}\,'S'M' \middle| \hat{H}_{so} \middle| \vec{d}\,SM \right\rangle = (-1)^{S'-M} \langle r \,|\, q_{M-M'} \,|\, s \rangle \begin{pmatrix} S' & 1 & S \\ -M' & M'-M & M \end{pmatrix} \left\langle \vec{d}\,'S' \| Z(i,j) \| \vec{d}\,S \right\rangle \quad (145)$$

Drake and Schlesinger [**44**] show that the reduced matrix element $\left\langle \vec{d}\,'S' \| Z(i,j) \| \vec{d}\,S \right\rangle$ can be expressed as

$$\left\langle \vec{d}\,'S' \| Z(i,j) \| \vec{d}\,S \right\rangle = (-1)^{S_{N+1}+S-1/2} \frac{1}{\sqrt{6}} \begin{Bmatrix} S' & S & 1 \\ \frac{1}{2} & \frac{1}{2} & S_{N+1} \end{Bmatrix}^{-1} \left\langle \vec{d}\,'_{N+1} S_{N+1} M_{N+1} \middle| \hat{E}_{n+1,j} \hat{E}_{i,n+1} + \tfrac{1}{2} \hat{E}_{ij} \middle| \vec{d}_{N+1} S_{N+1} M_{N+1} \right\rangle \quad (146)$$

where $N+1$ is the index of the *extra* orbital, $n+1$ is the index of the *extra* electron, and

$$\begin{Bmatrix} S' & S & 1 \\ \frac{1}{2} & \frac{1}{2} & S_{N+1} \end{Bmatrix} \quad (147)$$

is the Wigner 6-j symbol [**46**]. Thus we see that the generators are now spin-free at the expense of adding an orbital and an electron to the system.

Now we proceed to simplify the matrix elements of the spin-orbit Hamiltonian (equations (144) and (146)). Since CSFs can couple through the spin-orbit operator only if their total spins differ by 0 or ± 1, there are only three scenarios for S_{N+1}:

1. it is a half integer above the spins of equal-spin CSFs,
2. it is a half integer below the spins of equal-spin CSFs
3. it is the average value of the spins of CSFs of different spins.

For example, when coupling two doublets, S_{N+1} could be a triplet (scenario 1), or a singlet (scenario 2); when coupling a singlet to a triplet, S_{N+1} must be a doublet (scenario 3). Given these three scenarios, the coefficient and 6-j symbol in equation (146) take on only one of three possible values [**11**]:

1. $$-\sqrt{\frac{(S+1)(2S+1)}{S}}$$

2. $$\sqrt{\frac{S(2S+1)}{S+1}} \qquad (148)$$

3. $$\sqrt{S+1}$$

(where S is the total spin of the ket) respectively pertaining to the above scenarios. (In scenario 3 it is assumed that $S' = S+1$). Yabushita et al. [**11**] define

$$\begin{aligned}\left(F_{ij}\right)_{N+1} &\equiv \left\langle \vec{d}\,'_{N+1}\, S_{N+1}\, M_{N+1} \middle| \hat{E}_{n+1,j}\hat{E}_{i,n+1} + \tfrac{1}{2}\hat{E}_{ij} \middle| \vec{d}_{N+1}\, S_{N+1}\, M_{N+1} \right\rangle \\ &= \left\langle \vec{d}\,'_{N+1}\, S_{N+1}\, M_{N+1} \middle| \hat{e}_{i,n+1,n+1,j} + \tfrac{1}{2}\hat{E}_{ij} \middle| \vec{d}_{N+1}\, S_{N+1}\, M_{N+1} \right\rangle \end{aligned} \qquad (149)$$

Just as in the previous subsection, these matrix elements will be the product of segment values. The quantity $\left(F_{ij}\right)_{N+1}$ can then be expressed as the product

$$\left(F_{ij}\right)_{N+1} = \left(F_{ij}\right)_{N} W\left(T_{N+1}, b_{N+1}\right) \qquad (150)$$

The segment $k = N+1$ can take on only three symbols, pertaining to the above three scenarios:

1. $$T_{N+1} = \{W;1,1;0\}$$

2. $$T_{N+1} = \{W;2,2;0\} \qquad (151)$$

3. $$T_{N+1} = \{\overline{RL};1,2;0\}$$

which have corresponding segment values [**11**]

1. $$W\left(T_{N+1}, b_{N+1}\right) = -\sqrt{\frac{S}{2(S+1)}}$$

2. $$W\left(T_{N+1}, b_{N+1}\right) = \sqrt{\frac{S+1}{2S}} \qquad (152)$$

3. $$W\left(T_{N+1}, b_{N+1}\right) = 1$$

Thus the reduced matrix element $\left\langle \vec{d}\,'S' \| Z(i,j) \| \vec{d}\,S \right\rangle$ can be simplified in each scenario by considering the product of $\left(F_{ij}\right)_N$ with the appropriate quantity from equations (148) and from equations (152). Considering that for scenarios 1 and 2 $S = S'$ and for scenario 3 $S+1 = S'$, all three scenarios result in the same product:

$$\left\langle \vec{d}\,'S' \| Z(i,j) \| \vec{d}\,S \right\rangle = \sqrt{\frac{S'+S+1}{2}} \left(F_{ij}\right)_N \qquad (153)$$

In turn, the elements of the spin-orbit Hamiltonian are

$$\left\langle \vec{d}\,'S'M' \middle| \hat{H}_{so} \middle| \vec{d}\,SM \right\rangle = (-1)^{S'-M} \langle r \,|\, q_{M-M'} \,|\, s \rangle \begin{pmatrix} S' & 1 & S \\ -M' & M'-M & M \end{pmatrix} \sqrt{\frac{S'+S+1}{2}} \left(F_{ij}\right)_N \qquad (154)$$

Note that all references to the additional orbital and electron have been removed from this form of the spin-orbit Hamiltonian matrix. This method of calculating spin-orbit generators will be crucial in calculating the spin-orbit DCTs.

The real spin-orbit Hamiltonian

Molecular systems with even numbers of electrons can always be crafted to result in a real Hamiltonian [**11**]. Systems of odd numbers of electrons with point symmetry greater than D_2 or C_{2v} will also have a real Hamiltonian [**47**]; however, odd-electron systems with less than this level of symmetry will have a necessarily complex

Hamiltonian. Yabushita has implemented a technique which adds a non-interacting electron to such systems so the Hamiltonian will be real, albeit twice the dimension [**11**]. The advantage of such a system is that the arithmetic involved in diagonalizing a real Hamiltonian is less computationally costly than the arithmetic for a complex Hamiltonian, despite its larger size. This technique also fits well into the already-established real arithmetic of the COLUMBUS MRCI programs [**7**] [**8**] [**9**] [**10**]. The disadvantage of the extra-electron technique is that there are now twice as many states as expected, and half of them must be eliminated as they do not represent true states. Kedziora has proposed that in a future iteration of COLUMBUS, the extra-electron technique be abandoned in favor of a smaller, complex Hamiltonian with the correct number of eigenvalues and eigenvectors [**48**].

III. Formalism

Normally, energy eigenvalues and wavefunctions are calculated point-wise in the nuclear manifold, which would lend calculation of gradients and DCTs to a finite difference method; however, finite difference methods are less accurate than analytic methods, especially when automated [**49**]. Shepard has introduced a method to evaluate energy gradients of CI wavefunctions analytically [**3**]. These energy gradients can be expressed in terms of atom-centered basis functions and geometry-dependent coefficients; however, due to Shepard's method, derivatives need only be calculated explicitly for the original atom-centered basis functions, which are known analytically. Lischka et al. have adapted this method to calculate DCTs analytically [**5**], which is the method used in COLUMBUS. We shall outline these methods here, including the modifications necessary to accommodate the spin-orbit Hamiltonian.

Analytic Spin-Orbit Gradients

Constructing the Solution Wavefunctions

Constructing the orthogonal, geometry-dependent basis

Under the Born-Oppenheimer approximation, one normally chooses a point R_0 in the nuclear manifold and constructs an orthonormal electronic basis suited to it. At another point on the manifold, $R = R_0 + \delta$, the basis at R_0 is scrapped and a new basis is created. There is no explicit analytic connection between these two bases. Evaluation of the nuclear gradient on electronic functions requires knowledge of the bases at R_0

and R in the limit that $\delta \to 0$. To this end, it behooves us to construct a single geometry-dependent basis, rather than a distinct basis for every point. It is important to keep in mind that, although this basis will be constructed to apply to points on the manifold within a δ neighborhood of R_0, because of the limiting process, *it will never actually be evaluated at any point except* R_0. This fact will aid us in the construction and use of the basis.

In the following derivation by Shepard [**3**], we will pass through many bases. We will use bracketed superscripts to keep track. $[\chi]$ will indicate the atomic, non-orthogonal basis; $[C]$ will indicate the basis that is geometry-dependent and orthonormal at the reference geometry, but non-orthogonal elsewhere; and $[S]$ will indicate a basis which is geometry-dependent and everywhere orthonormal. Other bases will be notated as they are introduced.

For a given geometry R_0, we have a set of normal but non-orthogonal atom-centered one-electron functions $\left|\chi_\mu(R_0)\right\rangle$. Through an MCSCF step [**35**], an orthonormal set of molecular orbitals $\left|\phi_i(R_0)\right\rangle$ is constructed, with the relationship

$$\vec{\phi}(R_0) = \mathbf{C}(R_0)\,\vec{\chi}(R_0) \tag{155}$$

where

$$\vec{\chi}(R_0) \leftrightarrow \begin{pmatrix} \langle \chi_1(R_0)| \\ \langle \chi_2(R_0)| \\ \langle \chi_3(R_0)| \\ \vdots \end{pmatrix} \tag{156}$$

Let us now create a geometry-dependent basis in a similar manner:

$$\vec{\phi}^{[C]}(R) = \mathbf{C}(R_0)\vec{\chi}(R) \tag{157}$$

where the atomic orbitals are allowed to vary with geometry, but the coefficient matrix is not reevaluated at every point. Such a basis is, however, only orthogonal at R_0. To remedy this shortcoming, let us define the overlap matrix $\mathbf{S}^{[\chi]}$, such that

$$\mathbf{S}^{[\chi]}(R) = \vec{\chi}(R) \otimes \vec{\chi}^{\dagger}(R) \tag{158}$$

In the $[C]$ basis,

$$\mathbf{S}^{[C]} = \mathbf{C}(R_0)\mathbf{S}^{[\chi]}\mathbf{C}^{\dagger}(R_0) = \mathbf{C}(R_0)\vec{\chi}(R) \otimes \vec{\chi}^{\dagger}(R)\mathbf{C}^{\dagger}(R_0) = \vec{\phi}^{[C]}(R) \otimes \vec{\phi}^{[C]\dagger}(R) \tag{159}$$

Note that at R_0, $\mathbf{S}^{[C]}(R_0) = \mathbf{I}$. At every other geometry R, there exists a transformation $\mathbf{S}^{[C]-1/2}(R)$ such that

$$\mathbf{S}^{[C]-1/2}(R)\mathbf{S}^{[C]}(R)\mathbf{S}^{[C]-1/2}(R) = \mathbf{I} \tag{160}$$

This square root matrix can be defined by the expansion [**3**]

$$\mathbf{S}^{[C]-1/2}(R) = \mathbf{I} - \tfrac{1}{2}\left(\mathbf{S}^{[C]}(R) - \mathbf{I}\right) + \tfrac{3}{8}\left(\mathbf{S}^{[C]}(R) - \mathbf{I}\right)^2 - \ldots \tag{161}$$

which evaluates to $\mathbf{I}$ at R_0. Also, the derivative of the above expression evaluated at the reference geometry (which will soon be needed) evaluates to

$$\left.\frac{d}{dR}\mathbf{S}^{[C]^{-1/2}}(R)\right|_{R_0} = \frac{d}{dR}\mathbf{I} - \tfrac{1}{2}\left(\left.\frac{d}{dR}\mathbf{S}^{[C]}(R)\right|_{R_0} - \frac{d}{dR}\mathbf{I}\right)$$
$$+\tfrac{3}{4}\left(\mathbf{S}^{[C]}(R_0)-\mathbf{I}\right)\left(\left.\frac{d}{dR}S^{[C]}(R)\right|_{R_0} - \frac{d}{dR}\mathbf{I}\right)-\ldots \qquad (162)$$
$$= -\tfrac{1}{2}\frac{d}{dR}\mathbf{S}^{[C]}(R_0)$$

where the third and higher terms in the expansion evaluate to zero as $\mathbf{S}^{[C]}(R_0)=\mathbf{I}$.

With this transformation matrix, we can now construct the basis

$$\vec{\phi}^{[S]}(R) = \mathbf{S}^{[C]^{-1/2}}(R)\vec{\phi}^{[C]}(R) \qquad (163)$$

which is orthonormal at all geometries R.

Constructing a solution away from the reference geometry

We have created an orthonormal one-electron basis; however, the actual wave functions will be represented in the CSF space spanned by the Gel'fand-Tsetlin basis. Consider the following highly contrived yet didactic example. Suppose we are interested in a system of six electrons with four orbitals in a singlet configuration. Then there are 10 CSFs in the full-CI space, represented by the Weyl Tableaux in Figure 21. Recall that we construct the Gel'fand-Tsetlin basis with a set of spatial orbitals from a

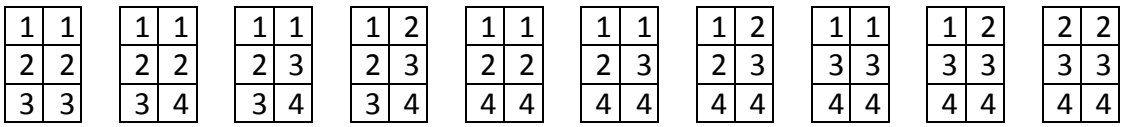

Figure 21. Gel'fand-Tsetlin basis for *N*=6, *n*=4 singlet

prior MCSCF step. Suppose in the MCSCF step, we want to leave the first and second orbitals doubly occupied. Then we are restricted to the MCCSF space of $\left|1\left(R_0\right)\right\rangle \otimes \left|2\left(R_0\right)\right\rangle \otimes \left|5\left(R_0\right)\right\rangle$, since they are the only CSFs in which this occurs. Assume that we already have the MCSCF solution at R_0. Let $\left|mc\left(R_0\right)\right\rangle$ be an eigenfunction of $\mathbf{H}\left(R_0\right)$. Figure 22 visualizes this eigenfunction in three-dimensional CSF-space.

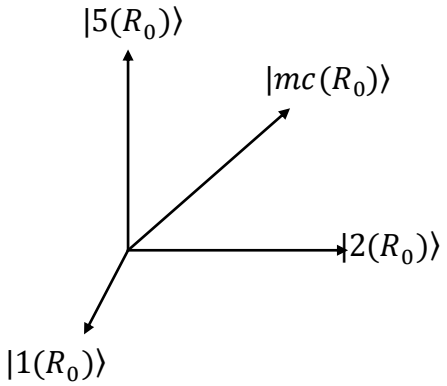

Figure 22. MCSCF solution vector projection in 3D CSF-space

Now let $\left|\psi\left(R\right)\right\rangle$ be an eigenfunction of $\mathbf{H}\left(R\right)$, which is confined to the space $\left|1\left(R\right)\right\rangle \otimes \left|2\left(R\right)\right\rangle \otimes \left|5\left(R\right)\right\rangle$. Since both of these functions are normal, they can be transformed one into the other by a unitary transformation:

$$\left|\psi\left(R\right)\right\rangle = \exp\left(\hat{A}\left(R\right)\right)\left|mc\left(R_0\right)\right\rangle \tag{164}$$

where $\hat{A}$ is the antihermitian product of parameters and unitary generators

$$\hat{A}(R) = \sum_{r<s} a_{rs}(R)\left(\hat{E}_{rs} - \hat{E}_{sr}\right) \tag{165}$$

These two wavefunctions are represented as coefficient vectors in a CSF space. They differ in two important ways: first, their CSF expansion coefficients are different; and second, the CSFs themselves differ as each set is composed of MOs that have resulted from a geometry-dependent optimization of energy. The unitary transformation $\exp\left(\hat{A}(R)\right)$ encompasses both of these differences, and so we can split it into two separate transformation operators: one that is a rotation of the CSF expansion coefficients, and one that is a rotation (and optimization) of the CSFs which make up the basis,

$$\left|\psi^{[K]}(R)\right\rangle = \exp\left(\hat{K}(R)\right)\exp\left(\hat{P}(R)\right)\left|mc^{[S]}(R_0)\right\rangle \tag{166}$$

where the coefficient rotation $\exp\left(\hat{P}(R)\right)$ acts on the function first, followed by the CSF rotation. Here we introduce the $[K]$ basis, which is geometry-dependent. Figure 23 shows an example of these two rotations.

A short discussion of essential and redundant orbital optimization is now relevant. The MCSCF step rotates the orbitals, which consequently rotate the CSFs. This procedure improves the solution to a subsequent (non-full) CI calculation. The MCSCF rotations can be partitioned into two sets: essential and redundant. Essential rotations are those that result in a lower eigenvalue in the MCSCF step, while redundant rotations have no effect on that eigenvalue after a reoptimization of the MCSCF CSF coefficients.

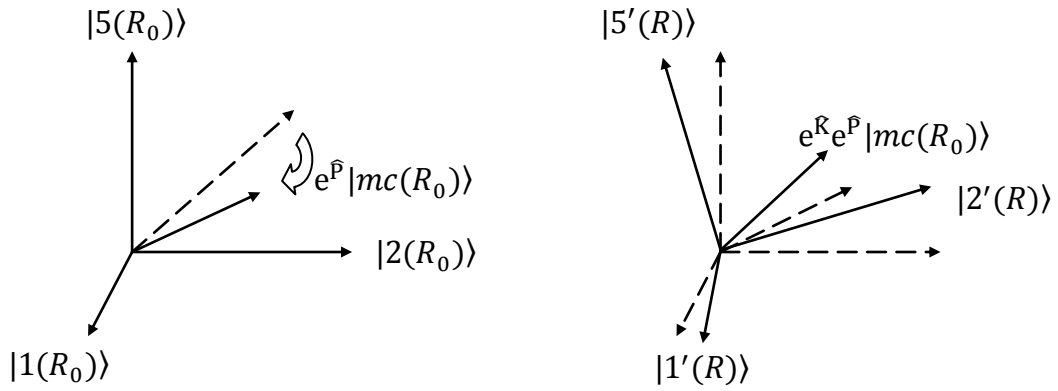

Figure 23. (Left) Rotation of a vector via CSF expansion coefficients; (Right) Rotation of a vector by rotating the CSFs

Redundant rotations take place in *invariant orbital subspaces.* The subsequent CI step will also rotate CSFs, but only via coefficients—not the orbitals. It too will have a partition of essential and redundant rotations. If the MCSCF invariant space is contained in the CI invariant space, any set of MCSCF invariant rotations will have no effect upon the CI eigenvalue; however, if some component of the MCSCF invariant space lies outside the CI invariant space, seemingly arbitrary rotations in the MCSCF step will produce different energies in the CI step. For this reason, an additional transformation, $\exp\left(\hat{Z}\left(R\right)\right)$, known as *orbital resolution* is required to ensure the CI energies are well-defined, and thus there is a well-defined limiting process to obtain the derivatives. Let us continue the example to see how this transformation affects the solution wavefunction.

Since we have left orbitals 1 and 2 doubly occupied in this example, the orbital subspace spanned by those orbitals is invariant. (For further discussion of invariant

subspaces, see [**3**].) We can, therefore, arbitrarily rotate orbitals 1 and 2 by the unitary operator $\exp\left(\hat{Z}(R)\right)$ in the invariant subspace and the CSFs will still span the same CSF space (see Figure 24). That is, a solution vector in the basis on the left side of Figure 24 can be expressed in the basis on the right by a rotation of the CSF expansion coefficients, $\exp\left(-\hat{Z}(R)\right)$, that exactly offsets the rotation of the CSFs in the invariant space (see Figure 25). Thus we have

$$\begin{aligned}\left|\psi^{[Z]}(R)\right\rangle &= \exp\left(\hat{Z}(R)\right)\exp\left(-\hat{Z}(R)\right)\left|\psi^{[K]}(R)\right\rangle \\ &= \exp\left(\hat{K}(R)\right)\exp\left(\hat{Z}(R)\right)\left[\exp\left(-\hat{Z}(R)\right)\exp\left(\hat{P}(R)\right)\right]\left|mc^{[S]}(R_0)\right\rangle \\ &= \exp\left(\hat{K}(R)\right)\exp\left(\hat{Z}(R)\right)\exp\left(\hat{P}(R)\right)\left|mc^{[S]}(R_0)\right\rangle\end{aligned} \quad (167)$$

where $\exp\left(-\hat{Z}(R)\right)$ as been rolled into $\exp\left(\hat{P}(R)\right)$, as they are both rotations of coefficients only. The two vectors, while physically the same, have distinct

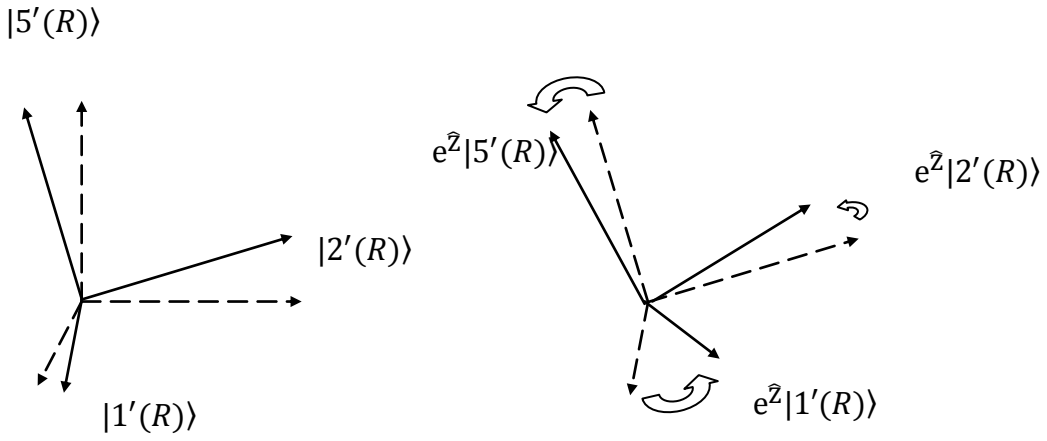

Figure 24. (Left) the MCSCF optimal CSFs; (Right) An arbitrary rotation in the invariant space leads to an equivalent optimal set of CSFs, where the energy is the same as the previously optimized energy

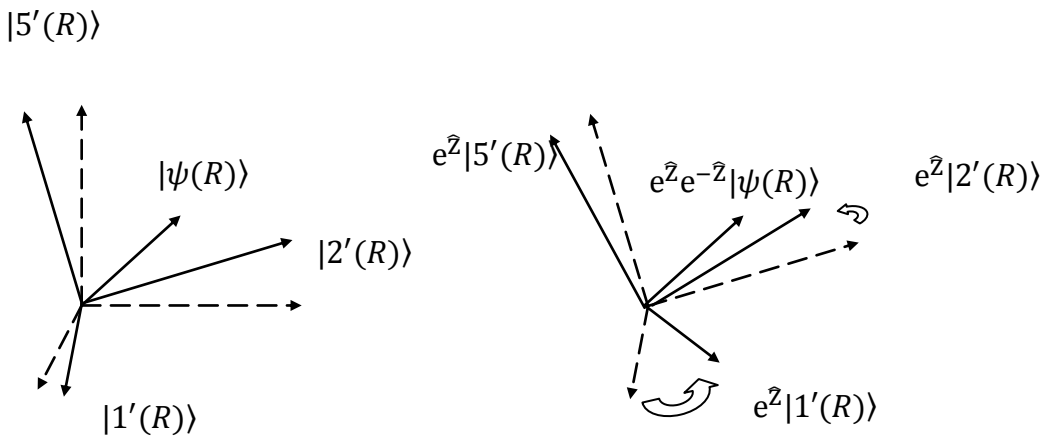

Figure 25. Different representations of the same vector due to a redundant rotation

representations. For this reason, we have introduced the $[Z]$, or *resolved basis*, as our final one.

Now suppose that, for our CI step, we relax the double occupancy restriction of orbital 2, but we keep orbital 1 doubly occupied and require at least one electron to be in

orbital 3 at all times. The CI space is $|1'(R)\rangle\otimes|2'(R)\rangle\otimes|3'(R)\rangle\otimes|6'(R)\rangle\otimes|8'(R)\rangle$. The CI solution will not contain the MCSCF solution at R because $|5'(R)\rangle$ is absent, but it will contain the projection onto the $|1'(R)\rangle\otimes|2'(R)\rangle$ space, which we explicitly highlight:

$$\begin{aligned}|CI(R)\rangle = &\left[\exp\left(\hat{Z}(R)\right)|1'(R)\rangle\langle 1'(R)|\exp\left(-\hat{Z}(R)\right)\right]|CI(R)\rangle \\ &+\left[\exp\left(\hat{Z}(R)\right)|2'(R)\rangle\langle 2'(R)|\exp\left(-\hat{Z}(R)\right)\right]|CI(R)\rangle \\ &+\sum_{m\notin MCSCF}|m(R)\rangle\langle m(R)|CI(R)\rangle\end{aligned} \tag{168}$$

Unless $\langle 5'(R)|\exp(\hat{Z}(R))|CI(R)\rangle = 0$, the eigenvalue will not be minimal, and will depend on the operator $\hat{K}$ chosen. Thus, while $\hat{Z}$ is redundant in the MCSCF step, it must be chosen such that $\langle 5'(R)|\exp(\hat{Z}(R))|CI(R)\rangle = 0$ in order to minimize the CI energy.

Given the correct orbital resolution, the CI solution vector at R can be expressed not only as a rotation of the MCSCF solution at R_0, but as a rotation of the CI solution vector at R_0 as well. Thus the CI solution at R can be expressed as

$$\left|\psi_{CI}^{[Z]}(R)\right\rangle = \exp\left(\hat{K}(R)\right)\exp\left(\hat{Z}(R)\right)\exp\left(\hat{P}(R)\right)\left|\psi_{CI}^{[S]}(R_0)\right\rangle \tag{169}$$

All of the nuclear geometry dependence has now been removed from the wave function and resides in the optimization operators.

The Analytic Gradient

We can now use the CI solution wavefunctions at an arbitrary nuclear geometry to construct the analytic gradient. The CI solution vectors, which are vectors of CSF expansion coefficients, satisfy the (electronic) matrix Schrödinger equation

$$\mathbf{H}(R)\vec{c}^{\,I}(R) = \varepsilon^{I}(R)\vec{c}^{\,I}(R) \tag{170}$$

where ε^I is the eigenvalue of the CI wavefunction ψ_I, represented here by a vector of coefficients in the CSF space, $\vec{c}^{\,I}$. In this case, $\mathbf{H}$ is the electronic Hamiltonian matrix which includes both non-relativistic and fine-structure contibutions, including the spin-orbit Hamiltonian (see equation (12)):

$$\mathbf{H}(R) = \mathbf{H}_0(R) + \mathbf{H}_{so}(R) \tag{171}$$

We can take the derivative of the Schrödinger equation and left-multiply it by $\vec{c}^{\,J}$:

$$\vec{c}^{\,J}(R)\frac{\partial}{\partial R_x}\left(\mathbf{H}(R)\vec{c}^{\,I}(R)\right)=\vec{c}^{\,J}(R)\frac{\partial}{\partial R_x}\left(\varepsilon^I(R)\vec{c}^{\,I}(R)\right). \tag{172}$$

Applying the chain rule to both sides,

$$\begin{aligned}\vec{c}^{\,J}(R)\frac{\partial}{\partial R_x}\left(\mathbf{H}(R)\right)\vec{c}^{\,I}(R)+\varepsilon^J(R)\vec{c}^{\,J}(R)\frac{\partial}{\partial R_x}\left(\vec{c}^{\,I}(R)\right)=\\ \frac{\partial}{\partial R_x}\left(E^I\right)\vec{c}^{\,J}(R)\vec{c}^{\,I}(R)+\varepsilon^I(R)\vec{c}^{\,J}(R)\frac{\partial}{\partial R_x}\left(\vec{c}^{\,I}(R)\right)\end{aligned} \tag{173}$$

The first term on the right-hand side is the delta function $\vec{c}^{\,J}(R)\vec{c}^{\,I}(R)=\delta_{JI}$, yielding

$$\begin{aligned}\vec{c}^{\,J}(R)\frac{\partial}{\partial R_x}\left(\mathbf{H}(R)\right)\vec{c}^{\,I}(R)+\varepsilon^J(R)\vec{c}^{\,J}(R)\frac{\partial}{\partial R_x}\left(\vec{c}^{\,I}(R)\right)=\\ \frac{\partial}{\partial R_x}\left(\varepsilon^I\right)\delta_{JI}+\varepsilon^I(R)\vec{c}^{\,J}(R)\frac{\partial}{\partial R_x}\left(\vec{c}^{\,I}(R)\right)\end{aligned} \tag{174}$$

For the gradient, we will assume that $I=J$; later we will make the alternate assumption for the DCTs. We can now isolate the energy gradient,

$$\begin{aligned}\frac{\partial}{\partial R_x}\left(\varepsilon^J(R)\right)&=\vec{c}^{\,J}(R)\frac{\partial}{\partial R_x}\left(\mathbf{H}(R)\right)\vec{c}^{\,J}(R)+\varepsilon^J\vec{c}^{\,J}(R)\frac{\partial}{\partial R_x}\left(\vec{c}^{\,J}(R)\right)-\varepsilon^J\vec{c}^{\,J}(R)\frac{\partial}{\partial R_x}\left(\vec{c}^{\,J}(R)\right)\\ &=\vec{c}^{\,J}(R)\frac{\partial}{\partial R_x}\left(\mathbf{H}(R)\right)\vec{c}^{\,J}(R)\end{aligned} \tag{175}$$

Let us use the following shorthand notation for equation (175):

$$\varepsilon^x(R)=\left\langle\psi_I(R)\middle|\mathbf{H}(R)^x\middle|\psi_I(R)\right\rangle \tag{176}$$

where the superscript x denotes differentiation with respect to a nuclear coordinate.

Although this equation appears to be the Helmann-Feynman Theorem, it is not. The Helmann-Feynman Theorem applies to exact wavefunctions, whereas this formula applies to CI wavefunctions, which are only exact within the space spanned by the basis.

Following equation (171), let us split equation (176) into two pieces:

$$\varepsilon^x(R)=\left\langle\psi_I(R)\middle|\mathbf{H}_0(R)^x\middle|\psi_I(R)\right\rangle+\left\langle\psi_I(R)\middle|\mathbf{H}_{so}(R)^x\middle|\psi_I(R)\right\rangle \tag{177}$$

Shepard's formalism already addresses the first term on the right-hand side of equation (177) [**3**] (also see Appendix G for more detail), and so we will focus on the last term, following in a parallel manner.

Per Shepard's formalism, the spin-orbit gradient in the resolved $\left[Z\right]$ basis can be expressed in the orthogonal $\left[S\right]$ basis as

$$\begin{aligned}\left\langle \psi_I^{[Z]}\left(R_0\right)\middle|\mathbf{H}_{so}^{[Z]}\left(R_0\right)^x\middle|\psi_I^{[Z]}\left(R_0\right)\right\rangle &= \left\langle \psi_I^{[S]}\left(R_0\right)\middle|\mathbf{H}_{so}^{[S]}\left(R_0\right)^x\middle|\psi_I^{[S]}\left(R_0\right)\right\rangle \\ &+\left\langle \psi_I^{[S]}\left(R_0\right)\middle|\left[\mathbf{H}_{so}^{[S]}\left(R_0\right),\mathbf{Z}^{mc}\left(R_0\right)^x\right]\middle|\psi_I^{[S]}\left(R_0\right)\right\rangle \\ &+\left\langle \psi_I^{[S]}\left(R_0\right)\middle|\left[\mathbf{H}_{so}^{[S]}\left(R_0\right),\mathbf{K}^{mc}\left(R_0\right)^x\right]\middle|\psi_I^{[S]}\left(R_0\right)\right\rangle\end{aligned} \tag{178}$$

where higher orders of commutators are considered negligible, and the bra-ket notation indicates vector-matrix multiplication (*cf.* equation (269) in [**3**]). This result stems from the form of the solution wavefunction at an arbitrary geometry as expressed in equation (169). Let us first address the first term on the right-hand side of equation (178), then subsequently we shall address the final two terms, which are treated similarly to one another.

The First Term: The Orthogonal Basis Derivative Term

Using the methods of second quantization, the first term on the right-hand side of equation (178) can be reduced to

$$\begin{aligned}\left\langle \psi_I^{[S]}\left(R_0\right)\middle|\mathbf{H}_{so}^{[S]}\left(R_0\right)^x\middle|\psi_I^{[S]}\left(R_0\right)\right\rangle &= \sum_{r\mu sv} h_{r\mu sv}^{so[S]x}\left\langle \psi_I^{[S]}\left(R_0\right)\middle|E_{r\mu sv}\middle|\psi_I^{[S]}\left(R_0\right)\right\rangle \\ &= Tr\left(\mathbf{h}^{so[S]x}\left\langle \psi_I^{[S]}\left(R_0\right)\middle|\mathbf{E}_{r\mu sv}\middle|\psi_I^{[S]}\left(R_0\right)\right\rangle\right)\end{aligned} \tag{179}$$

where $E_{r\mu s\nu}$ is a non-spin-averaged unitary group generator, and the matrix $\mathbf{h}^{so}$ represents the operator $\hat{h}^{so}$ defined to be proportional to the spin-orbit operator:

$$\hat{h}^{so} = \sum_{l,m} \xi_l(r_e)\left(\vec{\hat{l}} \cdot \vec{\hat{s}}\right) |lm\rangle\langle lm| \tag{180}$$

(*cf.* equation (11); see [**11**]). The derivative of the spin-orbit integral matrix is not calculable by the present form of any integral program in the COLUMBUS suite; however, these terms are available in NWCHEM in C_1 symmetry [**50**]. When this operator is integrated over electronic coordinates between spin-orbitals, we see that

$$\begin{aligned} h^{[S]so}_{r\mu s\nu} &\equiv \left\langle r^{[S]}\mu \left| \hat{h}^{so} \right| s^{[S]}\nu \right\rangle = \left\langle r^{[S]} \left| \sum_{l,m} \xi_l(r_e)\left(\vec{l}\right) |lm\rangle\langle lm| s^{[S]} \right\rangle \cdot \langle \mu | \vec{s} | \nu \rangle \\ &= \sum_{\chi} \left\langle r^{[S]} \left| \sum_{l,m} \xi_l(r_e)\left(\hat{l}_\chi\right) |lm\rangle\langle lm| s^{[S]} \right\rangle \langle \mu | \hat{s}_\chi | \nu \rangle \end{aligned} \tag{181}$$

Let us define a new non-spin-averaged *density matrix*:

$$D^{[S]so}_{r\mu s\nu}(R_0) \equiv \left\langle \psi^{[S]}_I(R_0) \left| E_{r\mu s\nu} \right| \psi^{[S]}_I(R_0) \right\rangle = \sum_{ij} c^I_j c^I_i \left\langle \varphi^{[S]}_j(r:R_0) \left| E_{r\mu s\nu} \right| \varphi^{[S]}_i(r:R_0) \right\rangle \tag{182}$$

(*cf.* definition (34)) where $\varphi^{[S]}_j$ are the CSFs and c^I_j are the corresponding wavefunction coefficients. Combining equations (182), (181), and (179), we can rewrite the orthogonal basis derivative term:

$$\begin{aligned} &\left\langle \psi^{[S]}_I(R_0) \left| \mathbf{H}^{[S]}_{so}(R_0)^x \right| \psi^{[S]}_I(R_0) \right\rangle = \\ &\sum_{rs}\sum_{\chi} \left\langle r^{[S]}(r_e:R_0) \left| \sum_{l,m} \left[\xi_l(r_e)\left(\hat{l}_\chi\right) \right]^x |lm\rangle\langle lm| s^{[S]}(r_e:R_0) \right\rangle \sum_{\mu\nu} \langle \mu | \hat{s}_\chi | \nu \rangle \sum_{ij} c^I_j c^I_i \left\langle \varphi^{[S]}_j(r_e:R_0) \left| E_{r\mu s\nu} \right| \varphi^{[S]}_i(r_e:R_0) \right\rangle \end{aligned} \tag{183}$$

which we will separate into a spin-independent integral piece:

$$\left(q_{\chi}^{[S]}\left(R_0\right)\right)_{rs}^{x} \equiv \left\langle r^{[S]}\left(r_e : R_0\right)\middle|\sum_{l,m}\left[\xi_l\left(r_e\right)\left(\hat{l}_{\chi}\right)\right]^{x}\middle|lm\right\rangle\left\langle lm\middle|s^{[S]}\left(r_e : R_0\right)\right\rangle \tag{184}$$

and a spin-dependent density piece:

$$\left(Z_{\chi}^{[S]}\left(R_0\right)\right)_{rs} \equiv \sum_{\mu\nu}\left\langle\mu\middle|\hat{s}_{\chi}\middle|\nu\right\rangle\sum_{ij}c_j^J c_i^I\left\langle\varphi_j^{[S]}\left(r : R_0\right)\middle|E_{r\mu s\nu}\middle|\varphi_i^{[S]}\left(r : R_0\right)\right\rangle \tag{185}$$

which we will call the new *spin-orbit density matrix*. Thus we see that the first term on the right-hand side of equation (178) reduces to the trace of the matrices

$$\left\langle\psi_I^{[S]}\left(R_0\right)\middle|\mathbf{H}_{so}^{[S]}\left(R_0\right)^{x}\middle|\psi_I^{[S]}\left(R_0\right)\right\rangle = Tr\left(\mathbf{q}_{\chi}^{[S]}\left(R_0\right)^{x}\cdot\mathbf{Z}_{\chi}^{[S]}\left(R_0\right)\right) \tag{186}$$

As a result of this dissertation, the spin-orbit density matrices are now available in the COLUMBUS program CIDEN, and are traced with the derivatives of the one-electron integral matrices, $\mathbf{q}_{\chi}$, in our modified version of NWCHEM. (In NWCHEM, the integral matrices and their accompanying analytic gradients are multiplied by *i* to force them to be real.)

The Second and Third Terms

The nuclear dependence will now be dropped for brevity. In the second and third terms on the right-hand side of equation (178) , all three matrices have a second-quantized form:

$$\begin{aligned}\mathbf{H}_{so}^{[S]} &= \sum_{r\mu s\nu} h_{r\mu s\nu}^{so[S]}\hat{E}_{r\mu s\nu}\\ \mathbf{Z}^{mc} &= \sum_{rs} z_{rs}^{mc}\left(\hat{E}_{rs}-\hat{E}_{sr}\right)\\ \mathbf{K}^{mc} &= \sum_{rs} k_{rs}^{mc}\left(\hat{E}_{rs}-\hat{E}_{sr}\right)\end{aligned} \tag{187}$$

where

$$h^{so[S]}_{r\mu s\nu} = \sum_{rs}\sum_{\chi}\left(q_{\chi}\right)_{rs}\left\langle \mu\left|s_{\chi}\right|\nu\right\rangle \tag{188}$$

leading to the forms

$$\left\langle \psi^{[S]}_{I}\left|\left[\mathbf{H}^{[S]}_{so},\mathbf{Z}^{mcx}\right]\right|\psi^{[S]}_{I}\right\rangle = \sum_{rs} z^{mcx}_{rs}\left\langle \psi^{[S]}_{I}\left|\sum_{r'\mu s'\nu} h^{so[S]}_{r'\mu s'\nu}\left[\hat{E}_{r'\mu s'\nu},\left(\hat{E}_{rs}-\hat{E}_{sr}\right)\right]\right|\psi^{[S]}_{I}\right\rangle \tag{189}$$

and

$$\left\langle \psi^{[S]}_{I}\left|\left[\mathbf{H}^{[S]}_{so},\mathbf{K}^{mcx}\right]\right|\psi^{[S]}_{I}\right\rangle = \sum_{rs} k^{mcx}_{rs}\left\langle \psi^{[S]}_{I}\left|\sum_{r'\mu s'\nu} h^{so[S]}_{r'\mu s'\nu}\left[\hat{E}_{r'\mu s'\nu},\left(\hat{E}_{rs}-\hat{E}_{sr}\right)\right]\right|\psi^{[S]}_{I}\right\rangle \tag{190}$$

We must now determine the meaning of the commutator $\left[\hat{E}_{r'\mu s'\nu},\left(\hat{E}_{rs}-\hat{E}_{sr}\right)\right]$, which appears in both terms. Using the commutation rule for unitary group generators,

$$\left[\hat{E}_{r\mu s\nu},\hat{E}_{t\rho u\sigma}\right] = \hat{E}_{r\mu u\sigma}\delta^{\nu\rho}_{st} - \hat{E}_{sv t\rho}\delta^{\mu\sigma}_{ru} \tag{191}$$

we conclude that

$$\begin{aligned}\left[\hat{E}_{r'\mu s'\nu},\left(\hat{E}_{rs}-\hat{E}_{sr}\right)\right] = {} & \hat{E}_{r'\mu s\alpha}\delta^{\nu\alpha}_{s'r} - \hat{E}_{s'\nu r\alpha}\delta^{\mu\alpha}_{r's} + \hat{E}_{r'\mu s\beta}\delta^{\nu\beta}_{s'r} - \hat{E}_{s'\nu r\beta}\delta^{\mu\beta}_{r's} \\ & - \hat{E}_{r'\mu r\alpha}\delta^{\nu\alpha}_{s's} + \hat{E}_{s'\nu s\alpha}\delta^{\mu\alpha}_{r'r} - \hat{E}_{r'\mu r\beta}\delta^{\nu\beta}_{s's} + \hat{E}_{s'\nu s\beta}\delta^{\mu\beta}_{r'r}\end{aligned} \tag{192}$$

When the requisite sum over spin-orbitals is applied and the spin-orbit integrals included, we find

$$\begin{aligned}\sum_{r'\mu s'\nu} h^{so}_{r'\mu s'\nu}\left[\hat{E}_{r'\mu s'\nu},\left(\hat{E}_{rs}-\hat{E}_{sr}\right)\right] = {} & \sum_{r'\mu} h^{so}_{r'\mu r\alpha}\hat{E}_{r'\mu s\alpha} - \sum_{s'\nu} h^{so}_{s\alpha s'\nu}\hat{E}_{s'\nu r\alpha} \\ & + \sum_{r'\mu} h^{so}_{r'\mu r\beta}\hat{E}_{r'\mu s\beta} - \sum_{s'\nu} h^{so}_{s\beta s'\nu}\hat{E}_{s'\nu r\beta} - \sum_{r'\mu} h^{so}_{r'\mu s\alpha}\hat{E}_{r'\mu r\alpha} \\ & + \sum_{s'\nu} h^{so}_{r\alpha s'\nu}\hat{E}_{s'\nu s\alpha} - \sum_{r'\mu} h^{so}_{r'\mu s\beta}\hat{E}_{r'\mu r\beta} + \sum_{s'\nu} h^{so}_{r\beta s'\nu}\hat{E}_{s'\nu s\beta}\end{aligned} \tag{193}$$

Since $\mathbf{h}^{so}$ is symmetric, we take advantage of the fact that

$$h^{so}_{r\mu s\nu} = h^{so}_{s\nu r\mu} \tag{194}$$

as well as the freedom to choose independent summation indices to rewrite equation (193) as

$$\begin{aligned}\sum_{r'\mu s'\nu} h^{so}_{r'\mu s'\nu}\left[\hat{E}_{r'\mu s'\nu},\left(\hat{E}_{rs}-\hat{E}_{sr}\right)\right] &= \sum_{t\mu}\left(h^{so}_{r\alpha t\mu}\hat{E}_{t\mu s\alpha}+h^{so}_{r\beta t\mu}\hat{E}_{t\mu s\beta}\right)-\sum_{t\mu}\left(h^{so}_{s\alpha t\mu}\hat{E}_{t\mu r\alpha}+h^{so}_{s\beta t\mu}\hat{E}_{t\mu r\beta}\right)\\ &\quad -\sum_{t\mu}\left(h^{so}_{s\beta t\mu}\hat{E}_{t\mu r\beta}+h^{so}_{s\alpha t\mu}\hat{E}_{t\mu r\alpha}\right)+\sum_{t\mu}\left(h^{so}_{r\alpha t\mu}\hat{E}_{t\mu s\alpha}+h^{so}_{r\beta t\mu}\hat{E}_{t\mu s\beta}\right)\end{aligned} \tag{195}$$

which further reduces to

$$\sum_{r'\mu s'\nu} h^{so}_{r'\mu s'\nu}\left[\hat{E}_{r'\mu s'\nu},\left(\hat{E}_{rs}-\hat{E}_{sr}\right)\right] = 2\sum_{t\mu\nu} h^{so}_{r\nu t\mu}\hat{E}_{t\mu s\nu}-2\sum_{t\mu\nu} h^{so}_{s\nu t\mu}\hat{E}_{t\mu r\nu} \tag{196}$$

Each of the terms on the right-hand side of this equation is an element of a spin-contracted Fock matrix for the spin-orbit Hamiltonian. (See Appendix G for definitions of non-relativistic Fock matrices). Let us define

$$\begin{aligned}\left(F^{[S]}_{so}\right)_{rs} &\equiv \sum_{t\mu\nu} h^{so}_{r\nu t\mu}\left\langle\psi^{[S]}_I\middle|\hat{E}_{t\mu s\nu}\middle|\psi^{[S]}_I\right\rangle\\ &= \sum_t\sum_\chi\left(q^{[S]}_\chi\right)_{rt}\sum_{\nu\mu}\langle\nu|s_\chi|\mu\rangle\left\langle\psi^{[S]}_I\middle|\hat{E}_{t\mu s\nu}\middle|\psi^{[S]}_I\right\rangle\\ &= \sum_t\sum_\chi\left(q^{[S]}_\chi\right)_{rt}\left(Z^{[S]}_\chi\right)_{ts}\end{aligned} \tag{197}$$

and

$$\left(f^{so}_{orb}\right)_{rs} \equiv 2\left(\left(F^{[S]}_{so}\right)_{rs}-\left(F^{[S]}_{so}\right)_{sr}\right) \tag{198}$$

so that equations (189) and (190) yield

$$\left\langle\psi^{[S]}_I\middle|\left[\mathbf{H}^{[S]}_{so},\mathbf{Z}^{mcx}\right]\middle|\psi^{[S]}_I\right\rangle = \sum_{rs} z^{mcx}_{rs}\left(f^{so}_{orb}\right)_{rs} = \vec{z}^{\,mcx}\cdot\vec{f}^{\,so}_{orb} \tag{199}$$

and

$$\left\langle\psi^{[S]}_I\middle|\left[\mathbf{H}^{[S]}_{so},\mathbf{K}^{mcx}\right]\middle|\psi^{[S]}_I\right\rangle = \sum_{rs} k^{mcx}_{rs}\left(f^{so}_{orb}\right)_{rs} = \vec{k}^{\,mcx}\cdot\vec{f}^{\,so}_{orb} \tag{200}$$

respectively, yielding

$$\left\langle \psi_I^{[Z]}(R_0) \middle| \mathbf{H}_{so}^{[Z]}(R_0)^x \middle| \psi_I^{[Z]}(R_0) \right\rangle = Tr\left(\mathbf{q}_\chi^{[S]}(R_0) \cdot \mathbf{Z}_\chi^{[S]}(R_0) \right) + \vec{z}^{mcx} \cdot \vec{f}_{orb}^{so} + \vec{k}^{mcx} \cdot \vec{f}_{orb}^{so} \quad (201)$$

Orbital Resolution Vector

It has been shown by Shepard that the form of the orbital resolution vector, $\vec{z}$, depends on the method of resolution [**3**]; if several methods are used, the contribution from each method must be summed. The three methods available in the MCSCF program are natural orbital (NO) resolution, F-Fock matrix resolution, and Q-Fock matrix resolution; however, the F-Fock matrix resolution is not available for use in gradients and DCTs at this time. The other two methods result in the following forms of the orbital resolution vector:

1. Natural Orbital

$$\vec{z}_{rs}^{NOx} = \frac{D_{rs}^{[K]x}}{D_{ss}^{[K]} - D_{rr}^{[K]}} \quad (202)$$

2. Q-Fock Matrix

$$\vec{z}_{rs}^{Qx} = \frac{Q_{rs}^{[K]x}}{Q_{ss}^{[K]} - Q_{rr}^{[K]}} \quad (203)$$

where the natural orbital resolution uses the one-electron non-relativistic transition density matrix defined in equation (35), and the Q-Fock resolution uses the Fock matrix

$$Q_{rs}^{[K]} \equiv 2h_{rs}^{[K]} + \sum_{tu} \left(2g_{rstu}^{[K]} - g_{rtsu}^{[K]} \right) D_{tu}^{[K]} \quad (204)$$

The Product $\vec{z}^{x} \cdot \vec{f}$

While the product of the orbital resolution vector gradient with the orbital gradient vector will remain the same for the non-relativistic term, the spin-orbit term will require a few modifications based on the results presented above. That product can be expressed as:

$$\vec{z}^{NOx} \cdot \vec{f}^{so}_{orb} = 2\sum_{r>s} D^{[K]x}_{rs} \left(\frac{\left(F_{so}\right)_{rs} - \left(F_{so}\right)_{sr}}{D^{[K]}_{ss} - D^{[K]}_{rr}} \right) \equiv \sum_{rs} D^{[K]x}_{rs} \left(A^{D}_{so}\right)_{rs} \tag{205}$$

$$\vec{z}^{Qx} \cdot \vec{f}^{so}_{orb} = 2\sum_{r>s} Q^{[K]x}_{rs} \left(\frac{\left(F_{so}\right)_{rs} - \left(F_{so}\right)_{sr}}{Q^{[K]}_{ss} - Q^{[K]}_{rr}} \right) \equiv \sum_{rs} Q^{[K]x}_{rs} \left(A^{Q}_{so}\right)_{rs} \tag{206}$$

(The undefined diagonal elements are resolved by defining $\mathbf{A}$ to be zero on the diagonal.) Note that these new $\mathbf{A}^{X}_{so}$ matrices differ from Shepard's formalism only in that they have the spin-orbit Fock matrices in the numerator, while all other matrices remain the same. The result is that these terms are evaluated parallel to Shepard's formalism, with the exception that the $\mathbf{A}^{X}_{so}$ matrices are substituted for the non-relativistic variety.

The derivative of the Q-Fock matrix (definition (204)) is

$$Q^{[K]x}_{rs} = 2h^{[K]x}_{rs} + \sum_{tu} \left(2g^{[K]x}_{rstu} - g^{[K]x}_{rtsu} \right) D^{[K]}_{tu} + \sum_{tu} \left(2g^{[K]}_{rstu} - g^{[K]}_{rtsu} \right) D^{[K]x}_{tu} \tag{207}$$

When partially transformed into the [S] basis, this derivative is

$$\begin{aligned} Q^{[K]x}_{rs} = {} & 2h^{[S]x}_{rs} + 2\left\{ h^{[S]}, K^{x} \right\}_{rs} + \sum_{tu} \left(2g^{[S]x}_{rstu} - g^{[S]x}_{rtsu} \right) D^{[S]}_{tu} \\ & + \sum_{tu} \left(2\left\{ g^{[S]}, K^{x} \right\}_{rstu} - \left\{ g^{[S]}, K^{x} \right\}_{rtsu} \right) D^{[S]}_{tu} + \sum_{tu} \left(2g^{[K]}_{rstu} - g^{[K]}_{rtsu} \right) D^{[K]x}_{tu} \end{aligned} \tag{208}$$

where $\{\mathbf{A},\mathbf{B}\} = \mathbf{AB} + \mathbf{B}^{\dagger}\mathbf{A}$. Three types of terms exist in this gradient:

1. Terms involving derivatives of integral matrices
2. Terms involving derivatives of K
3. Terms involving derivatives of transition density matrices.

The natural orbital resolution will only involve the third type of term because it has no Fock matrices.

Q-Matrix Terms, Type 1

These terms have the form

$$\begin{aligned}\left(\vec{z}^{Qx}\cdot\vec{f}_{orb}^{\,so}\right)^{I} &= \sum_{rs} 2h_{rs}^{[S]x}\left(A_{so}^{Q}\right)_{rs} + \sum_{rstu}\left(2g_{rstu}^{[S]\,x} - g_{rtsu}^{[S]\,x}\right)D_{tu}^{[S]}\left(A_{so}^{Q}\right)_{rs} \\ &= Tr\left(\mathbf{h}^{[S]x}\mathbf{D}_{so}^{Q}\right) + \tfrac{1}{2}Tr\left(\mathbf{g}^{[S]x}\mathbf{d}_{so}^{Q}\right)\end{aligned} \tag{209}$$

where we have defined

$$\begin{aligned}\left(D_{so}^{Q}\right)_{rs} &\equiv 2\left(A_{so}^{Q}\right)_{rs} \\ \left(d_{so}^{Q}\right)_{rstu} &\equiv 2\left(A_{so}^{Q}\right)_{rs}D_{tu}^{[S]} + 2\left(A_{so}^{Q}\right)_{tu}D_{rs}^{[S]} - \tfrac{1}{2}\left(A_{so}^{Q}\right)_{rt}D_{us}^{[S]} \\ &\quad -\tfrac{1}{2}\left(A_{so}^{Q}\right)_{ru}D_{st}^{[S]} - \tfrac{1}{2}\left(A_{so}^{Q}\right)_{su}D_{rt}^{[S]} - \tfrac{1}{2}\left(A_{so}^{Q}\right)_{st}D_{ru}^{[S]}\end{aligned} \tag{210}$$

Q-Matrix Terms, Type 2

These terms have the form

$$\begin{aligned}\left(\vec{z}^{Qx}\cdot\vec{f}_{orb}^{\,so}\right)^{II} &= \sum_{rs} 2\left\{h^{[S]},K^{x}\right\}_{rs}\left(A_{so}^{Q}\right)_{rs} + \sum_{rstu}\left(2\left\{g^{[S]},K^{x}\right\}_{rstu} - \left\{g^{[S]},K^{x}\right\}_{rtsu}\right)D_{tu}^{[S]}\left(A_{so}^{Q}\right)_{rs} \\ &= Tr\left(\left\{h^{[S]},\mathbf{K}^{x}\right\}\mathbf{D}_{so}^{Q}\right) + \tfrac{1}{2}Tr\left(\left\{g^{[S]},\mathbf{K}^{x}\right\}\mathbf{d}_{so}^{Q}\right) \\ &= Tr\left(\mathbf{K}^{x\dagger}\left(\mathbf{h}^{[S]}\mathbf{D}_{so}^{Q} + \mathbf{D}_{so}^{Q}\mathbf{h}^{[S]} + \tfrac{1}{2}\mathbf{g}^{[S]}\mathbf{d}_{so}^{Q} + \tfrac{1}{2}\mathbf{g}^{[S]}\mathbf{d}_{so}^{Q}\right)\right) \\ &= -2Tr\left(\mathbf{K}^{x}\mathbf{F}_{so}^{Q}\right) \\ &\equiv \vec{k}^{mcx}\cdot\vec{f}_{orb}^{\,Qso}\end{aligned} \tag{211}$$

where we have analogously defined

$$\mathbf{F}_{so}^{Q} \equiv \mathbf{h}^{[S]}\mathbf{D}_{so}^{Q} + \tfrac{1}{2}\mathbf{g}^{[S]}\mathbf{d}_{so}^{Q} \tag{212}$$

Q-Matrix Terms, Type 3

These terms have the form

$$\begin{aligned}
\left(\vec{z}^{\,Qx} \cdot \vec{f}_{orb}^{\,so}\right)^{III} &= \sum_{rstu}\left(2g_{rstu}^{[K]} - g_{rtsu}^{[K]}\right) D_{tu}^{[K]x}\left(A_{so}^{Q}\right)_{rs} \\
&= \sum_{tu}\left(Q_{so}^{A}\right)_{tu} D_{tu}^{[K]x} \\
&= \sum_{n}\sum_{tu} p_n^x \left\langle n_{\perp}^{[K]} \middle| \left(Q_{so}^{A}\right)_{tu}\left(\hat{E}_{tu} + \hat{E}_{ut}\right) \middle| mc^{[K]} \right\rangle \\
&= \sum_{n} p_n^x \left\langle n_{\perp}^{[K]} \middle| 2\mathbf{Q}_{so}^{A} \middle| mc^{[K]} \right\rangle \\
&\equiv \vec{p}^{\,x} \cdot \vec{f}_{csf}^{\,Qso}
\end{aligned} \tag{213}$$

where $\left\langle n_{\perp}^{[K]} \right|$ is the complement space of the MCSCF solution vector $\left| mc^{[K]} \right\rangle$, and we have defined

$$\left(\mathbf{Q}_{so}^{A}\right)_{rs} \equiv \sum_{tu}\left(2g_{rstu}^{[S]} - g_{rtsu}^{[S]}\right)\left(A_{so}^{Q}\right)_{rs} \tag{214}$$

Natural Orbital Terms, Type 3

These terms have the form

$$\begin{aligned}
\left(\vec{z}^{\,NOx} \cdot \vec{f}_{orb}^{\,so}\right)^{III} &= \sum_{rs} D_{rs}^{[K]x}\left(A_{so}^{D}\right)_{rs} \\
&= \sum_{n}\sum_{rs} p_n^x \left\langle n_{\perp}^{[K]} \middle| \left(A_{so}^{D}\right)_{rs}\left(\hat{E}_{rs} + \hat{E}_{sr}\right) \middle| mc^{[K]} \right\rangle \\
&= \sum_{n} p_n^x \left\langle n_{\perp}^{[K]} \middle| 2\mathbf{A}_{so}^{D} \middle| mc^{[K]} \right\rangle \\
&\equiv \vec{p}_n^{\,x} \cdot \vec{f}_{csf}^{\,Dso}
\end{aligned} \tag{215}$$

Combining equations (215), (213), (211), and (209) into equation (201), we have the more refined form of the spin-orbit gradient:

$$\left\langle \psi_I^{[Z]} \middle| \mathbf{H}_{so}^{[Z]x} \middle| \psi_I^{[Z]} \right\rangle = Tr\left(\mathbf{h}^{[S]x}\mathbf{D}_{so}^{Q}\right) + \tfrac{1}{2}Tr\left(\mathbf{g}^{[S]x}\mathbf{d}_{so}^{Q}\right) + Tr\left(\mathbf{q}_{\chi}^{[S]x}\cdot\mathbf{Z}_{\chi}^{[S]}\right) + \left(\vec{k}^{x\dagger}\ \vec{p}^{x\dagger}\right)\begin{pmatrix} \vec{f}_{orb}^{\,so} + \vec{f}_{orb}^{\,Qso} \\ \vec{f}_{csf}^{\,Qso} + \vec{f}_{csf}^{\,Dso} \end{pmatrix} \tag{216}$$

Matrix Turnover

We can simplify the final term in equation (216) by defining

$$\begin{aligned} \vec{\lambda}^{mcx} &\equiv \left(\vec{k}^{x\dagger}\ \vec{p}^{x\dagger}\right) \\ \vec{f}_{so}^{\,total} &\equiv \begin{pmatrix} \vec{f}_{orb}^{\,so} + \vec{f}_{orb}^{\,Qso} \\ \vec{f}_{csf}^{\,Qso} + \vec{f}_{csf}^{\,Dso} \end{pmatrix} \end{aligned} \tag{217}$$

$\vec{\lambda}^{mcx}$ is known as the *first-order response* of the MCSCF wave function, and is shown by Shepard [**3**] to be equal to

$$\vec{\lambda}^{mcx} = -\tfrac{\partial}{\partial R_x}\begin{pmatrix} \vec{f}_{orb}^{\,mc} \\ \vec{f}_{csf}^{\,mc} \end{pmatrix}\left(\mathbf{G}^{mc}\right)^{-1} \tag{218}$$

at the reference geometry, where $\mathbf{G}^{mc}$ is the Hessian matrix, $\vec{f}_{orb}^{\,mc}$ is the orbital gradient vector and $\vec{f}_{csf}^{\,mc}$ is the CSF gradient vector. Thus we have that the last term in equation (216) is equal to

$$\left(\vec{k}^{x\dagger}\ \vec{p}^{x\dagger}\right)\begin{pmatrix} \vec{f}_{orb}^{\,so} + \vec{f}_{orb}^{\,Qso} \\ \vec{f}_{csf}^{\,Qso} + \vec{f}_{csf}^{\,Dso} \end{pmatrix} = \vec{\lambda}^{mcx}\mathbf{G}^{mc-1}\vec{f}_{so}^{\,total} \tag{219}$$

To the right-most matrix-vector product we assign the symbol

$$\vec{\lambda}^{so} \equiv -\mathbf{G}^{mc-1}\vec{f}_{so}^{\,total} \tag{220}$$

which we separate into orbital and CSF pieces:

$$\vec{\lambda}^{mcx}\mathbf{G}^{mc-1}\vec{f}_{so}^{\,total} = \vec{f}_{orb}^{\,mcx}\cdot\vec{\lambda}_{orb}^{so} + \vec{f}_{csf}^{\,mcx}\cdot\vec{\lambda}_{csf}^{so} \tag{221}$$

Analogously to Shepard's method, we assert that the orbital piece has the form

$$\vec{f}_{orb}^{\,mc\,x} \cdot \vec{\lambda}_{orb}^{\,so} = Tr\left(\mathbf{h}^{[S]x}\mathbf{D}_{so}^{\Lambda}\right) + \tfrac{1}{2}Tr\left(\mathbf{g}^{[S]x}\mathbf{d}_{so}^{\Lambda}\right) \tag{222}$$

where

$$\begin{aligned} \mathbf{D}_{so}^{\Lambda} &\equiv -\left\{\mathbf{D}^{[S]}, \mathbf{\Lambda}_{orb}^{so}\right\} \\ \mathbf{d}_{so}^{\Lambda} &\equiv -\left\{\mathbf{D}^{[S]}, \mathbf{\Lambda}_{orb}^{so}\right\} \end{aligned} \tag{223}$$

and $\mathbf{\Lambda}_{orb}^{so}$ is the matrix form of the vector $\vec{\lambda}_{orb}^{\,so}$. Similarly, we have

$$\vec{f}_{csf}^{\,mc\,x} \cdot \vec{\lambda}_{csf}^{\,so} = Tr\left(\mathbf{h}^{[S]x}\mathbf{D}_{so}^{\lambda}\right) + \tfrac{1}{2}Tr\left(\mathbf{g}^{[S]x}\mathbf{d}_{so}^{\lambda}\right) \tag{224}$$

where

$$\begin{aligned} \left(D_{so}^{\lambda}\right)_{rs} &\equiv \sum_{n}\left(\lambda_{csf}^{so}\right)_{n}\left\langle n_{\perp}\left|\hat{E}_{rs} - \hat{E}_{sr}\right|mc\right\rangle \\ \left(d_{so}^{\lambda}\right)_{rstu} &\equiv \sum_{n}\left(\lambda_{csf}^{so}\right)_{n}\tfrac{1}{2}\left\langle n_{\perp}\left|\hat{e}_{rstu} + \hat{e}_{srtu} + \hat{e}_{rsut} + \hat{e}_{srut}\right|mc\right\rangle \end{aligned} \tag{225}$$

Substituting equations (224) and (222) into (216), we find that the spin-orbit gradient is

$$\varepsilon_{so}^{x} = Tr\left(\mathbf{h}^{[S]x}\left(\mathbf{D}_{so}^{Q} + \mathbf{D}_{so}^{\Lambda} + \mathbf{D}_{so}^{\lambda}\right)\right) + \tfrac{1}{2}Tr\left(\mathbf{g}^{[S]x}\left(\mathbf{d}_{so}^{Q} + \mathbf{d}_{so}^{\Lambda} + \mathbf{d}_{so}^{\lambda}\right)\right) + Tr\left(\mathbf{q}^{[S]x} \cdot \mathbf{Z}^{[S]}\right) \tag{226}$$

which we simplify as

$$\varepsilon_{so}^{x} = Tr\left(\mathbf{h}^{[S]x}\left(\mathbf{D}_{so}^{tot}\right)\right) + \tfrac{1}{2}Tr\left(\mathbf{g}^{[S]x}\left(\mathbf{d}_{so}^{tot}\right)\right) + Tr\left(\mathbf{q}^{[S]x} \cdot \mathbf{Z}^{[S]}\right) \tag{227}$$

This form of the spin-orbit energy gradient must be transformed back to the atomic orbital (AO) basis so that it can be traced with the analytic AO basis gradient integrals. Note that the corrections due to orbital resolution result in traces with the non-relativistic integral matrices rather than the spin-orbit integral matrices. This is due to the fact that the spin-orbit integral matrices were not involved in the MCSCF step.

For this reason, $\mathbf{D}_{so}^{tot}$ and $\mathbf{d}_{so}^{tot}$ can be summed up with the non-relativistic effective density matrices and traced accordingly. This fact makes coding the spin-orbit effective density matrices in the program CIGRD as simple as adding the spin-orbit Fock matrix to the non-relativistic Fock matrix before any further calculations are performed.

Transformation to the Atomic Basis

The three traces in equation (227) are in the $\left[S\right]$ basis, and must be transformed to the atomic basis. The density matrices do not change; however, the integral matrices transform as:

$$\mathbf{h}^{[S]x} = \mathbf{h}^{[C]x} - \tfrac{1}{2}\left\{\mathbf{h}^{[C]}, \mathbf{S}^{[C]x}\right\} \tag{228}$$

(where the braces indicate the anticommutator) leading to the transformation of equation (227):

$$\begin{aligned}\varepsilon_{so}^{x} = {} & Tr\left(\mathbf{h}^{[C]x}\left(\mathbf{D}_{so}^{tot\,[C]}\right)\right) + \tfrac{1}{2}Tr\left(\mathbf{g}^{[C]x}\left(\mathbf{d}_{so}^{tot\,[C]}\right)\right) + Tr\left(\mathbf{q}^{[C]x}\cdot\mathbf{Z}^{[C]}\right) \\ & - \tfrac{1}{2}Tr\left(\left\{\mathbf{h}^{[C]}, \mathbf{S}^{[C]x}\right\}\mathbf{D}_{so}^{tot[C]}\right) - \tfrac{1}{4}Tr\left(\left\{\mathbf{g}^{[C]}, \mathbf{S}^{[C]x}\right\}\mathbf{d}_{so}^{tot\,[C]}\right) - \tfrac{1}{2}Tr\left(\left\{\mathbf{q}^{[C]}, \mathbf{S}^{[C]x}\right\}\cdot\mathbf{Z}^{[C]}\right)\end{aligned} \tag{229}$$

Shepard has also shown that the fourth and fifth trace operations in equation (229) are equal to

$$\begin{aligned}\tfrac{1}{2}Tr\left(\left\{\mathbf{h}^{[C]}, \mathbf{S}^{[C]x}\right\}\mathbf{D}_{so}^{tot\,[C]}\right) &= Tr\left(\mathbf{S}^{[C]x}\mathbf{F}_{so}^{1sc[C]}\right) \\ \tfrac{1}{4}Tr\left(\left\{\mathbf{g}^{[C]}, \mathbf{S}^{[C]x}\right\}\mathbf{d}_{so}^{tot\,[C]}\right) &= Tr\left(\mathbf{S}^{[C]x}\mathbf{F}_{so}^{2sc[C]}\right)\end{aligned} \tag{230}$$

where $\mathbf{F}_{so}^{1sc[C]}$ and $\mathbf{F}_{so}^{2sc[C]}$ are effective Fock matrices defined as

$$\left(F_{so}^{1sc[C]}\right)_{rs} \equiv \sum_{t} h_{rt}^{[C]}\left(D_{so}^{tot\,[C]}\right)_{ts}$$
$$\left(F_{so}^{2sc[C]}\right)_{rs} \equiv \sum_{tuv} g_{rtuv}^{[C]}\left(d_{so}^{tot\,[C]}\right)_{stuv} \tag{231}$$
$$\left(F_{so}^{sc[C]}\right)_{rs} \equiv \left(F_{so}^{1sc[C]}\right)_{rs} + \tfrac{1}{2}\left(F_{so}^{2sc[C]}\right)_{rs}$$

In a similar fashion, the last trace operation in equation (229) becomes

$$\tfrac{1}{2}Tr\left(\left\{\mathbf{q}^{[C]},\mathbf{S}^{x[C]}\right\}\cdot\mathbf{Z}^{[C]}\right) = Tr\left(\mathbf{S}^{x[C]}\mathbf{F}_{so}^{[C]}\right) \tag{232}$$

This Fock matrix was defined in equation (197). Substituting equations (232) and (230) into (229), the spin-orbit gradient is defined completely in terms of traces of products of integral and density matrices in the $[C]$ basis, whose form is equivalent in the atomic basis. After the transformation of the matrices from the MCSCF molecular orbital basis to the AO basis, the spin-orbit energy gradient becomes

$$\varepsilon^{x}_{so} = Tr\left(\mathbf{h}^{x[\chi]}\left(\mathbf{D}_{so}^{tot\,[\chi]}\right)\right) + \tfrac{1}{2}Tr\left(\mathbf{g}^{x[\chi]}\left(\mathbf{d}_{so}^{tot\,[\chi]}\right)\right) + Tr\left(\mathbf{q}^{x[\chi]}\cdot\mathbf{Z}^{[\chi]}\right) - Tr\left(\mathbf{S}^{x[\chi]}\left(\mathbf{F}_{so}^{tot[\chi]} + \mathbf{F}_{so}^{[\chi]}\right)\right) \tag{233}$$

These terms are added to the non-spin-orbit form of the gradient,

$$\varepsilon_0^{x} = Tr\left(\mathbf{h}^{x[\chi]}\mathbf{D}^{tot[\chi]}\right) + \tfrac{1}{2}Tr\left(\mathbf{g}^{x[\chi]}\mathbf{d}^{tot[\chi]}\right) - Tr\left(\mathbf{S}^{x[\chi]}\mathbf{F}_{tot}^{[\chi]}\right) \tag{234}$$

(see Appendix G) to yield

$$\begin{aligned}\varepsilon^{x} = {} & Tr\left(\mathbf{h}^{x[\chi]}\left(\mathbf{D}^{tot\,[\chi]} + \mathbf{D}_{so}^{tot\,[\chi]}\right)\right) + \tfrac{1}{2}Tr\left(\mathbf{g}^{x[\chi]}\left(\mathbf{d}^{tot\,[\chi]} + \mathbf{d}_{so}^{tot\,[\chi]}\right)\right) \\ & + Tr\left(\mathbf{q}^{x[\chi]}\cdot\mathbf{Z}^{[\chi]}\right) - Tr\left(\mathbf{S}^{x[\chi]}\left(\mathbf{F}_{so}^{tot[\chi]} + \mathbf{F}_{so}^{[\chi]} + \mathbf{F}_{tot}^{[\chi]}\right)\right)\end{aligned} \tag{235}$$

In the actual implementation, the standard Fock matrices $\mathbf{F}$ and $\mathbf{F}_{so}$ are added together early in the program CIGRD. The effect of this combination is to eliminate the

distinction between the various spin-orbit Fock and density matrices defined in this section and their spin-contracted counterparts; that is,

$$\begin{aligned}\mathbf{D}^{tot}+\mathbf{D}_{so}^{tot}&\rightarrow\mathbf{D}^{tot}\\ \mathbf{d}^{tot}+\mathbf{d}_{so}^{tot}&\rightarrow\mathbf{d}^{tot}\\ \mathbf{F}_{tot}+\mathbf{F}_{so}^{tot}&\rightarrow\mathbf{F}_{tot}\end{aligned} \tag{236}$$

thus simplifying the definition of the energy gradient:

$$\begin{aligned}\varepsilon^{x}=&Tr\left(\mathbf{h}^{x[\chi]}\left(\mathbf{D}^{tot[\chi]}\right)\right)+\tfrac{1}{2}Tr\left(\mathbf{g}^{x[\chi]}\left(\mathbf{d}^{tot[\chi]}\right)\right)\\ &+Tr\left(\mathbf{q}^{x[\chi]}\cdot\mathbf{Z}^{[\chi]}\right)-Tr\left(\mathbf{S}^{x[\chi]}\left(\mathbf{F}_{so}^{[\chi]}+\mathbf{F}_{tot}^{[\chi]}\right)\right)\end{aligned} \tag{237}$$

Analytic Derivative Coupling Terms

Elements of the derivative coupling term matrix $\mathbf{P}$ have the form

$$f_{JI}(R)^{x}=\left\langle\psi_{J}(R)\right|\tfrac{\partial}{\partial R_{x}}\left|\psi_{I}(R)\right\rangle \tag{238}$$

(where we are using Lischka's notation for the DCT [**5**]). The wavefunctions ψ_I are expanded in the CSF space as

$$\left|\psi_{I}(r:R)\right\rangle=\sum_{i}c_{i}^{I}(R)\left|\varphi_{i}(r:R)\right\rangle \tag{239}$$

Using this form, the elements of the DCT matrix are

$$f_{JI}(R)^{x}=\sum_{ij}c_{j}^{J}(R)\left\langle\varphi_{j}(r:R)\right|\tfrac{\partial}{\partial R_{x}}\left(c_{i}^{I}(R)\left|\varphi_{i}(r:R)\right\rangle\right) \tag{240}$$

Applying the chain rule,

$$\begin{aligned}f_{JI}(R)^{x}=&\sum_{ij}c_{j}^{J}(R)\left\langle\varphi_{j}(r:R)\right|\tfrac{\partial}{\partial R_{x}}\left(c_{i}^{I}(R)\right)\left|\varphi_{i}(r:R)\right\rangle\\ &+\sum_{ij}c_{j}^{J}(R)\left\langle\varphi_{j}(r:R)\right|c_{i}^{I}(R)\tfrac{\partial}{\partial R_{x}}\left(\left|\varphi_{i}(r:R)\right\rangle\right)\end{aligned} \tag{241}$$

In the first term, the derivative operation on the CI coefficients does not participate in the integration, leaving only the delta function $\left\langle \varphi_j\left(r:R\right)\middle|\varphi_i\left(r:R\right)\right\rangle = \delta_{ij}$. In the second term, the CI coefficients again exit the integration, but the gradient operation remains. This leaves

$$f_{JI}\left(R\right)^x = \sum_i c_i^J\left(R\right)\tfrac{\partial}{\partial R_x}\left(c_i^I\left(R\right)\right) + \sum_{ij} c_j^J\left(R\right)c_i^I\left(R\right)\left\langle \varphi_j\left(r:R\right)\middle|\tfrac{\partial}{\partial R_x}\middle|\varphi_i\left(r:R\right)\right\rangle \qquad (242)$$

The first term is a vector dot-product, and emphasizes the change in the CI coefficients; thus it is called by Lischka et al. the CI DCT

$$f_{JI}^{CI}\left(R\right)^x = \sum_i c_i^J\left(R\right)\tfrac{\partial}{\partial R_x}c_i^I\left(R\right) \equiv \vec{c}^{\,J}\left(R\right)\tfrac{\partial}{\partial R_x}\vec{c}^{\,I}\left(R\right) \qquad (243)$$

The second term emphasizes the change in the CSFs, and is called the CSF DCT:

$$f_{JI}^{CSF}\left(R\right)^x \equiv \sum_{ij} c_j^J\left(R\right)c_i^I\left(R\right)\left\langle \varphi_j\left(r:R\right)\middle|\tfrac{\partial}{\partial R_x}\varphi_i\left(R\right)\right\rangle \qquad (244)$$

The addition of the spin-orbit operator to the Hamiltonian will significantly alter the CI DCT, which will be discussed below. In COLUMBUS, the CSFs are formed from the orbitals defined in the MCSCF step which does not account for the spin-orbit operator. For this reason, the CSF DCT is unchanged by the addition of the spin-orbit operator at the CI step. Lischka's formalism for the CSF DCT is reviewed in Appendix H.

The CI DCT

Recall that we found the energy gradient by assuming $I = J$ in equation (174). To solve for the CI DCTs, we make the alternate assumption, i.e, $I \neq J$. Applying this assumption to equation (174) yields

$$\vec{c}^{\,J}(R)\tfrac{\partial}{\partial R_x}\left(\vec{c}^{\,I}(R)\right)=\left(\varepsilon^I(R)-\varepsilon^J(R)\right)^{-1}\vec{c}^{\,J}(R)\tfrac{\partial}{\partial R_x}\left(\mathbf{H}(R)\right)\vec{c}^{\,I}(R) \tag{245}$$

As we did with the energy gradient, we can split the Hamiltonian into two pieces,

$$\begin{aligned} f_{JI}^{CI}(R)^x &= \left(\varepsilon^I(R)-\varepsilon^J(R)\right)^{-1}\vec{c}^{\,J}(R)\tfrac{\partial}{\partial R_x}\left(\mathbf{H}_0(R)\right)\vec{c}^{\,I}(R) \\ &\quad+\left(\varepsilon^I(R)-\varepsilon^J(R)\right)^{-1}\vec{c}^{\,J}(R)\tfrac{\partial}{\partial R_x}\left(\mathbf{H}_{so}(R)\right)\vec{c}^{\,I}(R) \end{aligned} \tag{246}$$

and define

$$\begin{aligned} f_{JI}^{CI\,0}(R)^x &\equiv \Delta\varepsilon(R)^{-1}\vec{c}^{\,J}(R)\tfrac{\partial}{\partial R_x}\left(\mathbf{H}_0(R)\right)\vec{c}^{\,I}(R) \\ f_{JI}^{CI\,so}(R)^x &\equiv \Delta\varepsilon(R)^{-1}\vec{c}^{\,J}(R)\tfrac{\partial}{\partial R_x}\left(\mathbf{H}_{so}(R)\right)\vec{c}^{\,I}(R) \end{aligned} \tag{247}$$

Thus the CI DCT is very similar to the CI energy gradient, with the notable exception that it has an energy difference in the denominator, and the coefficient vectors are from different (rather than the same) wavefunctions. For this reason, the formalism for the analytic spin-orbit CI DCT exactly mirrors that of the analytic spin-orbit energy gradient, with the addition of the energy difference in the denominator and the substitution of *transition density matrices* in place of the standard matrices:

$$\begin{aligned} \Delta\varepsilon\, f_{JI}^{so\,x} &= Tr\left(\mathbf{h}^{x[\chi]}\left(\mathbf{D}_{so}^{tot\,JI[\chi]}\right)\right)+\tfrac{1}{2}Tr\left(\mathbf{g}^{x[\chi]}\left(\mathbf{d}_{so}^{tot\,JI[\chi]}\right)\right) \\ &\quad+Tr\left(\mathbf{q}^{x[\chi]}\cdot\mathbf{Z}^{JI[\chi]}\right)-Tr\left(\mathbf{S}^{x[\chi]}\left(\mathbf{F}_{so}^{sc\,JI[\chi]}+\mathbf{F}_{so}^{JI[\chi]}\right)\right) \end{aligned} \tag{248}$$

This quantity is added to the standard CI DCT (see equation (407) in Appendix G) and the standard CSF DCT (see equation (432) in Appendix H) to produce the full form of the DCT:

$$\begin{aligned}\Delta\varepsilon\, f_{JI}^{CI+CSF+so\,x} &= Tr\left(\mathbf{h}^{x[\chi]}\left(\mathbf{D}_{tot}^{JI[\chi]}+\mathbf{D}_{tot}^{CSF\,JI[\chi]}+\mathbf{D}_{so}^{tot\,JI[\chi]}\right)\right)+Tr\left(\mathbf{q}^{x[\chi]}\cdot\mathbf{Z}^{JI[\chi]}\right)\\ &+\tfrac{1}{2}Tr\left(\mathbf{g}^{x[\chi]}\left(\mathbf{d}_{tot}^{JI[\chi]}+\mathbf{d}_{tot}^{CSF\,JI[\chi]}+\mathbf{d}_{so}^{tot\,JI[\chi]}\right)\right)\\ &-Tr\left(\mathbf{S}^{x[\chi]}\left(\mathbf{F}_{tot}^{JI[\chi]}+\mathbf{F}_{so}^{sc\,JI[\chi]}+\mathbf{F}_{so}^{JI[\chi]}\right)\right)+\Delta\varepsilon\,Tr\left(\mathbf{D}^{IJ[\chi]a}\left(R_0\right)f_{orb}^{CSF[\chi]}\left(R_0\right)^{x}\right)\end{aligned} \tag{249}$$

In the actual implementation, just as with their standard counterparts in the formulation of the energy gradient, the spin-orbit density and Fock matrices are combined with their spin-contracted counterparts,

$$\begin{aligned}\mathbf{D}_{tot}^{JI[\chi]}+\mathbf{D}_{so}^{tot\,JI[\chi]} &\rightarrow \mathbf{D}_{tot}^{JI[\chi]}\\ \mathbf{d}_{tot}^{JI[\chi]}+\mathbf{d}_{so}^{tot\,JI[\chi]} &\rightarrow \mathbf{d}_{tot}^{JI[\chi]}\\ \mathbf{F}_{tot}^{JI[\chi]}+\mathbf{F}_{so}^{sc\,JI[\chi]} &\rightarrow \mathbf{F}_{tot}^{JI[\chi]}\end{aligned} \tag{250}$$

to yield a cleaner formulation of the DCT:

$$\begin{aligned}\Delta\varepsilon\, f_{JI}^{CI+CSF+so\,x} &= Tr\left(\mathbf{h}^{x[\chi]}\left(\mathbf{D}_{tot}^{JI[\chi]}+\mathbf{D}_{tot}^{CSF\,JI[\chi]}\right)\right)+Tr\left(\mathbf{q}^{x[\chi]}\cdot\mathbf{Z}^{JI[\chi]}\right)\\ &+\tfrac{1}{2}Tr\left(\mathbf{g}^{x[\chi]}\left(\mathbf{d}_{tot}^{JI[\chi]}+\mathbf{d}_{tot}^{CSF\,JI[\chi]}\right)\right)-Tr\left(\mathbf{S}^{x[\chi]}\left(\mathbf{F}_{tot}^{JI[\chi]}+\mathbf{F}_{so}^{JI[\chi]}\right)\right)\\ &+\Delta\varepsilon\,Tr\left(\mathbf{D}^{IJ[\chi]a}\left(R_0\right)f_{orb}^{CSF[\chi]}\left(R_0\right)^{x}\right)\end{aligned} \tag{251}$$

IV. Results and Discussion

Test Case and Implementation

In order to validate the formalism presented in Chapter III, we have implemented it in a hybrid of NWCHEM and COLUMBUS codes, and have chosen K He with a Stuttgart basis [**51**] [**52**]as a test case. K He was chosen was because of its relative simplicity for speedy calculations, the availability of a spin-orbit potential, evidence of an avoided crossing (where DCTs should be significant), and its possible application to a Diode-Pumped Alkali Laser (DPAL). Energy surfaces for the excited states of K He are shown below in Figure 26.

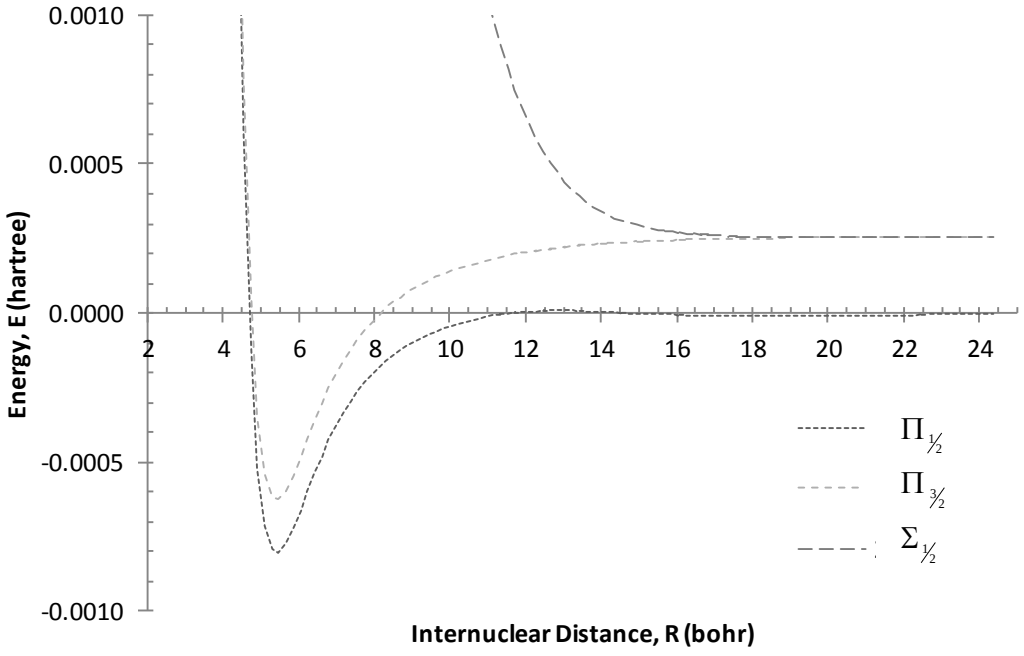

Figure 26. K He MRCI energy surfaces

Calculation of spin-orbit gradients and DCTs requires derivatives of spin-orbit integrals and potentials. COLUMBUS typically uses one of two integral programs: ARGOS, which is capable of handling spin-orbit potentials and integrals; or DALTON, which can produce gradients of atomic integrals. Since neither program currenty does both, NWCHEM has been leveraged to produce the spin-orbit integrals to be fed into COLUMBUS, as well to calculate the spin-orbit integral gradients used in the traces in equations (235) and (249). Kedziora has modified NWCHEM to write the integrals into the Standard Integral File System (SIFS) format used by all COLUMBUS programs. The disadvantage of using NWCHEM for integrals is that, unlike DALTON or ARGOS, symmetry-adapted integrals are not available. This shortcoming requires that all calculations must be done in the C_1 symmetry group, thus increasing calculation time, memory, and space required.

The current COLUMBUS code that produces the MRCI wavefunctions, including MCDRT, MCSCF, MCUFT, MOFMT, CIDRT, TRAN, CISRT, and CIUDG, has not been modified. The density program, CIDEN, has been modified to correctly interpret the multi-headed spin-orbit DRT or Shavitt graph (see Figure 20) and to produce the anti-symmetric spin-orbit density matrices $\mathbf{Z}_{\chi}$ in equation (185). CIGRD, which produces the effective density matrices and the Fock matrix, has been modified to create the spin-orbit Fock matrix $\mathbf{F}_{so}$ defined in equation (197). This matrix is then added to the standard Fock matrix defined in equation (365) of Appendix G. This sum effectively combines the matrices defined in equations (205) and (206) into those defined in

equation (380), as well as combining $\mathbf{F}_{so}^{sc}$ with $\mathbf{F}_{tot}$ in equation (235). A separate symmetric version of $\mathbf{F}_{so}$ is also supplied, as required by equation (235).The spin-orbit density matrices, which do not require an effective counterpart, are passed through to the CIGRD output files. After transformation to the atomic basis, the symmetric density and Fock matrices are passed back into NWCHEM, rather than DALTON, to evaluate the atomic integral gradients and perform the final traces. For DCTs, the antisymmetric (non-spin-orbit) density matrix is still passed to DALTON to evaluate the final trace operation in equation (249).

The Density Matrices

Modification of the density matrices for use with spin-orbit DRTs, as well as the creation of the spin-orbit density matrices, is the cornerstone of the implementation. We can validate these matrices by using them to calculate the energy expectation value of the wavefunctions:

$$\langle \psi_I | \hat{H} | \psi_I \rangle = Tr(\mathbf{h}\mathbf{D}) + \tfrac{1}{2} Tr(\mathbf{g}\mathbf{d}) + \sum_{\chi} Tr(\mathbf{q}_{\chi}\mathbf{Z}_{\chi}) \qquad (252)$$

(see equations (32), (184), and (185)). Note that this is also the trace of the total Fock matrix:

$$
\begin{aligned}
Tr\left(\mathbf{F}\right) &= \sum_{p} F_{pp} \\
&= \sum_{p}\left(\sum_{t} h_{pt} D_{tp} + \tfrac{1}{2} \sum_{tuv} g_{ptuv} d_{ptuv} + \sum_{\chi} \sum_{t} \left(\mathbf{q}_{\chi}\right)_{pt} \left(\mathbf{Z}_{\chi}\right)_{tp} \right) \\
&= \sum_{pt} h_{pt} D_{tp} + \tfrac{1}{2} \sum_{ptuv} g_{ptuv} d_{ptuv} + \sum_{\chi} \sum_{pt} \left(\mathbf{q}_{\chi}\right)_{pt} \left(\mathbf{Z}_{\chi}\right)_{tp} \\
&= Tr\left(\mathbf{h}\mathbf{D}\right) + \tfrac{1}{2} Tr\left(\mathbf{g}\mathbf{d}\right) + \sum_{\chi} Tr\left(\mathbf{q}_{\chi}\mathbf{Z}_{\chi}\right)
\end{aligned}
\tag{253}
$$

This value should be nearly equal to the energy eigenvalues calculated by CIUDG, which approximately solve the Schrödinger equation:

$$
\hat{H}\left|\tilde{\psi}_{I}\right\rangle \approx \varepsilon^{I}\left|\tilde{\psi}_{I}\right\rangle \rightarrow \varepsilon^{I} \approx \left\langle \tilde{\psi}_{I}\right|\hat{H}\left|\tilde{\psi}_{I}\right\rangle \tag{254}
$$

where $\left|\tilde{\psi}_{I}\right\rangle$ is the approximate eigenvector. The difference between these values is dependent upon the convergence tolerance of the MRCI eigenvalues.

Figure 27 compares the MRCI eigenvalue surfaces with the Fock energy surfaces for the test case for the p-manifold excited states. Point-wise differences are on the order of 10^{-10} hartree or smaller. Each of these states is normally doubly degenerate, but due to the addition of the ghost electron [**11**], each state is quadruply degenerate. It is sufficient to specify the energy or gradient of only the lowest of each quadruplet.

Since the effective density matrices differ from the standard density matrices in that they account for rotations in the MCSCF invariant space, the energy expectation value they construct should also be approximately equal to the MRCI eigenvalues. Figure 28 compares these values with the MRCI eigenvalues. Their difference should now depend not only on the convergence of the MRCI wavefunctions, but also upon the

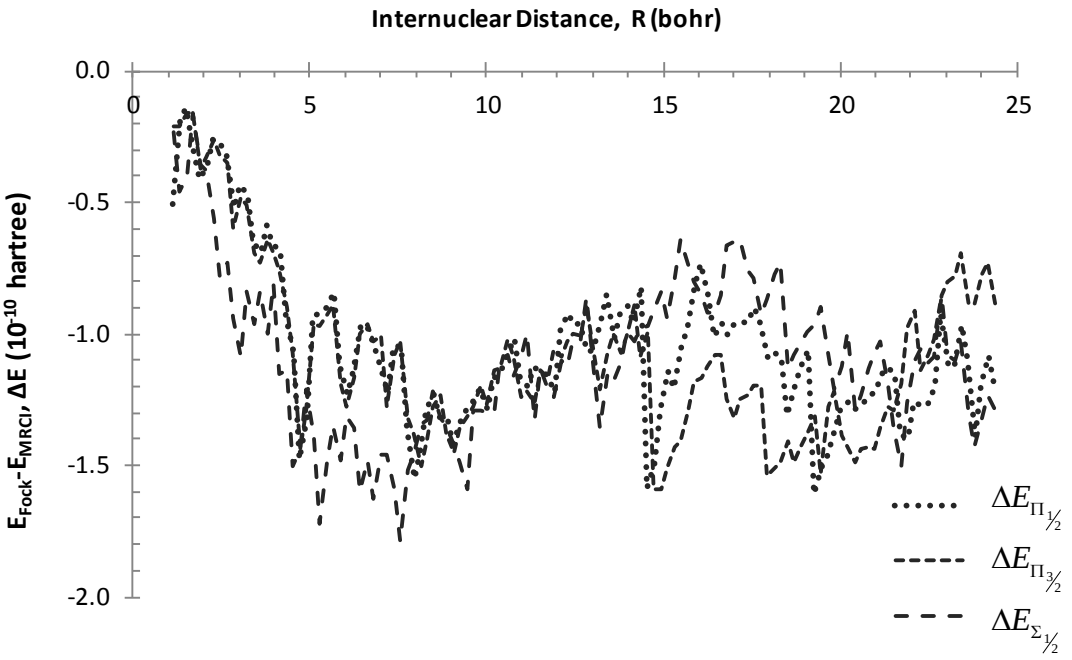

Figure 27. K He Fock - MRCI energy difference

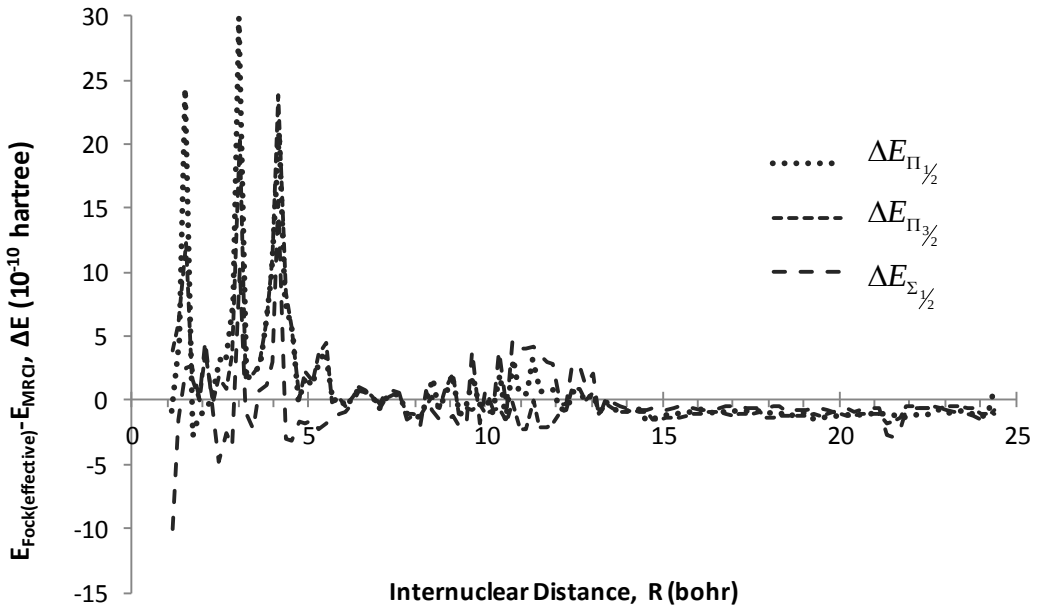

Figure 28. K He Effective Fock – MRCI energy difference

convergence tolerance of the MCSCF Hessian inverse. Point-wise differences are in general on the order of 10^{-10}, but grow an order of magnitude when approaching the repulsion wall. Since energies themselves are only converged to 10^{-6} hartree in this calculation, these small energy differences are most likely numerical artifacts due to the different methods used to calculate either energy.

Analytic Gradients

Analytic gradients have merit on their own, in that they can be used for geometry optimization algorithms [**53**]. Adding this open-shell spin-orbit capability to analytic gradients has the potential to improve such optimizations. While this is a contribution in its own right, our interest in them is that the code required to produce the gradients is a very large part of the code that produces the DCTs. The successful calculation of these gradients partially validates the calculation of the DCTs.

The linear geometry of K He allows for easy calculation of a finite-difference gradient to which the analytic gradient can be compared. Figure 29 through Figure 31 compare finite-central-difference gradients using a 0.2 Å split to analytic gradients. Differences, for the most part, are less than 1%.

Derivative Coupling Terms and the Adiabatic Mixing Angle

Effects of the Arbitrary Rotation of Wavefunctions

DCTs suffer an additional complexity that the gradients do not. Each MRCI wavefunction may have an arbitrary phase factor, which does not affect the energy

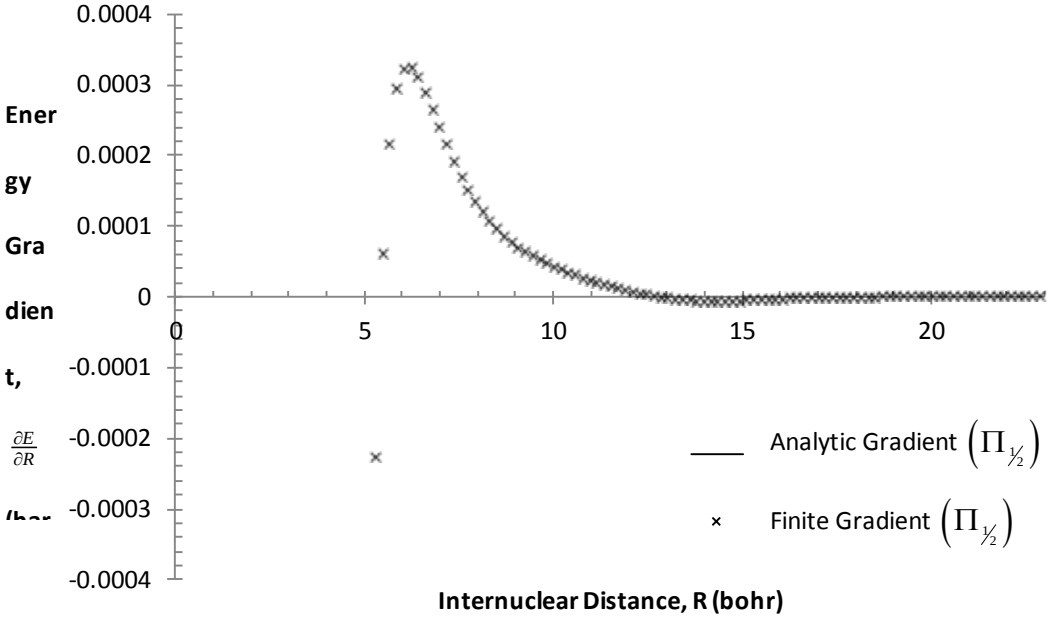

Figure 29. Finite vs. analytic gradient of K He $\Pi_{1/2}$ state

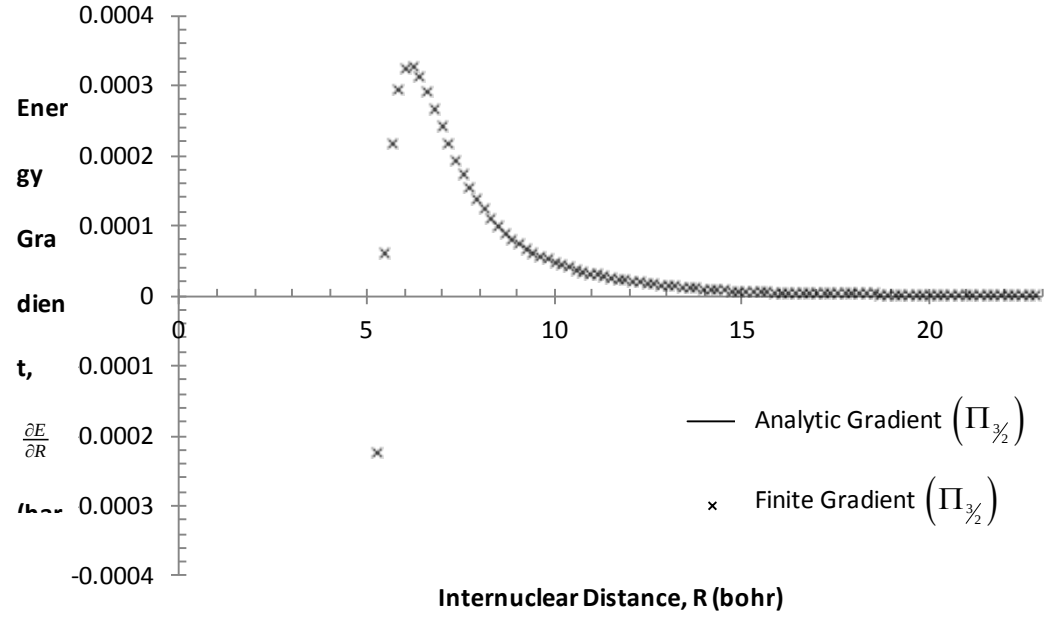

Figure 30. Finite vs. analytic gradient of K He $\Pi_{3/2}$ state

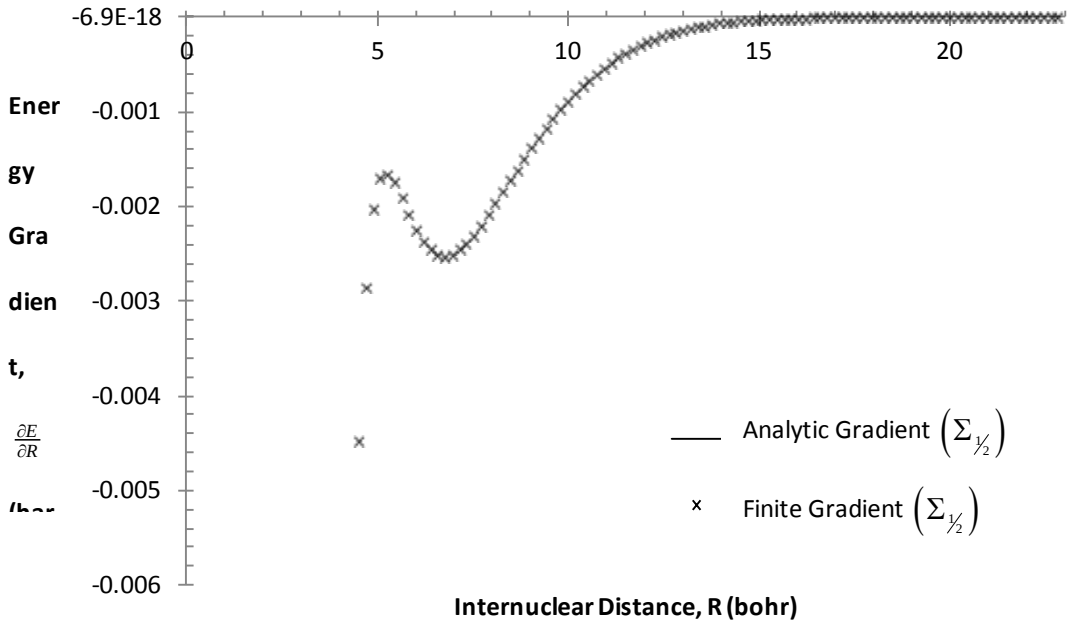

Figure 31. Finite vs. analytic gradient of K He $\Sigma_{1/2}$ state

expectation value or its gradient. Let

$$\left|\psi_I^{'}\right\rangle = e^{-i\theta}\left|\psi_I\right\rangle \tag{255}$$

Then for an operator $\hat{A}$

$$\begin{aligned}\left\langle\psi_I^{'}\middle|\hat{A}\middle|\psi_I^{'}\right\rangle &= e^{i\theta}\left\langle\psi_I\middle|\hat{A}e^{-i\theta}\middle|\psi_I\right\rangle \\ &= e^{i\theta}e^{-i\theta}\left\langle\psi_I\middle|\hat{A}e^{-i\theta}\middle|\psi_I\right\rangle \\ &= \left\langle\psi_I\middle|\hat{A}\middle|\psi_I\right\rangle\end{aligned} \tag{256}$$

and so the phase factor is superfluous. If we instead consider a transition property between different wavefunctions, we find that the phase does indeed matter:

$$\begin{aligned}\left\langle \psi_I^{'} \middle| \hat{A} \middle| \psi_J^{'} \right\rangle &= e^{i\theta_I} \left\langle \psi_I \middle| \hat{A} e^{-i\theta_J} \middle| \psi_J \right\rangle \\ &= e^{i\theta_I} e^{-i\theta_J} \left\langle \psi_I \middle| \hat{A} e^{-i\theta} \middle| \psi_J \right\rangle \\ &= e^{i(\theta_I - \theta_J)} \left\langle \psi_I \middle| \hat{A} \middle| \psi_J \right\rangle\end{aligned} \tag{257}$$

Since COLUMBUS only uses real wavefunctions, the arbitrary phase is limited to ± 1, but it will still require careful deliberation, especially as the DCT crosses the axis.

In addition to the arbitrary phase angle, there will also be an arbitrary mixing angle between degenerate wavefunctions; the doubling of degeneracy due to the ghost electron only compounds this issue, creating a quadruple-degeneracy. To understand how this mixing angle affects the DCTs, consider an arbitrary vector in the space spanned by the $\Sigma_{1/2}$ states:

$$\left| \psi \right\rangle = \sum_{i=1}^{4} \left| \Sigma_{1/2}^{i} \right\rangle \left\langle \Sigma_{1/2}^{i} \middle| \psi \right\rangle \tag{258}$$

We can project this vector into the space of gradients of the $\Pi_{1/2}$ states:

$$\sum_{j=1}^{4} \tfrac{\partial}{\partial R} \left| \Pi_{1/2}^{j} \right\rangle \left\langle \Pi_{1/2}^{j} \middle| \tfrac{\partial}{\partial R} \middle| \psi \right\rangle = \sum_{j=1}^{4} \tfrac{\partial}{\partial R} \left| \Pi_{1/2}^{j} \right\rangle \sum_{i=1}^{4} \left\langle \Pi_{1/2}^{j} \middle| \tfrac{\partial}{\partial R} \middle| \Sigma_{1/2}^{i} \right\rangle \left\langle \Sigma_{1/2}^{i} \middle| \psi \right\rangle \tag{259}$$

From this equation we conclude that

$$\left\langle \Pi_{1/2}^{j} \middle| \tfrac{\partial}{\partial R} = \sum_{i=1}^{4} \left\langle \Pi_{1/2}^{j} \middle| \tfrac{\partial}{\partial R} \middle| \Sigma_{1/2}^{i} \right\rangle \left\langle \Sigma_{1/2}^{i} \right| \tag{260}$$

that is, the DCTs are simply the projections of the gradients of the $\Pi_{1/2}$ states onto the $\Sigma_{1/2}$ space. Let us apply an arbitrary unitary transformation to the basis of the $\Sigma_{1/2}$ space (for all practical purposes, we treat the space and its *dual* equivalently):

$$\frac{\partial}{\partial R}\left|\Pi^{j}_{1/2}\right\rangle = \sum_{i=1}^{4}\hat{U}\left|\Sigma^{i}_{1/2}\right\rangle\left\langle\Sigma^{i}_{1/2}\right|\hat{U}^{\dagger}\frac{\partial}{\partial R}\left|\Pi^{j}_{1/2}\right\rangle \tag{261}$$

While the gradient wavefunction itself has not changed, the DCTs have been changed by the transformation. This means that, unfortunately, a DCT such as $\left\langle\Pi^{j}_{1/2}\frac{\partial}{\partial R}\middle|\Sigma^{k}_{1/2}\right\rangle$, being a projection onto a single arbitrary basis function, is not well-defined. The Euclidean norm of the gradient wavefunction, however, is well defined. That is,

$$\begin{aligned}\sqrt{\sum_{i=1}^{4}\left\|\left\langle\Pi^{j}_{1/2}\frac{\partial}{\partial R}\middle|\hat{U}^{\dagger}\Sigma^{i}_{1/2}\right\rangle\right\|^{2}} &= \sqrt{\sum_{i=1}^{4}\left\langle\Pi^{j}_{1/2}\frac{\partial}{\partial R}\middle|\hat{U}^{\dagger}\Sigma^{i}_{1/2}\right\rangle\left\langle\Sigma^{i}_{1/2}\hat{U}\middle|\frac{\partial}{\partial R}\Pi^{j}_{1/2}\right\rangle} \\ &= \sqrt{\sum_{i=1}^{4}\left\langle\Pi^{j}_{1/2}\frac{\partial}{\partial R}\middle|\Sigma^{i}_{1/2}\right\rangle\left\langle\Sigma^{i}_{1/2}\middle|\frac{\partial}{\partial R}\Pi^{j}_{1/2}\right\rangle} \\ &= \sqrt{\left\langle\Pi^{j}_{1/2}\frac{\partial}{\partial R}\middle|\frac{\partial}{\partial R}\Pi^{j}_{1/2}\right\rangle} \\ &= \left\|\frac{\partial}{\partial R}\left|\Pi^{j}_{1/2}\right\rangle\right\|\end{aligned} \tag{262}$$

Thus we see that the physically meaningful quantity is the norm of the DCTs. This norm, as we shall presently show, is the true DCT for a rotated basis.

From the four $\left|\Pi_{1/2}\right\rangle$ wavefunctions to the four $\left|\Sigma_{1/2}\right\rangle$ wavefunctions there are a total of 16 different DCTs, represented within the matrix

$$\mathbf{p} = \begin{pmatrix} \left\langle\Pi^{1}_{1/2}\middle|\frac{\partial}{\partial R}\Sigma^{1}_{1/2}\right\rangle & \left\langle\Pi^{1}_{1/2}\middle|\frac{\partial}{\partial R}\Sigma^{2}_{1/2}\right\rangle & \left\langle\Pi^{1}_{1/2}\middle|\frac{\partial}{\partial R}\Sigma^{3}_{1/2}\right\rangle & \left\langle\Pi^{1}_{1/2}\middle|\frac{\partial}{\partial R}\Sigma^{4}_{1/2}\right\rangle \\ \left\langle\Pi^{2}_{1/2}\middle|\frac{\partial}{\partial R}\Sigma^{1}_{1/2}\right\rangle & \left\langle\Pi^{2}_{1/2}\middle|\frac{\partial}{\partial R}\Sigma^{2}_{1/2}\right\rangle & \left\langle\Pi^{2}_{1/2}\middle|\frac{\partial}{\partial R}\Sigma^{3}_{1/2}\right\rangle & \left\langle\Pi^{2}_{1/2}\middle|\frac{\partial}{\partial R}\Sigma^{4}_{1/2}\right\rangle \\ \left\langle\Pi^{3}_{1/2}\middle|\frac{\partial}{\partial R}\Sigma^{1}_{1/2}\right\rangle & \left\langle\Pi^{3}_{1/2}\middle|\frac{\partial}{\partial R}\Sigma^{2}_{1/2}\right\rangle & \left\langle\Pi^{3}_{1/2}\middle|\frac{\partial}{\partial R}\Sigma^{3}_{1/2}\right\rangle & \left\langle\Pi^{3}_{1/2}\middle|\frac{\partial}{\partial R}\Sigma^{4}_{1/2}\right\rangle \\ \left\langle\Pi^{4}_{1/2}\middle|\frac{\partial}{\partial R}\Sigma^{1}_{1/2}\right\rangle & \left\langle\Pi^{4}_{1/2}\middle|\frac{\partial}{\partial R}\Sigma^{2}_{1/2}\right\rangle & \left\langle\Pi^{4}_{1/2}\middle|\frac{\partial}{\partial R}\Sigma^{3}_{1/2}\right\rangle & \left\langle\Pi^{4}_{1/2}\middle|\frac{\partial}{\partial R}\Sigma^{4}_{1/2}\right\rangle \end{pmatrix} \tag{263}$$

In reality, $\mathbf{p}$ is an off-diagonal submatrix of the entire DCT matrix for all wavefunctions; however, if we are only interested in the coupling between the $\left\{\Pi^{j}_{1/2}\right\}$ space and the

$\left\{\Sigma^i_{1/2}\right\}$ space, we need only consider the matrix formed between these eight wavefunctions and their duals, for which the diagonal blocks are zero:

$$\mathbf{P} = \begin{pmatrix} 0 & \mathbf{p} \\ -\mathbf{p}^\dagger & 0 \end{pmatrix} \tag{264}$$

If we assume that $\mathbf{p}$ is not singular, then there exists a similarity transformation by which it may be diagonalized:

$$\mathbf{p}^d = \mathbf{v}^{-1}\mathbf{p}\,\mathbf{v} \tag{265}$$

It follows that the off-diagonal blocks of the matrix $\mathbf{P}$ can be diagonalized by the transformation

$$\mathbf{P}' \equiv \begin{pmatrix} 0 & \mathbf{p}^d \\ -\mathbf{p}^{d\dagger} & 0 \end{pmatrix} = \begin{pmatrix} \mathbf{v}^{\dagger -1} & 0 \\ 0 & \mathbf{v} \end{pmatrix}^\dagger \begin{pmatrix} 0 & \mathbf{p} \\ -\mathbf{p}^\dagger & 0 \end{pmatrix} \begin{pmatrix} \mathbf{v}^{\dagger -1} & 0 \\ 0 & \mathbf{v} \end{pmatrix} \tag{266}$$

We now find $\mathbf{P}'$ in a new basis in which the original, arbitrarily rotated and phased wavefunctions have been re-rotated to yield a *canonical* set of wavefunctions $\left\{\left|\Pi'_{1/2}\right\rangle\right\}$ and $\left\{\left|\Sigma'_{1/2}\right\rangle\right\}$. This transformation has reduced the number of DCTs from sixteen to four (the four eigenvalues of the off-diagonal block), each of which couples only one $\left|\Pi'_{1/2}\right\rangle$ wavefunction to only one $\left|\Sigma'_{1/2}\right\rangle$ wavefunction. Considering that now each row and column of $\mathbf{P}'$ contains only one non-zero element, equation (260) tells us that each $\frac{\partial}{\partial R}\left|\Pi'^{j}_{1/2}\right\rangle$ is collinear with a distinct $\left|\Sigma'^{i}_{1/2}\right\rangle$, and that the length of the derivative wavefunction is the DCT. Since the wavefunctions in each respective space are, for our

purposes, indistinguishable, there should be no distinction of the coupling between any two pairs, and we should expect all four new DCTs to have the same magnitude.

As an example of the preceeding discussion, consider the DCTs of the K He system at 5.0 Å (9.4 bohr). The calculated DCTs are found in the matrix

$$\mathbf{p} = \begin{pmatrix} 6.68\times10^{-6} & -2.42\times10^{-6} & -1.72\times10^{-4} & 5.11\times10^{-2} \\ -5.10\times10^{-2} & 1.63\times10^{-5} & -6.51\times10^{-6} & 5.33\times10^{-6} \\ -5.54\times10^{-6} & 1.04\times10^{-3} & 5.11\times10^{-2} & 1.75\times10^{-4} \\ -1.84\times10^{-5} & -5.11\times10^{-2} & 1.04\times10^{-3} & 1.56\times10^{-6} \end{pmatrix} \tag{267}$$

which is diagonalized by the matrix

$$\mathbf{v} = \begin{pmatrix} 3.47\times10^{-3} - 4.09\times10^{-1}i & 4.80\times10^{-4} + 4.08\times10^{-1}i & 7.06\times10^{-1} & 9.88\times10^{-3} - 4.09\times10^{-1}i \\ 3.47\times10^{-3} + 4.09\times10^{-1}i & 4.80\times10^{-1} - 4.08\times10^{-1}i & 7.06\times10^{-1} & 9.88\times10^{-3} - 4.09\times10^{-1}i \\ 5.78\times10^{-1} & 2.89\times10^{-1} + 5.00\times10^{-1}i & 1.02\times10^{-3} - 7.34\times10^{-3}i & -2.89\times10^{-1} + 5.00\times10^{-1}i \\ 5.78\times10^{-1} & 2.89\times10^{-1} - 5.00\times10^{-1}i & 1.02\times10^{-3} + 7.34\times10^{-3}i & -2.89\times10^{-1} - 5.00\times10^{-1}i \end{pmatrix} \tag{268}$$

When the matrix $\mathbf{P}$ built from the matrix in equiation (267) is subjected to the transformation in equation (266), the resultant DCT matrix is

$$\mathbf{P}' = \begin{pmatrix} 0 & 0 & 0 & 0 & 5.11\times10^{-2} - 5.05\times10^{-4}i & 0 & 0 & 0 \\ 0 & 0 & 0 & 0 & 0 & 5.11\times10^{-2} + 5.05\times10^{-4}i & 0 & 0 \\ 0 & 0 & 0 & 0 & 0 & 0 & -2.55\times10^{-2} - 4.43\times10^{-2}i & 0 \\ 0 & 0 & 0 & 0 & 0 & 0 & 0 & -2.55\times10^{-2} + 4.43\times10^{-2}i \\ -5.11\times10^{-2} - 5.05\times10^{-4}i & 0 & 0 & 0 & 0 & 0 & 0 & 0 \\ 0 & -5.11\times10^{-2} + 5.05\times10^{-4}i & 0 & 0 & 0 & 0 & 0 & 0 \\ 0 & 0 & 2.55\times10^{-2} - 4.43\times10^{-2}i & 0 & 0 & 0 & 0 & 0 \\ 0 & 0 & 0 & 2.55\times10^{-2} + 4.43\times10^{-2}i & 0 & 0 & 0 & 0 \end{pmatrix} \tag{269}$$

While each of the DCTs in $\mathbf{P}'$ is complex, we have the option of effecting an arbitrary phase rotation between each pair of wavefunctions, allowing us to remove the imaginary portion of each DCT:

$$\mathbf{P}' = \begin{pmatrix} 0 & 0 & 0 & 0 & -0.0511 & 0 & 0 & 0 \\ 0 & 0 & 0 & 0 & 0 & -0.0511 & 0 & 0 \\ 0 & 0 & 0 & 0 & 0 & 0 & -0.0511 & 0 \\ 0 & 0 & 0 & 0 & 0 & 0 & 0 & -0.0511 \\ 0.0511 & 0 & 0 & 0 & 0 & 0 & 0 & 0 \\ 0 & 0.0511 & 0 & 0 & 0 & 0 & 0 & 0 \\ 0 & 0 & 0.0511 & 0 & 0 & 0 & 0 & 0 \\ 0 & 0 & 0 & 0.0511 & 0 & 0 & 0 & 0 \end{pmatrix} \tag{270}$$

As hypothesized, we see that, in the canonical basis, the DCTs between each distinct pair of wavefunctions are indeed of the same magnitude. From this exercise we also conclude that we need only calculate four DCTs, not sixteen. From the four distinct elements of any given row or column of the DCT matrix, we can calculate a Euclidean norm, which is the DCT in the canonical basis.The radial DCT in the canonical basis, calculated as the norm of the DCTs in the first row of $\mathbf{P}$, is shown in Figure 32.

Adiabatic Mixing Angle

This exercise has shown that, despite the eight wavefunctions involved, we are effectively seeking the adiabatic mixing angle for only two wavefunctions and so we can calculate the adiabatic mixing angle according to equation (103). Figure 33 shows the result of that integration (as integrated from $R = \infty$). Figure 34 shows the non-adiabatic surfaces and the resultant mixed diabatic surfaces. Figure 35 shows the off-diagonal diabatic coupling surface. The strength of the coupling surface depends upon both the size of the coupling angle and the energy difference between the two adiabatic surfaces; thus the coupling surface continues to grow well past the area where DCTs are strong, into a region which, for most interactions, would be energetically disallowed. These are the surfaces that may be used in nuclear dynamics calculations.

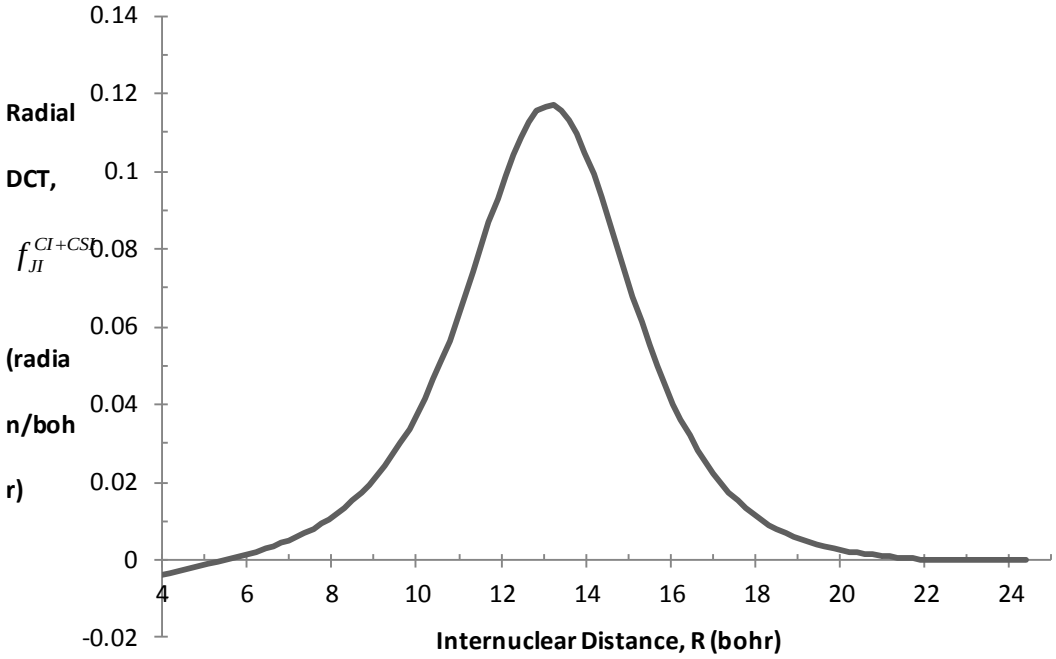

Figure 32. Radial DCT between $\Pi_{1/2}$ and $\Sigma_{1/2}$ states

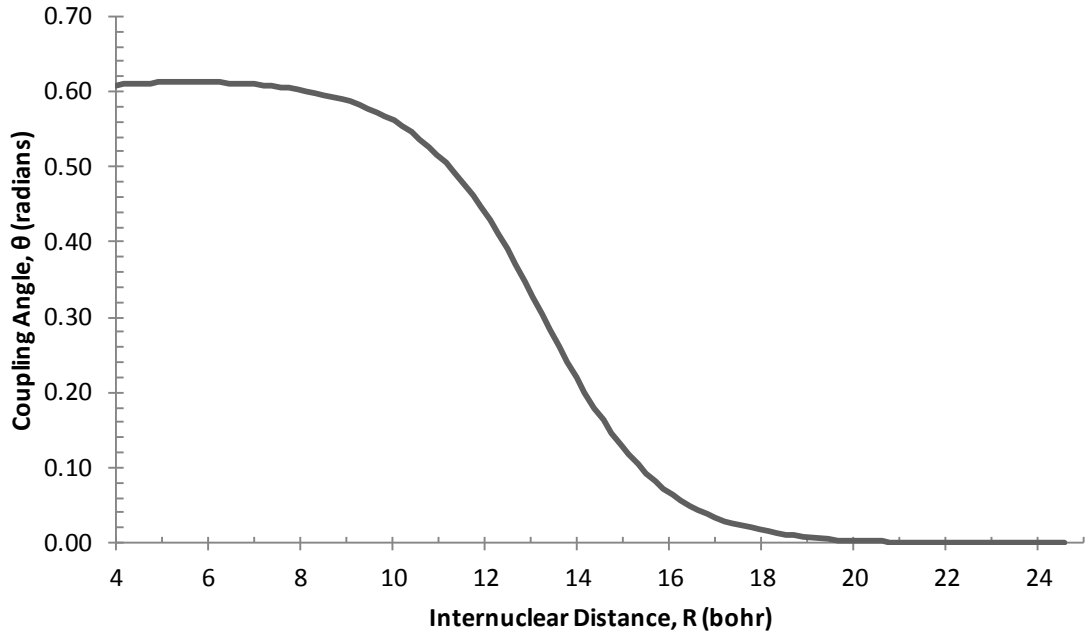

Figure 33. Radial coupling angle between $\Pi_{1/2}$ and $\Sigma_{1/2}$ states

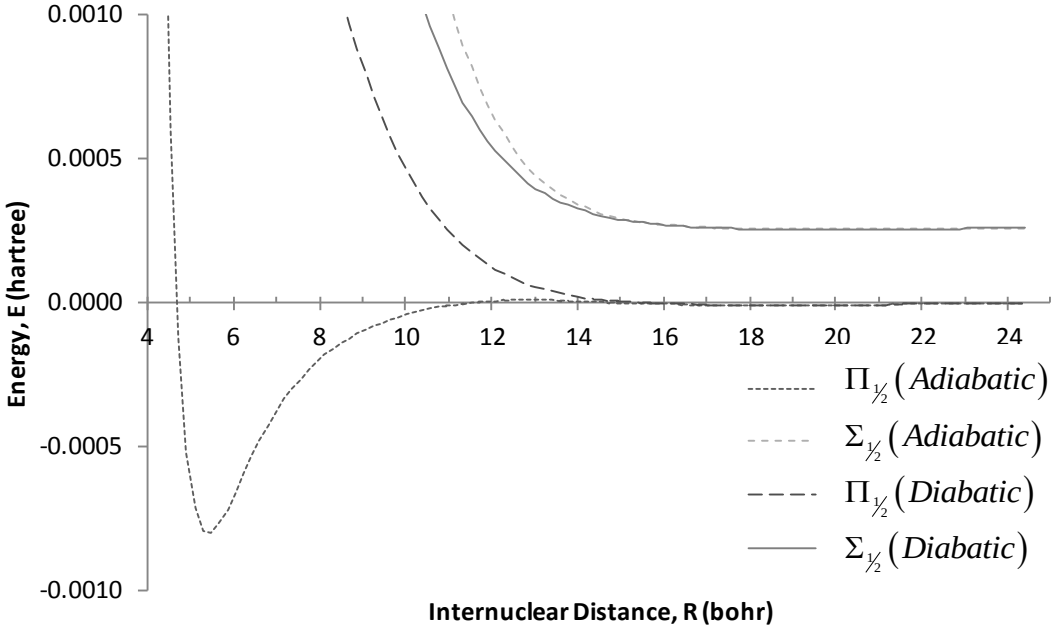

Figure 34. Diabatic vs adiabatic K He surfaces

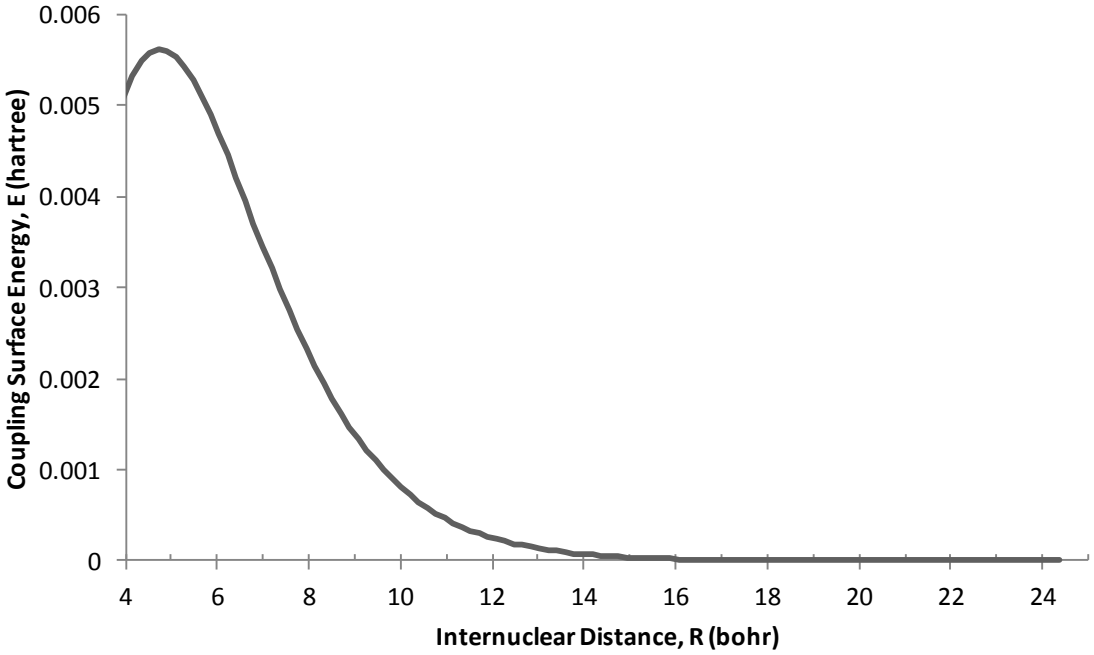

Figure 35. Diabatic K He coupling surface

Validation

We have two sources of validation of our DCT calculations. First, since the analytic gradient algorithm is such a large part of the DCT algorithm, the correct gradients in the previous section speak to the fidelity of the DCTs calculated with the same code. Second, Werner established a method to estimate the coupling angle using the MRCI wavefunction coefficients [**12**]:

$$\theta_{\Sigma_{1/2}-\Pi_{1/2}} \approx \arcsin\left(\frac{\sqrt{\sum_{i\in\Pi_{1/2}}\left(c_i^{\Sigma_{1/2}}\right)^2}}{\sum_i\left(c_i^{\Sigma_{1/2}}\right)^2}\right) \tag{271}$$

where the Euclidean norm is taken of the coefficients of the $\Sigma_{1/2}$ eigenvector, $c_i^{\Sigma_{1/2}}$, which coincide with CSFs that have $\Pi_{1/2}$ symmetry (for simplicity, only the reference CSFs are considered in an MRCI calculation). We can generalize this method to spin-orbit wavefunctions by using the Euclidean norm of all coefficients pertaining to CSFs whose physical occupation is appropriate. Figure 36 shows our calculated mixing angle compared to the angle estimated via the Werner method. Similarly, Figure 37 compares our DCT calculation with the derivative of Werner's angle. The Werner angle matches the angle calculated with the DCTs by less than 0.02 radians, an acceptable error given the rudimentary nature of the approximation.

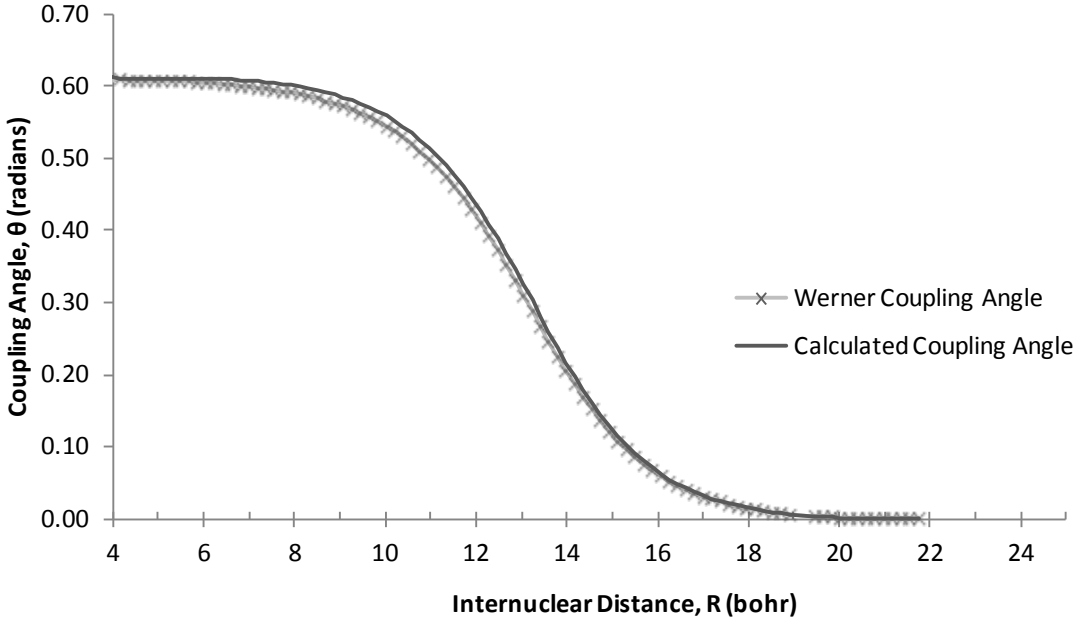

Figure 36. Coupling angle as calculated via DCTs vs. calculated via CI coefficients

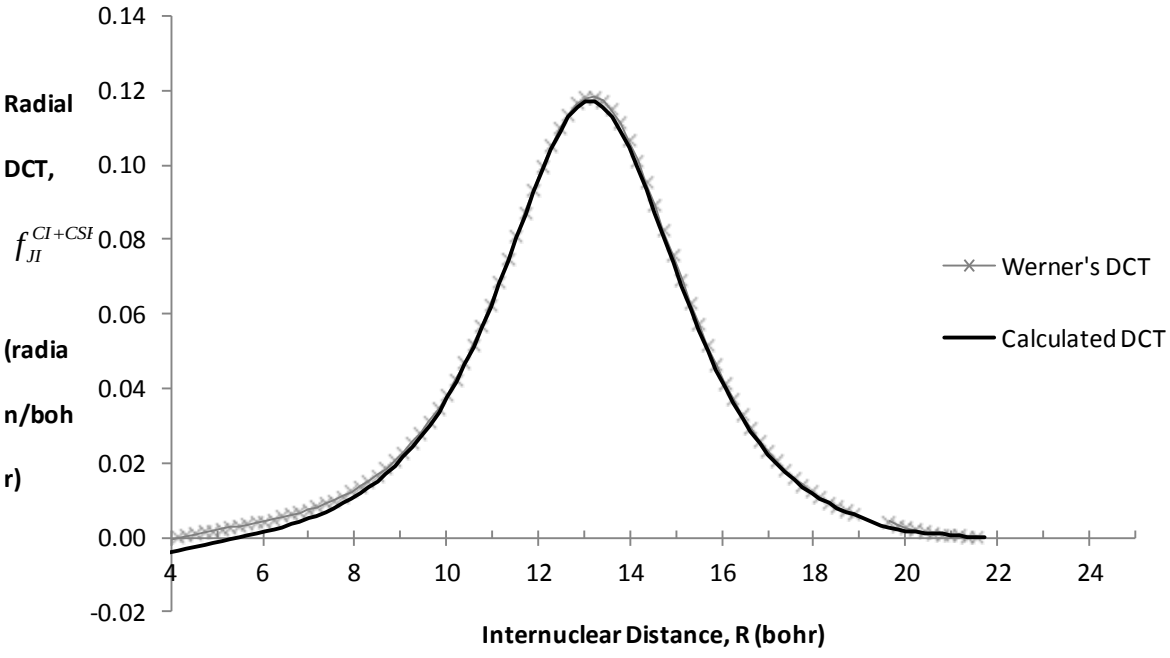

Figure 37. DCT as calculated vs. derivative of Werner's angle

V. Conclusion

A tool has been developed to calculate energy gradients and DCTs of spin-orbit wavefunctions at the MRCI level. While several approximation methods have been in place, no method has been available that actually calculates these quantities for spin-orbit CI wavefunctions until now. This work makes such a method available, having been aggregated to the MRCI, DCT, and spin-orbit methods already in place in COLUMBUS.

With this formalism in place, spin-orbit energy gradients and DCTs can now be analytically calculated for large-atom systems where spin-orbit contributions to the Hamiltonian are non-negligible, such as open-shell systems like the Alkali-noble-gas mixtures that may be used in a DPAL. While the energy gradients will be useful in geometry optimization problems, the DCTs will provide diabatic potential energy surfaces for nuclear dynamics calculations.

K He

We have calculated such surfaces specifically for the K He system. The maximum derivative coupling for K He appears to occur well outside the energy well of the $\Pi_{1/2}$ manifold (13.2 bohr separation), indicating that, despite its small magnitude (0.117 radian/bohr), the derivative coupling may play a non-negligible role in the dynamics, and should be taken into account for a relevant DPAL-related analysis. Additionally, the coupling surface (Figure 35) becomes non-negligible at about the same geometry and

continues to grow well into the repulsion wall, indicating that coupling may continue to manifest itself throughout the potential well. While the DCT and coupling surface provide some insight, the true value of this sample calculation won't be known until these surfaces are used for wave packet propagation.

Werner's Coupling Angle

While we have used Werner's method of approximating the coupling angle [**12**] to validate our COLUMBUS calculations, our conclusions also speak strongly to the utility of the Werner angle. From our results, we may conclude that the Werner method has been successfully extended to apply to spin-orbit MRCI wavefunctions. While a single point calculation of K He required on the order of 24 CPU-hours to compute the DCT-derived coupling angle, calculation of the Werner angle required approximately half of that time. This work has shown that, depending on the fidelity one requires, it may be preferable in future calculations to simply compute the Werner angle rather than the DCTs in the interest of resource management. This recommendation comes with the caveat that the ease of calculation of the Werner angle depends on the complexity of the DRT and of the molecular geometry. For sufficiently complex molecules, this may not be a feasible calculation, and the interested party may need to return to the DCT-based calculation.

Recommendations for Further Work

This dissertation is not an end in and of itself, but has provided a tool for many future works.

Spin-Orbit Density Matrix

In the formalism presented here, we have introduced a new mathematical tool, the spin-orbit density matrix (see, e.g., equation (185)). While the standard one-electron density matrix exhibits a number of interesting properties (e.g., the trace is equal to the total number of electrons, and each diagonal element gives the approximate electron occupation of a given orbital), we have not, in this work, explored the full meaning and properties of the spin-orbit density matrix. Such an exploration could bring new understanding and utility to the spin-orbit density matrix.

Relativistic Geometry Optimization

With the energy gradient method in place, it will certainly prove enlightening to compare current non-relativistic optimized geometries to those calculated with the spin-orbit Hamiltonian. This analysis could reveal how important the spin-orbit effects are to the geometries of simple diatoms to complex proteins.

Wave Packet Propagation

The diabatic surfaces computed herein may now be used in wave packet propagation methods to further explore the dynamics of K He. The diabatic surfaces of similar systems, such as Rb He and Cs He can also be calculated with similar resources and likewise employed.

Analysis of Angular DCTs

Because of our interest in the radial coupling mechanism, this dissertation has primarily focused on the radial DCT, which is calculated as the z-component of the position of either the potassium or helium atom changes. However, the DCT is truly a multi-atom gradient with a different component for each of the six coordinates (in the case of K He). Figure 38 shows the remaining off-axis DCTs of K He. The first property to

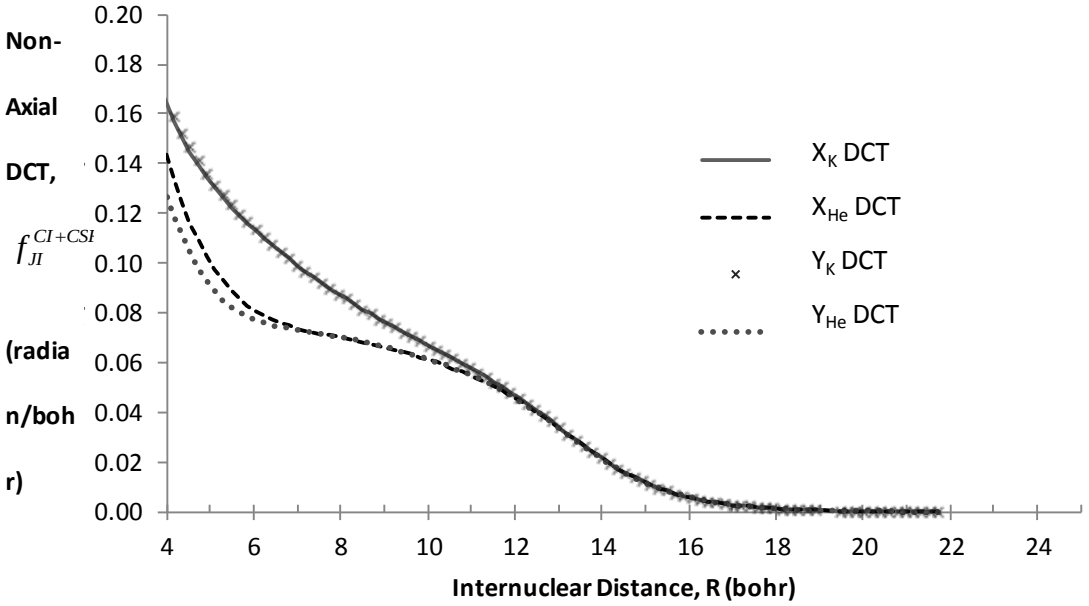

Figure 38. X- and Y-DCTs of K He

note is that movement of the helium or potassium produces different couplings, which is to be expected as these are not symmetric atoms. One should also note that, despite the supposed symmetry around the axis, the X- and Y- DCTs for helium are not equal as

the geometry approaches the repulsion wall. This unexpected phenomenon may be an artifact of forcing the use of C_1 symmetry. When using this symmetry, all states in the SA-MCSCF step are in the same irrep, and must be unequally weighted in order to account for the effects of orbital resolution on the density matrices (consider equations (202) and (203)). Whether this compromise, or one like it, is the cause for the difference in the X- and Y-DCTs, cannot be known without further exploration; however, given the agreement with the Werner coupling angle, the answer seems to have no impact on the fidelity of the radial DCT.

The Cartesian DCTs can be transformed to three internal DCTs (radial and two angular) and three center-of-mass DCTs by means of a Jacobi transformation [**54**]. The angular DCTs, shown in Figure 39, are of the form $\left\langle \Pi^i_{1/2} \left| \frac{\partial}{\partial\theta} \right| \Sigma^j_{1/2} \right\rangle$, and are in fact an off-diagonal element of the nuclear angular momentum operator, $\hat{J}^n$. This equivalence can provide another source of validation of the DCTs, if $\hat{J}^n$ can be calculated in an alternative manner. Yarkony [**55**] contends that if an operator, such as total angular momentum, commutes with the Hamiltonian,

$$\left[\hat{H}, \hat{J}\right] = 0 \tag{272}$$

then it is true that

$$\begin{aligned} 0 &= \left\langle \Psi_I \left| \left[\hat{H}, \hat{J}\right] \right| \Psi_J \right\rangle \\ &= E_I \left\langle \Psi_I \left| \hat{J} \right| \Psi_J \right\rangle - \left\langle \Psi_I \left| \hat{J} \right| \Psi_J \right\rangle E_J \\ &= \left(E_I - E_J\right) \left\langle \Psi_I \left| \hat{J} \right| \Psi_J \right\rangle \end{aligned} \tag{273}$$

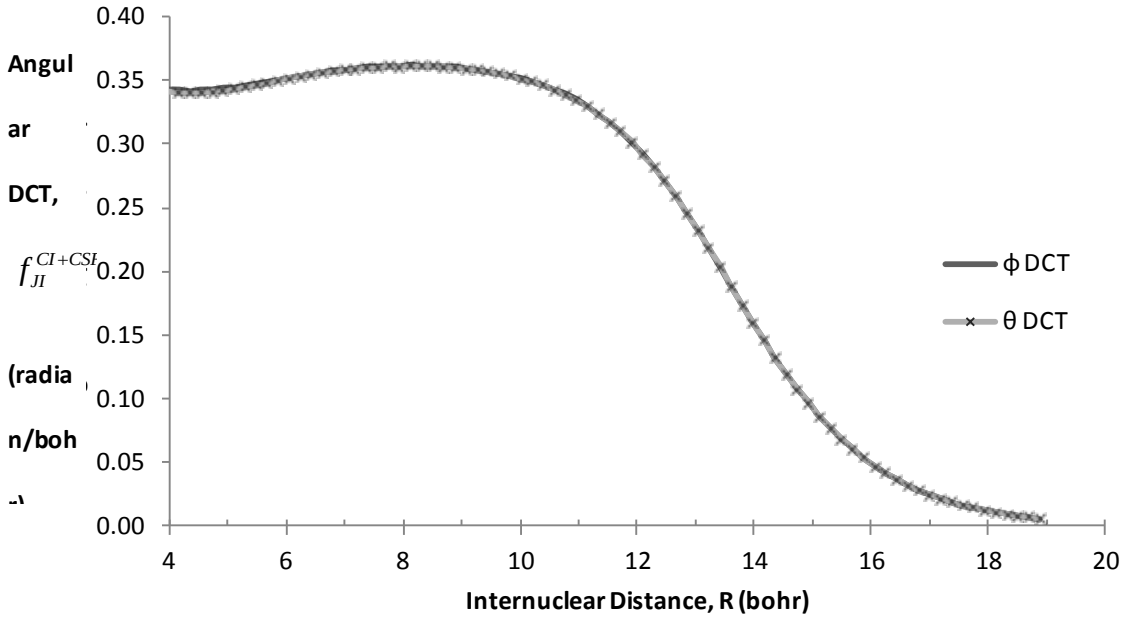

Figure 39. Angular DCTs of K He

If we consider that this total operator consists of both nuclear and electronic components,

$$\hat{J} = \hat{J}^n + \hat{J}^e \tag{274}$$

then equation (273) implies that

$$\langle \Psi_I | \hat{J}^n | \Psi_J \rangle = -\langle \Psi_I | \hat{J}^e | \Psi_J \rangle \tag{275}$$

That is, the representation of the nuclear angular momentum operator (or angular DCTs) is equal and opposite to the representation of the electronic angular momentum operator. In non-relativistic MRCI calculations, since spin is not considered, the total angular momentum is $\hat{L}$, the orbital angular momentum. The comparison of angular DCTs to $\hat{L}_e$ is readily made, as its matrix elements are quickly calculated by COLUMBUS

from the available orbital angular momentum integrals. However, for the spin-orbit Hamiltonian, in which orbital angular momentum is not a good quantum number, equation (272) does not hold for $\hat{L}$, but rather for total angular momentum, $\hat{L}+\hat{S}$. Spin integrals, unlike orbital angular momentum integrals, are not readily available in NWCHEM or COLUMBUS, and so a comparison of the angular DCTs to electronic angular momentum is not possible at this time. If NWCHEM's integral program can be modified to produce the spin integrals, and COLUMBUS to produce the elements of the spin operator, then another source of validation of the DCTs would be available.

Appendix A. The Hamiltonian

This appendix provides a brief introduction to the energy operator, or *Hamiltonian.* Energy is important because it drives the dynamics of a system, the understanding of which is the ultimate goal of this research.

> The reason for the preeminent position of energy eigenfunctions in the theory is, of course, that they form the stationary states of isolated systems in which energy must be conserved. . . . Moreover, because of their simple time dependence. . . they can be used to build up a description of the time evolution of non-stationary systems as well. [**56**]

Origin

Formally, the Hamiltonian is derived from the Lagrangian via the Legendre transformation [**25**]:

$$H(q,p,t)=\sum_i \dot{q}_i p_i - L(q,\dot{q},t) \tag{276}$$

where q, $\dot{q}$, and p are generalized position, velocity, and momentum, respectively, and the Lagrangian is defined as the difference of kinetic and potential energies:

$$L=T-V \tag{277}$$

However, when the Lagrangian of a system can be expressed as a sum of functions which do not mix degrees of generalized velocities, that is,

$$L=L_0(q,t)+L_1(q,\dot{q},t)+L_2(q,\dot{q},t) \tag{278}$$

where L_1 is of first degree in $\dot{q}$ and L_2 is of second degree in $\dot{q}$, then the Hamiltonian is just the total energy:

$$H = T + V \tag{279}$$

In our quantum mechanical treatment of nuclei and electrons, the kinetic energy will only depend upon the square of the velocity and the potential energy will have no velocity dependence, and so it follows that the Lagrangian does indeed take the form of equation (278), and thus the Hamiltonian will take the form of equation (279). Although the above equations are classical in nature, often the procedure for creating quantum mechanical formulae is to merely replace the classical functions with operators [**26**]. This will be the case for the Hamiltonian operator, which will take the form

$$\hat{H} = \hat{T} + \hat{V} \tag{280}$$

Kinetic and Potential Energy Operators

From the classical, non-relativistic analog, the kinetic energy operator will take on the form

$$\hat{T} = \frac{\hat{p}^2}{2m} \tag{281}$$

where $\hat{p}$ is the (linear) momentum operator. To extract the form of the momentum operator in position-space, first consider that diffraction experiments indicate that a free particle with a known momentum has a wavefunction of the form [**40**]

$$\psi(\vec{r},t) = \exp\left[\frac{i}{\hbar}\left(\vec{p}\cdot\vec{r} - \varepsilon t\right)\right] \tag{282}$$

where $\vec{r}$ is the position, ε is the energy, and $\hbar$ is the reduced Planck's constant. It is a postulate of quantum mechanics that the operator of an observable quantity is

hermitian, and thus obeys an eigenvalue equation with real eigenvalues [**26**]; in the case of momentum and energy,

$$\begin{aligned} \hat{p}\psi &= p\psi \\ \hat{H}\psi &= \varepsilon\psi \end{aligned} \tag{283}$$

To preserve these relationships, the momentum operator in the position-space representation (as opposed to the momentum- or k-space representation) and the energy operator take the form

$$\begin{aligned} \hat{p} &\to -i\hbar\nabla \\ \hat{H} &\to i\frac{\partial}{\partial t} \end{aligned} \tag{284}$$

and so the non-relativistic Hamiltonian will always contain a second spatial derivative.

The form of the potential energy operator will depend on the nature of the particular system; however, we can say generally that it will be a function of position but not of velocity,

$$\hat{V} \to V\left(\vec{r}\right) \tag{285}$$

(in the case of a free particle, this potential is zero). Thus we can cast the Hamiltonian as a solvable differential equation in position space,

$$H = -\frac{\hbar^2}{2m}\nabla^2 + V\left(\vec{r}\right) \tag{286}$$

The Schrödinger Equation

The Schrödinger wave equation defines the relationship between the time derivative of a wavefunction and its spatial derivative. For a single particle, it is

$$H\psi = \left(-\frac{\nabla^2}{2m} + V(\vec{r}) \right) \psi = i \frac{\partial}{dt} \psi \tag{287}$$

and is one of the postulates of quantum mechanics [**26**]. In equation (284) we found that the energy operator is expressed as $i \frac{\partial}{\partial t}$, which also appears on the right-hand side of equation (287) with eigenvalues of energy, ε (see equation (283)). Consequently, the time-derivative operator can be replaced by its eigenvalues, and the Schrödinger equation itself takes the form of an eigenvalue equation,

$$H\psi = \left(-\frac{\nabla^2}{2m} + V(\vec{r}) \right) \psi = \varepsilon \psi \tag{288}$$

This is the *time-independent Schrödinger equation* [**26**]. The Hamiltonian may change from system to system, but the basic eigenvalue relationship with the wavefunctions and energy will remain. It is this eigenvalue relationship that drives the mathematics of quantum chemistry.

Appendix B. The Breit-Pauli Hamiltonian

The Dirac Equation

Quantum chemistry relies on approximate solutions of the Schrödinger equation, which itself can be considered an approximation. If wielded carefully, this equation will yield most of the information about the energy of a system; however, in some cases it is insufficient for the accuracy required. By assuming the kinetic energy takes the form in equation (281), which leads to the Hamiltonian in equation (8), we have neglected some of the less significant, relativistic effects one finds when electron speed approaches a non-negligible fraction of the speed of light.

Close scrutiny of the Schrödinger equation ((288)) reveals that it is not Lorentz invariant; that is, it does not treat space and time on equal footing. A more suitable equation for exploring relativistic effects is the *Dirac equation for a single electron* [**57**]

$$\left(c\vec{\alpha} \cdot \left(\hat{p} + \frac{1}{c}\vec{A} \right) + \beta c^2 - \varphi \right) \vec{\psi} = i \frac{\partial}{\partial t} \vec{\psi} \tag{289}$$

where $\vec{A}$ is the vector potential, φ is the scalar electrostatic potential, $\vec{\alpha}$ is a three-component vector of 4x4 matrices, and β is a single 4x4 matrix [**57**]. Although at first glance this equation appears to be the Schrödinger equation with a different Hamiltonian, the matrix nature of the equation means that the solutions, $\vec{\psi}$, are four-component *spinors* rather than scalar wavefunctions. The electrostatic potential may include the nuclear potential, and the vector potential has been included in the *canonical* or *generalized momentum* [**58**] [**59**]. Since the momentum only appears once,

the Dirac equation has only a first spatial derivative, symmetric to the first time derivative. Solutions to the Dirac equation simultaneously satisfy the simple relativistic wave equation, the Klein-Gordon equation, the continuity equation, and the principle of linear superposition [**57**].

The Breit Equation

When introducing additional electrons, an electron interaction term must be added to equation (289). The non-relativistic two-electron operator,

$$-\tfrac{1}{2}\sum_{i,j}\frac{1}{r_{ij}} \tag{290}$$

where $r_{ij}=\left|\vec{r}_i-\vec{r}_j\right|$, assumes instantaneous Coulombic forces and thus is not Lorentz invariant. A fully covariant description of the electron interaction lies in the complicated Bethe-Salpeter equation [**60**]. A truncation of the expansion of that equation leads to the *Breit operator*

$$\varphi_i=\sum_{\alpha,i}\frac{Z_\alpha}{\vec{r}_{\alpha i}}\,\tfrac{1}{2}\sum_{i,j}\frac{1}{r_{ij}}-\frac{1}{2r_{ij}}\left(\vec{\alpha}_i\cdot\vec{\alpha}_j+\frac{\left(\vec{\alpha}_i\cdot r_{ij}\right)\left(\vec{\alpha}_j\cdot r_{ij}\right)}{r_{ij}^2}\right) \tag{291}$$

which, while not completely Lorentz-invariant, is correct to the order of α^4, where α is the fine structure constant ($=c^{-1}$) [**60**]. Since this operator involves the direct product of the $\vec{\alpha}$ matrices, it will involve 16x16 matrices. The resulting electronic Hamiltonian (*cf.* equation (8)) is

$$\hat{H}_e = \sum_i \left(c\vec{\alpha}_i \cdot \left(\hat{p}_i + \frac{1}{c}\vec{A}_i \right) + \beta_i c^2 \right) + \tfrac{1}{2}\sum_{i,j} \left(\frac{1}{r_{ij}} - \frac{1}{2r_{ij}} \left(\vec{\alpha}_i \cdot \vec{\alpha}_j + \frac{\left(\vec{\alpha}_i \cdot r_{ij}\right)\left(\vec{\alpha}_j \cdot r_{ij}\right)}{r_{ij}^2} \right) \right) - \sum_{\alpha,i} \frac{Z_\alpha}{\vec{r}_{\alpha i}} \quad (292)$$

The potential term involving the nuclei retains its non-relativistic form and is included in the electrostatic potential term in equation (289):

$$\varphi_i = \sum_{\alpha,i} \frac{Z_\alpha}{\vec{r}_{\alpha i}} \quad (293)$$

By means of a Foldy-Wouthuysen transform, the Hamiltonian is reduced into this final form, the *Breit-Pauli Hamiltonian* [**60**]:

$$\begin{aligned} \hat{H}_e = \sum_i & c^2 - \varphi_i + \frac{\pi_i^2}{2} - \frac{\pi_i^4}{8c^2} + \tfrac{1}{2}\left(\vec{\sigma}_i \cdot \vec{B}_i\right) - \frac{1}{8c^2}\vec{\sigma}_i \cdot \left(\vec{\pi}_i \times \vec{E}_i - \vec{E}_i \times \vec{\pi}_i\right) \\ & - \frac{\pi_i^2}{4c^2}\left(\vec{\sigma}_i \cdot \vec{B}_i\right) + \frac{1}{8c^2}\left(\nabla \cdot \vec{E}_i\right) + \tfrac{1}{2}\sum_{i,j} \frac{1}{r_{ij}} - \frac{1}{2c^2 r_{ij}} \left(\left(\vec{\pi}_i \cdot \vec{\pi}_j\right) + \frac{\left(\vec{\pi}_i \cdot \vec{r}_{ij}\right)\left(\vec{\pi}_j \cdot \vec{r}_{ij}\right)}{r_{ij}^2} \right) \\ & - \frac{1}{4c^2 r_{ij}^3}\left[\vec{\sigma}_i \cdot \left(\vec{r}_{ij} \times \vec{\pi}_i\right) - \vec{\sigma}_j \cdot \left(\vec{r}_{ij} \times \vec{\pi}_j\right)\right] + \frac{1}{2c^2 r_{ij}^3}\left[\vec{\sigma}_i \cdot \left(\vec{r}_{ij} \times \vec{\pi}_j\right) - \vec{\sigma}_j \cdot \left(\vec{r}_{ij} \times \vec{\pi}_i\right)\right] \end{aligned} \quad (294)$$

where $\vec{\pi}_i$ is the gauge-covariant momentum of electron *i* [**32**], $\vec{E}_i\left(\vec{B}_i\right)$ is the total electric(magnetic) field at electron *i*, and $\vec{\sigma}_i$ is the spin of the i^{th} electron. Tinkham justifies this simplification to the Breit-Pauli Hamiltonian by the relatively low energies addressed in quantum chemistry [**56**].

This Hamiltonian can be sorted into seven operators:

1. The non-relativistic Hamiltonian

$$H_0 = \sum_i \frac{p_i^2}{2} - \varphi_i + \tfrac{1}{2}\sum_{ij} \frac{1}{r_{ij}} \quad (295)$$

2. The mass-velocity correction term

$$H_1 = -\sum_i \frac{p_i^4}{8c^2} \tag{296}$$

3. The orbit-orbit term

$$H_2 = -\tfrac{1}{2}\sum_{i,j} \frac{1}{2c^2 r_{ij}} \left(\left(\vec{p}_i \cdot \vec{p}_j \right) + \frac{\left(\vec{p}_i \cdot \vec{r}_{ij} \right)\left(\vec{p}_j \cdot \vec{r}_{ij} \right)}{r_{ij}^2} \right) \tag{297}$$

4. The spin-orbit term

$$H_3 = \frac{1}{2c^2} \left[\sum_i \vec{\sigma}_i \cdot \left(\vec{E}_i \times \vec{p}_i \right) + \sum_{i,j} 2\vec{\sigma}_i \cdot \left(\frac{\vec{r}_{ij}}{r_{ij}^3} \times \vec{p}_j \right) \right] \tag{298}$$

5. The Darwin term

$$H_4 = \sum_i \frac{i}{4c^2} \left(\vec{p}_i \cdot \vec{E}_i \right) \tag{299}$$

6. The spin-spin term

$$H_5 = \tfrac{1}{2}\sum_{i,j} \frac{1}{c^2} \left[-\frac{2\pi}{3} \left(\vec{\sigma}_i \cdot \vec{\sigma}_j \right) \delta^3 \left(\vec{r}_{ij} \right) + \frac{1}{4r_{ij}^3} \left(\vec{\sigma}_i \cdot \vec{\sigma}_j - 3\frac{\left(\vec{\sigma}_i \cdot \vec{r}_{ij} \right)\left(\vec{\sigma}_j \cdot \vec{r}_{ij} \right)}{r_{ij}^2} \right) \right] \tag{300}$$

7. The external magnetic interaction term

$$H_6 = \tfrac{1}{c}\sum_i \tfrac{1}{2} \left(\vec{\sigma}_i \cdot \vec{B}_i \right) + \left(\vec{A}_i \cdot \vec{p}_i \right) \tag{301}$$

The electron rest-mass energy, c^2, also appears in the Hamiltonian, but will be ignored since it serves only as an energy offset. Although the Dirac equation acts on four-component spinors, the above seven terms have scalar functions as their eigenvectors. "[T]here is really no longer any serious difficulty in principle in writing down a basic Hamiltonian which is accurate enough for all practical purposes in extranuclear physics"

[**56**]. Thus, they can be appended to the non-relativistic Hamiltonian in the Schrödinger equation, leading to more accurate eigenvectors and eigenvalues.

Fine Structure and the Spin-Orbit Operator

The orders of magnitude of the H_1, H_3, and H_4 terms are on the order of α^2 times smaller than the non-relativistic Hamiltonian; these are grouped together as the *fine structure terms* [**61**]. The others are the *hyperfine structure terms,* and are at least an order of magnitude smaller than the fine structure terms [**61**]. For this reason, one can disregard the hyperfine structure terms and still get a much-improved solution compared to the non-relativistic Hamiltonian.

Let us focus on the spin-orbit term, H_3, as the other fine structure terms, H_1 and H_4, have little effect in the valence region. By dissecting the electric field term in equation (298), we can see the spin-orbit term separates into one- and two- electron pieces. The field is due both from the nuclei and the electrons:

$$\vec{E}_i = -\sum_{\alpha} \frac{Z_\alpha}{r_i^3} \vec{r}_i + \sum_j \frac{1}{r_{ij}^3} \vec{r}_{ij} \tag{302}$$

(where no external field is assumed) and so the cross product $\vec{E}_i \times \vec{p}_i$ is

$$\vec{E}_i \times \vec{p}_i = -\sum_{\alpha} \frac{Z_\alpha}{r_{i\alpha}^3} \left(\vec{r}_{i\alpha} \times \vec{p}_i \right) + \sum_j \frac{1}{r_{ij}^3} \left(\vec{r}_{ij} \times \vec{p}_i \right) \tag{303}$$

We recognize $\left(\vec{r}_{i\alpha} \times \vec{p}_i \right)$ as the orbital angular momentum of the i^{th} electron with respect to the α^{th} nucleus, and $\left(\vec{r}_{ij} \times \vec{p}_i \right)$ as the angular momentum of the i^{th} electron with respect to the j^{th} electron:

$$\begin{aligned}\left(\vec{r}_{i\alpha}\times\vec{p}_i\right)&\equiv\vec{L}_{i\alpha}\\ \left(\vec{r}_{ij}\times\vec{p}_i\right)&\equiv\vec{L}_{ij}\end{aligned}\tag{304}$$

Making these substitutions, equation (298) takes the form

$$H_3=\frac{1}{2c^2}\left[-\sum_{i\alpha}\frac{Z_\alpha}{r_{i\alpha}^3}\vec{\sigma}_i\cdot\vec{L}_{i\alpha}+\sum_{i,j}\frac{1}{r_{ij}^3}\vec{\sigma}_i\cdot\left(\vec{L}_{ij}-2\vec{L}_{ji}\right)\right]\tag{305}$$

Equation (305), more so than equation (298), shows the separate one- and two-electron spin-orbit terms. We can notate these as

$$\begin{aligned}h^{so}(i)&=-\frac{1}{2c^2}\sum_\alpha\frac{Z_\alpha}{r_{i\alpha}^3}\vec{\sigma}_i\cdot\vec{L}_{i\alpha}\\ g^{so}(i,j)&=\frac{1}{2c^2}\sum_j\frac{1}{r_{ij}^3}\vec{\sigma}_i\cdot\left(\vec{L}_{ij}-2\vec{L}_{ji}\right)\end{aligned}\tag{306}$$

The one-electron term grows rapidly with respect to nuclear size as compared to the two-electron term, and so the latter is less important for larger elements [**62**]. In any case, the effects of the two-electron term may be effectively included in the AREP. The revised electronic Hamiltonian is

$$H_e=-\sum_i\frac{\nabla_i^2}{2}+\tfrac{1}{2}\sum_{i,j}\frac{1}{\left|\vec{r}_i-\vec{r}_j\right|}-\sum_{\alpha,i}\left(\frac{Z_\alpha}{\left|\vec{r}_\alpha-\vec{r}_i\right|}-\frac{1}{c^2}\frac{Z_\alpha}{\left|\vec{r}_\alpha-\vec{r}_i\right|^3}\vec{\sigma}_i\cdot\vec{L}_{i\alpha}\right)\tag{307}$$

(again, *cf.* equation (8)).

Appendix C. Creation and Annihilation Operators

In this appendix, we discuss the creation and annihilation operators, used to second-quantize the Hamiltonian, in greater depth. While not a proof, this section employs a simple example involving small Slater determinants that the reader should find helpful in demonstrating their properties. In this section, we will use kets to represent both Slater determinants and functions—to differentiate, we leave electron dependence off of the determinant notation.

Annihilation

For a given function, we recognize that

$$|\chi_\alpha(i)\rangle\otimes|\chi_\beta(j)\rangle\otimes|\chi_\gamma(k)\rangle\otimes\ldots\equiv|\chi_\alpha(i)\chi_\beta(j)\chi_\gamma(k)\ldots\rangle \tag{308}$$

Consider the action of the operator

$$\sqrt{N}\sum_i\langle\chi_1(i)| \tag{309}$$

on an example Slater determinant,

$$|\chi_1\chi_2\chi_3\rangle\equiv\tfrac{1}{\sqrt{6}}\begin{vmatrix}|\chi_1(1)\rangle & |\chi_2(1)\rangle & |\chi_3(1)\rangle\\ |\chi_1(2)\rangle & |\chi_2(2)\rangle & |\chi_3(2)\rangle\\ |\chi_1(3)\rangle & |\chi_2(3)\rangle & |\chi_3(3)\rangle\end{vmatrix} \tag{310}$$

This is equal to

$$\begin{aligned}&\tfrac{1}{\sqrt{2}}\big(\langle\chi_1(1)|+\langle\chi_1(2)|+\langle\chi_1(3)|\big)\big(|\chi_1(1)\chi_2(2)\chi_3(3)\rangle-|\chi_1(1)\chi_3(2)\chi_2(3)\rangle+\\&|\chi_3(1)\chi_1(2)\chi_2(3)\rangle-|\chi_2(1)\chi_1(2)\chi_3(3)\rangle+|\chi_2(1)\chi_3(2)\chi_1(3)\rangle-|\chi_3(1)\chi_2(2)\chi_1(3)\rangle\big)\end{aligned} \tag{311}$$

A $\langle \chi_1(i)|$bra will only create a non-zero inner product with a ket that includes $|\chi_1(i)\rangle$ in its direct product. The resultant inner product will integrate out the i^{th} electronic variable since, by orthonormality, we assume

$$\left\langle \chi_\alpha(i) | \chi_\beta(i) \right\rangle = \delta_{\alpha\beta} \tag{312}$$

The resultant sum of functions is

$$\begin{aligned} &\tfrac{1}{\sqrt{2}}\left(|\chi_2(2)\chi_3(3)\rangle - |\chi_3(2)\chi_2(3)\rangle + |\chi_3(1)\chi_2(3)\rangle\right) - \\ &\tfrac{1}{\sqrt{2}}\left(|\chi_2(1)\chi_3(3)\rangle + |\chi_2(1)\chi_3(2)\rangle - |\chi_3(1)\chi_2(2)\rangle\right) \end{aligned} \tag{313}$$

While this does not appear to be a Slater determinant at first glance, when each *pair* of electrons is considered alone, we see that there are in fact three determinants:

$$|\chi_2\chi_3\rangle + |\chi_3\chi_2\rangle + |\chi_2\chi_3\rangle \tag{314}$$

Since $|\chi_2\chi_3\rangle = -|\chi_3\chi_2\rangle$, equation (314) reduces to the determinant $|\chi_2\chi_3\rangle$. Thus the operator in (309) has annihilated the χ_1 spin-orbital from the determinant. For that reason, we can equate it to an annihilation operator [**40**]:

$$\sqrt{N}\sum_i \langle \chi_1(i)| \equiv \hat{a}_1 \tag{315}$$

with the action

$$\hat{a}_1 |\chi_1\chi_2\chi_3\rangle = |\chi_2\chi_3\rangle \tag{316}$$

If we were to split up the spin-orbital into its spatial and spin components, we define

$$\sqrt{N}\sum_i \langle r(i)\mu(\omega_i)| \equiv \hat{a}_{r\mu} \tag{317}$$

Creation

Next consider the action of the operator

$$\frac{1}{\sqrt{N+1}}\sum_i |\chi_1(i)\rangle \tag{318}$$

on the Slater determinant $|\chi_2\chi_3\rangle$. The operator, by adding an orbital to the product, must effectively also add a third electron. Thus, in three-electron space, there are three forms of the determinant $|\chi_2\chi_3\rangle$ that must be considered in the product:

$$\begin{aligned}&\tfrac{1}{\sqrt{2}}\left(|\chi_2(1)\chi_3(2)\rangle - |\chi_3(1)\chi_2(2)\rangle\right)\\ &-\tfrac{1}{\sqrt{2}}\left(|\chi_2(1)\chi_3(3)\rangle - |\chi_3(1)\chi_2(3)\rangle\right)\\ &\tfrac{1}{\sqrt{2}}\left(|\chi_2(2)\chi_3(3)\rangle - |\chi_3(2)\chi_2(3)\rangle\right)\end{aligned} \tag{319}$$

(Note that the second determinant was multiplied by -1. This is because of the anti-symmetric nature of electrons, which requires that the wavefunction, upon exchange of electrons, must have opposite sign. The sign change is not present in the third determinant because two electrons were exchanged, thus cancelling the sign change [**26**].) The direct product with the operator is then

$$\begin{aligned}&\tfrac{1}{\sqrt{6}}\left(|\chi_1(1)\rangle + |\chi_1(2)\rangle + |\chi_1(3)\rangle\right)\otimes[\left(|\chi_2(1)\chi_3(2)\rangle - |\chi_3(1)\chi_2(2)\rangle\right) -\\ &\left(|\chi_2(1)\chi_3(3)\rangle - |\chi_3(1)\chi_2(3)\rangle\right) + \left(|\chi_2(2)\chi_3(3)\rangle - |\chi_3(2)\chi_2(3)\rangle\right)]\end{aligned} \tag{320}$$

A $|\chi_1(i)\rangle$ ket will only create a non-zero direct product with a ket that does not already have a function of the i^{th} electronic variable. The resultant function is

$$\begin{aligned}&\tfrac{1}{\sqrt{6}}[\left(|\chi_2(1)\chi_3(2)\chi_1(3)\rangle - |\chi_3(1)\chi_2(2)\chi_1(3)\rangle\right)\\ &-\left(|\chi_2(1)\chi_1(2)\chi_3(3)\rangle - |\chi_3(1)\chi_1(2)\chi_2(3)\rangle\right)\\ &+\left(|\chi_1(1)\chi_2(2)\chi_3(3)\rangle - |\chi_1(1)\chi_3(2)\chi_2(3)\rangle\right)]\end{aligned} \tag{321}$$

which is the determinant $|\chi_1\chi_2\chi_3\rangle$. Thus the operator in (318) has created the χ_1 spin-orbital in the determinant. For that reason, we can equate it to a creation operator [**40**]:

$$\frac{1}{\sqrt{N+1}}\sum_i |\chi_1(i)\rangle \equiv \hat{a}_1^\dagger \tag{322}$$

with the action

$$\hat{a}_1^\dagger |\chi_2\chi_3\rangle = |\chi_1\chi_2\chi_3\rangle \tag{323}$$

As in the case for the annihilation operator, we can split the spin-orbital into spatial and spin components:

$$\frac{1}{\sqrt{N+1}}\sum_i |r(i)\mu(\omega_i)\rangle \equiv \hat{a}_{r\mu}^\dagger \tag{324}$$

The creation and annihilation operators obey the anticommutation relationship [**40**]:

$$\left\{\hat{a}_{r\mu}^\dagger, \hat{a}_{r\mu}\right\} \equiv \hat{a}_{r\mu}^\dagger \hat{a}_{r\mu} + \hat{a}_{r\mu}\hat{a}_{r\mu}^\dagger = \hat{1}. \tag{325}$$

These are the creation and annihilation operators introduced in the main body of the text.

Appendix D. The Spatial Orbital Basis

In order to represent the Hamiltonian, the first task is to build a suitable basis for a single electron; from that set, a basis for the multi-electron wavefunctions can be built as a direct product space. This one-electron basis must meet three criteria:

1. It must be orthonormal
2. It must be easy to integrate (for computational savings)
3. It must predict the lowest possible energy (as a consequence of the *variation principle*)

Orthonormality

For a single atom, the direct product of spherical harmonics in θ and φ, with associated Laguerre polynomials in r provides a set of orthonormal orbitals with which to construct wave functions [**28**]. These orbitals are, in fact, the eigenfunctions of the hydrogen atom Hamiltonian [**26**] and are known as *Slater Orbitals* [**20**]; however, for polyatomic molecules, hydrogenic basis functions located at different atomic centers are not orthogonal, having an overlap matrix defined by

$$\mathbf{S}_{\mu\nu} = \left\langle \chi_\mu \middle| \chi_\nu \right\rangle \tag{326}$$

where the χ_k are the orbitals. Such a basis, which we will refer to as an *atom-centered basis* or *atomic orbitals*, must be transformed non-unitarily into a non-localized set of orthonormal Molecular Orbitals (MO), often referred to as a Linear Combination of Atomic Orbitals (LCAO) [**20**]. These MOs are defined as

$$|\phi_i\rangle = \sum_\mu c_{\mu i} |\chi_\mu\rangle \tag{327}$$

Since the molecular orbitals are required to be orthonormal, a transformation will reduce the overlap matrix to the identity matrix.

Integratability

Slater orbitals, while more physically accurate, are unwieldy for computation. For example, the *1S* Slater orbital is

$$\chi(R) = \left(\frac{\zeta^3}{\pi}\right)^{1/2} \exp(-\zeta |R|) \tag{328}$$

which exhibits cusp behavior at the origin. Figure 40 shows the square root of the probability of finding an electron as a function of R, in atomic units. Integration against other Slater orbitals at other origins proves to be computationally intensive. For this reason, an alternative set of *Gaussian orbitals* is often chosen instead. The pivotal

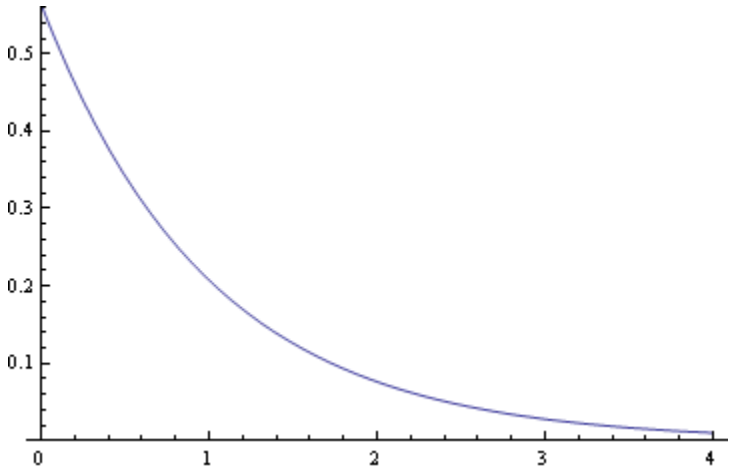

Figure 40. 1S Slater Orbital, ζ=1.0

difference between the Slater orbital and the Gaussian orbital, which has the form

$$\chi(R) = \left(\frac{2\alpha}{\pi}\right)^{3/4} \exp\left(-\alpha |R|^2\right) \tag{329}$$

is that in the latter the argument is squared in the exponent. When two Gaussian functions are integrated, the result is a Gaussian, regardless of their origins, making the task of integration much easier. Figure 41 compares a Gaussian orbital to the previous Slater orbital. The Gaussian is thicker towards the origin and falls off faster, while it exhibits no cusp. Although it is not a very accurate representation of the Slater orbital, the ability to develop efficient integration algorithms with Gaussian orbitals means that more of these can be used. Figure 42 shows a linear combination of three Gaussian orbitals against the original Slater orbital. The figure shows that, although not quite a match at the cusp, this orbital is much closer to the Slater orbital, and is still more easily integrated. A basis created from such functions is labeled a STO-3G basis. *STO* indicates

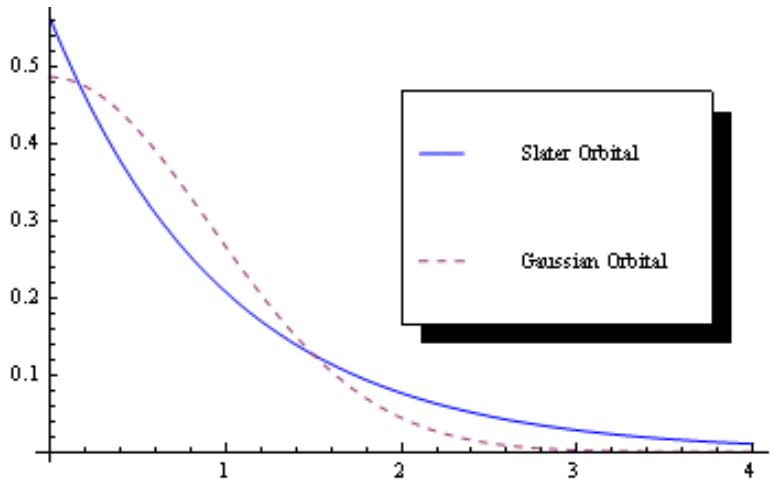

Figure 41. Gaussian orbital, α=0.6

that it is a Slater-Type Orbital (as opposed to a Slater orbital) and 3G indicates the orbitals are each made from three Gaussians [**20**]. Although the HF method itself can be applied to either Slater orbitals or STOs, the integration advantage of the STOs makes them a staple in computational chemistry packages.

Lowest Possible Energy

The variation principle [**20**] states that, for an approximate eigenvector $|\tilde{\psi}\rangle$, the eigenvalue will be related to the true energy by

$$\langle\tilde{\psi}|\hat{H}|\tilde{\psi}\rangle \geq \varepsilon_0 \tag{330}$$

Thus, given several different bases, the one that produces the lowest eigenvalue is the best choice.

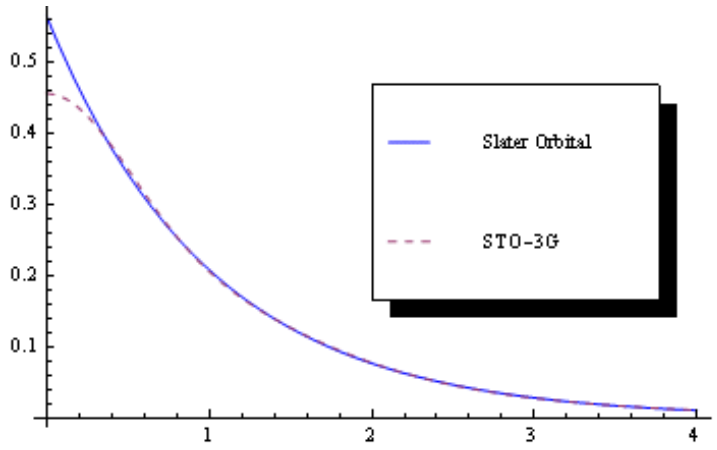

Figure 42. Linear combination of three Gaussian orbitals [20]

Appendix E. Self Consistent Field Method

The Fock Operator

For our purposes, the Hartree-Fock method results in the best possible ground state of a molecule given a molecular orbital basis derived from a single Slater determinant. While we will ultimately be interested in optimizing the basis for excited states, this method nevertheless provides a *first guess* from which a more suitable basis may be formed. From the preceding section, we have found that the orbitals must satisfy orthonormality,

$$\left\langle \phi_i \middle| \phi_j \right\rangle = \delta_{ij} \tag{331}$$

and are defined by the variation principle. Using a single Slater determinant for the *ansatz* $\tilde{\psi}$ leads to the constraint equation [**20**]

$$\hat{h}(i)\phi_a(i) + \sum_{j\neq i}\left[\int dj\, \phi_b^*(j)\frac{1}{r_{ij}}\right]\phi_a(i) - \sum_{j\neq i}\int\left[dj\, \phi_b^*(j)\phi_a(j)\frac{1}{r_{ij}}\right]\phi_b(i) = \varepsilon_i\phi_a(i) \tag{332}$$

where $\hat{h}$ is the single-electron operator from equation (13). The integral in the second term in equation (332) is called the *Coulomb operator*, $\hat{J}_b(j)$ and represents the average instantaneous coulomb potential between electron i and electron j. The third term in equation (332) looks almost exactly the same, except that the electrons have been exchanged between the two orbitals. For this reason, this integral is known as the *exchange operator*, and has the following property:

$$K_b(i)\phi_a(i) = \left[\int dj\, \phi_b^*(j)\frac{1}{r_{ij}}\phi_a(j)\right]\phi_b(i) \tag{333}$$

The exchange operator is a result of the antisymmetric nature of electrons (due to the Pauli exclusion principle), and doesn't have a simple classical analog. The form of the operator in equation (333) allows us to rewrite equation (332) as

$$\left[\hat{h}(i)+\sum_{j\neq i}J_b(i)-\sum_{j\neq i}K_b(i)\right]\phi_a(i)=\varepsilon_i\phi_a(i) \tag{334}$$

The operator on the left is called the *Fock operator*, $\hat{f}(i)$ [**20**]. The orbitals must obey the pseudo-eigenvalue equation

$$\hat{f}\left|\phi_i\right\rangle=\varepsilon_i\left|\phi_i\right\rangle \tag{335}$$

which are the Hartree-Fock equations. This is not a true eigenvalue equation because the operator $\hat{f}$ depends upon the eigenvectors $\left|\phi_i\right\rangle$,and it must be solved iteratively. That is, a guess for the eigenvectors is proffered, from which the Fock operator may be calculated, from which new eigenvectors can be calculated, and so on until the eigenvectors reach self-consistency.

Pople-Nebset Equations

The HF method is further subdivided into a number of different cases. We will not review them all, but instead will present one of the more general of these,the *unrestricted open-shell Hartree-Fock method* (UHF), as an example.

Unrestricted refers to the fact that spin-up electrons will be allowed a different set of spatial orbitals than the spin-down electrons. Thus equation (327) is split into two separate equations for spin-up and spin-down:

$$\left|\phi_i^\alpha\right\rangle = \sum_\mu c_{\mu i}^\alpha \left|\chi_\mu\right\rangle$$
$$\left|\phi_i^\beta\right\rangle = \sum_\mu c_{\mu i}^\beta \left|\chi_\mu\right\rangle \tag{336}$$

There are also two Fock operators,

$$\hat{f}^\alpha \equiv \left\langle\alpha\right| \hat{f} \left|\alpha\right\rangle$$
$$\hat{f}^\beta \equiv \left\langle\beta\right| \hat{f} \left|\beta\right\rangle \tag{337}$$

Plugging these definitions into the HF equations leads to, for example,

$$\sum_\mu c_{\mu i}^\alpha \hat{f} \left|\chi_\mu\right\rangle = \varepsilon_i \sum_\mu c_{\mu i}^\alpha \left|\chi_\mu\right\rangle \tag{338}$$

which, when integrated against $\left\langle\chi_\nu\right|$, yields

$$\sum_\mu \mathbf{F}_{\nu\mu} c_{\mu i}^\alpha = \varepsilon_i \sum_\mu \mathbf{S}_{\nu\mu} c_{\mu i}^\alpha \tag{339}$$

where $\mathbf{S}$ is the overlap matrix (see equation (326)) and $\mathbf{F}$ is the *Fock matrix* whose elements are defined as

$$\mathbf{F}_{\nu\mu}^\alpha = \left\langle\chi_\nu\right| \hat{f}^\alpha \left|\chi_\mu\right\rangle \tag{340}$$

with symmetric equations for spin-down (note this is not the same second-quantized Fock matrix used in the formalism in the main body of the text). Equation (339) is equivalent to the matrix equation

$$\mathbf{F}^\alpha \mathbf{C}^\alpha = \mathbf{S}^\alpha \mathbf{C}^\alpha \varepsilon^\alpha \tag{341}$$

which are known as the *Pople-Nebset equations* [**20**]. By transforming this equation into a basis in which the overlap matrix becomes the identity matrix, the Pople-Nebset

equations become pseudo-eigenvalue equations. This transformation is effected as follows:

1. Since $\mathbf{S}$ is hermitian, diagonalize it by the transform

$$\mathbf{s} = \mathbf{U}^{\dagger}\mathbf{S}\mathbf{U} \tag{342}$$

2. Create the matrix $\mathbf{s}^{-1/2}$, a diagonal matrix whose entries are the inverse of the positive square roots of the eigenvalues of $\mathbf{s}$.

3. Define the transformation

$$\mathbf{X} \equiv \mathbf{U}\mathbf{s}^{-1/2}\mathbf{U}^{\dagger} \tag{343}$$

4. Using this transformation, create the matrices

$$\begin{aligned} \mathbf{C}^{\alpha}{}' &= \mathbf{X}^{-1}\mathbf{C}^{\alpha} \\ \mathbf{F}^{\alpha}{}' &= \mathbf{X}^{\dagger}\mathbf{F}^{\alpha}\mathbf{X} \end{aligned} \tag{344}$$

   along with their spin-down counterparts, to create the equations

$$\mathbf{F}^{\alpha}{}'\mathbf{C}^{\alpha}{}' = \mathbf{C}^{\alpha}{}'\varepsilon^{\alpha} \tag{345}$$

Both $\mathbf{F}^{\alpha}$ and $\mathbf{F}^{\beta}$ depend on $\mathbf{C}^{\alpha}$ and $\mathbf{C}^{\beta}$, so the two equations are not independent.

Thus, in order to solve these equations, one must:

1. Make an initial guess at $\mathbf{F}^{\alpha}$ and $\mathbf{F}^{\beta}$

2. Transform $\mathbf{F}^{\alpha}{}'$ and $\mathbf{F}^{\beta}{}'$

3. Calculate their eigenvectors and eigenvalues; equate these to $\mathbf{C}^{\alpha}{}'$, $\mathbf{C}^{\beta}{}'$, ε^{α} and ε^{β}

4. Transform these back to $\mathbf{C}^{\alpha}$ and $\mathbf{C}^{\beta}$, use these to calculate a new $\mathbf{F}^{\alpha}$ and $\mathbf{F}^{\beta}$ and so forth, until self-consistency is achieved.

When the single-electron orbitals have been determined, the final step of the SCF method is to create an antisymmetric Slater determinant from the lowest N orbitals:

$$\left|\varphi_0\right\rangle \equiv \left|\phi_a \phi_b ... \phi_N\right\rangle \tag{346}$$

This is the electronic ground state, used to determine the ground-state energy

$$\varepsilon_0 = \left\langle \psi_0 \left| \hat{H} \right| \psi_0 \right\rangle \tag{347}$$

As a final note, since $\mathbf{C}$ is a square matrix, there will be as many MOs created as AOs used, regardless of the number of electrons involved. Because the MOs not occupied by an electron don't affect the energy, those unoccupied orbitals are orthonormalized but not energy-optimized by this process. If one is interested only in the ground state, these extra orbitals are of little value anyway; however, if one is interested in excited states, these orbitals are not ideal. The MCSCF method, to be briefly discussed next, addresses this concern by further performing the SCF method to higher states. Although the SCF MOs can be used directly in a subsequent CI calculation, an intermediate MCSCF step can reduce the effort of the CI by identifying and eliminating those orbitals that will have less impact on the CI result.

Multi-Configuration Self-Consistent Field

MCSCF is a complicated but useful generalization of the SCF procedure. While the SCF method optimizes the molecular orbitals by adjusting the SCF coefficients (see equation (327)), and the CI method optimizes the CI coefficients of the determinants to

create the eigenfunctions of the Hamiltonian (see equation (351)), the MCSCF method combines both of these optimizations, but usually on a smaller scale than the CI:

1. The ground-state orbitals are optimized
2. Several determinants are constructed (not just the ground state)
3. A linear combination of determinants is optimized for the ground-state energy
4. New orbitals are optimized based on the CI coefficients

The process is continued until self-consistency of the involved orbitals is achieved. This procedure specifically optimizes the orbitals for the ground state; the method can also be adapted to optimize the orbitals for some excited state. For the construction of derivative coupling terms, there are several (but commonly two) states of importance. Rather than optimizing to any single state, the orbitals are constructed to have the best average optimization for all states involved. This method is called the *State-Averaged MCSCF* (SA-MCSCF) [**3**].

The scope of this project does not involve the modification of the MCSCF procedure, and only relies upon it inasmuch as it prepares orbitals for a multi-electron basis; hence, we will not give more than this rudimentary explanation here. Nevertheless, the interested reader may wish to refer to Shepard's paper, which thoroughly outlines the subject [**35**].

Appendix F. Configuration Interaction

The method of Configuration Interaction (CI) is an improvement upon the SCF method [**20**]. It is also the principle computational tool with which we calculate eigenfunctions for the derivative coupling terms. The goal of CI is to solve the matrix equation

$$\mathbf{H}\vec{c}^{\,I} = \varepsilon^{I}\vec{c}^{\,I} \tag{348}$$

where $\mathbf{H}$ is the Hamiltonian matrix, ε^{I} represents an energy eigenvalue corresponding to the eigenvectors $\vec{c}^{\,I}$, which fulfill the relationship

$$\left|\psi_{I}\right\rangle = \sum_{i} c_{i}^{I}\left|\varphi_{i}\right\rangle \tag{349}$$

While the SCF method used the lowest N orbitals to create a single Slater determinant, disregarding higher orbitals, CI uses some or all of the orbitals to create a family of Slater determinants in which to represent the Hamiltonian. The ground state of this Hamiltonian will no longer be a single determinant (see equation (346)), but a linear combination of determinants. This Hamiltonian yields two advantages over the SCF Hamiltonian: first, the ground state will be at least as good as the SCF ground state, leading to an equal or lower (and hence better) ground-state energy; and second, the Hamiltonian allows for excited states.

Given a system of n spin-orbitals and N electrons, one can make a total of $\binom{n}{N}$ Slater determinants. Each determinant may be constructed by replacing an occupied

ground-state MCSCF orbitals with one of the unoccupied (or *virtual*) MCSCF orbitals. For instance, if the spin-orbital $|\phi_a\rangle$ is included in the ground state, one can construct all the determinants that replace $|\phi_a\rangle$ with an orbital not included in the ground state, $|\phi_r\rangle$. This is a singly-excited determinant, denoted by $|\varphi_a^r\rangle$. There are $N(n-N)$ such singly-excited determinants [**20**]. Similarly, we can remove two spin-orbitals at a time and replace them, constructing the family of doubly-excited determinants, $|\varphi_{ab}^{rs}\rangle$, of which there are $\binom{N}{2}\binom{n-N}{2}$. Clearly one can continue constructing determinants in this fashion until all combinations are exhausted. Representing in such an N-electron basis gives what is called a *full CI Hamiltonian:*

$$\hat{H} \rightarrow \begin{pmatrix} \langle\varphi_0|\hat{H}|\varphi_0\rangle & \langle\varphi_0|\hat{H}|\varphi_a^r\rangle\ldots & \langle\varphi_0|\hat{H}|\varphi_{ab}^{rs}\rangle & \cdots \\ \vdots & \vdots & \vdots & \\ \langle\varphi_a^r|\hat{H}|\varphi_0\rangle\ldots & \langle\varphi_a^r|\hat{H}|\varphi_a^r\rangle\ldots & \langle\varphi_a^r|\hat{H}|\varphi_{ab}^{rs}\rangle & \cdots \\ \vdots & \vdots & \vdots & \\ \langle\varphi_{ab}^{rs}|\hat{H}|\varphi_0\rangle\ldots & \langle\varphi_{ab}^{rs}|\hat{H}|\varphi_a^r\rangle\ldots & \langle\varphi_{ab}^{rs}|\hat{H}|\varphi_{ab}^{rs}\rangle & \cdots \\ \vdots & \vdots & \vdots & \ddots \end{pmatrix} \tag{350}$$

(If $n=N$, the CI space reduces to a single determinant.) Because the Hamiltonian is hermitian, only the upper triangle must be calculated. Furthermore, orthogonality restrictions dictate that a number of the elements will be zero [**20**]. Nevertheless, the size of this matrix grows rapidily with the number of basis orbitals and electrons. For this reason, larger molecules almost never receive a full CI treatment. Commonly, the Hamiltonian is restricted to be represented only in the ground state, singly-excited

determinants, and doubly-excited determinants; this treatment is aptly named the *Singles and Doubles CI* (SDCI or CISD) [**3**]. This method calculates even lower energies if it is preceded by an MCSCF step.

It should be noted that, rather than using bare Slater determinants, the CSFs of the Gel'fand-Tsetlin basis used in COLUMBUS employ a spin-adapted linear combination of Slater determinants; this does not change the general concept discussed here.

Once the elements of the Hamiltonian are calculated, its eigenvectors are constructed from the Slater determinants,

$$\left|\psi^I\right\rangle = \xi_0^I \left|\varphi_0\right\rangle + \sum_{ar} \left(\xi_a^r\right)^I \left|\varphi_a^r\right\rangle + \sum_{abrs} \left(\xi_{ab}^{rs}\right)^I \left|\varphi_{ab}^{rs}\right\rangle \tag{351}$$

by a matrix diagonalization or similar procedure. These are the wavefunctions that will be used to calculate derivative coupling terms.

The interested reader may wish to reference Shavitt's more complete review of the CI method [**63**].

Multi-Reference CI

COLUMBUS uses *Multi-Reference Singles and Doubles CI* (MRSDCI or MR-CISD). This method differs from the standard SDCI in that, rather than taking single- and double- excitations only from the ground state CSF, these excitations are taken from a set of CSFs, known as the *reference CSFs* determined from the MCSCF step. In cases where information is needed about excited states, especially nearly-degenerate states, MR methods are successful where single-reference methods may fail [**9**].

Direct CI

The Hamiltonian matrices calculated in computational chemistry can have dimensions on the order of hundreds of millions of elements in practical calculations; however, usually it is only the lowest handful of eigenvalues and eigenvectors which are needed. Such a requirement hardly justifies the diagonalization of the entire matrix which, for an $n \times n$ Hamiltonian can require on the order of n^3 operations [**64**], which is too costly when only a few eigenvalues are required. Furthermore, calculations in normal diagonalization routines require the whole Hamiltonian be used, which is a fierce burden on computer memory. Nesbet proposed a method [**64**] which Shavitt modified [**65**], now known as *Direct-CI*, which uses only a small portion of the Hamiltonian for each calculation, producing one eigenvalue and eigenvector at a time, so that the effort required is proportional to the number of eigenvectors sought. This method attempts to solve for the eigenvalues and eigenvectors of equation (348) iteratively, without solving all equations at once. The Davidson method [**66**], itself built upon an earlier method proposed by Roos [**67**], is the basis for the current direct CI method used in COLUMBUS [**68**].

Appendix G. The Non-Relativistic Energy Gradient

This appendix outlines Shepard's formalism for obtaining the non-relativistic energy gradients [**3**]. It is intended to be a quick overview for readers of this paper. For a more in-depth understanding, please see Shepard's referenced paper.

The energy gradient, in the resolved basis,

$$\varepsilon(R)^x = \left\langle \psi_I^{[Z]}(R) \middle| \hat{H}^{[Z]}(R)^x \middle| \psi_I^{[Z]}(R) \right\rangle \tag{352}$$

can be represented in the $[S]$ basis as:

$$\begin{aligned} &\left\langle \psi_I^{[Z]}(R) \middle| \hat{H}^{[Z]}(R)^x \middle| \psi_I^{[Z]}(R) \right\rangle = \\ &\quad \left\langle \psi_I^{[S]}(R) \middle| \left[\exp\left(-\hat{Z}(R)\right) \exp\left(-\hat{K}(R)\right) \hat{H}^{[S]}(R) \exp\left(\hat{K}(R)\right) \exp\left(\hat{Z}(R)\right) \right]^x \middle| \psi_I^{[S]}(R) \right\rangle \end{aligned} \tag{353}$$

When the exponentials are expanded as a series, they form commutators with the Hamiltonian according to the Baker-Campbell-Hausdorff theorem:

$$\begin{aligned} \left\langle \psi_I^{[Z]}(R) \middle| \hat{H}^{[Z]}(R)^x \middle| \psi_I^{[Z]}(R) \right\rangle = &\left\langle \psi_I^{[S]}(R) \middle| \hat{H}^{[S]}(R)^x \middle| \psi_I^{[S]}(R) \right\rangle \\ &+ \left\langle \Psi_I^{[S]}(R) \middle| \left[\hat{H}^{[S]}(R), \hat{Z}(R) \right]^x \middle| \psi_I^{[S]}(R) \right\rangle \\ &+ \left\langle \psi_I^{[S]}(R) \middle| \left[\hat{H}^{[S]}(R), \hat{K}(R) \right]^x \middle| \psi_I^{[S]}(R) \right\rangle + \ldots \end{aligned} \tag{354}$$

where higher-order terms are ignored in this derivation [**3**]. Since each of the rotation operators is unitary, it can be expressed as

$$\exp\left(\hat{A}(R)\right) = \exp\left(\sum_{r \prec s} a_{rs}(R) \left(\hat{E}_{rs} - \hat{E}_{sr} \right) \right) \tag{355}$$

(*cf.* equation(115)). Here, we have combined each generator with its transpose so that the parameters are unrestricted. (This adjustment was primarily made to coincide with

Shepard's notation [**3**], but the concept is unchanged.) Thus equation (354) can be expressed as

$$\begin{aligned}\left\langle \psi_I^{[Z]}(R)\middle|\hat{H}^{[Z]}(R)^x\middle|\psi_I^{[Z]}(R)\right\rangle &= \left\langle \psi_I^{[S]}(R)\middle|\hat{H}^{[S]}(R)^x\middle|\psi_I^{[S]}(R)\right\rangle \\ &+\left\langle \psi_I^{[S]}(R)\middle|\left(\sum_{rs} z_{rs}(R)\left[\hat{H}^{[S]}(R),\hat{E}_{rs}-\hat{E}_{sr}\right]\right)^x\middle|\psi_I^{[S]}(R)\right\rangle \\ &+\left\langle \psi_I^{[S]}(R)\middle|\left(\sum_{rs} k_{rs}(R)\left[\hat{H}^{[S]}(R),\hat{E}_{rs}-\hat{E}_{sr}\right]\right)^x\middle|\psi_I^{[S]}(R)\right\rangle\end{aligned} \quad (356)$$

The following notational substitutions are made for simplicity:

$$\begin{aligned}\sum_{r<s} z_{rs}(R)\left[\hat{H}^{[S]}(R),\hat{E}_{rs}-\hat{E}_{sr}\right] &= \vec{z}(R)\cdot\vec{f}_{red}^{\,CI}(R) \\ \sum_{r<s} k_{rs}(R)\left[\hat{H}^{[S]}(R),\hat{E}_{rs}-\hat{E}_{sr}\right] &= \vec{k}(R)\cdot\vec{f}_{ess}^{\,CI}(R)\end{aligned} \quad (357)$$

where $\vec{f}^{\,CI}$ is the orbital gradiant vector, and the dot product represents a sum of operators rather than a scalar quantity. (There is, in fact, only one such vector; however, since rotations are partitioned into redundant and essential classes, the orbital gradient vector can be so partitioned as well.) Then equation (356) is simplified as

$$\begin{aligned}\left\langle \psi_I^{[Z]}(R)\middle|\hat{H}^{[Z]}(R)^x\middle|\psi_I^{[Z]}(R)\right\rangle &= \left\langle \psi_I^{[S]}(R)\middle|\hat{H}^{[S]}(R)^x\middle|\psi_I^{[S]}(R)\right\rangle \\ &+\left(\vec{z}(R)\cdot\vec{f}_{red}^{\,CI}(R)\right)^x+\left(\vec{k}(R)\cdot\vec{f}_{ess}^{\,CI}(R)\right)^x\end{aligned} \quad (358)$$

which, expanded and evaluated at R_0, is equal to

$$\begin{aligned}\left\langle \psi_I^{[Z]}(R_0)\middle|\hat{H}^{[Z]}(R_0)^x\middle|\psi_I^{[Z]}(R_0)\right\rangle &= \left\langle \psi_I^{[S]}(R_0)\middle|\hat{H}^{[S]}(R_0)^x\middle|\psi_I^{[S]}(R_0)\right\rangle \\ &+\left(\vec{z}(R_0)^x\cdot\vec{f}_{orb}^{\,red}(R_0)\right)+\left(\vec{k}(R_0)^x\cdot\vec{f}_{orb}^{\,ess}(R_0)\right) \\ &+\left(\vec{z}(R_0)\cdot\vec{f}_{orb}^{\,red}(R_0)^x\right)+\left(\vec{k}(R_0)\cdot\vec{f}_{orb}^{\,ess}(R_0)^x\right)\end{aligned} \quad (359)$$

At the reference geometry, $\left|\psi_{CI}\left(R\right)\right\rangle = \left|\psi_{CI}\left(R_0\right)\right\rangle$ and so $\hat{K}\left(R_0\right) = \hat{Z}\left(R_0\right) = 0$, and so all their parameters must be zero. This leads to the elimination of two terms in the above equation

$$\begin{aligned}\left\langle \psi_I^{[Z]}\left(R_0\right)\right| \hat{H}^{[Z]}\left(R_0\right)^x \left|\psi_I^{[Z]}\left(R_0\right)\right\rangle &= \left\langle \psi_I^{[S]}\left(R_0\right)\right| \hat{H}^{[S]}\left(R_0\right)^x \left|\psi_I^{[S]}\left(R_0\right)\right\rangle \\ &+\left(\vec{z}\left(R_0\right)^x \cdot \vec{f}_{orb}^{\,red}\left(R_0\right)\right)+\left(\vec{k}\left(R_0\right)^x \cdot \vec{f}_{orb}^{\,ess}\left(R_0\right)\right)\end{aligned} \tag{360}$$

Consider the first term, expanding the Hamiltonian in its second-quantized form:

$$\begin{aligned}\left\langle \psi_I^{[S]}\left(R_0\right)\right| \hat{H}^{[S]}\left(R_0\right)^x \left|\psi_I^{[S]}\left(R_0\right)\right\rangle &= \left\langle \psi_I^{[S]}\left(R_0\right)\right| \sum_{rs}\left(h_{rs}^{[S]}\left(R_0\right)\right)^x E_{rs} \\ &+\tfrac{1}{2}\sum_{rstu}\left(g_{rstu}^{[S]}\left(R_0\right)\right)^x \mathbf{e}_{rstu}\left|\psi_I^{[S]}\left(R_0\right)\right\rangle \\ &=\sum_{rs}\left(h_{rs}^{[S]}\left(R_0\right)\right)^x \left\langle \psi_I^{[S]}\left(R_0\right)\right| E_{rs}\left|\psi_I^{[S]}\left(R_0\right)\right\rangle \\ &+\tfrac{1}{2}\sum_{rstu}\left(g_{rstu}^{[S]}\left(R_0\right)\right)^x \left\langle \psi_I^{[S]}\left(R_0\right)\right| e_{rstu}\left|\psi_I^{[S]}\left(R_0\right)\right\rangle\end{aligned} \tag{361}$$

We use the density matrices (see equation (34)) to simplify equation (361):

$$\begin{aligned}\left\langle \psi_I^{[S]}\left(R_0\right)\right| \hat{H}\left(R_0\right)^x \left|\psi_I^{[S]}\left(R_0\right)\right\rangle &= \sum_{rs}\left(h_{rs}^{[S]}\left(R_0\right)\right)^x D_{rs}^{[S]}\left(R_0\right)+\tfrac{1}{2}\sum_{rstu}\left(g_{rstu}^{[S]}\left(R_0\right)\right)^x d_{rstu}^{[S]}\left(R_0\right) \\ &= Tr\left[\left(h^{[S]}\left(R_0\right)\right)^x \cdot D^{[S]}\left(R_0\right)\right]+\tfrac{1}{2}Tr\left[\left(g^{[S]}\left(R_0\right)\right)^x \cdot d^{[S]}\left(R_0\right)\right]\end{aligned} \tag{362}$$

where the nuclear derivatives now only act upon the coefficient matrices, as the generators, and hence density matrices, are geometry-independent.

Now consider the second term in equation (360). The orbital gradient vector is non-zero as a consequence of the CI step, which optimizes the CSF coefficients but not the orbitals [**3**]. For an MCSCF step, or a full CI, the orbital gradient vector is zero;

however, for the sake of generality we will assume that it is non-zero. Its form, which is derived elsewhere [**5**] [**35**], is

$$\left(\vec{f}_{orb}\right)_{JI} = \left(1-P_{rs}\right)\left\langle \psi_I^{[Z]} \middle| \sum_u h_{ru}^{[Z]}\left(E_{us}+E_{su}\right) + \sum_{tuv} g_{rtuv}^{[Z]}\left(e_{stuv}+e_{tsuv}\right) \middle| \psi_I^{[Z]} \right\rangle \tag{363}$$

where P_{rs} is the permutation operator that exchanges orbital r with orbital s. Although the unitary generators (and hence density matrices) are not symmetric, only the symmetric portion of those matrices will appear in the product with the symmectric matrices $\mathbf{h}$ and $\mathbf{g}$. Hence,

$$\begin{aligned} \vec{f}^{CI} &= 2\left(1-P_{rs}\right)\sum_u h_{ru}^{[Z]} D_{us}^{[Z]} + \sum_{tuv} g_{rtuv}^{[Z]} d_{stuv}^{[Z]} \\ &= 2\left(\sum_u h_{ru}^{[Z]} D_{us}^{[Z]} + \sum_{tuv} g_{rtuv}^{[Z]} d_{stuv}^{[Z]} + \sum_u h_{su}^{[Z]} D_{ur}^{[Z]} + \sum_{tuv} g_{stuv}^{[Z]} d_{rtuv}^{[Z]} \right) \end{aligned} \tag{364}$$

Let us define the Fock matrices [**3**] [**5**]

$$\begin{aligned} F_{rs}^{1[Z]} &\equiv \sum_u h_{ru}^{[Z]} D_{us}^{[Z]} \\ F_{rs}^{2[Z]} &\equiv \sum_{tuv} g_{rtuv}^{[Z]} d_{stuv}^{[Z]} \\ F_{rs}^{[Z]} &\equiv F_{rs}^{1JI[Z]} + F_{rs}^{2[Z]} \end{aligned} \tag{365}$$

which allow the orbital gradient vector to be simplified as

$$\vec{f}^{CI} = 2\left(F_{rs}^{[Z]} - F_{sr}^{[Z]}\right) \tag{366}$$

Since an analytic derivative is never taken of this vector, it is not necessary to further transform it.

To determine the elements of the $\vec{z}\left(R\right)$ vector, $Z_{pq}\left(R\right)$, we note the transformation

$$D_{pq}^{[Z]}(R)=\left[\exp\left(-\mathbf{Z}(R)\right)\mathbf{D}^{[K]}(R)\exp\left(\mathbf{Z}(R)\right)\right]_{pq} \tag{367}$$

Using the Baker-Campbell-Hausdorff theorem again, we expand the exponentials and find the relationship

$$D_{pq}^{[Z]}(R)=D_{pq}^{[K]}(R)+\left[\mathbf{D}^{[K]}(R),\mathbf{Z}(R)\right]_{pq} \tag{368}$$

where higher-order commutators are ignored. We can break this commutator into its two component terms, which we can then express as summations:

$$D_{pq}^{[Z]}(R)=D_{pq}^{[K]}(R)+\sum_{\mu}\left(D_{p\mu}^{[K]}(R)Z_{\mu q}(R)-Z_{p\mu}(R)D_{\mu q}^{[K]}(R)\right) \tag{369}$$

Let us take the gradient of this equation and evaluate it at the reference geometry:

$$D_{pq}^{[Z]}(R_0)^{x}=D_{pq}^{[K]}(R_0)^{x}+\sum_{\mu}\left(D_{p\mu}^{[K]}(R_0)\left(Z_{\mu q}(R_0)^{x}\right)-\left(Z_{p\mu}(R_0)^{x}\right)D_{\mu q}^{[K]}(R_0)\right) \tag{370}$$

where we have used the fact that $\mathbf{Z}(R_0)=\mathbf{0}$. To complete the evaluation of this equation, consider that, within the invariant subspace of interest, the basis was resolved by diagonalizing the density matrix [**3**]. Then the equation

$$D_{pq}^{JI[Z]}=D_{pp}^{JI[Z]}\delta_{pq} \tag{371}$$

must hold. When this equality is recognized, equation (370) becomes

$$\begin{aligned}\left(D_{pp}^{[Z]}(R_0)\delta_{pq}\right)^{x}&=D_{pq}^{[K]}(R_0)^{x}\\&\quad+\sum_{\mu}\left(D_{p\mu}^{[K]}(R_0)\delta_{p\mu}\left(Z_{\mu q}(R_0)\right)^{x}-\left(Z_{p\mu}(R_0)\right)^{x}D_{\mu q}^{[K]}(R_0)\delta_{\mu q}\right)\end{aligned} \tag{372}$$

Evaluation for $p\neq q$ yields

$$0 = D_{pq}^{[K]}\left(R_0\right)^x + \left(D_{pp}^{[K]}\left(R_0\right) - D_{qq}^{[K]}\left(R_0\right)\right)\mathbf{Z}_{pq}\left(R_0\right)^x \rightarrow$$
$$Z_{pq}\left(R_0\right)^x = \frac{D_{pq}^{[K]}\left(R_0\right)^x}{D_{qq}^{[K]}\left(R_0\right) - D_{pp}^{[K]}\left(R_0\right)} \tag{373}$$

(For $p = q$, equation (372) is not useful for identifying $Z_{pq}\left(R_0\right)^x$).

Diagonalizing the density matrix is not the only method for resolving bases. The diagonalization of Fock matrices, such as those defined in equation (365) as well as the Fock matrix defined by

$$Q_{pq}^{[Z]}\left(R\right) = 2h_{pq}^{[Z]}\left(R\right) + \sum_{rs}\left[\left(2g_{pqrs}^{[Z]}\left(R\right) - g_{pqrs}^{[Z]}\left(R\right)\right)D_{rs}^{[Z]}\left(R\right)\right] \tag{374}$$

may also be used. The analogue of equation (367) is true for these Fock matrices as well. Thus, depending on the method of resolution used, we find that

$$Z_{pq}\left(R_0\right)^x = \frac{F_{pq}^{[K]}\left(R_0\right)^x}{F_{qq}^{[K]}\left(R_0\right) - F_{pp}^{[K]}\left(R_0\right)} \tag{375}$$

and

$$Z_{pq}\left(R_0\right)^x = \frac{Q_{pq}^{[K]}\left(R_0\right)^x}{Q_{qq}^{[K]}\left(R_0\right) - Q_{pp}^{[K]}\left(R_0\right)} \tag{376}$$

as well. Each of these may contribute to the DCT, and so we find that the vector product $\vec{z}\left(R_0\right)^x \cdot \vec{f}_{red}^{\,CI}\left(R_0\right)$ has contributions equal to

$$\left(\vec{z}\left(R_0\right)^x \cdot \vec{f}_{red}^{\,CI}\left(R_0\right)\right)^{\mathbf{D}} = \sum_{p \neq q} D_{pq}^{[K]}\left(R_0\right)^x A_{pq}^{\mathbf{D}} \tag{377}$$

$$\left(\vec{z}\left(R_0\right)^x \cdot \vec{f}_{red}^{\,CI}\left(R_0\right)\right)^{\mathbf{F}} = \sum_{p \neq q} F_{pq}^{JI[K]}\left(R_0\right)^x A_{pq}^{\mathbf{F}} \tag{378}$$

and

$$\left(\vec{z}\left(R_0\right)^x \cdot \vec{f}_{red}^{\,CI}\left(R_0\right)\right)^{\mathbf{Q}} = \sum_{p\neq q} Q_{pq}^{[K]}\left(R_0\right)^x A_{pq}^{\mathbf{Q}} \tag{379}$$

where

$$A_{pq}^{\mathbf{X}} = \frac{F_{pq}^{[Z]}\left(R_0\right) - F_{qp}^{[Z]}\left(R_0\right)}{X_{qq}^{[K]}\left(R_0\right) - X_{pp}^{[K]}\left(R_0\right)} \tag{380}$$

is not differentiated, and can be calculated as needed. The first factor under each summation, which is a derivative, must be further transformed into the atomic basis. The gradient of each Fock matrix will involve gradients of one- and two-electron integral matrices $\left(\mathbf{h}^x, \mathbf{g}^x\right)$ and gradients of density matrices $\left(\mathbf{D}^x, \mathbf{d}^x\right)$ (see equations (374) and (365)), while transforming back to the $\left[S\right]$ basis will involve a gradient of the $\mathbf{K}\left(R\right)$ matrix for both Fock and density matrix gradients. This transformation and differentiation will yield three types of terms: those involving gradients of integral matrices, involving gradients of $\mathbf{K}\left(R\right)$, and involving gradients of density matrices.

The terms involving gradients of the integral matrices will take the form

$$Tr\left(\mathbf{h}^{[S]}\left(R_0\right)^x \mathbf{D}^{\mathbf{X}}\right) + \tfrac{1}{2} Tr\left(\mathbf{g}^{[S]}\left(R_0\right)^x \mathbf{d}^{\mathbf{X}}\right) \tag{381}$$

where

$$\begin{aligned} D_{pq}^{\mathbf{Q}} &\equiv 2A_{pq}^{\mathbf{Q}} \\ d_{pqrs}^{\mathbf{Q}} &\equiv -\tfrac{1}{2}\left(A_{qs}^{\mathbf{Q}} D_{pr}^{[S]}\left(R_0\right) - A_{pr}^{\mathbf{Q}} D_{ps}^{[S]}\left(R_0\right)\right) \\ \mathbf{D}^{\mathbf{F}} &\equiv \tfrac{1}{2}\left\{\mathbf{D}^{[S]}\left(R_0\right); \mathbf{A}^{\mathbf{F}}\right\} \\ \mathbf{d}^{\mathbf{F}} &\equiv \tfrac{1}{2}\left\{\mathbf{d}^{[S]}\left(R_0\right); \mathbf{A}^{\mathbf{F}}\right\} \end{aligned} \tag{382}$$

in which the operation $\{;\}$ is the matrix anticommutator. The terms involving gradients of the $\mathbf{K}(R)$ matrix will all take the form

$$\vec{k}(R_0)^x \cdot \vec{f}^{CI\,\mathbf{X}} \tag{383}$$

which can be added onto the similar term in equation (360). The terms involving gradients of density matrices will take the form

$$\vec{p}(R_0)^x \cdot \vec{f}_{csf}^{\,\mathbf{X}} \tag{384}$$

where $\vec{p}(R)$ is the vector of parameters for the rotation of CSF coefficients (see equation (167)) and $\vec{f}_{csf}$ is analogous to $\vec{f}^{CI}$, but where the commutator is taken with the generators of $\exp(\hat{P})$. Now the vector product

$$\left(\vec{k}(R_0)^x\ \vec{p}(R_0)^x\right)\begin{pmatrix} \vec{f}^{CI} + \vec{f}^{CI\,\mathbf{Q}} + \vec{f}^{CI\,\mathbf{F}} \\ \vec{f}^{CI\,\mathbf{Q}} + \vec{f}^{CI\,\mathbf{D}} + \vec{f}^{CI\,\mathbf{F}} \end{pmatrix} \tag{385}$$

can be cast as [**3**]

$$Tr\left(\mathbf{h}^{[S]}(R_0)^x\left(\mathbf{D}^{\mathbf{\Lambda}} + \mathbf{D}^{\boldsymbol{\lambda}}\right)\right) + \tfrac{1}{2}Tr\left(\mathbf{g}^{[S]}(R_0)^x\left(\mathbf{d}^{\mathbf{\Lambda}} + \mathbf{d}^{\boldsymbol{\lambda}}\right)\right) \tag{386}$$

Thus all terms in equation (360) are written as traces of gradients of integral matrices multiplied by various density matrices. Substituting the results of (381) and (386) into equation (362)yields

$$\begin{aligned} \left\langle \psi_I^{[Z]}(R_0)\middle|\hat{H}^{[Z]}(R_0)^x\middle|\psi_I^{[Z]}(R_0)\right\rangle &= Tr\left(\mathbf{h}^{[S]}(R_0)^x\left(\mathbf{D}^{[S]}(R_0) + \mathbf{D}^{\mathbf{Q}} + \mathbf{D}^{\mathbf{F}} + \mathbf{D}^{\mathbf{\Lambda}} + \mathbf{D}^{\boldsymbol{\lambda}}\right)\right) \\ &\quad + \tfrac{1}{2}Tr\left(\mathbf{g}^{[S]}(R_0)^x\left(\mathbf{d}^{[S]}(R_0) + \mathbf{d}^{\mathbf{Q}} + \mathbf{d}^{\mathbf{F}} + \mathbf{d}^{\mathbf{\Lambda}} + \mathbf{d}^{\boldsymbol{\lambda}}\right)\right) \\ &= Tr\left(\mathbf{h}^{[S]}(R_0)^x\,\mathbf{D}_{tot}^{[S]}(R_0)\right) + \tfrac{1}{2}Tr\left(\mathbf{g}^{[S]}(R_0)^x\,\mathbf{d}_{tot}^{[S]}(R_0)\right) \end{aligned} \tag{387}$$

These integral matrices have analytic forms in the original atomic basis to which we should like to transform them. Recall that the transformation between the $\left[C\right]$ and $\left[S\right]$ bases is

$$\mathbf{h}^{[S]}(R)=\mathbf{S}^{[C]^{-1/2}}(R)\mathbf{h}^{[C]}(R)\mathbf{S}^{[C]^{-1/2}}(R) \tag{388}$$

It follows then that the derivative of this equation evaluated at the reference geometry is

$$\begin{aligned}\mathbf{h}^{[S]}(R_0)^x &= \mathbf{S}^{[C]^{-1/2}}(R_0)^x\,\mathbf{h}^{[C]}(R_0)\mathbf{S}^{[C]^{-1/2}}(R_0)\\ &+\mathbf{S}^{[C]^{-1/2}}(R_0)\mathbf{h}^{[C]}(R_0)^x\,\mathbf{S}^{[C]^{-1/2}}(R_0)+\mathbf{S}^{[C]^{-1/2}}(R_0)\mathbf{h}^{[C]}(R_0)\mathbf{S}^{[C]^{-1/2}}(R_0)^x\end{aligned} \tag{389}$$

Using equation (161), we find that

$$\begin{aligned}\mathbf{S}^{[C]^{-1/2}}(R_0)&=\mathbf{1}\\ \mathbf{S}^{[C]^{-1/2}}(R_0)^x&=-\tfrac{1}{2}\mathbf{S}^{[C]}(R_0)^x\end{aligned} \tag{390}$$

and equation (389) is simplified as

$$\begin{aligned}\mathbf{h}^{[S]}(R_0)^x &= -\tfrac{1}{2}\mathbf{S}^{[C]}(R_0)^x\,\mathbf{h}^{[C]}(R_0)+\mathbf{h}^{[C]}(R_0)^x-\tfrac{1}{2}\mathbf{h}^{[C]}(R_0)\mathbf{S}^{[C]}(R_0)^x\\ &=\mathbf{h}^{[C]}(R_0)^x-\tfrac{1}{2}\left\{\mathbf{S}^{[C]}(R_0)^x,\mathbf{h}^{[C]}(R_0)\right\}\end{aligned} \tag{391}$$

Similarly,

$$\mathbf{g}^{[S]}(R_0)^x=\mathbf{g}^{[C]}(R_0)^x-\tfrac{1}{4}\left\{\mathbf{S}^{[C]}(R_0)^x,\mathbf{g}^{[C]}(R_0)\right\} \tag{392}$$

leading to the transformation of equation (387):

$$\begin{aligned}\left\langle \psi_I^{[Z]}(R_0)\middle|\hat{H}^{[Z]}(R_0)^x\middle|\psi_I^{[Z]}(R_0)\right\rangle = & Tr\left[\mathbf{h}^{[C]}(R_0)^x\,\mathbf{D}_{tot}^{[C]}(R_0)\right] \\ & +\tfrac{1}{2}Tr\left[\mathbf{g}^{[C]}(R_0)^x\,\mathbf{d}_{tot}^{JJ[C]}(R_0)\right] \\ & -\tfrac{1}{2}Tr\left[\left\{\mathbf{h}^{[C]}(R_0),\mathbf{S}^{[C]}(R_0)^x\right\}\cdot\mathbf{D}_{tot}^{[C]}(R_0)\right] \\ & -\tfrac{1}{4}Tr\left[\left\{\mathbf{g}^{[C]}(R_0),\mathbf{S}^{[C]}(R_0)^x\right\}\cdot\mathbf{d}_{tot}^{[C]}(R_0)\right]\end{aligned} \tag{393}$$

in which we have used the fact that the density matrices in the two bases are the same at the reference geometry. Let us simplify the arguments of the trace. We have, using simplified notation:

$$Tr\left(\{\mathbf{h},\mathbf{S}\}\mathbf{D}\right) = Tr\left(\mathbf{hSD}+\mathbf{ShD}\right) = \sum_{ijk}\mathbf{h}_{ij}\mathbf{S}_{jk}\mathbf{D}_{ki}+\mathbf{S}_{ij}\mathbf{h}_{jk}\mathbf{D}_{ki} \tag{394}$$

Since $\mathbf{h}$ and $\mathbf{S}$ are symmetric, this is

$$\sum_{ijk}\mathbf{h}_{ij}\mathbf{S}_{jk}\mathbf{D}_{ki}+\mathbf{S}_{ij}\mathbf{h}_{jk}\mathbf{D}_{ki} = \sum_{ijk}\mathbf{S}_{kj}\mathbf{h}_{ji}\mathbf{D}_{ik}^T+\mathbf{S}_{ij}\mathbf{h}_{jk}\mathbf{D}_{ki} \tag{395}$$

The density matrix is not symmetric; however, since $\mathbf{h}$ and $\mathbf{S}$ are, only the symmetric portion of $\mathbf{D}$ contributes to the trace. Thus

$$\sum_{ijk}\mathbf{S}_{kj}\mathbf{h}_{ji}\mathbf{D}_{ik}^T+\mathbf{S}_{ij}\mathbf{h}_{jk}\mathbf{D}_{ki} = \sum_{ijk}\mathbf{S}_{kj}\mathbf{h}_{ji}\mathbf{D}_{ik}+\mathbf{S}_{ij}\mathbf{h}_{jk}\mathbf{D}_{ki} = 2Tr\left(\mathbf{SF}^1\right) \tag{396}$$

where the Fock matrices were defined in equation (365). If we apply this derivation to the terms in equation (393), we find that

$$-\tfrac{1}{2}Tr\left[\left\{\mathbf{h}^{[C]}(R_0),\mathbf{S}^{[C]}(R_0)^x\right\}\cdot\mathbf{D}_{tot}^{[C]}(R_0)\right] = -Tr\left[\mathbf{S}^{[C]}(R_0)^x\,\mathbf{F}_{tot}^{1[C]}\right] \tag{397}$$

and, through a similar derivation,

$$-\tfrac{1}{4}Tr\left[\left\{\mathbf{g}^{[C]}(R_0),\mathbf{S}^{[C]}(R_0)^x\right\}\cdot\mathbf{d}_{tot}^{[C]}(R_0)\right] = -Tr\left[\mathbf{S}^{[C]}(R_0)^x\,\mathbf{F}_{tot}^{2[C]}\right] \tag{398}$$

Equation (393) can consequently be written

$$\left\langle \psi_I^{[Z]}(R_0)\middle|\hat{H}^{[Z]}(R_0)^x\middle|\psi_I^{[Z]}(R_0)\right\rangle = Tr\left[\mathbf{h}^{[C]}(R_0)^x\,\mathbf{D}_{tot}^{[C]}(R_0)\right] + \tfrac{1}{2}Tr\left[\mathbf{g}^{[C]}(R_0)^x\,\mathbf{d}_{tot}^{[C]}(R_0)\right] - Tr\left[\mathbf{S}^{[C]}(R_0)^x\,\mathbf{F}_{tot}^{[C]}(R_0)\right] \tag{399}$$

The transfer to the atomic basis is relatively simple. Any operator in the $[C]$ basis can be expressed in the $[\chi]$ basis by the transformation

$$\mathbf{A}^{[C]}(R) = \mathbf{C}^T(R_0)\,\mathbf{A}^{[\chi]}(R)\,\mathbf{C}(R_0) \tag{400}$$

(see equation (157)). Since $\mathbf{C}(R_0)$ is constant with respect to nuclear coordinates,

$$\mathbf{A}^{[C]}(R)^x = \mathbf{C}^T(R_0)\,\mathbf{A}^{[\chi]}(R)^x\,\mathbf{C}(R_0) \tag{401}$$

however, density matrices transform as [**3**]

$$\mathbf{D}^{[C]}(R) = \mathbf{C}^{-1}(R_0)\,\mathbf{D}^{[\chi]}(R)\left(\mathbf{C}^{-1}(R_0)\right)^T \tag{402}$$

Thus equation (399) can be restated as

$$\begin{aligned}\left\langle \psi_I^{[Z]}(R_0)\middle|\hat{H}^{[Z]}(R_0)^x\middle|\psi_I^{[Z]}(R_0)\right\rangle = {} & Tr\left[\mathbf{C}^T(R_0)\mathbf{h}^{[\chi]}(R_0)^x\,\mathbf{D}_{tot}^{JI[\chi]}(R_0)\left(\mathbf{C}^{-1}\right)^T(R_0)\right] \\ & + \tfrac{1}{2}Tr\left[\mathbf{C}^T(R_0)\mathbf{g}^{[\chi]}(R_0)^x\,\mathbf{d}_{tot}^{JI[\chi]}(R_0)\left(\mathbf{C}^{-1}\right)^T(R_0)\right] \\ & - Tr\left[\mathbf{C}^T(R_0)\mathbf{S}^{[\chi]}(R_0)^x\,\mathbf{F}_{tot}^{[\chi]}(R_0)\left(\mathbf{C}^{-1}\right)^T(R_0)\right]\end{aligned} \tag{403}$$

Since

$$Tr(\mathbf{AB}) = Tr(\mathbf{BA}) \tag{404}$$

it follows that the last matrix in each trace argument can be brought to the front, and so the transformation has no effect on the form of the trace:

$$\left\langle \psi_I^{[Z]}(R_0)\middle|\hat{H}^{[Z]}(R_0)^x\middle|\psi_I^{[Z]}(R_0)\right\rangle = Tr\left[(R_0)\mathbf{h}^{[\chi]}(R_0)^x\,\mathbf{D}_{tot}^{[\chi]}(R_0)\right] + \tfrac{1}{2}Tr\left[\mathbf{g}^{[\chi]}(R_0)^x\,\mathbf{d}_{tot}^{[\chi]}(R_0)\right] - Tr\left[\mathbf{S}^{[\chi]}(R_0)^x\,\mathbf{F}_{tot}^{[\chi]}(R_0)\right] \tag{405}$$

Thus the gradient is now written with derivatives only of matrices whose elements are known analytically, *i.e.* derivatives of

$$\begin{aligned}
\mathbf{h}_{ij}^{[\chi]}(R) &= \int dr\, \chi_i^*(r;R)\left[-\tfrac{1}{2}\nabla_{el}^2 - \sum_\alpha \frac{Z_\alpha}{|R_\alpha - r|}\right]\chi_j(r;R) \\
\mathbf{g}_{ijkl}^{[\chi]}(R) &= \int\int dr_1 dr_2\, \chi_i^*(r_1;R)\,\chi_k^*(r_2;R)\left[\frac{1}{|r_1 - r_2|}\right]\chi_j(r_1;R)\,\chi_l(r_2;R) \\
\mathbf{S}_{ij}^{[\chi]}(R) &= \int dr\, \chi_i^*(r;R)\,\chi_j(r;R)
\end{aligned} \tag{406}$$

while the density matrices can be calculated as needed. Thus there is no need to use finite differences to estimate the gradient, nor to create analytic functions of the CI coefficients.

The CI DCT is derived in the same manner, with the exception that transition density matrices are used, and the entire quantity must afterward be divided by the energy difference:

$$\begin{aligned}
\Delta E(R_0)\, f_{JI}^{CI}(R_0)^x &= \left\langle \psi_J^{[Z]}(R_0)\middle|\hat{H}^{[Z]}(R_0)^x\middle|\psi_I^{[Z]}(R_0)\right\rangle \\
&= Tr\left[(R_0)\mathbf{h}^{[\chi]}(R_0)^x\,\mathbf{D}_{tot}^{JI[\chi]}(R_0)\right] \\
&\quad + \tfrac{1}{2}Tr\left[\mathbf{g}^{[\chi]}(R_0)^x\,\mathbf{d}_{tot}^{JI[\chi]}(R_0)\right] - Tr\left[\mathbf{S}^{[\chi]}(R_0)^x\,\mathbf{F}_{tot}^{JI[\chi]}(R_0)\right]
\end{aligned} \tag{407}$$

Appendix H. The CSF DCT

The CSF DCT is [**5**] [**49**]

$$f_{JI}^{CSF}\left(R\right)^{x} \equiv \sum_{ij} c_j^J\left(R\right) c_i^I\left(R\right) \left\langle \varphi_j\left(r:R\right) \middle| \tfrac{\partial}{\partial R_x} \varphi_i\left(R\right) \right\rangle \tag{408}$$

(see equation (244) in the main text). Unlike the CI DCT, in this case the gradient is taken of the basis function. Since the Gel'fand-Tsetlin basis functions can be written as linear combinations of Slater determinants, let us consider the gradient of a determinant:

$$\tfrac{\partial}{\partial R_x} \left| \phi_a \phi_b \phi_c \ldots \right\rangle = \left| \tfrac{\partial}{\partial R_x} \left(\phi_a\right) \phi_b \phi_c \ldots \right\rangle + \left| \phi_a \tfrac{\partial}{\partial R_x} \left(\phi_b\right) \phi_c \ldots \right\rangle + \left| \phi_a \phi_b \tfrac{\partial}{\partial R_x} \left(\phi_c\right) \ldots \right\rangle + \ldots \tag{409}$$

The $n!n$ terms in this expansion each contain nuclear derivatives of functions of all electronic variables; however, one can also separate the terms into a set containing nuclear derivatives of functions only of electron 1, a set containing nuclear derivatives of functions only of electron 2, etc. For example, consider the simple Slater determinant

$$\left| \phi_a \phi_b \right\rangle = \frac{1}{\sqrt{2}} \left(\left| \phi_a\left(1\right) \phi_b\left(2\right) \right\rangle - \left| \phi_b\left(1\right) \phi_a\left(2\right) \right\rangle \right) \tag{410}$$

Its nuclear gradient can be written as

$$\begin{aligned} \tfrac{\partial}{\partial R_x} \left| \phi_a \phi_b \right\rangle &= \frac{1}{\sqrt{2}} \left(\left| \tfrac{\partial}{\partial R_x} \left(\phi_a\left(1\right) \right) \phi_b\left(2\right) \right\rangle - \left| \phi_b\left(1\right) \tfrac{\partial}{\partial R_x} \left(\phi_a\left(2\right) \right) \right\rangle + \left| \phi_a\left(1\right) \tfrac{\partial}{\partial R_x} \left(\phi_b\left(2\right) \right) \right\rangle - \left| \tfrac{\partial}{\partial R_x} \left(\phi_b\left(1\right) \right) \phi_a\left(2\right) \right\rangle \right) \\ &= \frac{1}{\sqrt{2}} \left(\left| \tfrac{\partial}{\partial R_x} \left(\phi_a\left(1\right) \right) \phi_b\left(2\right) \right\rangle - \left| \tfrac{\partial}{\partial R_x} \left(\phi_b\left(1\right) \right) \phi_a\left(2\right) \right\rangle + \left| \phi_a\left(1\right) \tfrac{\partial}{\partial R_x} \left(\phi_b\left(2\right) \right) \right\rangle - \left| \phi_b\left(1\right) \tfrac{\partial}{\partial R_x} \left(\phi_a\left(2\right) \right) \right\rangle \right) \end{aligned} \tag{411}$$

which can be separated into two terms as discussed above. Thus we can recast the nuclear derivative as

$$\frac{\partial}{\partial R_x} \equiv \sum_i \hat{\delta}(i) \tag{412}$$

where

$$\hat{\delta}(i)\left|\phi_k(j;R)\right\rangle = \left|\frac{\partial}{\partial R_x}\phi_k(i;R)\right\rangle \delta_{ij} \tag{413}$$

Since $\frac{\partial}{\partial R_x}$ is then effectively a one-electron operator, it can be represented in the molecular orbital basis by the product of generator matrices with integral matrices much like the one-electron Hamiltonian (see equation (31))

$$\frac{\partial}{\partial R_x} = \sum_{r,s} \hat{E}_{rs}\delta_{rs} \tag{414}$$

where

$$\delta_{rs} \equiv \left\langle \phi_r(i;R)\right|\hat{\delta}(i)\left|\phi_s(i;R)\right\rangle \tag{415}$$

We can substitute this definition into definition (408):

$$\begin{aligned}
\sum_{ij} c_{Ii}^{\dagger}(R)c_{Jj}(R)\left\langle \varphi_i(r;R)\right|\frac{\partial}{\partial R_x}\varphi_j(r;R)\right\rangle &= \sum_{ij} c_{Ii}^{\dagger}(R)c_{Jj}(R)\left\langle \varphi_i(R)\right|\sum_{rs}\hat{E}_{rs}\left\langle \phi_r(i;R)\right|\hat{\delta}(i)\left|\phi_s(i;R)\right\rangle\left|\varphi_j(R)\right\rangle \\
&= \sum_{rs}\sum_{ij} c_{Ii}^{\dagger}(R)\left\langle \varphi_i(R)\right|\hat{E}_{rs}c_{Jj}(R)\left|\varphi_j(R)\right\rangle\left\langle \phi_r(R)\right|\hat{\delta}\left|\phi_s(R)\right\rangle \\
&= \sum_{rs}\left\langle \Psi_I(R)\right|\hat{E}_{rs}\left|\Psi_J(R)\right\rangle\left\langle \phi_r(R)\right|\hat{\delta}\left|\phi_s(R)\right\rangle \\
&= \sum_{rs} D_{rs}^{IJ[Z]}(R)\left\langle \phi_r^{[Z]}(R)\right|\frac{\partial}{\partial R_x}\phi_s^{[Z]}(R)\right\rangle
\end{aligned} \tag{416}$$

where all pieces can be assumed at this point to be expressed in the $[Z]$ basis. Thus, rather than acting on the Gel'fand-Tsetlin basis functions, we can assume the gradient acts upon the molecular orbitals directly. We can now transform this form of the CSF

DCT back into the $[C]$ basis just as we have done with the CI DCT. The derivative of a MO evaluated at the reference geometry can be expressed as the transformation

$$\begin{aligned}\left|\tfrac{\partial}{\partial R_x}\phi_s^{[Z]}(R_0)\right\rangle &= \tfrac{\partial}{\partial R_x}\left[\exp(\mathbf{K}(R))\exp(\mathbf{Z}(R))\left|\phi_s^{[S]}(R)\right\rangle\right] \\ &= \tfrac{\partial}{\partial R_x}\left[(1+\mathbf{K}(R)+\ldots)(1+\mathbf{Z}(R)+\ldots)\left|\phi_s^{[S]}(R)\right\rangle\right] \\ &= \tfrac{\partial}{\partial R_x}\left[(1+\mathbf{K}(R)+\mathbf{Z}(R)+\ldots)\left|\phi_s^{[S]}(R)\right\rangle\right] \\ &= \left|\tfrac{\partial}{\partial R_x}\phi_s^{[S]}(R_0)\right\rangle + \tfrac{\partial}{\partial R_x}(\mathbf{K}(R_0))\left|\phi_s^{[S]}(R_0)\right\rangle + \tfrac{\partial}{\partial R_x}(\mathbf{Z}(R_0))\left|\phi_s^{[S]}(R_0)\right\rangle\end{aligned} \tag{417}$$

where all other terms contain at least one factor of $\hat{K}(R_0)$ or $\hat{Z}(R_0)$ and thus evaluate to zero. Transforming from the $[S]$ basis back to the $[C]$ basis is effected by

$$\begin{aligned}\left|\tfrac{\partial}{\partial R_x}\phi_s^{[Z]}(R_0)\right\rangle &= \tfrac{\partial}{\partial R_x}\left(\mathbf{S}^{[C]-1/2}(R_0)\right)\left|\phi_s^{[C]}(R_0)\right\rangle + \mathbf{S}^{[C]-1/2}(R_0)\tfrac{\partial}{\partial R_x}\left|\phi_s^{[C]}(R_0)\right\rangle \\ &+ \tfrac{\partial}{\partial R_x}(\mathbf{K}(R_0))\mathbf{S}^{[C]-1/2}(R_0)\left|\phi_s^{[C]}(R_0)\right\rangle + \tfrac{\partial}{\partial R_x}(\mathbf{Z}(R_0))\mathbf{S}^{[C]-1/2}(R_0)\left|\phi_s^{[C]}(R_0)\right\rangle\end{aligned} \tag{418}$$

(see equation (163)), which, using equation (390), simplifies to

$$\begin{aligned}\left|\tfrac{\partial}{\partial R_x}\phi_s^{[Z]}(R_0)\right\rangle &= -\tfrac{1}{2}\tfrac{\partial}{\partial R_x}\left(\mathbf{S}^{[C]}(R_0)\right)\left|\phi_s^{[C]}(R_0)\right\rangle + \tfrac{\partial}{\partial R_x}\left|\phi_s^{[C]}(R_0)\right\rangle \\ &+ \tfrac{\partial}{\partial R_x}(\mathbf{K}(R_0))\left|\phi_s^{[C]}(R_0)\right\rangle + \tfrac{\partial}{\partial R_x}(\mathbf{Z}(R_0))\left|\phi_s^{[C]}(R_0)\right\rangle\end{aligned} \tag{419}$$

Since

$$\left\langle\phi_r^{[Z]}(R_0)\right| = \left\langle\phi_r^{[K]}(R_0)\right| = \left\langle\phi_r^{[S]}(R_0)\right| = \left\langle\phi_r^{[C]}(R_0)\right| \tag{420}$$

it follows that integrating equation (419) against $\left\langle\phi_r^{[Z]}(R_0)\right|$ yields

$$\begin{aligned}\left\langle\phi_r^{[Z]}(R_0)\left|\tfrac{\partial}{\partial R_x}\phi_s^{[Z]}(R_0)\right\rangle\right. &= -\tfrac{1}{2}\left\langle\phi_r^{[C]}(R_0)\left|\tfrac{\partial}{\partial R_x}\left(\mathbf{S}^{[C]}(R_0)\right)\right|\phi_s^{[C]}(R_0)\right\rangle + \left\langle\phi_r^{[C]}(R_0)\left|\tfrac{\partial}{\partial R_x}\right|\phi_s^{[C]}(R_0)\right\rangle \\ &+ \left\langle\phi_r^{[C]}(R_0)\left|\tfrac{\partial}{\partial R_x}(\mathbf{K}(R_0))\right|\phi_s^{[C]}(R_0)\right\rangle + \left\langle\phi_r^{[C]}(R_0)\left|\tfrac{\partial}{\partial R_x}(\mathbf{Z}(R_0))\right|\phi_s^{[C]}(R_0)\right\rangle\end{aligned} \tag{421}$$

Elements of $\tfrac{\partial}{\partial R_x}\mathbf{S}^{[C]}(R_0)$ are

$$\left(\tfrac{\partial}{\partial R_x}\mathbf{S}^{[C]}(R_0)\right)_{rs} = \left\langle \tfrac{\partial}{\partial R_x}\phi_r^{[C]}(R_0)\middle|\phi_s^{[C]}(R_0)\right\rangle + \left\langle \phi_r^{[C]}(R_0)\middle|\tfrac{\partial}{\partial R_x}\phi_s^{[C]}(R_0)\right\rangle \tag{422}$$

and so the first two terms on the right-hand side of equation (421) can be combined:

$$\begin{aligned}\left\langle \phi_r^{[Z]}(R_0)\middle|\tfrac{\partial}{\partial R_x}\phi_s^{[Z]}(R_0)\right\rangle = \tfrac{1}{2}\left(\left\langle \phi_r^{[C]}(R_0)\middle|\tfrac{\partial}{\partial R_x}\phi_s^{[C]}(R_0)\right\rangle - \left\langle \tfrac{\partial}{\partial R_x}\phi_r^{[C]}(R_0)\middle|\phi_s^{[C]}(R_0)\right\rangle\right)\\ + \left\langle \phi_r^{[C]}(R_0)\middle|\tfrac{\partial}{\partial R_x}\left(\mathbf{K}(R_0)\right)\middle|\phi_s^{[C]}(R_0)\right\rangle + \left\langle \phi_r^{[C]}(R_0)\middle|\tfrac{\partial}{\partial R_x}\left(\mathbf{Z}(R_0)\right)\middle|\phi_s^{[C]}(R_0)\right\rangle\end{aligned} \tag{423}$$

If we use the parameter-generator form of $\mathbf{K}$ and $\mathbf{Z}$ (see equation (355)),

$$\begin{aligned}\mathbf{K}(R_0) &= \sum_{r'<s'} k_{r's'}(R_0)\left(E_{r's'} - E_{s'r'}\right)\\ \mathbf{Z}(R_0) &= \sum_{r'<s'} z_{r's'}(R_0)\left(E_{r's'} - E_{s'r'}\right)\end{aligned} \tag{424}$$

then the final terms in equation (423) become

$$\begin{aligned}\left\langle \phi_r^{[C]}(R_0)\middle|\tfrac{\partial}{\partial R_x}\left(\mathbf{K}(R_0)\right)\middle|\phi_s^{[C]}(R_0)\right\rangle &= \sum_{r'<s'} \tfrac{\partial}{\partial R_x}\left(k_{r's'}(R_0)\right)\left\langle \phi_r^{[C]}(R_0)\middle|\left(E_{r's'} - E_{s'r'}\right)\middle|\phi_s^{[C]}(R_0)\right\rangle\\ \left\langle \phi_r^{[C]}(R_0)\middle|\tfrac{\partial}{\partial R_x}\left(\mathbf{Z}(R_0)\right)\middle|\phi_s^{[C]}(R_0)\right\rangle &= \sum_{r'<s'} \tfrac{\partial}{\partial R_x}\left(z_{r's'}(R_0)\right)\left\langle \phi_r^{[C]}(R_0)\middle|\left(E_{r's'} - E_{s'r'}\right)\middle|\phi_s^{[C]}(R_0)\right\rangle\end{aligned} \tag{425}$$

as only the parameters ($k_{r's'}$ and $z_{r's'}$) have nuclear dependence, while the generators ($E_{r's'}$ and $E_{s'r'}$) participate in the integral. Because of the annihilation/creation form of the generators (see equation (30)), those integrals become delta functions:

$$\begin{aligned}\left\langle \phi_r^{[C]}(R_0)\middle|\tfrac{\partial}{\partial R_x}\left(\mathbf{K}(R_0)\right)\middle|\phi_s^{[C]}(R_0)\right\rangle &= \sum_{r'<s'} \tfrac{\partial}{\partial R_x}\left(k_{r's'}(R_0)\right)\left(\delta_{r'r}\delta_{s's} - \delta_{r's}\delta_{s'r}\right)\\ \left\langle \phi_r^{[C]}(R_0)\middle|\tfrac{\partial}{\partial R_x}\left(\mathbf{Z}(R_0)\right)\middle|\phi_s^{[C]}(R_0)\right\rangle &= \sum_{r'<s'} \tfrac{\partial}{\partial R_x}\left(z_{r's'}(R_0)\right)\left(\delta_{r'r}\delta_{s's} - \delta_{r's}\delta_{s'r}\right)\end{aligned} \tag{426}$$

Because of the restricted sum, only one of those delta products will ever be non-zero; thus these equations reduce to

$$\begin{aligned}\left\langle \phi_r^{[C]}(R_0)\middle|\tfrac{\partial}{\partial R_x}\left(\mathbf{K}(R_0)\right)\middle|\phi_s^{[C]}(R_0)\right\rangle &= \tfrac{\partial}{\partial R_x}k_{rs}(R_0)\\ \left\langle \phi_r^{[C]}(R_0)\middle|\tfrac{\partial}{\partial R_x}\left(\mathbf{Z}(R_0)\right)\middle|\phi_s^{[C]}(R_0)\right\rangle &= \tfrac{\partial}{\partial R_x}z_{rs}(R_0)\end{aligned} \tag{427}$$

The various forms of $\frac{\partial}{\partial R_x} z_{rs}\left(R_0\right)$ were discussed in equations (373)-(376). From equation (423) let us define

$$f_{orbrs}^{CSF[C]}\left(R_0\right)^x \equiv \tfrac{1}{2}\left(\left\langle \phi_r^{[C]}\left(R_0\right)\middle|\tfrac{\partial}{\partial R_x}\phi_s^{[C]}\left(R_0\right)\right\rangle - \left\langle \tfrac{\partial}{\partial R_x}\phi_r^{[C]}\left(R_0\right)\middle|\phi_s^{[C]}\left(R_0\right)\right\rangle\right) \tag{428}$$

(which is antisymmetric) so that the entire CSF DCT becomes

$$\begin{aligned}\sum_{ij} c_{Ii}^{\dagger}\left(R_0\right)c_{Jj}\left(R_0\right)\left\langle \varphi_i\left(r;R_0\right)\middle|\tfrac{\partial}{\partial R_x}\varphi_j\left(r;R_0\right)\right\rangle = \\ \sum_{r<s} D_{rs}^{IJ[C]}\left(R_0\right)\left(f_{orbrs}^{CSF[C]}\left(R_0\right)^x + \tfrac{\partial}{\partial R_x}k_{rs}\left(R_0\right) + \tfrac{\partial}{\partial R_x}z_{rs}\left(R_0\right)\right) \\ = Tr\left(\mathbf{D}^{IJ[C]a}\left(R_0\right) f_{orb}^{CSF[C]}\left(R_0\right)^x\right) + \sum_{r\neq s} D_{rs}^{IJ[C]}\left(R_0\right)\tfrac{\partial}{\partial R_x}k_{rs}\left(R_0\right) \\ + \sum_{r\neq s}\tfrac{\partial}{\partial R_x} D_{rs}^{IJ[K]}\left(R_0\right)A_{rs}^{CSF\,IJ\,\mathbf{D}} + \sum_{r\neq s}\tfrac{\partial}{\partial R_x} F_{rs}^{IJ[K]}\left(R_0\right)A_{rs}^{CSF\,IJ\,\mathbf{F}} \\ + \sum_{r\neq s}\tfrac{\partial}{\partial R_x} Q_{rs}^{IJ[K]}\left(R_0\right)A_{rs}^{CSF\,IJ\,\mathbf{Q}}\end{aligned} \tag{429}$$

where we have defined

$$A_{pq}^{CSF\,IJ\,\mathbf{X}} = \frac{D_{pq}^{IJ[C]}\left(R_0\right)}{X_{qq}^{IJ[C]}\left(R_0\right) - X_{pp}^{IJ[C]}\left(R_0\right)} \tag{430}$$

(see equation (380)) and the antisymmetric part of the one-electron density matrix is sufficient for the trace with the CSF orbital gradient vector. The last three terms are treated analogously to the terms in equations (377)-(379), with the appropriate substitution of the $A_{pq}^{CSF\,IJ\,\mathbf{X}}$ term The second term joins them in a manner similar to (385), with the resulting form

$$\begin{aligned} &Tr\left(\mathbf{h}^{[C]}\left(R_0\right)^x\left(\mathbf{D}^{CSF\,IJ\,\mathbf{F}} + \mathbf{D}^{CSF\,IJ\,\mathbf{Q}} + \mathbf{D}^{CSF\,IJ\,\mathbf{\Lambda}} + \mathbf{D}^{CSF\,IJ\,\mathbf{\lambda}}\right)\right) \\ &+\tfrac{1}{2}Tr\left(\mathbf{g}^{[C]}\left(R_0\right)^x\left(\mathbf{d}^{CSF\,IJ\,\mathbf{F}} + \mathbf{d}^{CSF\,IJ\,\mathbf{Q}} + \mathbf{d}^{CSF\,IJ\,\mathbf{\Lambda}} + \mathbf{d}^{CSF\,IJ\,\mathbf{\lambda}}\right)\right)\end{aligned} \tag{431}$$

where $\mathbf{D}^{CSF\,IJ\,\mathbf{X}}$ and $\mathbf{d}^{CSF\,IJ\,\mathbf{X}}$ are defined analogously to those found in equation (387). These traces can now be transformed into the atomic basis similar to equation (403):

$$\begin{aligned}\sum_{ij} c_{Ii}^{\dagger}\left(R_0\right) c_{Jj}\left(R_0\right)\left\langle \varphi_i\left(r;R_0\right)\left|\tfrac{\partial}{\partial R_x}\varphi_j\left(r;R_0\right)\right\rangle\right. = \\ Tr\left(\mathbf{D}^{IJ[\chi]a}\left(R_0\right) f_{orb}^{CSF[\chi]}\left(R_0\right)^x\right) \\ + Tr\left(\mathbf{h}^{[\chi]}\left(R_0\right)^x\left(\mathbf{D}^{CSF\,IJ\,\mathbf{F}} + \mathbf{D}^{CSF\,IJ\,\mathbf{Q}} + \mathbf{D}^{CSF\,IJ\,\boldsymbol{\Lambda}} + \mathbf{D}^{CSF\,IJ\,\boldsymbol{\lambda}}\right)\right) \\ + \tfrac{1}{2} Tr\left(\mathbf{g}^{[\chi]}\left(R_0\right)^x\left(\mathbf{d}^{CSF\,IJ\,\mathbf{F}} + \mathbf{d}^{CSF\,IJ\,\mathbf{Q}} + \mathbf{d}^{CSF\,IJ\,\boldsymbol{\Lambda}} + \mathbf{d}^{CSF\,IJ\,\boldsymbol{\lambda}}\right)\right) \\ = Tr\left(\mathbf{D}^{IJ[\chi]a}\left(R_0\right) f_{orb}^{CSF[\chi]}\left(R_0\right)^x\right) \\ + Tr\left(\mathbf{h}^{[\chi]}\left(R_0\right)^x \mathbf{D}_{tot}^{CSF\,IJ}\right) + \tfrac{1}{2} Tr\left(\mathbf{g}^{[\chi]}\left(R_0\right)^x \mathbf{d}_{tot}^{CSF\,IJ}\right)\end{aligned} \tag{432}$$

At this point, the CSF DCT has been defined in terms of density matrices and gradients of integral matrices at the reference geometry. Combining this with the CI DCT term gives the whole DCT in terms of functions which can be differentiated analytically.

Appendix I. Angular Momentum

Definition

Classically, we consider angular momentum as the cross product of an object's linear momentum with its position with respect to some fixed point [**25**]:

$$J = r \times p \tag{433}$$

Since it is the cross product of two polar vectors, angular momentum is a pseudovector; that is, it rotates like a polar vector, but it remains invariant under inversion, unlike a polar vector. However, in this paper we will be dealing with special unitary groups which do not allow inversion, so angular momentum can be treated summarily as if it were a polar vector.

As with the Hamiltonian, we will derive the quantum mechanical equivalent of equation (433) by turning the classical quantities into operators [**61**]:

$$\hat{J} = \hat{r} \times \hat{p} \tag{434}$$

Recalling the quantum mechanical definition of the linear momentum operator, (284), we see that the angular momentum operator is, component-wise [**46**],

$$\hat{J} \to -i\left(y\tfrac{\partial}{\partial z} - z\tfrac{\partial}{\partial y}\right)\hat{i} - i\left(z\tfrac{\partial}{\partial x} - x\tfrac{\partial}{\partial z}\right)\hat{j} - i\left(x\tfrac{\partial}{\partial y} - y\tfrac{\partial}{\partial x}\right)\hat{k} \tag{435}$$

The formulation in equation (434) was used in Appendix B when exploring the spin-orbit Hamiltonian, where $\hat{L}$ was the orbital angular momentum of the electron. However, there we also found the set of spin operators $\hat{\sigma}_i$ of an electron was considered a set of angular momentum operators. An electron, though massive, is considered a point

particle in quantum chemistry, so it is a fallacy to attempt to connect this spin angular momentum with that of a spinning orb, and equation (434) does not apply. What we need, then, is a more general definition of angular momentum.

In an intuitive sense, angular momentum generates rotation. In a mathematical sense, angular momentum operators are the generators of rotation. A rotation $\hat{U}$ in three-space can be expressed as the exponentiation of it rotational parameters multiplied by the generators [**34**]:

$$\hat{U} = \exp\left(\theta_x \hat{J}_x + \theta_y \hat{J}_y + \theta_z \hat{J}_z\right) \tag{436}$$

This is certainly not the only parameterization of a three-dimensional rotation, but it is as valid as any. The set of rotations is a Lie group, and so the set of angular momentum operators forms its underlying Lie algebra. Lie algebras are defined by their commutation relations [**34**]. In this case, the operators obey the relations

$$\begin{aligned} \left[\hat{J}_x, \hat{J}_y\right] &= i\,\hat{J}_z \\ \left[\hat{J}_y, \hat{J}_z\right] &= i\,\hat{J}_x \\ \left[\hat{J}_z, \hat{J}_x\right] &= i\,\hat{J}_y \end{aligned} \tag{437}$$

which is a specific case of the general Lie algebra commutation relation

$$\left[\hat{O}_i, \hat{O}_j\right] = \sum_{i,j,k} c_{ijk} \hat{O}_k \tag{438}$$

It is easy to see that the angular momentum as formulated in equation (434) obeys the relations in equation (437) given the fundamental commutation relation between position and linear momentum,

$$\left[\hat{x}, \hat{p}_x\right] = i, etc. \tag{439}$$

however, we say that *any* set of operators that obeys the commutation relations presented in equation (437) are angular momentum operators [**46**]. Thus, even though the spin operators do not conform to the formulation in equation (434), they do obey the proper commutation relations and thus can be considered angular momentum operators.

Eigenvalue equations

As angular momentum is an observable quantity, it obeys an eigenvalue equation. In this section we will discover the possible eigenvalues and eigenfunctions associated with the angular momentum operators.

Commuting Operators

It is clear from equation (437) that none of the angular momentum operators commute; this implies that only one of the quantities, J_x, J_y, or J_z, can be observed precisely at any given moment of measurement [**26**]. This also implies that they form a rank 1 algebra (i.e., the largest abelian subalgebra is one-dimensional) and thus has one Casimir invariant operator [**34**]:

$$\hat{J}_x^2 + \hat{J}_y^2 + \hat{J}_z^2 \equiv \hat{J}^2 \tag{440}$$

(This operator is discovered by solving the secular equation for an arbitrary element in the algebra; this process is discussed in Gilmore [**34**] but I will not elaborate here.) The Casimir invariant is a multiple of the identity matrix, and thus commutes with all

elements of the algebra. This further implies that any one of the aforementioned quantities can be observed concurrently with the Casimir invariant; typically we choose J_z. Thus we have a maximal set of two commuting observables in the set of angular momenta, J_z and J^2, which share a set of eigenvectors. Geometrically, this implies that, while we cannot know the precise direction of the angular momentum vector, we can know its length and its projection onto the z-axis.

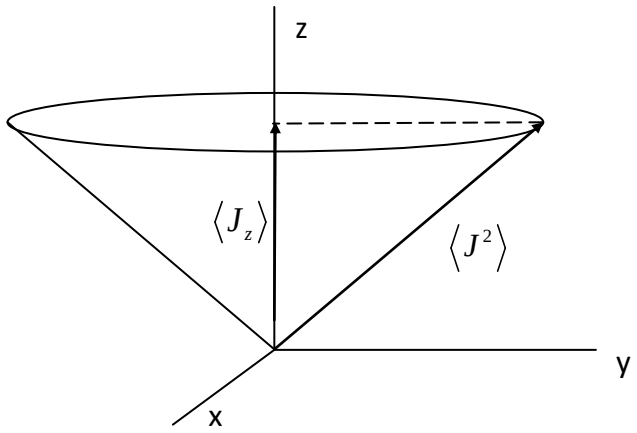

Figure 43. Uncertainty in angular momentum

Eigenvalues

Thus we have the following eigenvalue equations:

$$\begin{aligned} \hat{J}^2 \mid jm\rangle &= \lambda_j \mid jm\rangle \\ \hat{J}_z \mid jm\rangle &= \lambda_m \mid jm\rangle \end{aligned} \tag{441}$$

While the operations $\hat{J}_x \mid jm\rangle$ and $\hat{J}_y \mid jm\rangle$ are of lesser interest, the operations $\hat{J}_+ \mid jm\rangle$ and $\hat{J}_- \mid jm\rangle$, where we define

$$\begin{aligned}\hat{J}_+ &\equiv \hat{J}_x + i\hat{J}_y \\ \hat{J}_- &\equiv \hat{J}_x - i\hat{J}_y\end{aligned} \tag{442}$$

which are adjoints of each other, are of particular use. Using these in place of the $\hat{J}_x$ and $\hat{J}_y$ operators, we have a new Lie algebra with commutation relations [**46**]

$$\begin{aligned}\left[\hat{J}_z, \hat{J}_\pm\right] &= \pm\hat{J}_\pm \\ \left[\hat{J}_+, \hat{J}_-\right] &= 2\hat{J}_z \\ \left[\hat{J}^2, \hat{J}_\pm\right] &= 0\end{aligned} \tag{443}$$

Since $\hat{J}^2$ and $\hat{J}_\pm$ commute, the eigenvalue equation

$$\hat{J}^2\hat{J}_\pm \left| jm\right\rangle = \lambda_j \hat{J}_\pm \left| jm\right\rangle \tag{444}$$

implies that $\hat{J}_\pm \left| jm\right\rangle$ is also an eigenvector of $\hat{J}^2$ with eigenvalue λ_j, while the equation

$$\hat{J}_z\hat{J}_\pm \left| jm\right\rangle = \left(\pm\hat{J}_\pm + \hat{J}_\pm\hat{J}_z\right)\left| jm\right\rangle = \left(\lambda_m \pm 1\right)\hat{J}_\pm \left| jm\right\rangle \tag{445}$$

implies that it is also an eigenvector of $\hat{J}_z$ with eigenvalue $\left(\lambda_m \pm 1\right)$. Furthermore, equation (445) implies that

$$\hat{J}_\pm \left| jm\right\rangle = C_\pm \left| j\, m \pm 1\right\rangle \tag{446}$$

which shows that the eigenvalues of $\hat{J}_z$ differ by integer steps. Combining definition (440) with definition (442), we find a new form of the Casimir invariant,

$$\hat{J}^2 = \tfrac{1}{2}\hat{J}_+\hat{J}_- + \tfrac{1}{2}\hat{J}_-\hat{J}_+ + \hat{J}_z^2 \tag{447}$$

We can take the expectation value of this equation,

$$\begin{aligned}\left\langle jm \mid \hat{J}^2 \mid jm \right\rangle &= \tfrac{1}{2}\left\langle jm \mid \hat{J}_+\hat{J}_- \mid jm \right\rangle + \tfrac{1}{2}\left\langle jm \mid \hat{J}_-\hat{J}_+ \mid jm \right\rangle + \left\langle jm \mid \hat{J}_z^2 \mid jm \right\rangle \\ \lambda_j &= \tfrac{1}{2}\left(\left|C_-\right|^2 + \left|C_+\right|^2\right) + \lambda_m^2\end{aligned} \tag{448}$$

which implies the quantity $\lambda_j - \lambda_m^2$ must be positive. Since both λ_j and λ_m are real, this further implies that λ_j is non-negative and that λ_m is bound above and below by $\pm\sqrt{\lambda_j}$ [**69**]. Let $\left| jm_{\max} \right\rangle$ be the vector whose eigenvalue of $\lambda_{m_{\max}}$ is maximal. Then it is true that

$$\hat{J}_+ \left| jm_{\max} \right\rangle = 0 \tag{449}$$

and hence that

$$\hat{J}_-\hat{J}_+ \left| jm_{\max} \right\rangle = \left(\hat{J}^2 - \hat{J}_z^2 - \hat{J}_z\right) \left| jm_{\max} \right\rangle = 0 \tag{450}$$

Expanding this last equation, we find

$$\begin{aligned}0 &= \left(\hat{J}^2 - \hat{J}_z^2 - \hat{J}_z\right) \left| jm_{\max} \right\rangle \\ &= \lambda_j - \lambda_{m_{\max}}\left(\lambda_{m_{\max}} + 1\right)\end{aligned} \tag{451}$$

Thus we conclude that for maximal λ_m,

$$\lambda_j = \lambda_{m_{\max}}\left(\lambda_{m_{\max}} + 1\right) \tag{452}$$

By analogous argument, for the minimal value $\lambda_{m_{\min}}$

$$\lambda_j = \lambda_{m_{\min}}\left(\lambda_{m_{\min}} - 1\right) \tag{453}$$

Comparing equations (452) and (453) leads to the conclusion that

$$\lambda_{m_{\max}} = -\lambda_{m_{\min}} \tag{454}$$

Since the values of λ_m differ by integer steps (see equation (446)), this conclusion implies that λ_m must take on integer or half-integer values. If we let $\lambda_{m_{\max}}$ be assigned the symbol j, then the eigenvalue of $\hat{J}^2$ is $j(j+1)$ and if we let λ_m be assigned the symbol m, m ranges from $-j$ to j. The equations are

$$\begin{aligned}\hat{J}^2 \left| jm \right\rangle &= j(j+1) \left| jm \right\rangle \\ \hat{J}_z \left| jm \right\rangle &= m \left| jm \right\rangle\end{aligned} \tag{455}$$

Thus not only is the z-projection quantized, it is limited by the total angular momentum (see Figure 44). Table 4 shows the first several values of j and the possible values of m. Apart from the eigenvalue equations, we also have the equations involving $\hat{J}_+$ and $\hat{J}_-$. Using the relationship

$$\hat{J}^2 = \hat{J}_\pm \hat{J}_\mp + \hat{J}_z^2 \mp \hat{J}_z \tag{456}$$

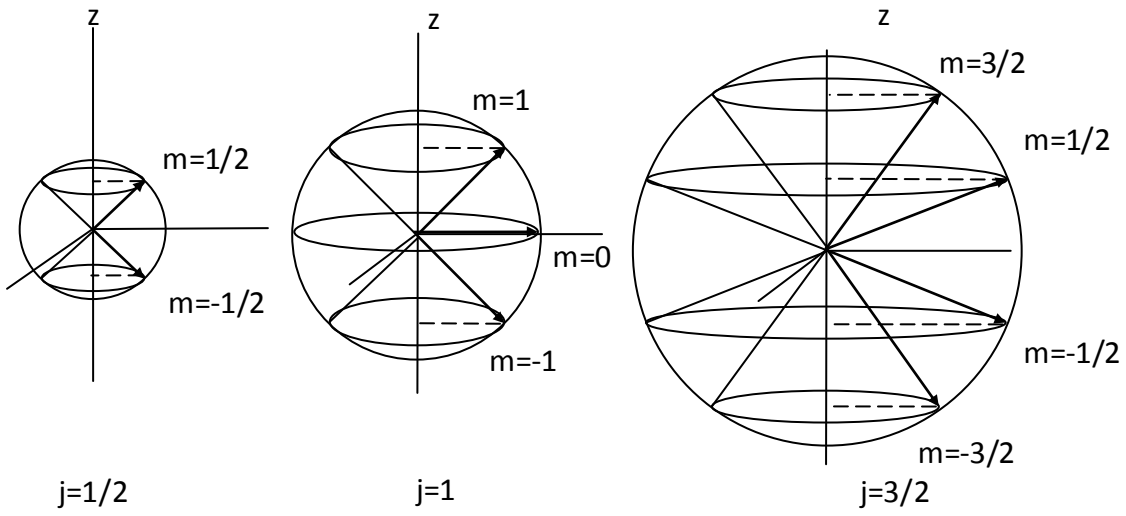

Figure 44. Angular momentum allowed observables

Table 4. Angular momentum values

j	m				
0	*0*				
1/2	*-1/2*	*1/2*			
1	*-1*	*0*	*1*		
3/2	*-3/2*	*-1/2*	*1/2*	*3/2*	
2	*-2*	*-1*	*0*	*1*	*2*

We find through integration that

$$\begin{aligned} \langle jm|\hat{J}^2|jm\rangle &= \langle jm|\hat{J}_{\pm}\hat{J}_{\mp}|jm\rangle + \langle jm|\hat{J}_z^2|jm\rangle \mp \langle jm|\hat{J}_z|jm\rangle \\ j(j+1) &= |C_{\mp}|^2 + m(m\mp 1) \end{aligned} \tag{457}$$

which leads to the equations

$$\hat{J}_{\pm}|jm\rangle = \sqrt{j(j+1)-m(m\pm 1)}\,|j\,m\pm 1\rangle \tag{458}$$

The eigenvalue equations (455) paired with the equations immediately above will be most useful in forming the matrix representation of the angular momentum operators in the succeeding section.

It is an interesting aside to note that, although angular momentum may have integer or half-integer values, the two sets never coincide. That is to say, a system with integer spin can never be made to have half integer spin, and vice versa. A system with an even number of electrons can be a singlet, triplet, quintuplet, etc., with the available spin states only being limited by the number of electrons; however, it will never be a

doublet, quartet, sextet, etc. The opposite is true for odd-electron systems. Fermions may be turned into one another, but can never be transformed into bosons. Orbital angular momentum only manifests itself in integer steps (see the spherical harmonics, below).

Physical Eigenfunctions

The eigenvalue equations (441) form solvable differential equations when the operators $\hat{J}^2$ and $\hat{J}_z$ are derived from equation (435) and the eigenvalues are replaced with $j(j+1)$ and m. Rather than Cartesian coordinates, it is easiest to solve these equations in spherical coordinates. By representing these equations in physical space, we are limited to representing angular momenta which reside in physical space (e.g., orbital angular momentum). This representation is limited to integer-value angular momenta, and so will not include spin (which does not reside in physical space). I will not belabor the transformation nor the solution at this point; suffice it to say that using the relationships

$$\begin{aligned} x &= r\sin\theta\cos\varphi \\ y &= r\sin\theta\cos\varphi \\ z &= r\cos\theta \end{aligned} \tag{459}$$

the angular momentum operators become in spherical coordinates [**46**]

$$\begin{aligned} \hat{J}_z &\to -i\frac{\partial}{\partial\varphi} \\ \hat{J}^2 &\to -\left[\frac{1}{\sin^2\theta}\frac{\partial^2}{\partial\varphi^2}+\frac{1}{\sin\theta}\frac{\partial}{\partial\theta}\left(\sin\theta\frac{\partial}{\partial\theta}\right)\right] \end{aligned} \tag{460}$$

When these are substituted into their respective eigenvalue equations, they form the familiar differential equations whose solutions are the spherical harmonics, $Y_{lm}(\theta,\varphi)$, a complete set of orthonormal functions, whose formula I include here for completeness:

$$|jm\rangle \to Y_{lm}(\theta,\varphi)$$

$$Y_{lm}(\theta,\varphi) = \frac{1}{\sqrt{2\pi}} \frac{(-1)^m}{2^l l!} \left[\frac{2l+1}{2} \frac{(l-m)!}{(l+m)!} \right]^{1/2} \sin^m\theta \left[\frac{d}{d(\cos\theta)} \right]^{l+m} (\cos^2\theta - 1)^l \exp(im\varphi) \quad (461)$$

Because the spherical harmonics are complete and orthonormal, they provide a very useful basis from which to build wavefunctions. When multiplied by a radial function, these functions are able to span the three-dimensional wave functions of single electrons; the direct product of N sets of these functions can form a physical basis for a multi-electron system.

Rotation of Eigenfunctions

When a rotation is applied to a spin eigenfunction, it becomes a linear combination of other spin eigenfunctions. However, these rotations do not allow mixing outside the irrep to which the eigenfunction belongs; that is, the total spin does not mix [**46**]:

$$\hat{R}|jm\rangle = \sum_{m'} D^j_{m'm}(\hat{R})|jm'\rangle \quad (462)$$

where the $D^j_{m'm}(\hat{R})$ are known as the *Wigner D matrices* [**37**].

Matrix Representation

The commutation relations in equation (437) define (to within a constant) the Lie algebra $su(2)$ [**34**]; thus the physics of angular momentum is inexorably connected to the mathematics of the $su(2)$ algebra. We gain great satisfaction from this association as the physics of rotation, generated by angular momentum, and the group of rotations, $SO(3)$, (one of the groups) generated by $su(2)$, should be connected, as we intuitively expect.

There are an infinite number of trios of matrices that obey the $su(2)$ commutation rules. The *defining representation* is the set of 2×2 matrices

$$\begin{pmatrix} 0 & i \\ i & 0 \end{pmatrix}, \begin{pmatrix} 0 & -1 \\ 1 & 0 \end{pmatrix}, \begin{pmatrix} -i & 0 \\ 0 & i \end{pmatrix} \tag{463}$$

which the reader will find obey the relations in equation (437) where i is replaced with -2. An adjustment of phase leads to the *Pauli spin matrices* [**46**]*:*

$$\begin{aligned} \sigma_x &\to \begin{pmatrix} 0 & 1 \\ 1 & 0 \end{pmatrix} \\ \sigma_y &\to \begin{pmatrix} 0 & -i \\ i & 0 \end{pmatrix} \\ \sigma_z &\to \begin{pmatrix} 1 & 0 \\ 0 & -1 \end{pmatrix} \end{aligned} \tag{464}$$

which form another equally valid defining representation of $su(2)$ generators.

[Note that the matrices in the collection (463) are antihermitian (symmetric imaginary components and antisymmetric real components) while those in (464) are hermitian. In

general, the physicist prefers hermitian operators, as, by postulate, they represent observable quantities and obey real eigenvalue equations; however, exponentiated antihermitian matrices are unitary, which are more appropriate for transformations. Thus when one wishes to study angular momentum *per se,* an hermitian representation is fitting; however, when one wishes to use angular momentum as a means to the end of rotations, an antihermitian representation may be more applicable.]

The *regular representation* is the set of 3×3 matrices derived directly from the commutation rules [**34**]:

$$\begin{pmatrix}0&0&0\\0&0&-1\\0&1&0\end{pmatrix},\begin{pmatrix}0&0&1\\0&0&0\\-1&0&0\end{pmatrix},\begin{pmatrix}0&-1&0\\1&0&0\\0&0&0\end{pmatrix} \tag{465}$$

In the previous section, we found a good basis to work in, the $|jm\rangle$ basis. Using equations (455) and (458), we can form the matrix representations of $\hat{J}^2, \hat{J}_z, \hat{J}_+$, and $\hat{J}_-$ in this infinite but discrete basis. Figure 45 Shows the first 10×10 block of each operator, where zeros have been excluded, although the block-diagonal form has been emphasized. $\hat{J}_x$ and $\hat{J}_y$ can be determined using equation (442). Each block or irrep labels a different value of j. For this reason, each block can be used separately as the case may require. For instance, the 2×2 blocks (which are the defining representation) can be used to generate rotations on two-component spinors such as spin, while the 3×3 blocks (which are a transformation of the regular representation) generate

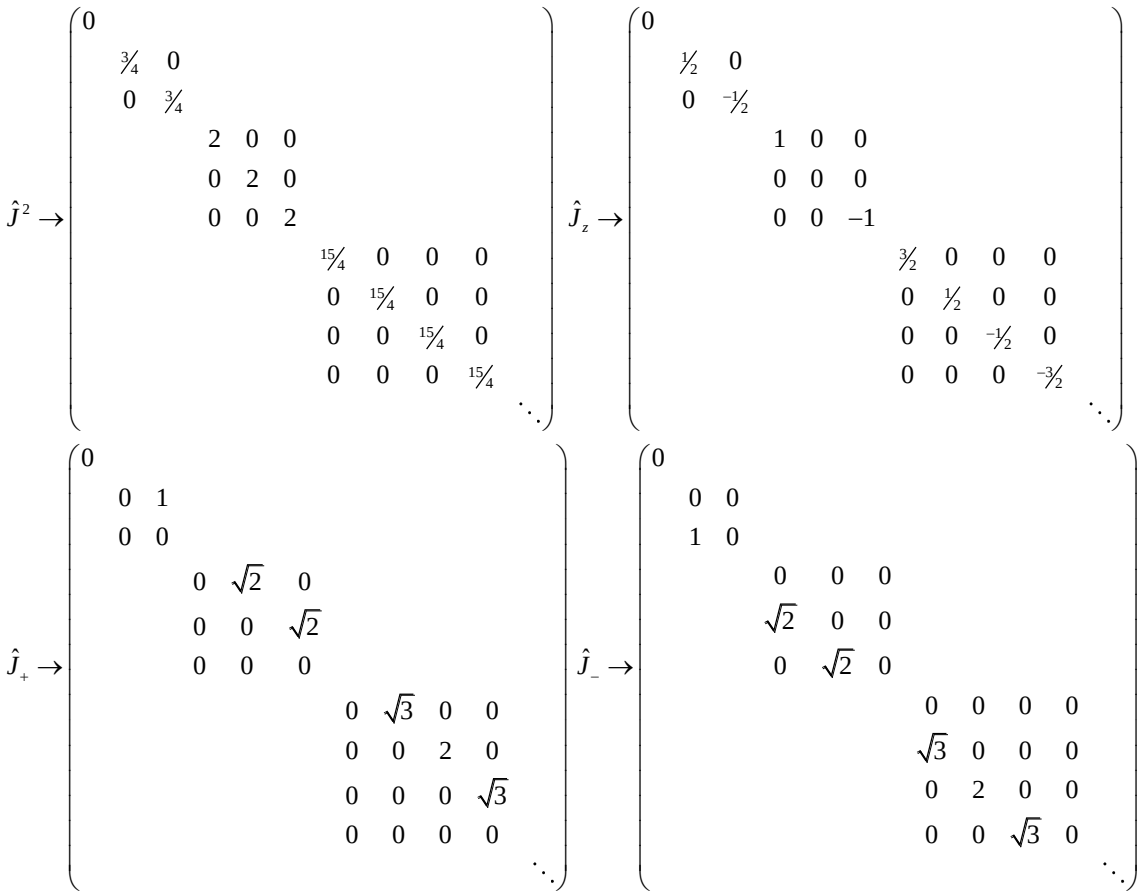

Figure 45. Irreps of angular momentum operators

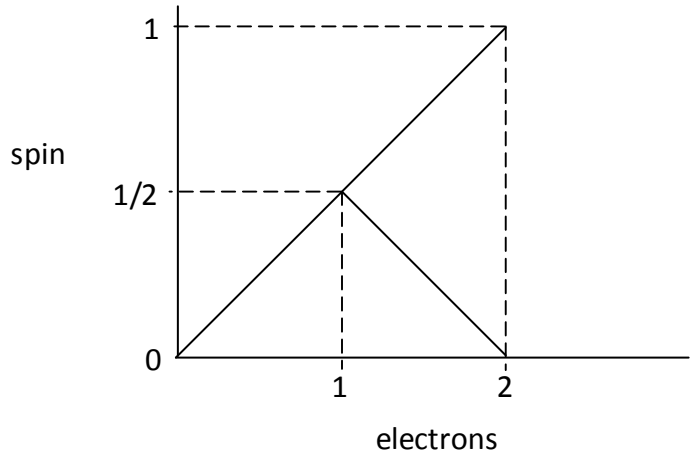

Figure 46. Addition of spin

rotations of rank-1 tensors, such as p-states and vectors in classical three-dimensional space. In this basis, both $\hat{J}^2$ and $\hat{J}_z$ are diagonal, as expected. Notice that each block of $\hat{J}^2$ is an identity matrix scaled by its eigenvalue $j(j+1)$. The elements of $\hat{J}_z$ are the eigenvalues m.

Coupling

Addition

In the previous section, we identified the set of simultaneous eigenfunctions of $\hat{J}^2$ and $\hat{J}_z$, $|jm\rangle$. If a system has two angular momenta associated with it, it is possible to form an eigenfunction of both sets of operators by taking the direct product of eigenfunctions from either set:

$$|j_1 m_1\rangle \otimes |j_2 m_2\rangle \equiv \left| \begin{matrix} j_1 & j_2 \\ m_1 & m_2 \end{matrix} \right\rangle \tag{466}$$

This is an eigenfunction for $\hat{J}_1^2$, $\hat{J}_2^2$, $\hat{J}_{1z}$,and $\hat{J}_{2z}$. Alternatively, we can add the two angular momenta together and form an eigenfunction of $\left(\hat{J}_{1z}+\hat{J}_{2z}\right)$, $\left(\hat{J}_1+\hat{J}_2\right)^2$, $\hat{J}_1^2$, and $\hat{J}_2^2$ [**46**]. While these two formulations are equally valid and differ only by a unitary transformation, the latter has an advantage for systems in which the angular momenta are allowed to couple. For such systems, the set of quantum numbers j_1, j_2, m_1, and m_2 are not good quantum numbers since they are allowed to change. The good quantum numbers, i.e., the eigenvalues that will not change, will be the *total* angular momentum and its z-projection. Even in the non-coupling case, this latter formulation forms a more

compact notation, with only two eigenvalues per function to consider, rather than $2N$. What more, this latter formulation allows the system to be easily expressed in the irrep basis discussed in the previous section.

Example: adding electron spin

Building a basis for the GUGA depends heavily upon *spin adaptation*, which is the process of transforming eigenfunctions into pure states of total j [**20**]. The following example of spin coupling illustrates that transformation.

Consider a system of two spin-1/2 particles such as electrons. Considering only the spin portion, each individual electron wave function can have either of the forms

$$\begin{aligned} \left|s=\tfrac{1}{2}, m_s=\tfrac{1}{2}\right\rangle &= \left|\tfrac{1}{2}\right\rangle \equiv \left|\alpha\right\rangle \\ \left|s=\tfrac{1}{2}, m_s=-\tfrac{1}{2}\right\rangle &= \left|-\tfrac{1}{2}\right\rangle \equiv \left|\beta\right\rangle \end{aligned} \tag{467}$$

We indicate the direct product merely by juxtaposition, so that the uncoupled functions are

$$\begin{aligned} &\left|\alpha\alpha\right\rangle \\ &\left|\alpha\beta\right\rangle \\ &\left|\beta\alpha\right\rangle \\ &\left|\beta\beta\right\rangle \end{aligned} \tag{468}$$

where

$$\left|\gamma\gamma'\right\rangle \equiv \left|\gamma\right\rangle \otimes \left|\gamma'\right\rangle \tag{469}$$

Now consider transforming to spin-coupled eigenfunctions. Since each electron has spin-1/2, the total spin can either be 1/2+1/2=1 or 1/2-1/2=0 (See Figure 46). The spin-1 eigenfunction has three possible z-projections, -1, 0, or 1, and thus forms a triplet. The

spin-0 eigenfunction has no z-projection, and is a singlet. We can indicate these eigenfunctions as

$$\begin{array}{l} |11\rangle \\ |10\rangle \\ |1\,-1\rangle \\ |0\,0\rangle \end{array} \tag{470}$$

We now need a way to define these spin-coupled functions in terms of the original, uncoupled functions which are more intuitive. The transformation

$$|\,jm\rangle = \sum_{m_1,m_2} |m_1 m_2\rangle\langle m_1 m_2\,|\,jm\rangle \tag{471}$$

has coefficients we define as

$$\langle m_1 m_2\,|\,jm\rangle \equiv c_{j m m_1 m_2} \tag{472}$$

known as *Clebsch-Gordan coefficients* [**46**], which are tabulated in various locations. Figure 47 shows the Clebsch-Gordan coefficients for small angular momenta [**70**]. Using these coefficients, we find the following relationships:

$$\begin{array}{ll} |11\rangle = |\alpha\alpha\rangle & |10\rangle = \frac{1}{\sqrt{2}}\left(|\alpha\beta\rangle + |\beta\alpha\rangle\right) \\ |1\,-1\rangle = |\beta\beta\rangle & |0\,0\rangle = \frac{1}{\sqrt{2}}\left(|\alpha\beta\rangle - |\beta\alpha\rangle\right) \end{array} \tag{473}$$

This result was gleaned from the 1/2x1/2 block of Figure 47. Now consider adding a third electron. Since the first two are already coupled, we are coupling an angular momentum of 1 or 0 to an angular momentum of 1/2. Thus we use the 1x1/2 block to find the first set of functions, and the second set (0x1/2) is trivial. We can now have total spins of 3/2 or 1/2 (see Figure 48). Note that there are two ways to have a spin-

1/2 system; either coupling 1 to -1/2 or coupling 0 to 1/2. Using Figure 47 again, we find the following eigenfunctions:

$$
\begin{aligned}
\left|\tfrac{3}{2}\,\tfrac{3}{2}\right\rangle &= \left|\alpha\alpha\alpha\right\rangle \\
\left|\tfrac{3}{2}\,\tfrac{1}{2}\right\rangle &= \tfrac{1}{\sqrt{3}}\left(\left|\alpha\alpha\beta\right\rangle + \left|\alpha\beta\alpha\right\rangle + \left|\beta\alpha\alpha\right\rangle\right) \\
\left|\tfrac{3}{2}\,\tfrac{-1}{2}\right\rangle &= \tfrac{1}{\sqrt{3}}\left(\left|\alpha\beta\beta\right\rangle + \left|\beta\alpha\beta\right\rangle + \left|\beta\beta\alpha\right\rangle\right) \\
\left|\tfrac{3}{2}\,\tfrac{-3}{2}\right\rangle &= \left|\beta\beta\beta\right\rangle \\
\left|\tfrac{1}{2}\,\tfrac{1}{2}\right\rangle &= \begin{cases} \tfrac{1}{\sqrt{6}}\left(2\left|\alpha\alpha\beta\right\rangle - \left(\left|\alpha\beta\alpha\right\rangle + \left|\beta\alpha\alpha\right\rangle\right)\right) \\ \tfrac{1}{\sqrt{2}}\left(\left|\alpha\beta\alpha\right\rangle - \left|\beta\alpha\alpha\right\rangle\right) \end{cases} \\
\left|\tfrac{1}{2}\,\tfrac{-1}{2}\right\rangle &= \begin{cases} \tfrac{1}{\sqrt{6}}\left(\left(\left|\alpha\beta\beta\right\rangle + \left|\beta\alpha\beta\right\rangle\right) - 2\left|\beta\beta\alpha\right\rangle\right) \\ \tfrac{1}{\sqrt{2}}\left(\left|\alpha\beta\beta\right\rangle - \left|\beta\alpha\beta\right\rangle\right) \end{cases}
\end{aligned}
\tag{474}
$$

Now we have a quartet and two degenerate doublets which give us the $2^3 = 8$ eigenfunctions. This process can continue indefinitely, coupling the spins of as many electrons as are in the system in question. As the number of electrons increases, so does the degeneracy of the multiplets. Figure 49 shows these degeneracies as the spin functions are constructed *genealogically* [**39**] [**71**]. Each path through the graph from left to right represents a different spin function.

Coupled rotated spin eigenfunctions

When we take the direct product of rotated eigenfunctions we can apply equation (466) to equation (462):

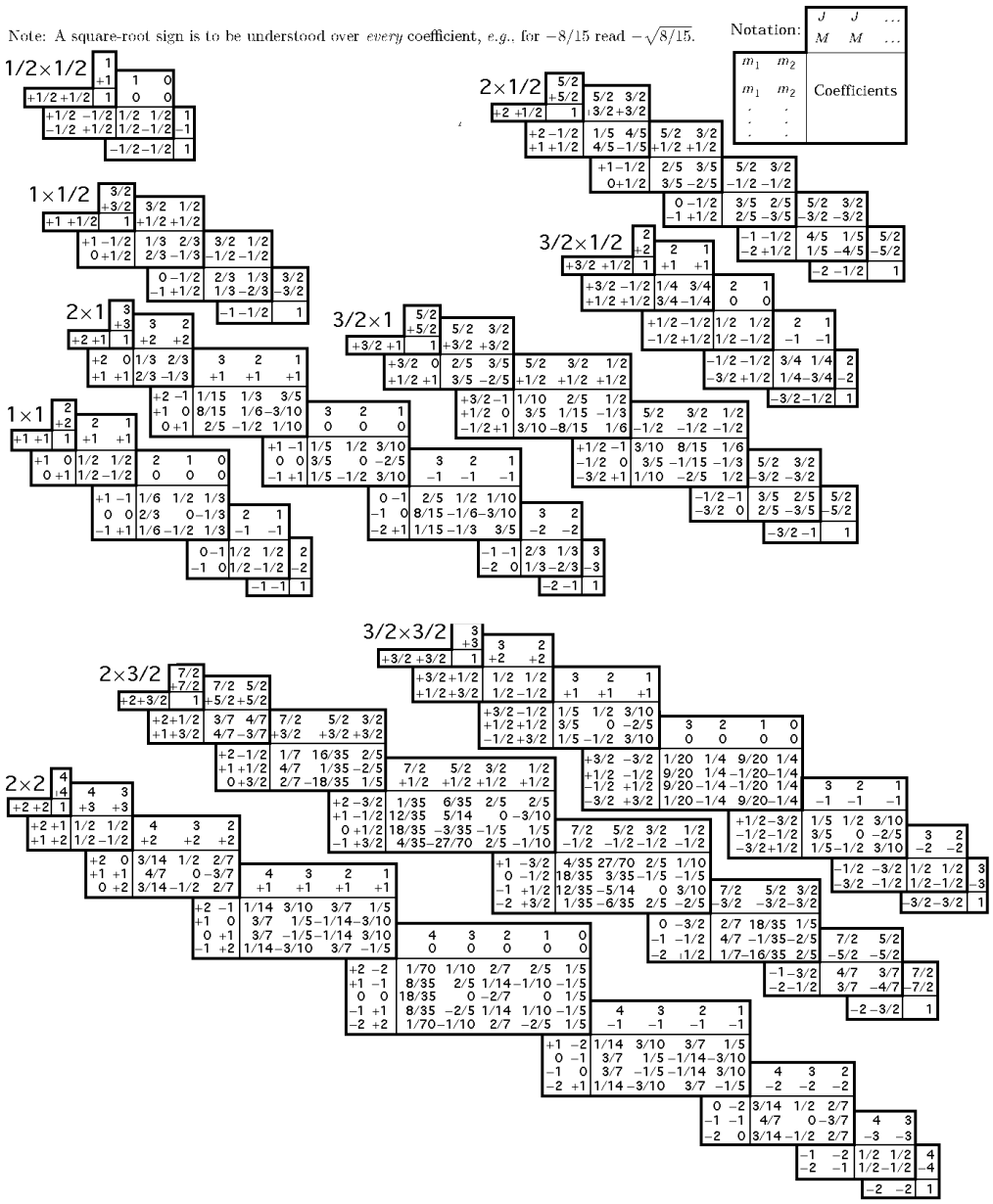

Figure 47. Clebsch-Gordan Coefficients [70]

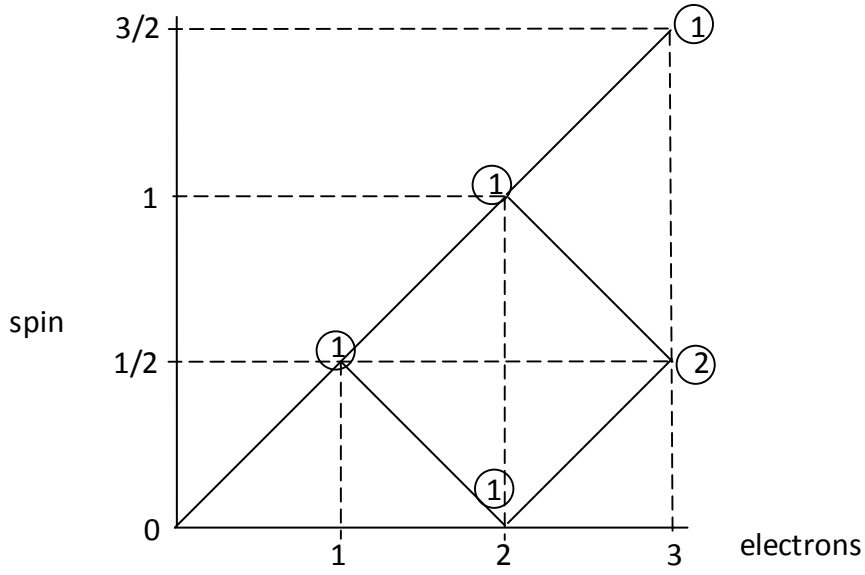

Figure 48. Addition of spin for three electrons

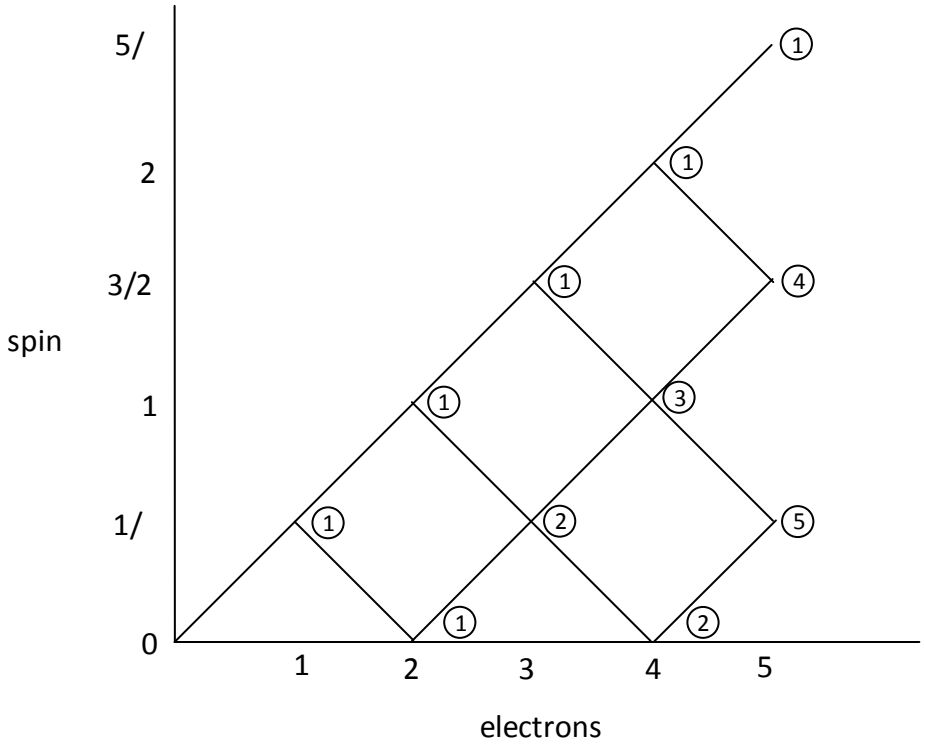

Figure 49. Genealogical construction of spin functions

$$\begin{aligned}\hat{R}\left|kq\right\rangle \otimes \hat{R}\left|jm\right\rangle &= \sum_{q'} D^{k}_{q'q}\left(\hat{R}\right)\left|kq'\right\rangle \otimes \sum_{m'} D^{j}_{m'm}\left(\hat{R}\right)\left|jm'\right\rangle \\ &= \sum_{q'm'} D^{k}_{q'q}\left(\hat{R}\right) D^{j}_{m'm}\left(\hat{R}\right)\left|kq'\right\rangle \otimes \left|jm'\right\rangle \\ &= \sum_{q'm'} D^{k}_{q'q}\left(\hat{R}\right) D^{j}_{m'm}\left(\hat{R}\right)\left|\begin{matrix} k & j \\ q' & m' \end{matrix}\right\rangle \\ &= \sum_{q'm'JM} D^{k}_{q'q}\left(\hat{R}\right) D^{j}_{m'm}\left(\hat{R}\right)\left|J\,M\right\rangle\left\langle J\,M\left|\begin{matrix} k & j \\ q' & m' \end{matrix}\right.\right\rangle\end{aligned} \tag{475}$$

where J ranges from $k+j$ to $\left|k-j\right|$ and M ranges appropriately for each J; the final term in the last equation is the Clebsch-Gordan coefficient.

Wigner-Eckart Theorem

For a given value of j, the set of simultaneous eigenvectors of $\hat{J}^2$ and $\hat{J}_z$, $\left|j-j\right\rangle, \left|j-(j-1)\right\rangle, \ldots \left|j\,j-1\right\rangle, \left|j\,j\right\rangle$, form a tensor of rank j. For instance, for $j=0$, the only eigenvector is $\left|0\,0\right\rangle$ and forms a rank-0 tensor by itself. For $j=1$, the three eigenvectors $\left|1-1\right\rangle, \left|10\right\rangle$, and $\left|11\right\rangle$ form a vector, or rank-1 tensor. Any tensor whose elements $T\left(k,q\right)$, when rotated, mix only among themselves is known as a *spherical tensor operator* [**46**]. Clearly this is the case for the tensors of spin eigenfunctions (see equation (462)). Each element of the spherical tensor operator, when applied to a spin eigenfunction, will thus act like the direct product of two angular momentum eigenfunctions:

$$T\left(k,q'\right)\left|d\,J\,M'\right\rangle = \left|\begin{matrix} k & J \\ q' & M' \end{matrix}\right\rangle \otimes \left|d\right\rangle \tag{476}$$

where d may be a collection of non-angular momentum eigenvalues which further identify the function. By completeness we can write an arbitrary eigenfunction $\left|d\,'J\,'M\,''\right\rangle$ as

$$\begin{aligned}\left|d\,'J\,'M\,''\right\rangle &= \sum_{q',M'}\left|\begin{matrix}k & J\\ q' & M'\end{matrix}\right\rangle\left\langle\begin{matrix}k & J\\ q' & M'\end{matrix}\right|d\,'J\,'M\,''\Big\rangle \\ &= \sum_{q',M'}\left|\begin{matrix}k & J\\ q' & M'\end{matrix}\right\rangle\left\langle\begin{matrix}k & J\\ q' & M'\end{matrix}\right|J\,'M\,''\Big\rangle\otimes\left|d\,'\right\rangle\end{aligned} \tag{477}$$

Let us now integrate this equation against the eigenfunction $\left|d\,K\,Q\right\rangle$:

$$\left\langle d\,K\,Q\middle|d\,'J\,'M\,''\right\rangle = \left\langle d\right|\otimes\sum_{q',M'}\left\langle K\,Q\left|\begin{matrix}k & J\\ q' & M'\end{matrix}\right\rangle\left\langle\begin{matrix}k & J\\ q' & M'\end{matrix}\right|J\,'M\,''\Big\rangle\otimes\left|d\,'\right\rangle \tag{478}$$

multiply both sides by $\left\langle\begin{matrix}k & J\\ q & M\end{matrix}\right|J\,'M\,''\Big\rangle$,

$$\begin{aligned}&\left\langle d\,K\,Q\middle|d\,'J\,'M\,''\right\rangle\left\langle\begin{matrix}k & J\\ q & M\end{matrix}\right|J\,'M\,''\Big\rangle = \\ &\qquad\left\langle d\right|\otimes\sum_{q',M'}\left\langle K\,Q\left|\begin{matrix}k & J\\ q' & M'\end{matrix}\right\rangle\left\langle\begin{matrix}k & J\\ q' & M'\end{matrix}\right|J\,'M\,''\Big\rangle\left\langle\begin{matrix}k & J\\ q & M\end{matrix}\right|J\,'M\,''\Big\rangle\otimes\left|d\,'\right\rangle\end{aligned} \tag{479}$$

and sum over all $J\,'$and $M\,''$:

$$\begin{aligned}&\sum_{J',M''}\left\langle d\,K\,Q\middle|d\,'J\,'M\,''\right\rangle\left\langle\begin{matrix}k & J\\ q & M\end{matrix}\right|J\,'M\,''\Big\rangle = \\ &\qquad\sum_{J',M''}\left\langle d\right|\otimes\sum_{q',M'}\left\langle K\,Q\left|\begin{matrix}k & J\\ q' & M'\end{matrix}\right\rangle\left\langle\begin{matrix}k & J\\ q' & M'\end{matrix}\right|J\,'M\,''\Big\rangle\left\langle\begin{matrix}k & J\\ q & M\end{matrix}\right|J\,'M\,''\Big\rangle\otimes\left|d\,'\right\rangle\end{aligned} \tag{480}$$

The last integral, a Clebsch-Gordan coefficient, is real and is its own conjugate:

$$\begin{aligned}&\sum_{J',M''}\left\langle d\,K\,Q\middle|d\,'J\,'M\,''\right\rangle\left\langle\begin{matrix}k & J\\ q & M\end{matrix}\right|J\,'M\,''\Big\rangle = \\ &\qquad\sum_{J',M''}\left\langle d\right|\otimes\sum_{q',M'}\left\langle K\,Q\left|\begin{matrix}k & J\\ q' & M'\end{matrix}\right\rangle\left\langle\begin{matrix}k & J\\ q' & M'\end{matrix}\right|J\,'M\,''\Big\rangle\left\langle J\,'M\,''\right|\begin{matrix}k & J\\ q & M\end{matrix}\Big\rangle\otimes\left|d\,'\right\rangle\end{aligned} \tag{481}$$

Through completeness, this forms a delta function on the right side:

$$\sum_{J',M''}\langle d\,K\,Q|d'\,J'\,M''\rangle\left\langle\begin{matrix}k & J\\ q & M\end{matrix}\middle|J'\,M''\right\rangle=\langle d|\otimes\sum_{q',M'}\left\langle K\,Q\middle|\begin{matrix}k & J\\ q' & M'\end{matrix}\right\rangle\delta_{q'q}\delta_{M'M}\otimes|d'\rangle$$
$$=\langle d|\otimes\left\langle K\,Q\middle|\begin{matrix}k & J\\ q & M\end{matrix}\right\rangle\otimes|d'\rangle \tag{482}$$

while on the left side, the integral over the spin functions also forms a delta function:

$$\langle d\,K\,Q|d'\,K\,Q\rangle\left\langle\begin{matrix}k & J\\ q & M\end{matrix}\middle|K\,Q\right\rangle=\langle d|\otimes\left\langle K\,Q\middle|\begin{matrix}k & J\\ q & M\end{matrix}\right\rangle\otimes|d'\rangle \tag{483}$$

Let us substitute equation (476) into equation(483):

$$\langle d\,K\,Q|d'\,K\,Q\rangle\left\langle\begin{matrix}k & J\\ q & M\end{matrix}\middle|K\,Q\right\rangle=\langle d\,K\,Q|T(k,q)|d'\,J\,M\rangle \tag{484}$$

and define

$$\langle d\,K\,Q|d'\,K\,Q\rangle\equiv\langle d\,K\,\|\,T_k\,\|\,d'\,K\rangle \tag{485}$$

to be the *reduced matrix element* of the spherical tensor operator T_k. Thus we have that the matrix element of a spherical tensor,

$$\langle d\,K\,Q|T(k,q)|d'\,J\,M\rangle=\left\langle\begin{matrix}k & J\\ q & M\end{matrix}\middle|K\,Q\right\rangle\langle d\,K\,\|\,T_k\,\|\,d'\,K\rangle \tag{486}$$

has been separated into geometrical (the Clebsch-Gordan coefficient) and dynamical (the reduced matrix element) components [**46**]. This separation allowed the reduced matrix element to be treated separately, which led to the definition of spin-orbit generators in terms of spin-free unitary generators [**44**].

Appendix J. The Symmetric Group

The symmetric group is the group of all (finite) permutations. It contains, as subgroups, the permutations of N objects, S_N, each with $N!$ elements. It bears importance not only because of the permutation of electrons, but also because of Cayley's theorem, which states that any finite group is isomorphic to a symmetric group [**72**].

Cyclic notation

Elements of this group are best expressed in *cyclic notation* [**72**]; for example, the symbol $(1\ 3\ 2)$ indicates that the first object moves to where the second object was, the third object moves to where the first object was, and the second object moves to where the third object was (this is the right-to-left convention; a left-to-right convention is equally valid). A cycle containing only two numbers is a *transposition*; a transposition of the form $(i \quad i+1)$ is called an *elementary transposition.* A product of cycles, e.g. $(1\ 2)(1\ 3)$, results in the permutation that takes 1 to 3, 3 (to 1) to 2, and 2 to 1. A few important theorems about the symmetric group in cyclic notation are:

1. Any permutation can be expressed as a product of transpositions or elementary transpositions; if the number of transpositions is even, the parity of the permutation is even (likewise for odd)

2. The set of even permutations in a group forms a subgroup called the *alternating group*

3. Cycles do not generally commute unless they are disjoint; i.e., they have no numbers in common

4. Any permutation can be expressed as a non-unique product of disjoint cycles

A number which is not permuted may be noted as a cycle by itself, or simply left off entirely. For example, the transpositions $(1\,2)$, $(1\,2)(3)$, and $(1\,2)(3)(4)$ are all equivalent. In this way, it is clear that the transposition $(1\,2)$ is not only an element of S_2, but also of S_3, S_4, *ad infinitum*. In fact, every group S_N is a subgroup of S_{N+1}, per the subgroup chain

$$S_1 \subset S_2 \subset S_3 \subset \ldots \subset S_{N-1} \subset S_N \tag{487}$$

Young tableaux

The regular representation of a permutation p_k in the group S_N is an $n!\times n!$ matrix. The basis vectors for this representation are constructed as

$$\begin{aligned} |p_k\rangle &\equiv p_k|1\rangle \\ \langle p_k| &\equiv \langle 1| p_k^{-1} \end{aligned} \tag{488}$$

(the latter property being true because symmetry operators are unitary [**37**]). We then construct the elements as

$$\left(R(p_k)\right)_{ij} = \langle p_i \mid p_k \mid p_j \rangle = \begin{cases} 1 & \text{if } p_i^{-1} p_k p_j = 1 \\ 0 & \text{otherwise} \end{cases} \tag{489}$$

In this form, the identity element will be diagonal, but in general the other permutations will have no structure. The irreducible representation basis vectors are specific linear combinations of the vectors in definition (488) which can be labeled by Young tableaux

[**39**]. Each Young frame of N boxes labels an irrep of S_N. For the group S_N, we take the N objects to be permuted (usually the numbers 1…N) and disperse them into each of the Young frames of n boxes using the following rules [**39**]:

1. No number is to be repeated
2. The number must be larger than the number to the left or above it

The frames filled with numbers by these rules are *standard Young tableaux*, and each one is a basis vector for the irreducible representation. Figure 50 explicitly shows all the Young tableaux that label S_5 irrep basis vectors. Each basis vector is labeled by a pair of those tableaux, but the pair must have the same frame. Thus, if k tableaux have the same frame in a group, they will be used to label k^2 basis vectors. Figure 51 shows an example basis vector label using two tableaux of the same shape. Using Figure 50, we see then that the S_5 irrep will have $1^2+4^2+5^2+6^2+5^2+4^2+1^2=120=5!$ basis vectors, the same as the regular representation. In the SGA, each box represents a spin-orbital, and each number represents an electron; thus the SGA involves permuting electrons among orbitals. Hence the number of electrons N matches the number of boxes in S_N.

The symmetrizer and antisymmetrizer

Two operators, the *symmetrizer* and the *antisymmetrizer*, relate the standard Young Tableaux to the operations they label [**39**]. The symmetrizer is the product over

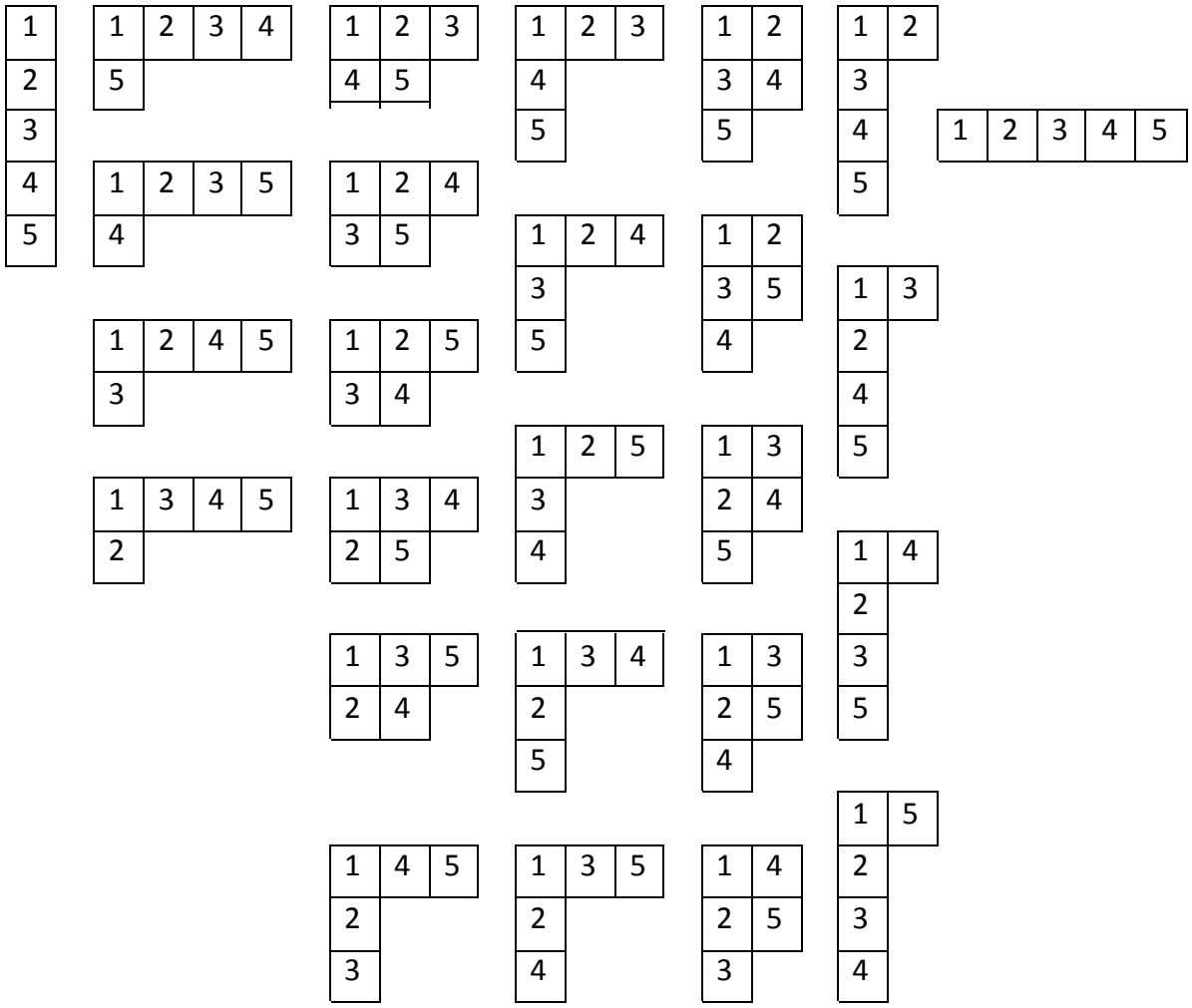

Figure 50. Young Tableaux for S_5

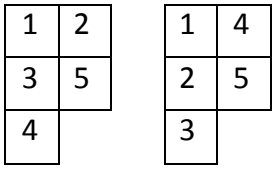

Figure 51. Example basis vector label for the S_5 irrep

all rows of the sum of all possible permutations in a single row of a tableau. The antisymmetrizer is the product over all columns of the sum of all possible even permutations and negative odd permutations in a single column of the tableau. For example, for the tableau

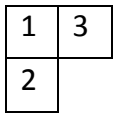

the first row, consisting of 1 and 3, includes the possible permutations (1) and $(1\,3)$; the second row only has the number 2, and so the only permutation is the identity (2). Thus the symmetrizer is

$$(2)\big[(1)+(1\,3)\big]=(1)+(13) \tag{490}$$

The first column, consisting of 1 and 2, includes the possible permutations (1), which is even, and $(1\,2)$, which is odd. The second column only has the number 3, so the only permutation is identity, (3), which is even. Thus the antisymmetrizer is

$$(3)\big[(1)-(1\,2)\big]=(1)-(1\,2) \tag{491}$$

The operation that the tableau labels is the product of the symmetrizer and the antisymmetrizer. Thus the above tableau labels the operation

$$\big[(1)+(1\,3)\big]\big[(1)-(1\,2)\big]=(1)-(1\,2\,3)+(1\,3)-(1\,2). \tag{492}$$

An example: The S_3 irreducible representation

Consider as a thorough example the group S_3. Using the above prescription, the Young tableaux are associated with the operations

$$\begin{array}{|c|c|c|}\hline 1 & 2 & 3 \\ \hline \end{array} \leftrightarrow (1)+(1\,2\,3)+(1\,3\,2)+(2\,3)+(1\,3)+(1\,2)$$

$$\begin{array}{|c|c|}\hline 1 & 2 \\ \hline 3 \\ \cline{1-1} \end{array} \leftrightarrow (1)-(1\,3\,2)-(1\,3)+(1\,2)$$

$$\begin{array}{|c|c|}\hline 1 & 3 \\ \hline 2 \\ \cline{1-1} \end{array} \leftrightarrow (1)-(1\,2\,3)+(1\,3)-(1\,2)$$

$$\begin{array}{|c|}\hline 1 \\ \hline 2 \\ \hline 3 \\ \hline \end{array} \leftrightarrow (1)+(1\,2\,3)+(1\,3\,2)-(2\,3)-(1\,3)-(1\,2)$$

Note that all these operations are orthogonal and, to within a constant, idempotent. Using the formulation in equation (488), these tableaux, which are now seen to be idempotent projectors, can be used to create the basis vectors

$$\left\langle \begin{array}{|c|c|c|}\hline 1 & 2 & 3 \\ \hline \end{array} \right| \leftrightarrow \tfrac{1}{\sqrt{6}}(1 \quad 1 \quad 1 \quad 1 \quad 1 \quad 1)$$

$$\left\langle \begin{array}{|c|c|}\hline 1 & 2 \\ \hline 3 \\ \cline{1-1} \end{array} \right| \leftrightarrow \tfrac{1}{2}(1 \quad -1 \quad 0 \quad 0 \quad -1 \quad 1)$$

$$\left\langle \begin{array}{|c|c|}\hline 1 & 3 \\ \hline 2 \\ \cline{1-1} \end{array} \right| \leftrightarrow \tfrac{1}{2}(1 \quad 0 \quad -1 \quad 0 \quad 1 \quad -1)$$

$$\left\langle \begin{array}{|c|}\hline 1 \\ \hline 2 \\ \hline 3 \\ \hline \end{array} \right| \leftrightarrow \tfrac{1}{\sqrt{6}}(1 \;\; 1 \;\; 1 \;\; -1 \;\; -1 \;\; -1)$$

where normalization has been enforced. Note that there are only four basis vectors here, but S_3 has 6. The two projectors from the dog-leg irrep can further be split each into a pair of nilpotent projectors. Consider the operation

$$\begin{array}{|c|c|}\hline 1 & 2 \\ \hline 3 \\ \cline{1-1} \end{array} \; (2\;3) \; \begin{array}{|c|c|}\hline 1 & 3 \\ \hline 2 \\ \cline{1-1} \end{array}$$

which yields the operation proportional to

$$\begin{array}{|c|c|}\hline 1 & 2 \\ \hline 3 \\ \cline{1-1} \end{array} \; \begin{array}{|c|c|}\hline 1 & 3 \\ \hline 2 \\ \cline{1-1} \end{array} \leftrightarrow (1\,2\,3) - (1\,3\,2) + (2\,3) - (1\,3) \qquad (493)$$

Likewise, the operation

$$\begin{array}{|c|c|}\hline 1 & 3 \\ \hline 2 \\ \cline{1-1} \end{array} \; (2\;3) \; \begin{array}{|c|c|}\hline 1 & 2 \\ \hline 3 \\ \cline{1-1} \end{array}$$

yields the operation proportional to

$$\begin{array}{|c|c|}\hline 1 & 3 \\ \hline 2 \\ \cline{1-1} \end{array} \; \begin{array}{|c|c|}\hline 1 & 2 \\ \hline 3 \\ \cline{1-1} \end{array} \leftrightarrow -(1\,2\,3) + (1\,3\,2) + (2\,3) - (1\,2) \qquad (494)$$

Both of these operations are nilpotent and are said to split the two projectors they use because they have the relationship

$$\left(\begin{array}{|c|c|}\hline 1 & 2 \\ \hline 3 \\ \cline{1-1} \end{array} \; \begin{array}{|c|c|}\hline 1 & 3 \\ \hline 2 \\ \cline{1-1} \end{array} \right) \left(\begin{array}{|c|c|}\hline 1 & 3 \\ \hline 2 \\ \cline{1-1} \end{array} \; \begin{array}{|c|c|}\hline 1 & 2 \\ \hline 3 \\ \cline{1-1} \end{array} \right) \propto \begin{array}{|c|c|}\hline 1 & 2 \\ \hline 3 \\ \cline{1-1} \end{array}$$

$$\left(\begin{array}{|c|c|}\hline 1 & 3 \\ \hline 2 \\ \cline{1-1} \end{array} \; \begin{array}{|c|c|}\hline 1 & 2 \\ \hline 3 \\ \cline{1-1} \end{array} \right) \left(\begin{array}{|c|c|}\hline 1 & 2 \\ \hline 3 \\ \cline{1-1} \end{array} \; \begin{array}{|c|c|}\hline 1 & 3 \\ \hline 2 \\ \cline{1-1} \end{array} \right) \propto \begin{array}{|c|c|}\hline 1 & 3 \\ \hline 2 \\ \cline{1-1} \end{array}$$

These projectors can be used to construct two additional basis vectors, just like the idempotent projectors. This action brings the total number of basis vectors to six, as required. These six vectors will block diagonalize all permutations of S_3 into a 1×1 symmetric block, a 1×1 antisymmetric block, and two 2×2 blocks. A Hamiltonian which commutes will all those permutations will also be thus block diagonalized in this basis. The interested reader may wish to consult Harter [**37**] for a parallel approach to finding a basis for C_{3v}.

Spin functions

As in the UGA, in the SGA each eigenfunction can be labeled by a pair of conjugate tableaux, one spatial and the other spin. Although the SGA uses the Young tableaux for the spatial piece, it uses the Weyl tableaux for the spin piece, just like the UGA. Figure 52 [**41**] combines the information from Figure 8 and Figure 49. Recall that in the UGA, although a spin state could be identified by the Young frame, the specific path taken to that state was ambiguous. In the SGA, that ambiguity is resolved. Surprisingly, it is the Young tableau of the spatial state rather than the Weyl tableau of the spin state that specifies this path. As an example, consider the triplet whose irrep is represented by the frame

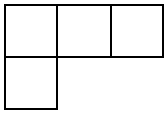

and thus whose conjugate spatial frame is

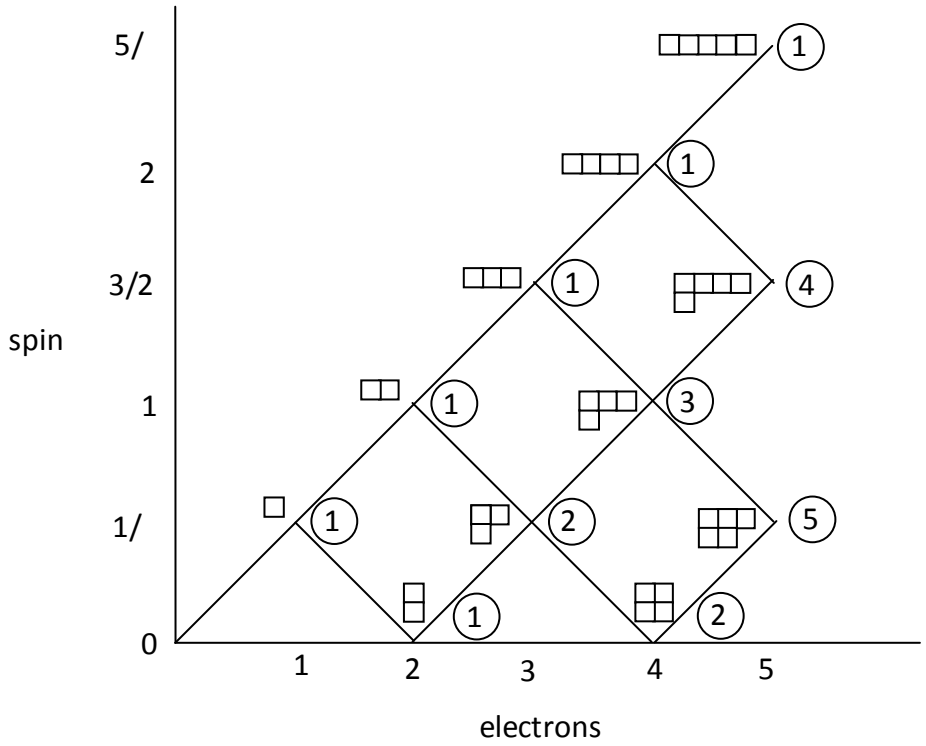

Figure 52. Genealogical construction of spin functions labled by multiplicities and Young frames

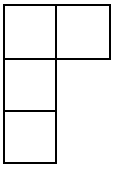

From Figure 52 it is clear that this spin state will a be triply degenerate triplet. While the spin state's Weyl tableau determines the z-projection m_s, the spatial state's Young tableau determines which triplet is involved. The three Young tableaux,

1	2
3	
4	

1	3
2	
4	

1	4
2	
3	

each specify a genealogical path. Take the first tableau, for example. 1 is in the first column, so we add it to the total spin. 2 appears in the second column, so we subtract it. 3 and 4 are both found in the first column, so we add both their spins. The resultant path of add, subtract, add, add is shown in Figure 53 [**41**]. Using spin coupling techniques, we recognize that this coupling path, doublet, singlet, doublet, triplet, is the triplet of spin functions

$$\begin{cases} \frac{1}{\sqrt{2}}\left(|\alpha\beta\alpha\alpha\rangle - |\beta\alpha\alpha\alpha\rangle\right) \\ \frac{1}{2}\left(|\alpha\beta\alpha\beta\rangle - |\beta\alpha\alpha\beta\rangle + |\alpha\beta\beta\alpha\rangle - |\beta\alpha\beta\alpha\rangle\right) \\ \frac{1}{\sqrt{2}}\left(|\alpha\beta\beta\beta\rangle - |\beta\alpha\beta\beta\rangle\right) \end{cases} \tag{495}$$

The second tableau then represents a doublet, triplet, doublet, triplet path outlined in Figure 54 [**41**]. This is the triplet

$$\begin{cases} \sqrt{\frac{2}{3}}|\alpha\alpha\beta\alpha\rangle - \sqrt{\frac{1}{6}}\left(|\alpha\beta\alpha\alpha\rangle + |\beta\alpha\alpha\alpha\rangle\right) \\ \sqrt{\frac{1}{3}}\left(|\alpha\alpha\beta\beta\rangle - |\beta\beta\alpha\alpha\rangle\right) + \sqrt{\frac{1}{12}}\left(|\alpha\beta\beta\alpha\rangle + |\beta\alpha\beta\alpha\rangle - |\alpha\beta\alpha\beta\rangle - |\beta\alpha\alpha\beta\rangle\right) \\ \sqrt{\frac{1}{6}}\left(|\alpha\beta\beta\beta\rangle + |\beta\alpha\beta\beta\rangle\right) - \sqrt{\frac{2}{3}}|\beta\beta\alpha\beta\rangle \end{cases} \tag{496}$$

Finally, the third Young tableau represents the doublet, triplet, quartet, triplet coupling in Figure 55 [**41**] which corresponds to the triplet

$$\begin{cases} \sqrt{\frac{3}{4}}|\alpha\alpha\alpha\beta\rangle + \sqrt{\frac{1}{12}}\left(|\alpha\beta\alpha\alpha\rangle + |\beta\alpha\alpha\alpha\rangle - |\alpha\alpha\beta\alpha\rangle\right) \\ \sqrt{\frac{1}{6}}\left(|\alpha\alpha\beta\beta\rangle + |\alpha\beta\alpha\beta\rangle + |\beta\alpha\alpha\beta\rangle - |\alpha\beta\beta\alpha\rangle - |\beta\alpha\beta\alpha\rangle - |\beta\beta\alpha\alpha\rangle\right) \\ \sqrt{\frac{1}{12}}\left(|\alpha\beta\beta\beta\rangle + |\beta\beta\alpha\beta\rangle - |\beta\alpha\beta\beta\rangle\right) - \sqrt{\frac{3}{4}}\left(\beta\beta\beta\alpha\right) \end{cases} \tag{497}$$

Although all three triplets are clearly different sets of functions, the spin-orbit Hamiltonian does not distinguish between them; in fact, any set of them could be mixed

and retain a definite spin, and any with the same m_s mixed would also retain a definite z-projection. For this reason, it is not necessary to specify exactly which genealogical path was taken to get to the spin state, and thus why the UGA does not suffer despite this disadvantage.

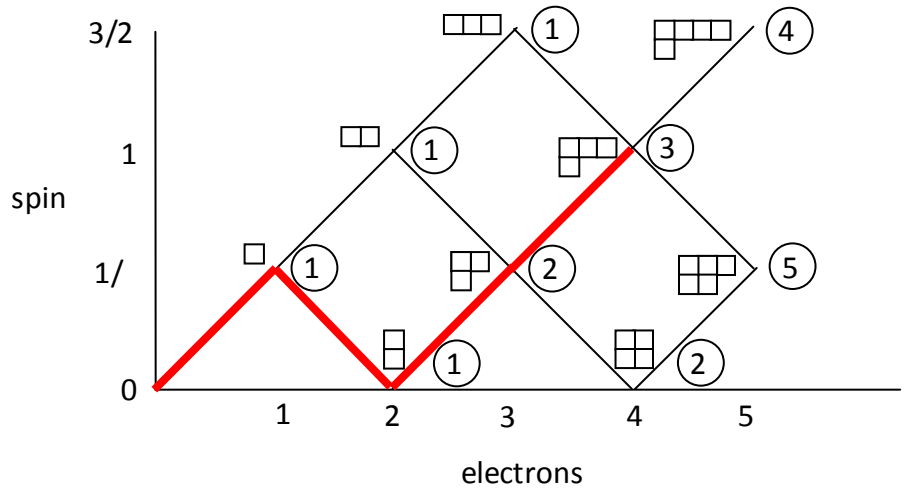

Figure 53. Spin state represented by the first Young Tableau

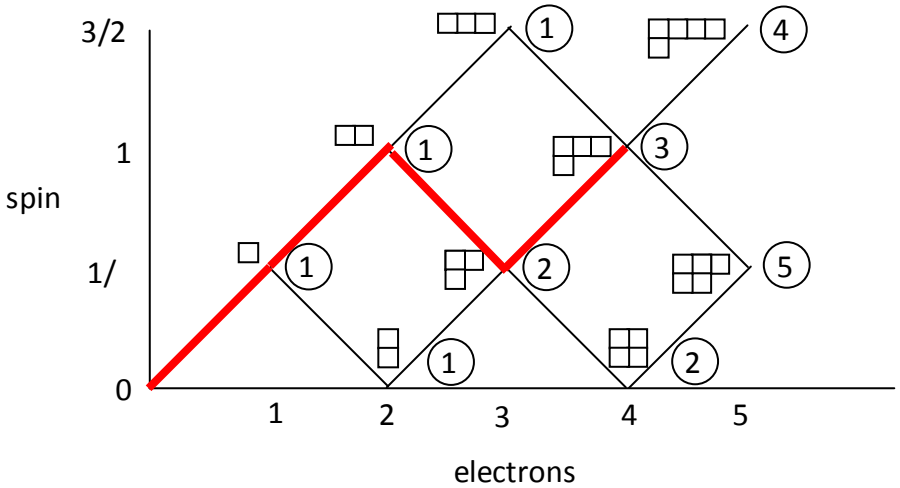

Figure 54. Spin state represented by the second Young Tableau

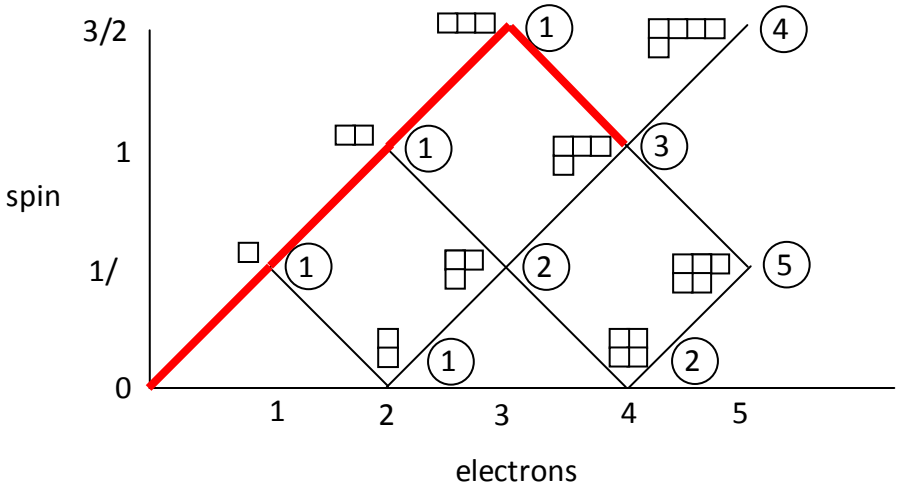

Figure 55. Spin state represented by the third Young Tableau

Bibliography

[1] R Shepard, "Geometrical energy derivative evaluation with MRCI wave functions," *International Journal of Quantum Chemistry*, vol. 31, no. 1, p. 33, 1987.

[2] R Shepard, H Lischka, P G Szalay, T Kovar, and M Ernzerhof, "A general multireference configuration interaction gradient program," *Journal of Chemical Physics*, vol. 96, p. 2085, 1992.

[3] R Shepard, "The Analytic Gradient Method for Configuration Interaction Wave Functions," *Modern Electronic Structure Theory*, vol. 1, p. 345, 1995.

[4] H Lischka, M Dallos, and R Shepard, *Molecular Physics*, vol. 100, p. 1647, 2002.

[5] H Lischka, P G Szalay, D R. Yarkony, and R Shepard, "Analytic evaluation of nonadiabatic coupling terms at the MR-CI level. I. Formalism," *Journal of Chemical Physics*, vol. 120, p. 7322, April 2004.

[6] M Dallos, H Lischka, R Shepard, D R Yarkony, and P G Szalay, "Analytic evaluation of nonadiabatic coupling terms at the MR-CI level. II. Minima on the crossing seam: Formaldehyde and the photodimerization of ethylene," *Journal of Chemical Physics*, vol. 120, p. 7330, 2004.

[7] H Lischka, R Shepard, F B Brown, and I Shavitt, "New implementation of the graphical unitary group approach for multireference direct configuration interaction calculations," *International Journal of Quantum Chemistry, Quantum Chemistry Symposium*, vol. S15, p. 91, 1981.

[8] R Shepard et al., "A progress report on the status of the COLUMBUS MRCI program system," *International Journal of Quantum Chemistry, Quantum Chemistry Symposium*, vol. 34, no. S22, p. 149, 1988.

[9] H Lischka et al., "High-Level multireference methods in the quantum-chemistry program system COLUMBES: Analytic MR-CISD and MR-AQCC gradients and MR-AQCC-LRT for excited states, GUGA spin-orbit CI and parallel CI density," *Physical Chemistry and Chemical Physics*, vol. 3, p. 664, 2001.

[10] H Lischka et al. (2006) COLUMBUS, an ab initio electronic structure program, release 5.9.1.

[11] S Yabushita, Z Zhang, and R M Pitzer, "Spin-orbit configuration interaction using the graphical unitary group approach and relativistic core potential and spin-orbit operators," *Journal of Physical Chemistry A*, vol. 103, p. 5791, 1999.

[12] H-J Werner, B Follmeg, and M H Alexander, "Adiabatic and diabatic potential energy surfaces for collisions of CN($X^2\Sigma^+$,$A\ ^2\Pi$) with He," *Journal of Chemical Physics*, vol. 89, no. 5, p. 3139, 1988.

[13] S Matsika and D R Yarkony, "On the effects of spin-orbit coupling on conical intersection seams in molecules with an odd number of electrons. I. Locating the seam," *Journal of Chemical Physics*, vol. 115, no. 5, p. 2038, 2001.

[14] S Matsika and D R Yarkony, "Spin-orbit coupling and conical intersections in molecules with an odd number of electrons. III. A perturbative determination of the electronic energies, derivative couplings and a rigorous diabatic representation near a conical intersection," *Journal of Chemical Physics*, vol. 116, no. 7, p. 2825, 2002.

[15] S Matsika and D R Yarkony, "Spin-orbit coupling and conical intersections. IV. A perturbative determination of the electronic energies, derivative couplings, and a rigorous diabatic representation near a conical intersection. The general case.," *Journal of Physical Chemistry B*, vol. 106, p. 8108, 2002.

[16] M R Manaa and D R Yarkony, "Nonadiabatic perturbations and fine structure splittings in the 1,2 $^3\Pi_g$ states of B_2: An analysis based on adiabatic and rigorous diabatic states," *Journal of Chemical Physics*, vol. 100, no. 11, p. 8204, 1994.

[17] G Parlant, J Rostas, G Taieb, and D R Yarkony, "On the electronic structure and dynamical aspects of the predissocoation of the $A\ ^2\Pi_\Omega$ states of MgCl. A rigorous quantum mechanical treatment incorporating spin-orbit and derivative coupling effects," *Journal of Chemical Physics*, vol. 93, no. 9, p. 6403, 1990.

[18] J J Dillon and D R Yarkony, "The photoelectron spectrum of the isopropoxide anion: Nonadiabatic effects due to conical intersections and the spin-orbit interacition," *Journal of Chemical Physics*, vol. 130, pp. 154312-1 , April 2009.

[19] AFRL DSRC. [Online]. http://www.afrl.hpc.mil/

[20] A Szabo and N S Ostlund, *Modern Quantum Chemistry*. Mineola, NY: Dover Publications, Inc, 1989.

[21] L R Kahn, P Baybutt, and D G Truhlar, "Ab initio effective core potentials: Reduction of all-electron molecular structure calculations to calculations involving only valence electrons," *Journal of Chemical Physics*, vol. 65, p. 3826, 1976.

[22] P A Christiansen, Y S Lee, and K S Pitzer, "Improved ab initio effective core potentials for molecular calculations," *Journal of Chemical Physics*, vol. 71, p. 4445, 1979.

[23] Y S Lee, W C Ermler, and K S Pitzer, "Ab initio effective core potentials including relativistic effects. I. Formalism and applications to the Xe and Au atoms," *Journal of Chemical Physics*, vol. 67, p. 5861, 1977.

[24] L A Fefee et al. (1997, Aug) Clarkson University Relativistic Effective Potential Database. [Online]. http://people.clarkson.edu/~pchristi/reps.html

[25] H Goldstein, C Poole, and J Safko, *Classical Mechanics*, 3rd ed. San Francisco: Addison Wesley, 2002.

[26] C Cohen-Tannoudji, B Diu, and F Laloë, *Quantum Mechanics*. New York: John Wiley & Sons, 1977, vol. 1.

[27] T Pascher, L S Cederbaum, and H Köppel, "Adiabatic and Quasidiabatic States in a Gauge Theoretical Framework," *Advances in Chemical Physics*, vol. 84, p. 293, 1993.

[28] B H Bransden and C J Joachain, *Physics of Atoms and Molecules*. New York: Longman, 1984.

[29] H Köppel, "Diabatic representation: methods for the construction of diabatic representations," *Unpublished article*, May 2002.

[30] W Domcke, D R Yarkony, and H Koppel, "Conical intersections," *Advanced Series in Physical Chemistry*, vol. 15, 2004.

[31] D R Yarkony, "Conical intersections: The new conventional wisdom," *The Journal of Physical Chemistry A*, vol. 105, p. 6277, 2001.

[32] K Moriyasu, *An Elementary Primer for Gauge Theory*. Singapore: World Scientific, 1983.

[33] B C Hall, *Lie Groups, Lie Algebras, and Representations*. New York: Springer-Verlag, 2004.

[34] R Gilmore, *Lie Groups, Physics, and Geometry*. Cambridge, MA: Cambridge University Press, 2008.

[35] R Shepard, "The multiconfiguration self-consistent field method," *Ab Initio Methods in Quantum Chemistry II: Advances in Chemical Physics*, vol. 69, p. 63, 1987.

[36] R Shepard, "An Introduction to GUGA in the COLUMBUS Program System," in *Relativistic and Electron Correlation Effects in Molecules and Solids*, G L Malli, Ed. New York: Plenum Press, 1994, p. 447.

[37] W G Harter, *Principles of Symmetry, Dynamics, and Spectroscopy*. New York: John Wiley & Sons, 1993.

[38] J Paldus, "Unitary Group Approach to Many-Electron Correlation Problem," *The Unitary Group From Lecture Notes in Chemistry*, vol. 22, 1981.

[39] R Pauncz, *The Symmetric Group in Quantum Chemistry*. Boca Raton: CRC Press, 1995.

[40] L I Schiff, *Quantum Mechanics*, 3rd ed. New York: McGraw-Hill Book Company, 1968.

[41] I Shavitt, Introduction to the Unitary Group Approach, Unpublished Presentation.

[42] I Shavitt, "The Graphical Unitary Group Approach and its Application to Direct Configuration Interaction Calculations," *The Unitary Group, from Lecture Notes in Chemistry*, vol. 22, 1981.

[43] I Shavitt, "Unitary group approach to configuration interaction calculations of the electronic structure of atoms and molecules," *The IMA Volumes in Mathematics and Its Applications: Mathematical Frontiers in Computational Physics*, vol. 15, 1988.

[44] G W F Drake and M Schlesinger, "Vector-coupling approach to orbital and spin-dependent tableau matrix elements in the theory of complex spectra," *Physical Review A*, vol. 15, no. 5, p. 1990, May 1977.

[45] R M Pitzer and N W Winter, "Spin-orbit (core) and core potential integrals," *International Journal of Quantum Chemistry*, vol. 40, no. 6, p. 773, 1991.

[46] R N Zare, *Angular Momentum*. New York: Wiley-Interscience, 1988.

[47] R M Pitzer and N W Winter, "Electronic-structure methods for heavy-atom molecules," *Journal of Physical Chemistry*, vol. 92, no. 11, p. 3061, 1988.

[48] G Kedziora, Personal communication, 2010.

[49] B H Lengsfield III, P Saxe, and D R Yarkony, "On the evaluation of nonadiabatic coupling matrix elements using SA-MCSCF/CI wave functions and analytic gradient methods. I," *Journal of Chemical Physics*, vol. 81, no. 10, p. 4549, 1984.

[50] M Valiev et al., "NWCHEM: a comprehensive and scalable open-source solution for large scale molecular simulations," *Computational Physics Communications*, vol. 181, p. 1477, 2010.

[51] F Weigend and R Ahlrichs, "Balanced basis sets of split valence, triple valence, and quadruple zeta valence quality for H to Rn: Design and assessment of accuracy," *Physical Chemistry Chemical Physics*, vol. 7, p. 3297, 2005.

[52] I S Lim, P Schwerdtfeger, B Metz, and H Stoll, "All-electron and relativistic pseudopotential studies for the group 1 element polarizabilities from K to element 119," *Journal of Chemical Physics*, vol. 122, no. 10, 2005.

[53] P Csaszar and P Pulay, "Geometry optimization by direct inversion in the iterative subspace," *Journal of Molecular Structure*, vol. 114, p. 31, 1984.

[54] L T Belcher, *Non-adiabatic energy surfaces of the B+H2 system*. Dayton, OH: Air Force Institute of Technology, 2005.

[55] D R Yarkony, "Vibronic Energies and the Breakdown of the Born-Oppenheimer Approximation in Diatomic Molecules: Adiabatic and Diabatic Representations," in *Computational Molecular Spectroscopy*. Chichester, West Sussex, England: John Wiley & Sons Ltd, 2000, ch. 14, p. 459.

[56] M Tinkham, *Group Theory and Quantum Mechanics*. New York: McGraw-Hill Book Company, 1964.

[57] K Balasubramanian, *Relativistic Effects in Chemistry Part A*. New York: John Wiley & Sons, 1997.

[58] M A Heald and J B Marion, *Classical Electromagnetic Radiation*, 3rd ed. Fort Worth, TX: Saunders College Publishing, 1995.

[59] J D Jackson, *Classical Electrodynamics*, 3rd ed. United States of America: John Wiley & Sons, 1999.

[60] H A Bethe and E E Salpeter, *Quantum Mechanics of One- and Two-Electron Atoms*. New York: SpringerVerlag, 1957.

[61] C Cohen-Tannoudji, B Diu, and F Laloë, *Quantum Mechanics*. New York: John Wiley & Sons, 1977, vol. 2.

[62] D G. Fedorov and M S Gordon, "A study of the relative importance of one-and two-electron contributions to spin-orbit coupling," *Journal of Chemical Physics*, vol. 112, p. 5611, April 2000.

[63] I Shavitt, "The method of configuration interaction," *Methods of Electronic Structure Theory (Modern Theoretical Chemistry)*, 1977.

[64] R K Nesbet, "Algorithm for diagonalization of large matrices," *Journal of Chemical Physics*, vol. 43, p. 311, 1965.

[65] I Shavitt, "Modification of Nesbet's algorithm for the iterative evaluation of eigenvalues and eigenvectors of large matrices," *Journal of Computational Physics*, vol. 6, p. 124, 1970.

[66] E R Davidson, "The iterative calculation of a few of the lowest eigenvalues and corresponding eigenvectors of large real-symmetric matrices," *Journal of Computational Physics*, vol. 17, p. 87, 1975.

[67] B Roos, "A new method for large-scale CI calculations," *Chemical Physics Letters*, vol. 15, no. 2, p. 153, 1972.

[68] R Shepard, I Shavitt, and H Lischka, "Reducing I/O costs for the eigenvalue procedure in large-scale configuration interaction calculations," *Journal of Computational Chemistry*, vol. 23, p. 1121, 2002.

[69] C M Marian, "Spin-orbit coupling in molecules," *Reviews in Computational Chemistry*, vol. 17, p. 99, 2001.

[70] Particle Data Group. (2009, June) The Review of Particle Physics. [Online]. http://pdg.lbl.gov/2008/reviews/clebrpp.pdf

[71] R Pauncz, *Spin Eigenfunctions*. New York: Plenum Press, 1979.

[72] S MacLane and G Birkhoff, *Algebra*, 3rd ed. Providence, RI: AMS Chelsea Publishing, 1999.

Vita

Captain Lachlan Belcher was commissioned into the US Air Force in 2003 from the US Air Force Academy, where he earned his Bachelor of Science degree in physics and mathematics. He earned his Master of Science degree at the Air Force Institute of Technology in 2005, after which he served as the ICBM Survivability Program Manager for the Minuteman III and Peacekeeper weapon systems at the 526th ICBM Systems Wing, Hill AFB, UT. He was admitted into the AFIT PhD program in 2007. He currently serves as the Deputy Chief of the Weapons Branch, Starfire Optical Range, Kirtland AFB, NM.

REPORT DOCUMENTATION PAGE

Form Approved
OMB No. 0704-0188

1. REPORT DATE *(DD-MM-YYYY)*	2. REPORT TYPE	3. DATES COVERED *(From - To)*
16-06-2011	PhD Dissertation	08/2007 - 06/2011

4. TITLE AND SUBTITLE
Gradients and Non-Adiabatic Derivative Coupling Terms for Spin-Orbit Wavefunctions

5a. CONTRACT NUMBER

5b. GRANT NUMBER

5c. PROGRAM ELEMENT NUMBER

6. AUTHOR(S)
Belcher, Lachlan T. Capt. USAF

5d. PROJECT NUMBER

5e. TASK NUMBER

5f. WORK UNIT NUMBER

7. PERFORMING ORGANIZATION NAME(S) AND ADDRESS(ES)
Air Force Institute of Technology
Graduate School of Engineering and Management (AFIT/EN)
2950 Hobson Way
WPAFB OH 45433

8. PERFORMING ORGANIZATION REPORT NUMBER
AFIT/DS/ENP/11-J01

9. SPONSORING/MONITORING AGENCY NAME(S) AND ADDRESS(ES)
High-Energy Laser Joint Technology Office
801 University Blvd SE
Ste 209
Albuquerque, NM 87106
505-248-8208; Harro.Ackermann@jto.hpc.mil

10. SPONSOR/MONITOR'S ACRONYM(S)
HEL JTO

11. SPONSORING/MONITORING AGENCY REPORT NUMBER

12. DISTRIBUTION AVAILABILITY STATEMENT
APPROVED FOR PUBLIC RELEASE; DISTRIBUTION UNLIMITED

13. SUPPLEMENTARY NOTES

14. ABSTRACT
Analytic gradients of electronic eigenvalues require one calculation per nuclear geometry, compared to 3n calculations for finite difference methods, where n is the number of nuclei. Analytic non-adiabatic derivative coupling terms, which are calculated in a similar fashion, are used to remove non-diagonal contributions to the kinetic energy operator, leading to more accurate nuclear dynamics calculations than those that employ the Born-Oppenheimer approximation and assume off-diagonal contributions are zero. The current methods and underpinnings for calculating both of these quantities for MRCI-SD wavefunctions in COLUMBUS are reviewed. Before this work, these methods were not available for wavefunctions of a relativistic MRCI-SD Hamiltonian. A formalism for calculating the density matrices, analytic gradients, and analytic derivative coupling terms for those wavefunctions is presented. The results of a sample calculation using a Stuttgart basis for K He are presented.

15. SUBJECT TERMS
Non-Adiabatic Chemistry, Quantum Chemistry, COLUMBUS, DPAL

16. SECURITY CLASSIFICATION OF:			17. LIMITATION OF ABSTRACT	18. NUMBER OF PAGES	19a. NAME OF RESPONSIBLE PERSON
a. REPORT	b. ABSTRACT	c. THIS PAGE	UU	227	Weeks, David E.
U	U	U			19b. TELEPONE NUMBER (*Include area code*) 937-255-3636 x 4561